(200)
R295
no. 80-146
[pt. 1]
Text

UNITED STATES
DEPARTMENT OF THE INTERIOR
GEOLOGICAL SURVEY

[Reports - Open file series] 80-146.

FINAL REPORT--

ENVIRONMENTAL STUDIES
SOUTHEASTERN UNITED STATES
ATLANTIC OUTER CONTINENTAL SHELF
1977

GEOLOGY

Edited by Peter Popenoe

U. S. GEOLOGICAL SURVEY
MENLO PARK
FEB 20 1980
LIBRARY

(200)
R290
no. 80-146
[pl. 1]
TEXT

USGS LIBRARY - MENLO PARK
3 1820 00087454 9

U.S. GEOLOGICAL SURVEY
MENLO PARK
FEB 20 1980
LIBRARY

FINAL REPORT--

ENVIRONMENTAL STUDIES
SOUTHEASTERN UNITED STATES
ATLANTIC OUTER CONTINENTAL SHELF
1977

GEOLOGY

Edited by Peter Popenoe

U.S. Geological Survey Open-File Report 80-146

[Reports. Open file

This report is preliminary and
has not been edited for
conformity with Geological
Survey standards and
nomenclature.

For the Period

1 October 1976 - 30 September 1977

Prepared for the

Bureau of Land Management

UNDER MEMORANDUM OF UNDERSTANDING

NO. AA550-MU6-56

This report has been reviewed by the Bureau of Land Management and approved for publication. Approval does not signify that the contents necessarily reflect the views and policies of the Bureau, nor does mention of trade names or commercial products constitute endorsement or recommendation for use.

U.S. GEOLOGICAL SURVEY
MENLO PARK
FEB 20 1980
LIBRARY

(200)
R29o
no. 80-146
[pl. 1]
TEXT

USGS LIBRARY - MENLO PARK
3 1820 00087454 9

U. S. GEOLOGICAL SURVEY
MENLO PARK
FEB 20 1980
LIBRARY

FINAL REPORT--

ENVIRONMENTAL STUDIES
SOUTHEASTERN UNITED STATES
ATLANTIC OUTER CONTINENTAL SHELF
1977

GEOLOGY

Edited by Peter Popenoe

U.S. Geological Survey Open-File Report 80-146

This report is preliminary and
has not been edited for
conformity with Geological
Survey standards and
nomenclature.

[Reports. Open file]

For the Period

1 October 1976 - 30 September 1977

Prepared for the

Bureau of Land Management

UNDER MEMORANDUM OF UNDERSTANDING

NO. AA550-MU6-56

This report has been reviewed by the Bureau of Land Management and approved for publication. Approval does not signify that the contents necessarily reflect the views and policies of the Bureau, nor does mention of trade names or commercial products constitute endorsement or recommendation for use.

U. S. GEOLOGICAL SURVEY
MENLO PARK
FEB 20 1980
LIBRARY

TABLE OF CONTENTS

CHAPTER 1. INTRODUCTION
by Peter Popenoe

CHAPTER 2. SESTON OF THE SOUTHEAST GEORGIA EMBAYMENT
by Larry J. Doyle, Peter R. Betzer, Martin Peacock, and Frederick Wall

CHAPTER 3. TURBIDITY IN THE SOUTHEAST GEORGIA EMBAYMENT
by Michael H. Bothner

CHAPTER 4. BOTTOM CURRENTS AND BOTTOM SEDIMENT MOBILITY IN THE OFFSHORE SOUTHEAST GEORGIA EMBAYMENT
by Bradford Butman, David W. Folger, and Stephanie Pfirman

CHAPTER 5. SURFICIAL SEDIMENTS OF THE U. S. ATLANTIC SOUTHEASTERN UNITED STATES CONTINENTAL SHELF
by Orrin H. Pilkey, Fred Keer, and Stephanie Keer

CHAPTER 6. VIBRACORE STUDIES: GEORGIA EMBAYMENT SHELF
by Mark Ayers, Blake W. Blackwelder, James D. Howard, Fred Keer, Harley Knebel, and Orrin H. Pilkey

CHAPTER 7. TRACE METAL CONCENTRATIONS IN SEDIMENT CORES FROM THE CONTINENTAL SHELF OFF THE SOUTHEASTERN UNITED STATES
by Michael Bothner, Phil Aruscavage, Wayne Ferrebee, and Joan Lathrop

CHAPTER 8. DISTRIBUTION AND OCCURRENCE OF REEFS AND HARDGROUNDS IN THE GEORGIA BIGHT
by Vernon J. Henry and Robert T. Giles

CHAPTER 9. SOUTHEAST GEORGIA EMBAYMENT HIGH-RESOLUTION SEISMIC-REFLECTION SURVEY
by Douglas W. Edsall

CHAPTER 10. THE GEOLOGY OF THE FLORIDA-HATTERAS SLOPE AND INNER BLAKE PLATEAU
by Charles Paull and William Dillon

CHAPTER 11. SOUTH ATLANTIC OUTER CONTINENTAL SHELF HAZARDS MAP
by Mahlon Ball, Peter Popenoe, Michael Vazzana, Elizabeth Coward, William Dillon, Thomas Durden, Jack Hampson, and Charles Paull

APPENDICES

APPENDIX I - CRUISE REPORTS
(in pocket at rear of volume) (on microfiche film)

APPENDICES 2A - 2G (to accompany Chapter 2)
(in pocket at rear of volume) (on microfiche film)

APPENDIX 3A (to accompany Chapter 2)
(in pocket at rear of volume) (on microfiche film)

CHAPTER 1

INTRODUCTION

Peter Popenoe[1]

---

[1] U. S. Geological Survey, Woods Hole, Massachusetts 02543

CHAPTER 1

INTRODUCTION

Peter Popenoe

This report is a Compendium of Work Elements of environmental research carried out during the Federal Fiscal Year 1977 on the Southeastern Atlantic Outer Continental Shelf (OCS) by the U. S. Geological Survey under its Memorandum of Understanding (MOU 550-MU6-56) with the Bureau of Land Management (BLM). The research is part of a broader effort by the Bureau to acquire relevant data on the environment for use in planning and decision making regarding the development of mineral resources on the Federal OCS. This report summarizes the results of field investigations carried out between October 1976 and September 1977 which constitute the first year of the program for the Southeastern Atlantic OCS area. Analyses of results were done chiefly in Fiscal Year 1978.

The objectives of the U. S. Geological Survey's geologic environmental research program were to: (1) measure the rate of sediment mobility over the sea bed and to monitor resultant changes in bottom morphology and texture; (2) determine the concentration, distribution and flux of suspended particulate matter in the water column; (3) determine the vertical distribution of trace metals in the near surface sediment at selected locations; (4) evaluate potential geologic hazards to oil and gas development due to surficial and intermediate depth structure and mass sediment transport events; (5) identify and determine the significance of outcrop and reef structures; and (6) support the activities of the chemical/biological benchmark contractor by obtaining supportive sediment texture, composition, and physical oceanographic information.

These studies cover investigations from the water column down to the deeper stratigraphy and they have been ordered within the volumn from the surface down. Chapter 1 through 4 discuss the sediments within the water column and the physical processes which act upon these sediments. Chapters 5 through 7 discuss the surficial and shallow stratigraphy. Chapter 8 discusses the distribution of reefs and hardgrounds, Chapters 9 and 10 the subsurface geology, and Chapter 11 discusses a hazards map which was compiled from the shallow seismic reflection data.

Three large maps (Map 8-A, showing the distribution of reefs and hardgrounds in the Georgia Bight; Map 9-A, a Geologic Map of the Florida-Hatteras Shelf, Slope, and inner Blake Plateau; and Map 11-A, the Hazards and Constraints Map) are included in a pocket in the rear of this volume. Also included in a pocket on microfiche film are three sets of Appendices. These Appendices are: (1) cruise reports of seven cruises that were conducted during the field operations; (2) Appendices to accompany Chapter 2, Seston of the Southeast Georgia Embayment; and (3) transmissometer and suspended matter data, Southeast Georgia Embayment which accompany Chapter 3, Turbidity in the Southeast Georgia Embayment. Appendices for Chapter 9 were considered important to the text so these are included following the chapter. In accordance with the Memorandum of Understanding, the basic data have been submitted to the Environmental Data Service (EDS) for public distribution.

CHAPTER 2

SESTON OF THE SOUTHEAST GEORGIA EMBAYMENT

Larry J. Doyle[1], Peter R. Betzer[1],
Martin Peacock[1], and Frederick Wall[1]

---

[1] University of South Florida, Department of Marine Science, St. Petersburg, Florida 33701

Chapter 2

Table of Contents

Page

Abstract. 2- 1

Introduction. 2- 2

Methods and Materials 2- 4

  Choice of Filters 2- 4

  Pre-Cruise Preparation. 2- 5

  On Board Processing 2- 6

  Laboratory. 2- 7

Results and Discussion. 2-10

  Seston Flux 2-10

  Composition of Suspended Sediments. 2-22

  The Dissolved Organic Problem 2-26

Conclusions 2-33

Literature Cited. 2-36

CHAPTER 2

LIST OF APPENDICES

Page

2A Total Suspended Load, % $CaCO_3$, % Mg and Mg/Ca Ratios 2

2B Cross-Sections of Total Suspended Load 14

2C Cross-Sections of Percent $CaCO_3$. 46

2D Particulate Organic Nitrogen Values. 77

2E Inorganic Content. 88

2F Mineralogy of Suspended Sediments. 93

2G SEM Photographic Atlas of Particle Types 97

These Appendices are on microfiche in packets located at the rear of this volume.

CHAPTER 2

SESTON OF THE SOUTHEAST GEORGIA EMBAYMENT

L. Doyle, P. Betzer, M. Peacock, F. Wall

ABSTRACT

To gain a 3-dimensional perspective on the distribution, concentration and composition of seston on the southeastern U.S. Atlantic Outer Continental Shelf, its potential as a pollutant sink, and its flux across the shelf, seasonal sampling was undertaken on a grid of 50 stations in 1977 during the Physical and Biological Oceanographic cruises of Texas Instruments, Inc. Water samples were collected from 2 and 3 depths with the aid of a transmissometer and analyzed in the laboratory for total suspended load, percent calcium carbonate and magnesium and their ratios, particulate organic nitrogen, total inorganic content, mineralogy, and SEM photoraphs were made of characteristic seston.

The suspended load was found to vary seasonally, being highest in the winter, slightly lower during the summer, and considerably lower during spring and fall. Inshore suspended loads were highest compared to offshore loads, probably reflecting input of sediment from the Savannah and Altamaha rivers and seasonal storms. Clay mineralogy of the water samples suggests that the fines which originate in the rivers are diluted by shelf waters and transported over the shelf to the slope where they become entrained by the Gulf Stream. Calcium carbonate was highest during winter and relatively stable in other seasons. High salinity water low in suspended particles extended over large areas of the shelf in summer and fall.

The study indicates that the shelf is not a sink for pollutants as

fine-grained particles are sparse on the shelf and that river-generated fines ultimately bypass the shelf to be deposited on the slope and rise. The study also points out that current methods of measuring particulate organic carbon are seriously in error.

INTRODUCTION

Only a few studies of the seston of the waters of the Atlantic Continental Margin have been undertaken. Most extensive among these is that of Manheim and others (1970), who investigated the suspended matter in surface samples from Cape Cod to the Florida Keys between May and June, 1965, and found that suspended sediments decrease rapidly seaward. In a more intensive study, Rodolfo and others (1971) characterized the suspended load of a single transect before and after the passage of Hurricane Gerda in September, 1969, and found that strong storm waves associated with passage of a hurricane resuspend significant amounts of sediment but that values quickly return to normal after storm passage. These excellent studies and other pertinent data are summarized by Emery and Uchupi (1972). However all are limited in their 3-dimensional and seasonal aspects.

This investigation was designed to occupy a grid of 50 stations (see Figure 2-1) on the continental margin between Cape Fear, North Carolina and Cape Canaveral, Florida. All 50 stations were occupied during the February-March and August cruises; 25 during the May and November cruises. Two depths were sampled at shallow stations and three at the deeper stations in order to provide a 3-dimensional characterization of the seston. Sampling was conducted over a period of 3 weeks to provide synopticity. The goals of the study include assessment of seston flux, sources, pathways, and sinks. Determination

Figure 2-1. Station locations. Transects are numbered in the figure. Stations within transects were lettered, A, B, etc. from closest to shore seaward.

Figure 2-1

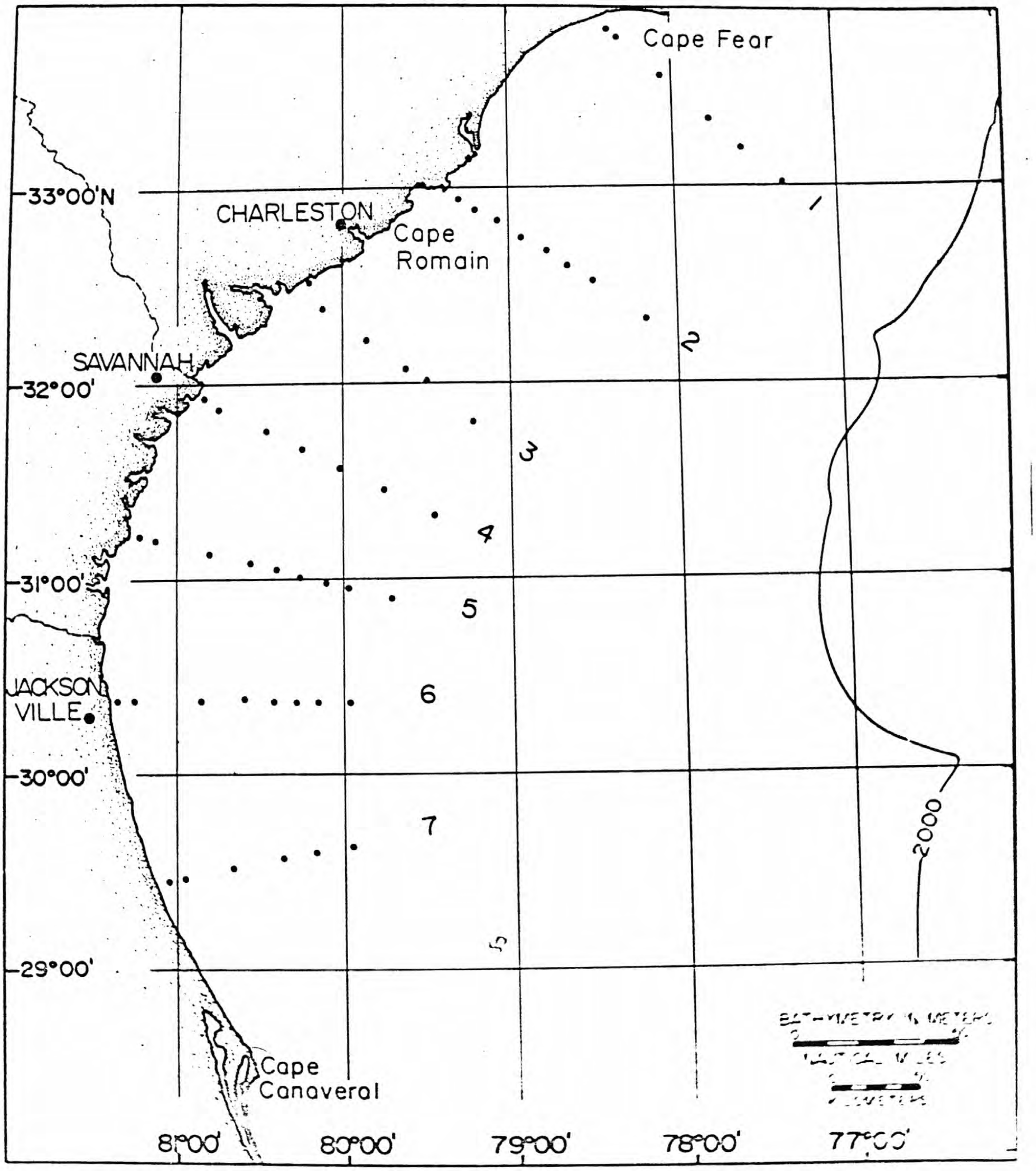

Cape Fear
33°00'N
CHARLESTON
Cape Romain
1
2
SAVANNAH
32°00'
3
4
31°00'
5
JACKSONVILLE
6
30°00'
7
2000
29°00'
BATHYMETRY IN METERS
NAUTICAL MILES
KILOMETERS
Cape Canaveral
81°00'
80°00'
79°00'
78°00'
77°00'

of pathways and sinks is a direct analog to likely pathways and sinks of pollutants associated with OCS development.

Shipboard sampling was carried out in 1977, aboard vessels furnished by Texas Instruments, Inc. Stations occupied were those of the benchmark study program managed by that company.

Physical and chemical oceanographic data for each station taken by Texas Instruments may be found in their final report to BLM. As required, data collected in this study are included as Appendices which are in the microfiche records in the pocket at the rear of this volume. Appendix 2A contains local suspended load, percent calcium carbonate, percent magnesium and Ca/Mg ratios. Appendix 2B shows cross-sections of total suspended load for each of the transects in Figure 2-1, seasonally. Appendix 2C shows similar cross-sections for calcium carbonate. Appendix 2D presents particulate organic nitrogen data, 2E total inorganic content, and 2F mineralogy. Appendix 2G is an atlas of SEM photographs which characterize the components of the seston.

METHODS AND MATERIALS

Choice of Filters

Total suspended load samples were collected on 47mm, 0.4 micrometer pore size Nuclepore filters. These filters were chosen over Millipore filters because of their physical and chemical properties including: (1) the pore sizes specified for Nuclepore membranes are highly precise and they have openings actually close to 0.4 micrometers; (2) they are not as hydroscopic as Millipore membranes and, therefore, provide more reproducible replicate weights; (3) their background of important trace constituents is considerably lower than Millipore membranes so that their use maximizes signal/noise ratios in trace metal analysis; and (4) their thickness (15 μm, about 1/10 that of Millipore HA membranes) and composition provide fewer adsorption sites for dissolved constituents. For compatibility with USGS-OCS studies of the mid and north Atlantic, which utilize Millipore membrances, separate total suspended load samples were taken using 47mm 0.45 μm pore size, Millipore filters for calibration of the transmissometer. Millipore filters were also used for collection of samples for suspended mineralogy. On the first two cruises 47mm, 0.45 μm pore size, Selas Flotronics silver filters were used for collection of particulate organic carbon samples, 25mm Selas silver filters on cruise 3, and Gelman glass fiber filters on cruise 4. As will be discussed subsequently, none of these membranes was satisfactory for the collection and determination of POC; and our data, as well as that of others, casts some doubt on the methods currently being used to measure POC numbers. Gelman glass fiber filters were used throughout for collection of particulate organic nitrogen.

Pre-Cruise Preparation

All pre-cruise preparations were carried out in a clean room or clean bench. Prior to each cruise the requisite number of Nuclepore filters and blanks was leached for 24 hours with 1.2 N Ultrex (Baker) HCl, triply rinsed with deionized water and dried over silica gel for 48 hours. Prior to each weighing, static electricity associated with the membranes was removed by passing them over a polonium source. Membranes were then weighed on a Perkin Elmer AD-2 microbalance. Variability was ± 5 micrograms. Thirty-five filters were loaded into acid-leached Millipore filter heads before each cruise. These filter heads were stored in sealed plastic bags and then used on offshore stations where low total suspended loads were expected. The remainder of the filters were sealed in acid-leached, polyethylene, snap top vials and used on the inshore stations. Loading and unloading at sea took place in a clean bench.

The Millipore filters for transmissometer calibration and the silver filters were weighed on the microbalance and stored in clean 47mm petri dishes. Glass fiber filters were precombusted at 500°C and stored in precombusted aluminum foil.

On Board Processing

Aboard the vessel, water samples were collected with 30 liter polyvinyl chloride (PVC) Niskin bottles attached to fiber hydrowire. Bottles were equipped with internal rubber closures during the first two cruises and externally activated ball valves on the last two cruises. Sampling depths were chosen using transmissometry, water depth and density data.

After the water samples had been collected, they were carried to the ship's lab for on-board processing. Filtration was carried out by pressurizing the Niskin bottles with 8 p.s.i. of doubly filtered (0.1 Micrometer) nitrogen through a plastic fitting in the top of the bottle. The completely closed system consisted of 3/8" I.D. teflon and silicon rubber tubing, which carried water from the Niskin bottles to the Millipore filter heads. Prior to each of the four cruises the filtering system was leached with 4 N HCl. Additionally, prior to filtering a new sample, the system was flushed with about one liter of that sample. Any time the tubing was disconnected it was immediately covered with polyethylene bags and sealed. Between 4 and 25 liters were filtered for total suspended load, 500 ml to one liter for particulate organic nitrogen and particulate organic carbon, and the remainder was filtered for suspended mineralogy until the filter clogged or all water was used. Volumes of filtered water were carefully measured and recorded. Various combinations of blanks for particulate organic carbon were used. A blank was inserted every fifth sample for particulate organic nitrogen.

The samples which were used for calibrating the transmissometer were collected with a five liter Niskin rosette system to which the transmissometer was attached. Since these bottles were not fitted for pressure filtration, seawater was pulled through paired Millipore filters by evacuation of a filtering flask in a closed filtering system.

After filtration, excess seawater and salt trapped on the filter were removed from the heads with 15 ml of deionized water and a hand-held Nalgene vacuum pump. Silver and glass fiber filters were placed in pre-combusted aluminum foil, transferred to 47mm plastic petri dishes, and refrigerated. All offshore samples were stored in their respective filter heads which were sealed in plastic bags for shipment to the shore-side laboratory. The other Nuclepore membranes were transferred to acid-cleaned, polyethylene snap top vials for shipment to the shore-side laboratory.

Laboratory

Wherever possible until the moment of analysis, all laboratory work was carried out in a clean room or clean bench. Nuclepore filters were placed in linear polyethylene funnels and further rinsed with about 12 ml of deionized water to remove any residual salt trapped on the filter. All other filters were placed in Millipore filter holders and rinsed by drawing 12 to 15 ml of deionized water through them. After a 48 hour desiccation over silica gel, the pads were reweighed on the Perkin Elmer micro balance. Total suspended load in micrograms per liter was calculated by dividing the difference between the tare weight and final weight by volume of water filtered.

Total suspended load samples on Nuclepore filters were then subjected to treatment for trace metal analysis for the weak acid soluble fraction as follows. The filters were placed in the same funnel assembly in which they were rinsed. Approximately 4 ml of 25% (^{v}/v) acetic acid solution was added and allowed to stand for two hours. After soaking, the solution was drained into acid-cleaned, one ounce, linear polyethylene bottles and the filters triply washed with deionized water, which was drained into the bottle with the filtrate. To prevent loss of metallic ions to the walls of the bottle (Robertson 1972), the pH was lowered to <1 by adding 0.5 ml of concentrated Ultrex (Baker) HCl. The solution was then transferred to an acid-washed 25 ml volumetric flask, brought to volume and returned to the one ounce bottle.

According to Chester and Hughes (1967) this solution contains the elements present in carbonates, those adsorbed onto mineral surfaces, and those present in easily reduced metal hydroxides and will affect to a negligible degree those present in the ferro-magnesium minerals. The solution was analyzed for Ca and Mg by atomic adsorption spectrometry. Calcium/magnesium ratios were determined for all samples and percent $CaCO_3$ was calculated by multiplying Ca values by 2.5.

The millipore filters which were used for transmissometer calibration were split using a Millipore filter cutter. One-half was saved for analysis with SEM, the other for analysis for total inorganic content. Total inorganic content was determined by combustion at 500°C using the techniques of Spencer and Manheim (1969). Results were not as consistent as desired, so samples from cruises one, three, and four were analyzed with an International Plasma low temperature asher (model 1101-448 AN). The asher oxidizes all organic material with a highly reactive oxygen (O_3) plasma, while temperatures remain below 40°C.

Halved filters were folded and placed on preweighed glass holders. They were then charred with 200 ml of acetone which prevents explosive oxidation of the filter in the asher. After charring, the glass holders were placed for at least 8 hours in the plasma, which completely oxidized the sample. Blank filter ash weights subtracted from total ash weights were 71 ± 18 μg. Replicate weighings of the glass holders alone showed a variation of ± 15 μg. Using the residual weight after oxidation in the low temperature asher, total inorganic content in μg/l was calculated.

Samples were prepared for suspended mineralogy determination by placing each filter in a 17 x 177 mm polypropylene centrifuge tube to which about 8 mls of filtered acetone were added. Tubes were shaken until the filter completely dissolved, after which they were spun in a Sorvall RC2-B centrifuge for 20 minutes at $3^{\circ}C$. The supernatant acetone was then carefully decanted. Eight mls of acetone were added to each tube, which was then sonified using a Heat Systems-Ultrasonics, Inc., Model W 185 cell disrupter with microtip and centrifuged and decanted as before. The process was repeated giving a total of three washes in acetone. Following the last acetone decantation about 5 mls of 1.2 N HCl was added, and the tube was sonified and allowed to stand for 3 hours to remove carbonate. The sample was then centrifuged and the acid decanted. About 5 ml of deionized water was then added and the tube was again sonified for at least 30 seconds to insure complete destruction of the pellet. To minimize the effect of differential settling rates, the contents of each tube were then vacuum-filtered, one ml at a time, through Selas Flotronic FM-25 silver filters (0.2 μm pore size, 25mm diameter) with a Millipore filtering apparatus.

After drying, silver filters were x-rayed at $2^{\circ}2\theta$ per minute. Each sample was x-rayed prior to any treatment. It was then glycolyzed for 12 hours, x-rayed, heated for 12 hours at 100°C, x-rayed, and heated for 4 hours at 300°C and x-rayed. Unless a 14 Å peak was present, samples were not subjected to heating at 550° C.

After carefully removing carbonate carbon with weak HCl, particulate organic carbon was determined by combusting the filters in an Angstrom carbon analyzer and measuring CO_2 conductivity.

Particulate organic nitrogen was determined with a Technicon II autoanalyzer. Samples were placed in digestion tubes with 25 ml surface seawater and 5 ml digestion mixtures of concentrated sulfuric acid, potassium sulfate, and mercuric sulfate (see EPA Manual of Methods for Chemical Analyses of Water and Wastes, 1974). Samples were digested for 1 hour at 180°C and then 1 1/2 hours at 370°C, allowed to cool and diluted to 75 ml with distilled water. Particulate organic nitrogen compounds are converted to ammonium sulfate in the digestion phase. Ammonia was measured by colorimetric technique on the autoanalyzer using an adaptation of the alkaline-phenol Technicon method L54-71W. Standards diluted in seawater and digested with precombusted glass fiber filters and blanks with seawater and precombusted glass fiber filters were run using the same procedure.

RESULTS AND DISCUSSION

Seston Flux

Distribution of the total suspended loads in surface and near bottom waters for the 4 seasonal cruises are shown in Figures 2-2 through 2-9. Seasonal cross sections showing the distribution of total suspended load for each transect are in Appendix 2B. It should be borne in mind that only half as many stations were occupied on the May and

November cruises as on the February-March and August cruises. This disparity may account for some of the lack of complexity in the data for the spring and fall cruises compared to the winter cruise and also for the apparent lack of high suspended load values inshore, because the inshore stations were not as thoroughly sampled in spring and fall as in winter and summer. Figures 2-2 through 2-9 and Appendix 2B show the total suspended load decreasing away from shore with lowest values found over the continental slope in the Florida Current. This trend is as expected and follows the pattern for surface waters reported in Manheim and others (1970) for May and June, 1965. Inshore suspended loads are highest in transects four and five and decrease to both the north and the south.

Suspended loads in transects four and five probably reflect the input of sediment from the Savannah and Altamaha rivers. Total suspended load values of over 1,000 µg/l are always found in waters of less than 33°/oo salinity. Decreasing suspended load offshore is mirrored by increase in salinity as the fresher, turbid inshore waters mix with more saline, less turbid offshore waters.

Figure 2-2 reflects the state of the total seston in near surface waters after an extremely harsh winter. Contours representing seston concentrations of 500 µg/l or less are much farther seaward than those of May (Figure 2-3). Surface contours lie still further inshore during the summer season (Figure 2-4), but by November (Figure 2-5) they have moved slightly seaward compared with the summer.

Near bottom data (Figures 2-6 through 2-9) show more subdued though generally similar patterns. Figures 2-8 and 2-9, which represent summer and fall conditions, show a shoreward bulge in the center portion of the study area. This water, low in suspended particulates and of high

Figure 2-2. Near surface total suspended load, February-March, 1977.

Figure 2-2

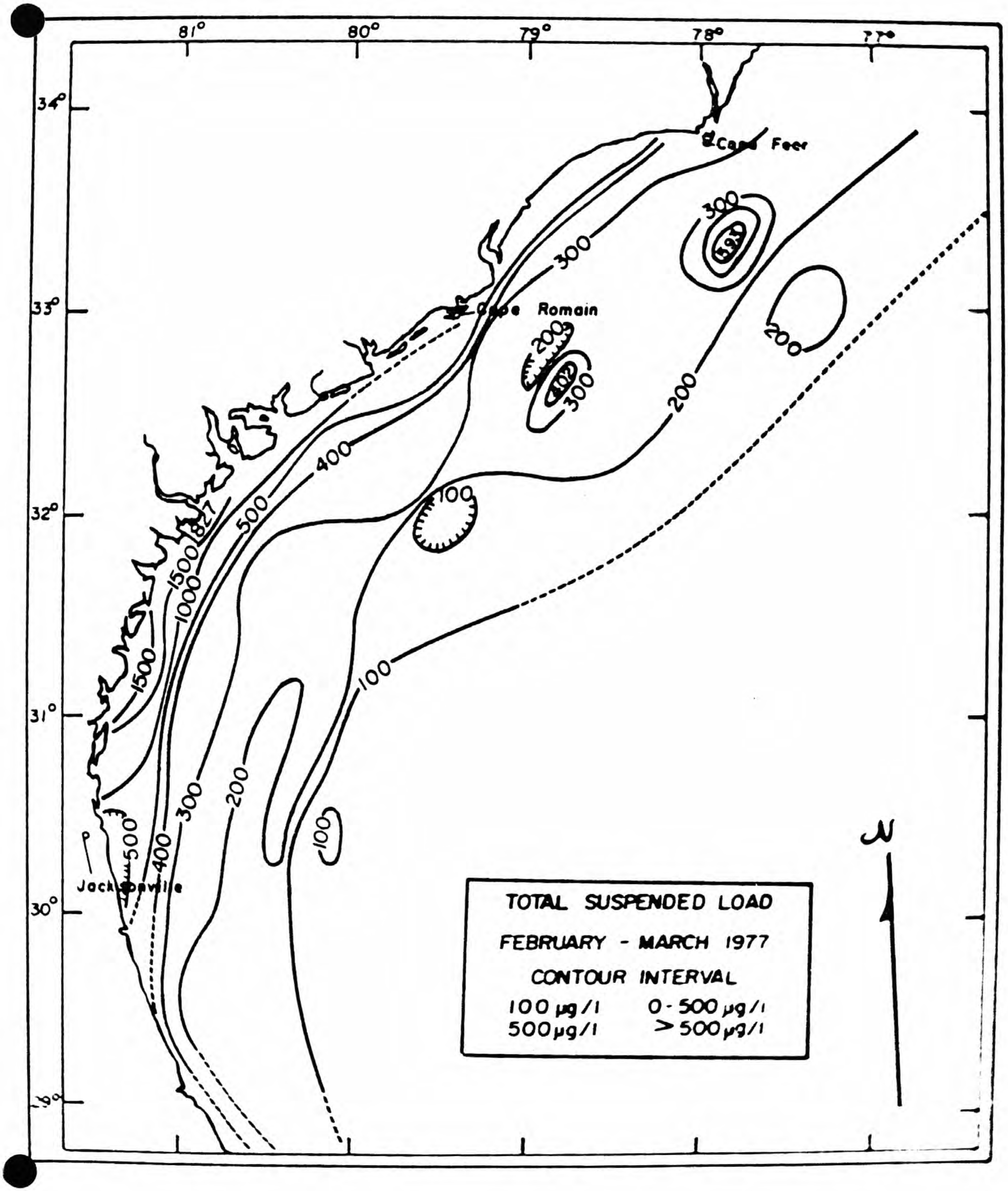
81°
80°
79°
78°
77°
34°
33°
32°
31°
30°
Cape Fear
Cape Romain
Jacksonville
300
300
200
200
300
200
200
400
500
827
1500
1000
1500
100
100
200
300
400
500
100
TOTAL SUSPENDED LOAD
FEBRUARY - MARCH 1977
CONTOUR INTERVAL
100 µg/l 0-500 µg/l
500µg/l >500µg/l
N

Figure 2-3. Near surface total suspended load, May 1977.

Figure 2-3

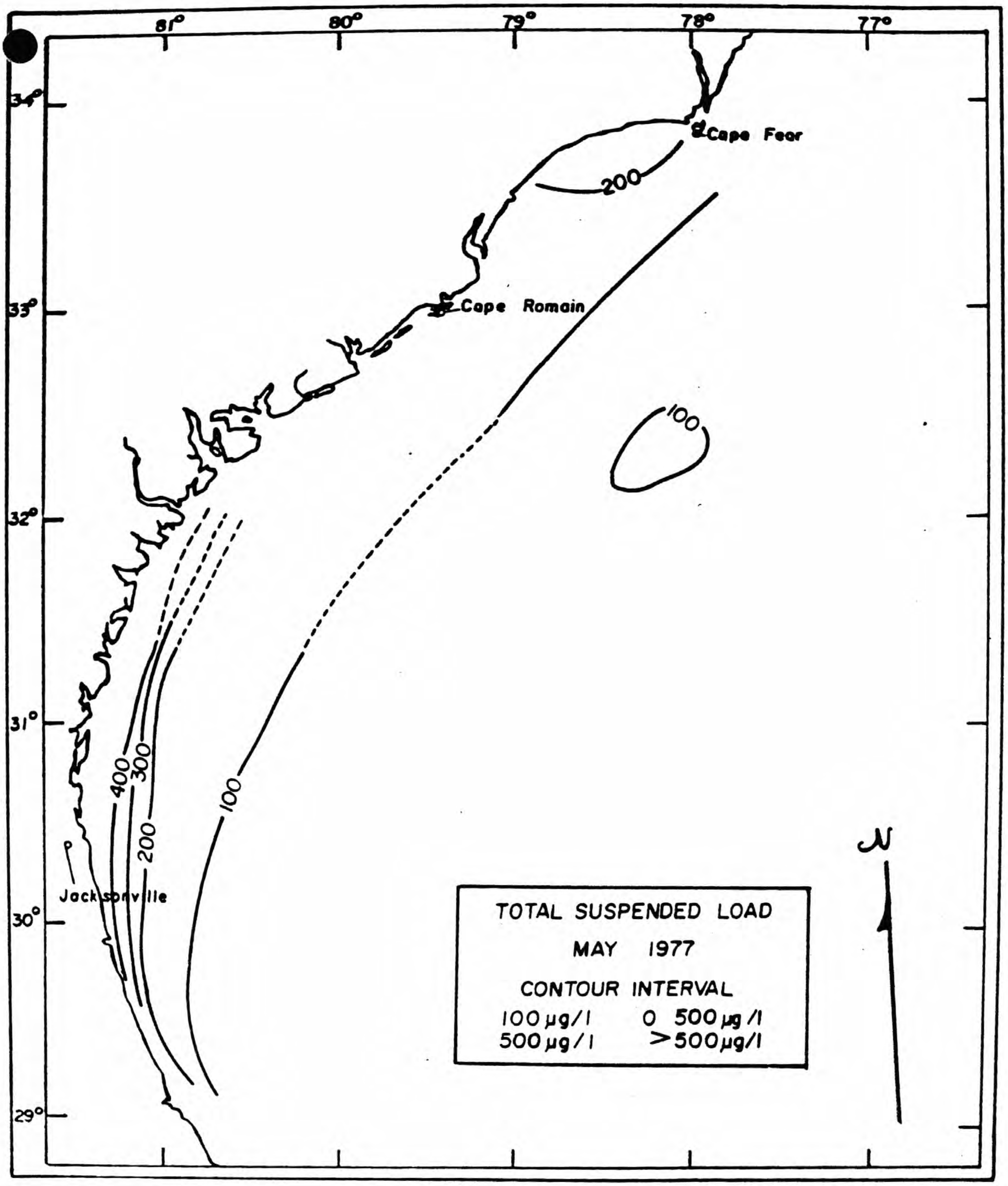
81°
80°
79°
78°
77°
34°
33°
32°
31°
30°
29°
Cape Fear
Cape Romain
Jacksonville
200
100
400
300
200
100
N
TOTAL SUSPENDED LOAD
MAY 1977
CONTOUR INTERVAL
100 µg/l 0 500 µg/l
500 µg/l >500 µg/l

Figure 2-4. Near surface total suspended load, August 1977.

Figure 2-4

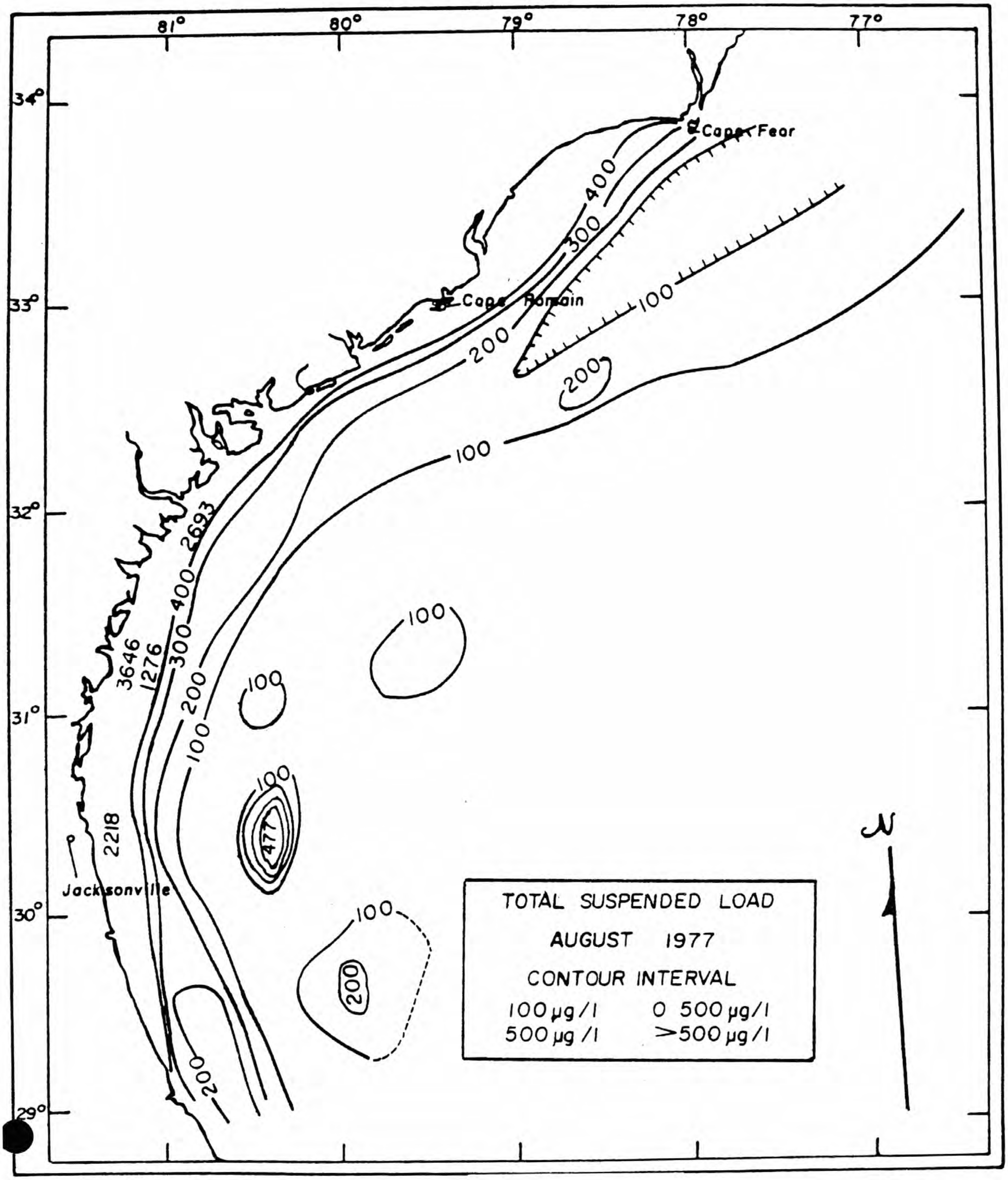
81°
80°
79°
78°
77°
34°
33°
32°
31°
30°
29°
Cape Fear
Cape Romain
Jacksonville
400
300
200
100
100
200
100
2693
400
3646
1276
300
200
100
100
100
100
477
2218
100
200
200
N
TOTAL SUSPENDED LOAD
AUGUST 1977
CONTOUR INTERVAL
100 µg/l 0 500 µg/l
500 µg/l >500 µg/l

Figure 2-5. Near surface total suspended load, November 1977.

Figure 2-5

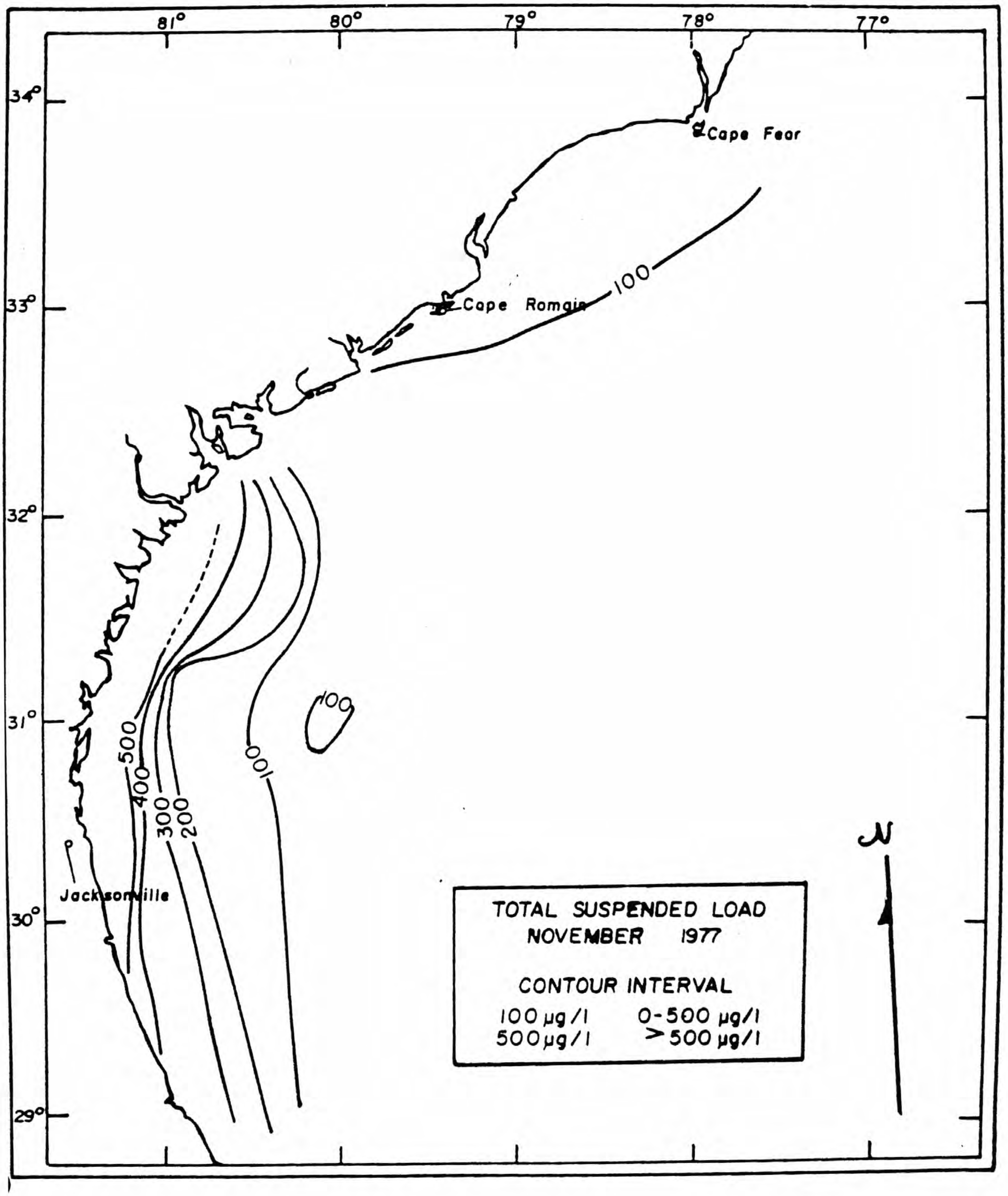
81°
80°
79°
78°
77°
34°
33°
32°
31°
30°
29°
Cape Fear
Cape Romain
100
100
100
500
400
300
200
Jacksonville
TOTAL SUSPENDED LOAD
NOVEMBER 1977
CONTOUR INTERVAL
100 µg/l 0-500 µg/l
500 µg/l >500 µg/l
N

Figure 2-6. Near bottom total suspended load, February-March, 1977.

Figure 2-6

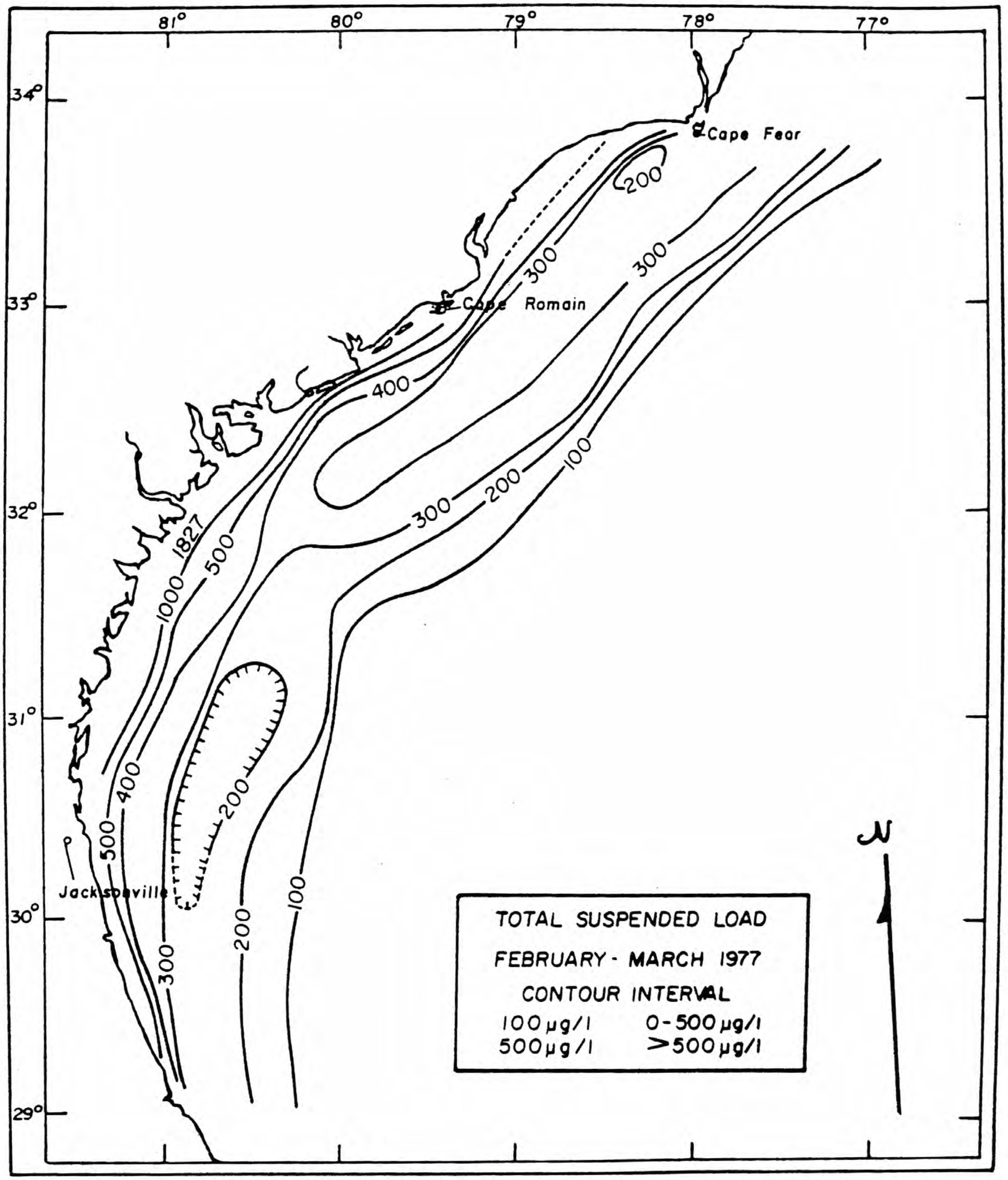

81°
80°
79°
78°
77°
34°
33°
32°
31°
30°
29°
Cape Fear
Cape Romain
Jacksonville
200
300
300
400
1827
1000
500
300
200
100
400
500
200
300
200
100
N
TOTAL SUSPENDED LOAD
FEBRUARY - MARCH 1977
CONTOUR INTERVAL
100 µg/l 0-500 µg/l
500 µg/l >500 µg/l

Figure 2-7. Near bottom total suspended load, May 1977.

Figure 2-7

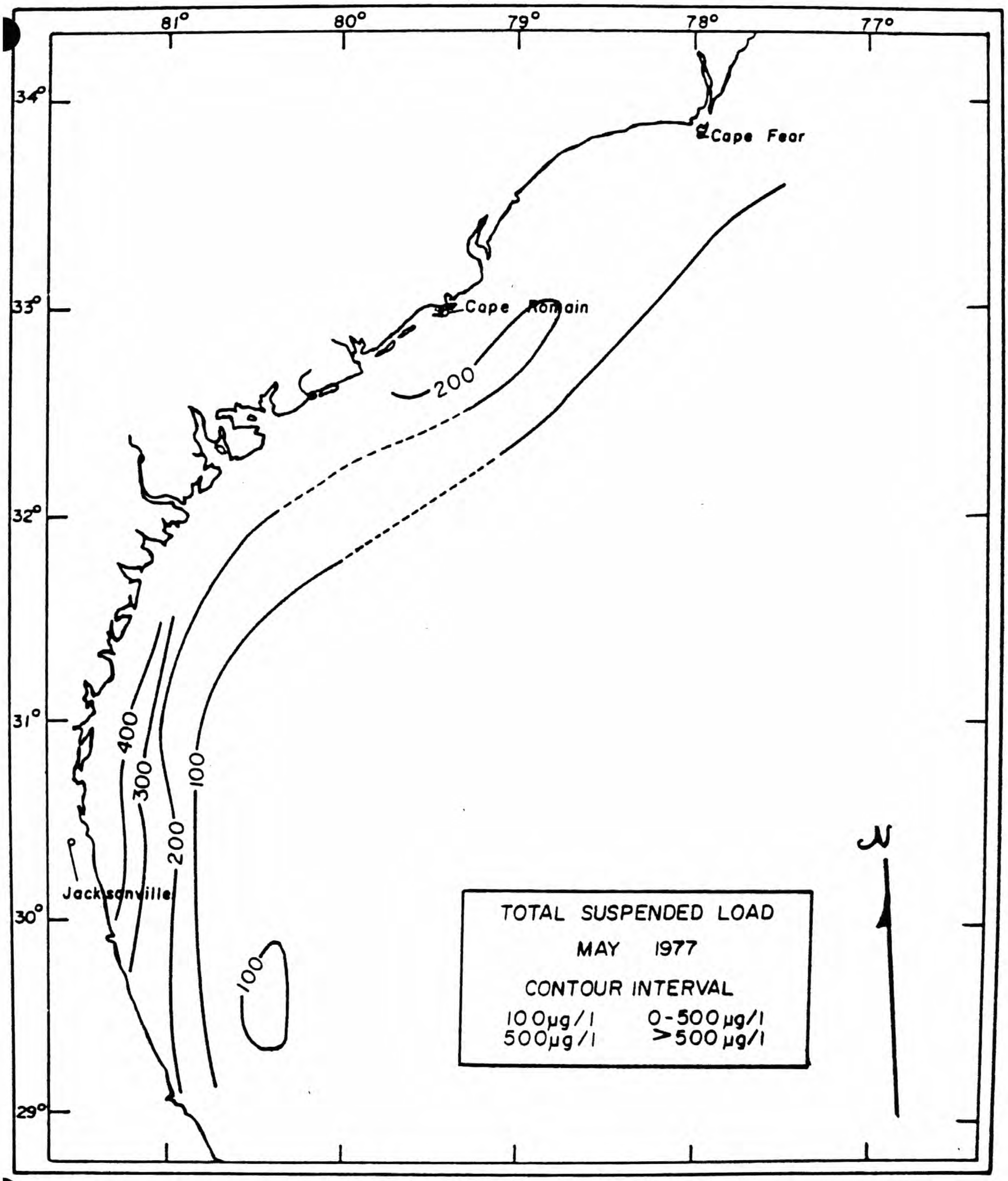
81°
80°
79°
78°
77°
34°
33°
32°
31°
30°
29°
Cape Fear
Cape Romain
Jacksonville
200
400
300
200
100
100
TOTAL SUSPENDED LOAD
MAY 1977
CONTOUR INTERVAL
100µg/l 0-500µg/l
500µg/l >500µg/l
N

Figure 2-8. Near bottom total suspended load August 1977.

Figure 2-8

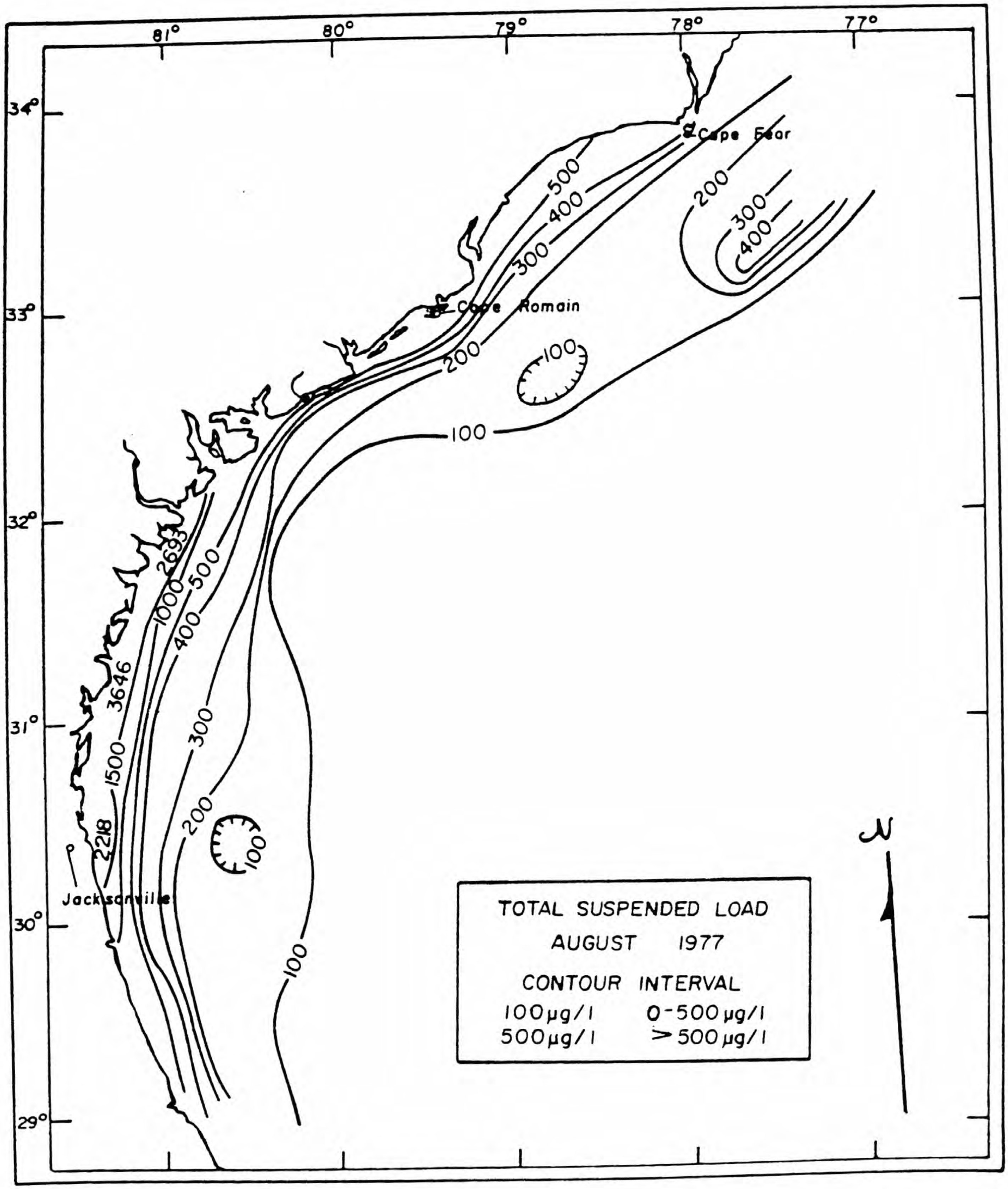

TOTAL SUSPENDED LOAD

AUGUST 1977

CONTOUR INTERVAL

100µg/l	0-500µg/l
500µg/l	> 500µg/l

81°
80°
79°
78°
77°
34°
33°
32°
31°
30°
29°
Cape Fear
Cape Romain
Jacksonville
500
400
300
200
100
2693
1000
3646
1500
2218
N

Figure 2-9. Near bottom total suspended load November 1977.

Figure 2-9

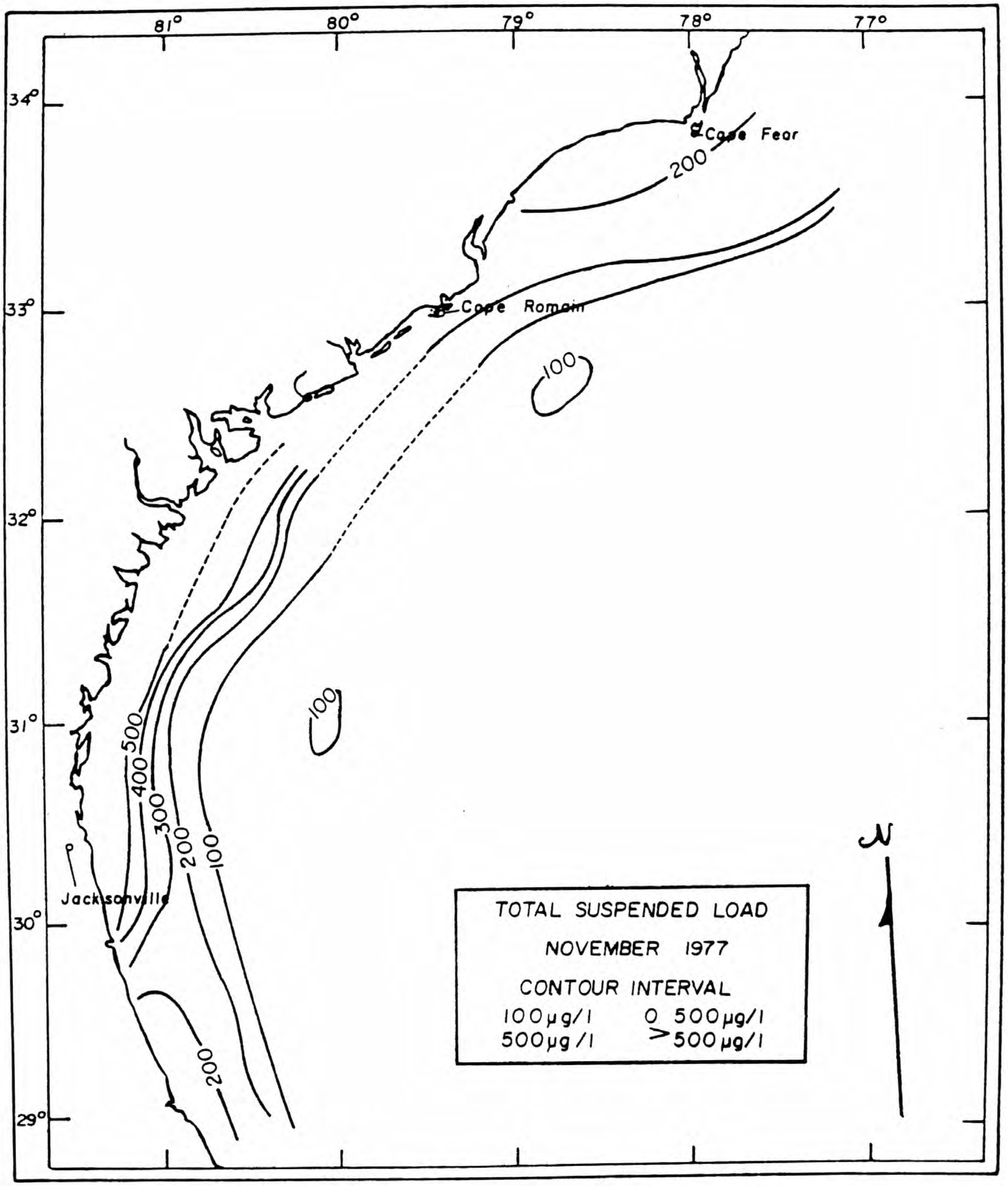
81°
80°
79°
78°
77°
34°
33°
32°
31°
30°
29°
Cape Fear
200
Cape Romain
100
100
500
400
300
200
100
200
Jacksonville
N
TOTAL SUSPENDED LOAD
NOVEMBER 1977
CONTOUR INTERVAL
100µg/l 0 500µg/l
500µg/l >500µg/l

salinity, is probably Florida Current water encroaching upon the shelf.

There are at least two alternative explanations of the general pattern of distribution of total suspended load in the southeast Atlantic Bight. One, which has been espoused by Manheim and others (1970), suggests that high seston concentrations inshore reflect contributions from rivers which quickly settle out. By their theory, little sediment escapes the estuary nearshore system to shelf and slope water, accounting for the high seston concentrations inshore rapidly decreasing over the open shelf and slope.

An alternative interpretation is that the rapid decrease in total suspended load in the offshore direction is due to the dilution and mixing of fresher waters of high suspended load with large volumes of shelf waters of comparatively low suspended load. In both alternatives, resuspension may contribute significantly to high suspended loads inshore.

Clay mineralogy of the suspended and surface sediments of the study area support the second interpretation. Rivers flowing into the waters of the Atlantic from the southeastern United States which carry an appreciable amount of fine sediments originate in the Piedmont province, where the dominant clay minerals are kaolinite and illite. Coastal plain sediments are dominated by smectite as are the sediments of the southeastern continental shelf (Pevear 1968). Only kaolinite and traces of illite were detected in the water column from inner shelf and slope water (see Appendix 2F). Slope bottom sediments have a mixed kaolinite, smectite, illite suite (Doyle and others, in press). These relationships suggest that at least some Piedmont river-borne fines are getting through the estuaries, and are by-passing the shelf in sufficient quantities to mask smectite resuspended from shelf sediments.

Masking is effective because silt and clay sizes make up only a small percentage of mid and outer southeastern shelf sediments (Pilkey and others, Chapter 5, this volume), so relatively small amounts of clay minerals are available for resuspension from the shelf sediments themselves.

Additional support for the latter interpretation is provided by Doyle and others (in press). They found that fine and sand-sized mica, the hydraulic equivalent of silt-sized particles, was not present in estuaries or on the shelf but became increasingly significant in slope, rise, and deep sea deposits, suggesting that some fines moved through the estuaries, over the shelf and were deposited on the outer portions of the continental margin.

In order to estimate the seasonal standing crop of particulates, the volume of shelf and slope water between Cape Fear and Cape Canaveral was estimated by dividing the region into areas based upon transect lines and lines drawn perpendicular to the isobaths from Cape Fear and Cape Canaveral. The seaward boundary was taken as a line joining the ends of all transects. Surface areas lying between 0 and 100 meters and between 100 and 400 meters were calculated for the entire study area with a polar planimeter. These were multiplied by weighted average depths calculated from bottom profiles of each transect. Water volume over depths between 0 and 100 meters was 3.373×10^3 km^3 and the surface area was 67, 454 km^2, while water volume over depths between 100 meters and 400 meters was 6.614×10^3 km^3 and the surface area was 22,300 km^2.

Using these numbers and the suspended sediment values from the various cruises, we constructed Table 2-1 which estimates the amount of total suspended load and calcium carbonate in the water column over the shelf and slope respectively, in metric tons. During all seasons sampled there was more suspended load and calcium carbonate over the shelf than over the slope. Table 2-1 also shows the sedimentation potential of the suspended load and of calcium carbonate. That is, the amount which would be deposited per cm^2 if the hypothetical situation arose whereby all material in suspension in the total water column were to settle out at once. Although it is obvious that such a situation never occurs in nature, such a calculation has the value of illustrating potential relationships of sedimentation rates between shelf and slope provinces.

Perusal of Table 2-1 shows that although the concentration of particles and $CaCO_3$ in suspension is less over the slope than over the shelf, the continental slope has a higher sedimentation potential in all cases but one than does the shelf because of a greater water volume. In many instances the slope then can act as a sediment and pollutant sink. Higher slope sedimentation potential is due to the presence of a much thicker water column and a reduced surface area. Higher sedimentation potential is a characteristic of continental slopes in general. The Florida Current, of course, must play a significant role in minimizing sedimentation rates on the Georgia Embayment shelf.

Winter and summer have the highest total suspended load; spring and fall the lowest. Some differences may again be an artifact of the reduced number of stations sampled in spring and fall. Despite the fact that the February-March sampling came at the end of a severe winter period, essentially the same amount of material was in suspension than as was the case in the following August.

Composition of Suspended Sediments

Appendix 2C shows the distribution of percent calcium carbonate in each sample of each transect over the 4 seasonal cruises. Values range

Table 2-1. Total suspended load and calcium carbonate in the water column over the shelf and slope (in metric tons).

	Suspended Matter				$CaCO_3$			
	TSL (total suspended load)		Sedimentation Potential		TSL (total suspended load)		Sedimentation Potential	
	Shelf	Slope	Shelf	Slope	Shelf	Slope	Shelf	Slope
Cruise 1	$1.32x10^6$m.t.	$4.49x10^5$m.t.	$1.96^{mg}/cm^2$	$2.01^{mg}/cm^2$	$1.20x10^5$m.t.	$5.25x10^4$m.t.	$1.178^{mg}/cm^2$	$0.235^{mg}/cm^2$
Cruise 2	$4.52x10^5$m.t.	$2.71x10^5$m.t.	$0.668^{mg}/cm^2$	$1.22^{mg}/cm^2$	$3.76x10^4$m.t.	$2.10x10^4$m.t.	$0.056^{mg}/cm^2$	$0.094^{mg}/cm^2$
Cruise 3	$1.24x10^6$m.t.	$4.76x10^5$m.t.	$1.85^{mg}/cm^2$	$2.13^{mg}/cm^2$	$5.84x10^4$m.t.	$3.71x10^4$m.t.	$0.086^{mg}/cm^2$	$0.166^{mg}/cm^2$
Cruise 4	$5.33x10^5$m.t.	$2.98x10^5$m.t.	$0.79^{mg}/cm^2$	$1.34^{mg}/cm^2$	$4.97x10^4$m.t.	$3.50x10^4$m.t.	$0.074^{mg}/cm^2$	$0.157^{mg}/cm^2$

from less than a percent to over 60% of the sample. Low values are usually associated with low salinity, high total suspended load and inshore water, while higher percentages are associated with open shelf and Florida Current water.

Table 2-1 shows the estimates of the total amount of calcium carbonate in suspension over shelf and slope for the 4 cruises. During the winter cruise about 1.7×10^5 metric tons or about 10% of the total suspended load was calcium carbonate, 5.9×10^4 metric tons or 8% in the spring, 9.6×10^4 metric tons or 5.5% in the summer, and 8.5×10^4 metric tons or 10.2% in the fall. While percentages change considerably, amounts of calcium carbonate in suspension remain relatively constant. Highest weight estimates occurred in the winter sampling and lowest during the spring. Winter highs may reflect resuspension of fine carbonates from the shelf due to storm waves.

During the November cruise (Appendix 2C, Part 4) the amounts of calcium carbonate in suspension change drastically from north to south. Transects 1 through 3 have extremely low percentages of calcium carbonate combined with low total suspended loads. Transects 4 through 7 have more normal calcium carbonate content. The change is dramatic and the reasons for it are not readily apparent. An SEM examination of several pads from northern and southern transects will be undertaken to attempt to resolve this paradox.

Magnesium analyses were run on the weak acid soluble fraction of suspended sediment samples and the data reported both as percent Mg and Ca/Mg ratios in Appendix 2A. Many ratios listed in Appendix 2A are much lower than would be expected from coccolith plates or from other carbonates alone. Lowest values appear to be in shallow waters and ratios usually increase with depth until they reach values which approximate those expected in carbonates. Relatively low ratios in surface and shallow waters increasing with depth, a pattern opposite to that which we find for magnesium, may be due to the magnesium in chlorophyll.

Appendix 2D shows the particulate organic nitrogen values determined for the 4 cruises. Since composition of particulate organic matter in seawater roughly reflects the composition of plankton, relatively high particulate organic nitrogen numbers in surface waters may refect high concentration of plankton and vice versa. Carbon analysis techniques for plankton are good. Carbon/nitrogen ratios in plankton range from about 5.3 to 12.5 (Emery and Uchupi 1972); so, by knowing values of particulate organic nitrogen, a gross estimate of particulate organic carbon and organic matter in suspension may be made. Below the euphotic zone C/N ratios in particulate organic matter drop substantially to an average of about 2.5 (Duursma 1960, as cited in Emery and Uchupi 1972) which, owing to potential overestimation of particulate organic carbon, may be regarded as a maximum value. Particulate organic nitrogen for the winter cruise averaged 15.2 µg/l, 17.3 µg/l during the spring cruise, only 7.9 µg/l during the summer cruise and 13.6 µg/l during the fall cruise. These averages suggest that the highest plankton crop occurred during spring as expected and the lowest during the summer.

Appendix 2D shows the mineralogy of selected samples from the winter and summer cruises. Results are reported as a blank, meaning undetectable, as trace T or as greater than trace of the acid insoluble residue. Feldspar and quartz are the most ubiquitous of the minerals present, followed by kaolinite. A few samples contained traces of illite.

In order to further characterize the seston, fractions of many filter pads were scanned with a SEM. Although most photographs are from the spring cruise they are representative of the types of seston seen on pads from all 3 cruises. It is difficult to get a quantitative estimate of composition from SEM because only a fraction of the entire pad is scanned and distribution of seston on the filter is patchy. However, it appears that there were far more coccoliths in the spring sampling than the winter or summer. Coccoliths appear to be predominate in the outer stations in the Florida Current during all seasons. Coccoliths, diatoms, and dinoflagellates (Appendix 2G, plates 1 through 15) make up most of the flora and fauna. A few foraminifera (not shown) are also present, as are whole coccopheres (plate 13). Aggregates are important constituents. These are often made up of coccoliths or fragments thereof. Some aggregates like those shown in plates 16 through 18 are probably fecal in origin; others origins are not so clear (plates 19 through 31). Probably some of these may be fecal pellets or partially degraded fecal material. A few mineral grains are found not bound into aggregates (plates 32 through 37). Often portions of the mount appear to be covered with an organic film. Most skeletal material does not appear corroded, but an exception is the diatom from Station 5B spring cruise shown in plate 10 which has been partially dissolved. Station 5B is inshore in shallow water and the corroded diatom suggests that some resuspension was occurring.

The Dissolved Organic Problem

Difficulties with seston analysis due to contamination, filtering medium, and type of filter have been discussed at length in the literature and are summarized by Riley (1970) among others. One problem which has not been adequately dealt with is that of dissolved organic carbon being adsorbed by the filter membrane and analyzed along with the particulate material, resulting in inflated particulate organic carbon values.

Menzel (1966) showed that adsorption of dissolved organic carbon occurred on both silver and glass fiber filters and the problem of retention of dissolved fatty acids and lipids by Millipore filters and Whatman and Gelman glass fiber filters has been discussed in detail by Quinn and Meyers (1971). They show that the problem can indeed be serious. Millipore filters retained 86% of the dissolved fatty acid or about 130 μg out of a possible 150 μg in 500 ml of filtration, while Gelman glass fiber filters retained about 50% of the dissolved fatty acid or about 75 μg out of a possible 150 μg in 500 ml of filtration.

Further problems in analysis of POC using glass fiber filters are exemplified by comparing the data of Betzer (1977) and Knauer (1977) who both studied the same suite of water samples from the eastern Gulf of Mexico. The former measured total suspended load on Nuclepore filters using the techniques outlined in this report. The latter measured POC on the same samples using precombusted glass fiber filters and standard analytical techniques. Table 2-2 shows the results. In the summer cruise, POC measurements on precombusted glass fiber filters exceeded the means for total suspended load estimates on Nuclepore filters. Conversion of POC to total organic content by even the most conservative estimate (a factor of 1.5 x POC) results in most values exceeding total suspended load numbers.

Glass fiber filters have still another unfortunate characteristic. They adsorb carbon dioxide from the atmosphere. Table 2-3 shows the carbon weight gain for precombusted glass fiber filters allowed to stand exposed to the air for varying lengths of time. As perusal of the table

GEOLOGICAL

Table 2-2. Comparison of TSL values on nuclepore filters with POC values from precombusted glass fiber filters 1975 - 1976 MAFLA.

SEASON	I		II		III		IV	
	TSL	POC	TSL	POC	TSL	POC	TSL	POC
Summer mean	79	80	101	110	78	160	170	240
(Range)	17-145	30-130	58-169	90-120	55-106	120-220	76-298	150-470
Fall mean	104	120	152	100	101	50	98	80
(Range)	53-197	60-220	104-210	70-150	54-144	30-100	37-158	40-110
Winter mean	351	140	352	130	141	90	287	150
(Range)	70-547	90-210	57-758	90-160	25-231	60-130	91-483	80-240

All numbers in μg/l
Roman numerals refer to sampling transects consisting of several stations

Table 2-3. Carbon absorbed from the air on glass fiber filters.

1 hour

#3	#36	#24
57.46 ug	53.84 ug	51.50 ug

Average 54.27 ug

1.5 hours

#20	#28	#45
54.76 ug	53.36 ug	52.10 ug

Average 53.40 ug

3.0 hours

#75	#50	#39
54.99 ug	54.52 ug	45.50 ug

Average 51.67 ug

20.5 hours

#48A	#52	#37
69.77 ug	61.97 ug	63.30 ug

Average 65.07 ug

26.5 hours

#2A	#108	#38
58.80 ug	52.40 ug	64.95 ug
#144 61.07 ug		

Average 59.30 ug

shows they can gain as much as 54 μg of carbon within 1 hour of exposure to air. Weight gain does not increase significantly after one hour.

Because of the difficulties encountered with glass fiber filters, silver filters were used in this study. Menzel (1966) has discussed the problem of adsorption of organics by these filters. In addition, the filters themselves contain carbon within the metal in large amounts compared to amounts in the particulate material collected. Table 2-4 shows analysis for carbon in 11 Selas silver filters from the same batch. Carbon values range from 292 μg to 493 μg carbon.

High carbon values and large variability preclude use of these filters for accurate POC measurements, especially when adsorption compounds the potential error. Most of the carbon is in the metal lattice and cannot be removed without burning and destroying the filter itself. Even modest heating (400°C) can distort and expand the pore size (Pilkey 1970).

Dissolved carbon is estimated to be on the order of 1,000 to 2,000 μg/l in surface waters and 300 to 700 μg/l in waters below 300 m (Menzel 1974). Since the quantity of dissolved organic carbon probably averages two orders of magnitude greater than the amount of particulate organic carbon and given Quinn and Myer's (1971) percentages of uptake of dissolved organics, masking of particulate organic carbon by the dissolved organic load is likely. Moreover, blank corrections by nesting filters in line are suspect because there may be considerable variability in uptake by different pads and a high percentage of the dissolved load may be retained by the top or sample filter compared to the blank filter below it.

There is no easy analytic solution to this problem. A possible alternative method may be to analyze a seawater sample for total organic

Table 2-4. Carbon in Selas flotronics silver filters.

Pad	ug C
1	349
2	477
3	442
4	493
5	461
6	467
7	396
8	382
9	359
10	292
11	307

carbon in a closed system, spin down another aliquot in an ultracentrifuge, analyze the supernatant liquid for dissolved carbon, and find particulate organic carbon by difference. However, such a method has the disadvantage of subtracting one relatively large number from another.

Historically all particulate organic carbon values arrived at with the use of glass fiber filters are probably too large by an unknown but significant factor and all dissolved organic carbon values derived after the sample has been passed through a filtering device are too small by some unknown factor. Values obtained with silver filters are also probably in error (Menzel 1966) and those obtained by filtration of relatively small amounts of water even more so, since carbon within the metal itself is a relatively large contributor to the signal. Total suspended load measurements are also too high by some indeterminant amount due to adsorption, even when blanks are used; especially those collected with Millipore filters. Total inorganic content should not be affected by the adsorption of organics and we have chosen to report this parameter, rather than total organic content.

Nuclepore filters should be less subject to POC contamination because of their structure (Lal 1977). Experimentation with Nuclepore organic adsorption to determine its magnitude is underway and results so far have supported this conclusion, although more work needs to be done. Due to the large differences in the volumes which are processed and the relatively rapid saturation of adsorption sites, the error in estimating total suspended load by Nuclepore filtration must be less than that for POC. For example only 1/2 to one liter of water is filtered for POC while 4 to 25 are filtered for total suspended load. In addition, total suspended load numbers generated by our method using Nuclepore filters have a high level of precision, 10 μg/l.

What numbers are reliable then? Best numbers are inorganic content, calcium carbonate, magnesium, and the trace metals expressed as weight per volume of filtered water. Total suspended load from Nuclepore filters also appears to be reliable. Adsorption of organics may of course also affect some trace metal values in that the partitioning of components between particulate and dissolved constituents may not be clear. Possible adsorption of dissolved nitrogen has not been formally assessed although low blank values (2nd filter) suggest that PON may be a more reliable estimate of organic content than POC.

We consider POC numbers generated in this study, like those in the literature, to be seriously in error. Therefore, these data will not be included. Although the generation of total inorganic content values by processing them through a low temperature asher is a potentially viable procedure, we only had 1/2 a Millipore pad available. Microscopic examination of the pads shows that matter is not distributed evenly on the pads but is patchy. Therefore these data included as Appendix 2E are also suspect.

CONCLUSIONS

1. Total suspended load values in all seasons decrease seaward. Highest values are associated with low salinity water (<33‰). During February-March higher suspended particulate loads extend farther out onto the shelf than at other seasons, probably because of winter storms combined with relatively high run-off.
2. During summer and fall high salinity water which was low in suspended particulates extended over large portions of the shelf.

Total suspended load estimates for the whole region are highest during the winter (1.77×10^6 metric tons), slightly lower during the summer (1.71×10^6 metric tons), and considerably lower during spring (0.72×10^6 metric tons) and fall (0.83×10^6 metric tons). Some of the disparity may be due to the fact that fewer inshore stations, expected to be relatively high in suspended load, were sampled in the spring and fall. However, these trends also hold for slope waters as well as shelf waters, suggesting that at least part of the trend is real.

3. Despite the fact that the continental margin had been subjected to an extreme winter, suspended particulate values for the February-March and August cruises were about the same. Similarity may result from quick relaxation and return to normal loads after storms in combination with small amounts of fines available for resuspension.
4. Calcium carbonate percentages were lowest inshore, where they were masked by high terrigenous content and were higher in more saline, cleaner shelf and Florida Current waters.
5. Estimates of standing crop of calcium carbonate were highest during the February-March cruise (17.3×10^4 metric tons), compared to (5.9×10^4 metric tons) in June, (9.5×10^4 metric tons) in August and (8.5×10^4 metric tons) in November. A large portion of the total calcium carbonate in the winter was found in shelf waters (12.0×10^4 metric tons). This high value indicates that resuspension of calcium carbonate from shelf bottom sediment may have been occurring.
6. Other than the winter values, the calcium carbonate crop remained relatively stable over the southeastern margin throughout the

seasons.

7. Coccoliths appear to be relatively most abundant during the May period.
8. Because of the thick, overlying water column combined with a relatively small surface area, the continental slope has a higher potential sedimentation rate than does the adjacent shelf.
9. Kaolinite dominates the clay mineral suite of the suspended sediments and of rivers rising in the Piedmont, while smectite is more important in shelf and Coastal Plain sediments. A mixed suite is found in slope sediments. These relationships suggest that river-borne fines are escaping from the estuaries, are passing over the shelf and reaching the slope system.
10. The continental slope is a potential sink for pollutants on some margins. On the southeastern U.S. continental margin, most fines and therefore most pollutants carried over the shelf will become entrained in the Florida Current.
11. We conclude that particulate organic carbon values generated by filtration through glass fiber filters and through silver filters are seriously in error. We strongly recommend that analysis of POC using the method of filtration through glass fiber filters or silver filters be discontinued and that alternate methods be investigated and developed. We further recommend that total inorganic content be determined rather than total organic content, which is also seriously suspect. Calcium should be measured using atomic absorption technique and $CaCO_3$ then expressed in µg/l, rather than % total suspended load. Nuclepore filters appear to be the best membrane for the determination of total suspended load.

LITERATURE CITED

Betzer, P.R., 1977. MAFLA final report, 1975-1976: BLM.

Chester, R. and Hughs, M.J., 1967. A chemical technique for the separation of ferro-manganese minerals, carbonate minerals, and adsorbed trace elements from pelagic sediments: Chemical Geology, vol. 2, pp. 249-262.

Doyle, L.J., Pilkey, O.H., and Woo, C.C., 1978. Sedimentary framework of the Eastern United States continental slope: Proceedings of joint SEPM/AAPG Slope Symposium, Oklahoma City, Oklahoma (in press).

Duursma, E.K., Dissolved organic carbon, nitrogen, and phosphorous in the sea: Netherlands Journal of Marine Research, vol. 1, 148 p.

Emery, K.O., and Uchupi, E., 1972. Western NorthAtlantic Ocean: America Assoc. Petroleum Geologist Memoir, 17, 532 p.

Knauer, G., 1977. MAFLA final report, 1975-1976: BLM.

Lal, D., 1977. The oceanic microcosm of particles: Science, vol. 198, pp. 997-1009.

Manheim, F.T., Meade, R.H., and Bond, G., 1970. Suspended matter in surface waters of the Atlantic continental marginfrom Cape Cod to the Florida Keys: Science, vol. 167, pp. 71-376.

Menzel, D.W., 1966. Bubbling of sea water and the production of organic particles: a re-evaluation: Deep-sea Research, vol. 13, pp. 963-966.

Menzel, D.W., 1974. Primary productivity, dissolved and particulate organic matter, and the sites of oxidation of organic matter, in The Sea, vol. IV, Edward D. Goldberg, ed., Wiley Interscience, New York, pp. 657-678.

Peavear, D.R., 1968. Clay mineral relationships in recent river nearshore marine, and continental slope sediments of the southeastern United States: PhD dissertation, University of Montana, 164 p.

Quinn, J.G., and Meyers, P.A., 1971. Retention of dissolved organic acids in seawater by various filters: Limn. and Ocean, vol. 16, pp. 129-131.

Riley, G.A., 1970. Particulate organic matter in sea water: Advances in Marine Biology, F.S. Russell and M. Yonge, eds., Academic Press, New York, vol. 8, pp. 1-118.

Robertson, D.E., 1972. Ultrapurity methods and techniques: M. Zeif and R. Speights eds., Marcel Dekker, New York, pp. 207-253.

Rodolfo, K.S., Buss, B.A., and Pilkey, O.H. Suspended sediment increase due to hurricane Gerda in continental shelf waters off Cape Lookout, North Carolina: Jour. Sed. Petrology, vol. 41, pp. 1121-1125.

Spencer, D.W., and Manheimm, F.T., 1969. Ash content and composition of Millipore HA filters: U.S. Geological Survey Professional Paper 650-D, pp. D288-D290.

CHAPTER 3

TURBIDITY IN THE SOUTHEAST GEORGIA EMBAYMENT

Michael H. Bothner[1]

---

[1] U. S. Geological Survey, Woods Hole, Massachusetts 02543

Chapter 3

Table of Contents

Page

Abstract. 3- 1

Introduction. 3- 1

Methods 3- 2

Results 3- 4

  March 1977. . . . . 3- 4

  June 1977 . . . . 3- 8

  August 1977 3-10

  November 1977 3-15

Summary 3-20

Literature Cited. 3-22

CHAPTER 3

TURBIDITY IN THE SOUTHEAST GEORGIA EMBAYMENT

Michael H. Bothner

ABSTRACT

Transmissometer profiles indicate that a surface or near-surface turbidity maximum is a persistent feature during the March, June and August sampling periods. This feature is typically 5-15 m thick and is related to higher concentrations of planktonic organisms. Resuspension of botom sediment, indicated by increasing turbidity near the bottom was commonly observed at stations closest to shore during each cruise. Areas of resuspension were also observed at stations on the middle shelf and at the shelf edge, although not consistently on each cruise.

The correlation coefficient between suspended matter concentration and light attenuation is generally >.7 for bottom water. Poorer correlations with data from surface and mid-depths may be related to greater differences in the composition of seston and dissolved organics and their effect on light transmission.

INTRODUCTION

The use of transmissometers in seston studies on the continental shelf off the Eastern United States provides qualitative information on the distribution of suspended particulate matter in the water column while at sea. This information permits the selection of major turbidity features in the water column for precise sampling.

The major features typically include a turbidity maximum in the pycnocline due to a higher standing stock of phytoplankton. Another interesting and important feature often found in the transmissometer profiles is an increase in turbidity as the instrument nears the water sediment interface. This increase in turbidity indicates higher concentrations of suspended material in the near-bottom water, in most cases due to active resuspension of bottom sediment. The occurrence of bottom sediment in suspension is significant to the general study of bottom sediment transport since suspended material can be transported by even gentle currents.

The beam transmissometer is a qualitative tool because the attenuation of light in water is affected by a number of independent factors. These include both the concentration and composition of suspended matter, and the concentration and nature of dissolved organic materials. Because these factors are often different in surface and bottom waters and in different water masses at the same depth, a good relationship between optical properties and suspended matter concentration is typically found only in restricted regions or depths where the composition of material and the level of dissolved organics are fairly uniform. The interpretation of the transmissometer profiles (and, thus, the suspended matter distributions) is improved when the transmissometer profiles are calibrated against analytically derived suspended matter data. In our studies, collection and analyses of the composition and concentration of suspended matter for calibration of the transmissometers were performed under the direction of Dr. Larry J. Doyle, University of South Florida, St. Petersburg, Florida.

METHODS

A transmissometer manufactured by Montedoro Whitney, Inc., San Luis Obispo, California, was used in this study to measure turbidity throughout the water column. The unit monitors transmission of white light with highest sensitivity at a wavelength of about 550 nm. It has a folded 1 m path length, and is powered by internal batteries. The instrument is capable of recording data internally and, with the proper interfacing, the data can be observed on deck in real time.

The instrument measures relative light transmission throughout the water column. To calculate the percent transmission, a value of transmission in sea water without suspended matter (I_o) is necessary. This value was estimated from transmission levels at depth in the Gulf Stream where suspended matter values were typically less than 50 $\mu g/l$. Extrapolation of the slope between extinction coefficient ($\alpha = \ln I_o/I$) and suspended matter concentration yielded the calculated value of light transmission in sea water having zero suspended matter. This definition of I_o includes the effect of dissolved organic matter. The value of I_o was found to vary somewhat during the cruise perhaps due to different concentrations of dissolved organics in the various water masses sampled. In addition, each replacement of the light source or optical prism resulted in a new I_o. Extinction coefficients generally are linearly related to the concentration of suspended matter for a water mass having suspended matter of similar composition and the same background of dissolved materials.

Areas of active resuspension were identified on the basis of increasing turbidity as the instrument approached the water-sediment interface. This technique excludes areas that may have significant amounts of resuspended sediment in bottom waters but show a uniform profile of low turbidity because resuspension processes are inactive at the time of sampling.

RESULTS

March 1977

During the March cruise the transmissometer was used in conjunction with a deck readout system which gave turbidity information in real time and permitted selection of suspended matter samples at depths of interesting turbidity trends. In addition, the deck readout provided a constant check on the operation of the transmissometer. Minor instrumental problems developed during the cruise resulting in some lost data, but these were corrected by Martin Peacock, University of South Florida, who was key operator of the system.

The relationship between the extinction coefficient (α) and the concentration of suspended matter were plotted for surface and mid-depth samples together (Figure 3-1). This was done because both depths contain predominately biogenic material. The correlation coefficient is only 0.43 which perhaps reflects a difference in composition of suspended matter (differences in species of phytoplankton) or differences in the amounts of dissolved organic matter. Transmissometer profiles showed layers of high turbidity generally less than 15 meters thick in surface and near surface waters at almost every station (Figure 3-2). These features are undoubtedly related to higher phytoplankton concentrations. Tabulation of extinction coefficients and concentrations of total suspended matter are presented in Appendix 3-A on microfiche at the rear of this volume.

The transmissometer depth profiles were examined to identify areas where turbidity increases as the instrument approached the water sediment interface (Figure 3-3). Such increases are thought to indicate areas of active sediment resuspension at the time of sampling. The correlation coefficient between and particulate concentrations is

Figure 3-1. Plot of total suspended matter concentration (mg/l) against extinction coefficient at the same depth. Equation of least squares regression line $Y = 988X = 21$, $r^2 = 0.43$ (*X and Y values divided by 2 to facilitate plotting).

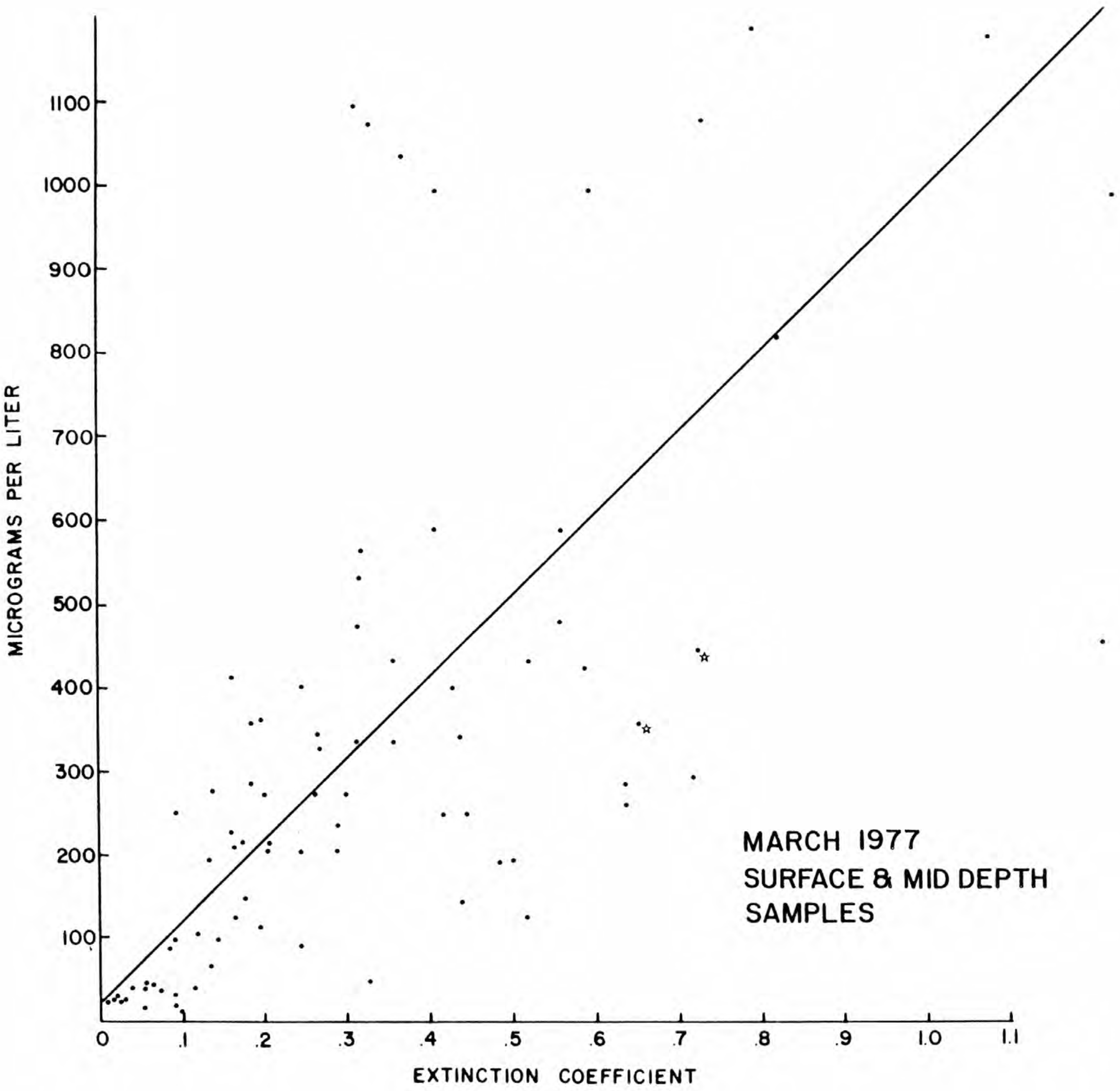
MICROGRAMS PER LITER
1100
1000
900
800
700
600
500
400
300
200
100
0
.1
.2
.3
.4
.5
.6
.7
.8
.9
1.0
1.1
EXTINCTION COEFFICIENT
MARCH 1977
SURFACE & MID DEPTH
SAMPLES

Figure 3-1

Figure 3-2. Occurrence of turbidity increases in surface or near-surface waters.

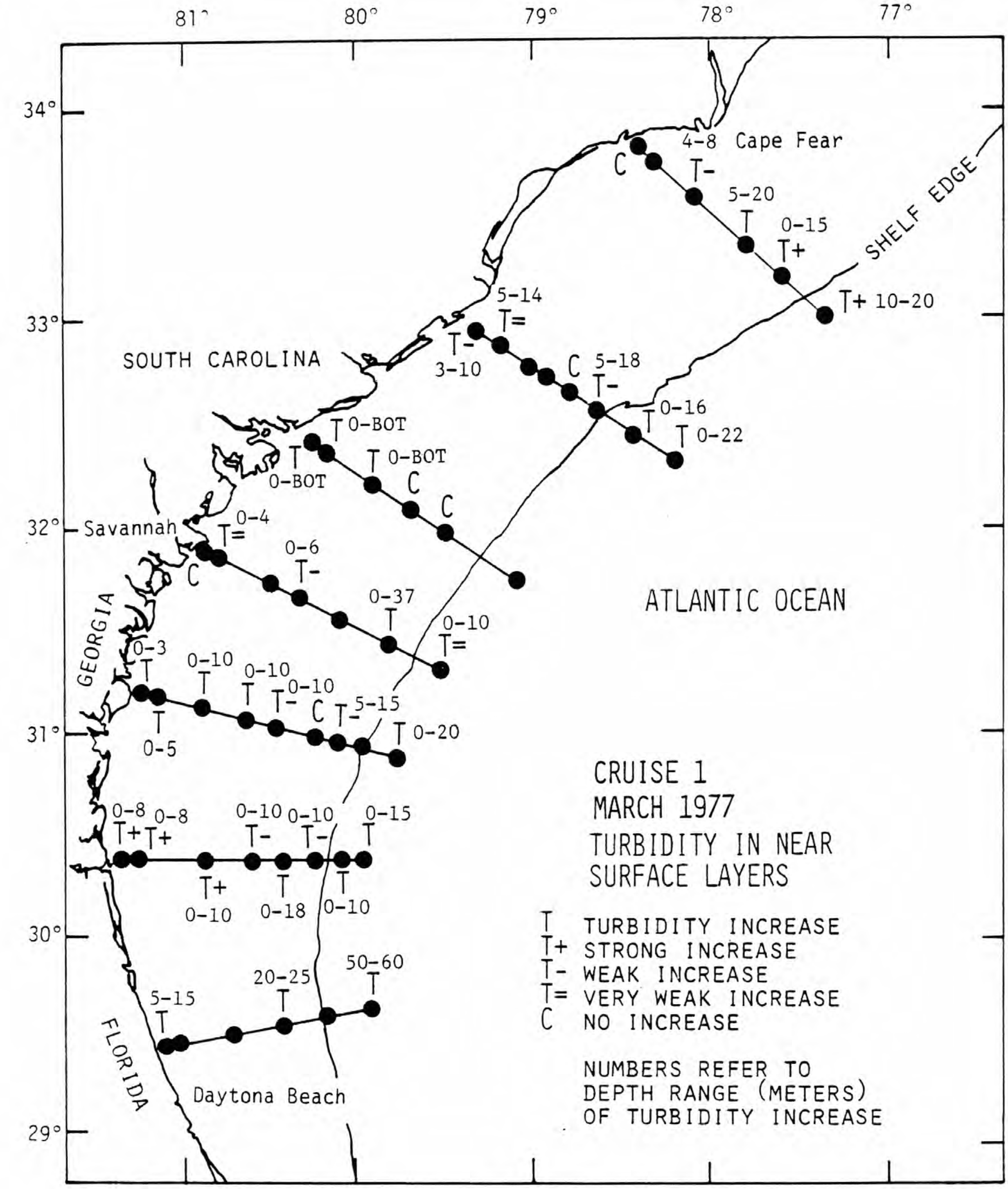
81°
80°
79°
78°
77°
34°
33°
32°
31°
30°
29°
Cape Fear
SHELF EDGE
SOUTH CAROLINA
Savannah
GEORGIA
FLORIDA
Daytona Beach
ATLANTIC OCEAN
C
4-8
T-
5-20
T
0-15
T+
T+ 10-20
5-14
T=
T-
3-10
C 5-18
T-
T 0-16
T 0-22
T 0-BOT
T
0-BOT
T 0-BOT
C
C
0-4
T=
C
0-6
T-
0-37
T
0-10
T=
0-3
T
0-10
T
0-10
T
0-10
T-
C
5-15
T-
T 0-20
T
0-5
0-8
T+
0-8
T+
0-10
T-
0-10
T-
0-15
T
T+
0-10
T
0-18
T
0-10
5-15
T
20-25
T
50-60
T
CRUISE 1
MARCH 1977
TURBIDITY IN NEAR SURFACE LAYERS
T TURBIDITY INCREASE
T+ STRONG INCREASE
T- WEAK INCREASE
T= VERY WEAK INCREASE
C NO INCREASE
NUMBERS REFER TO DEPTH RANGE (METERS) OF TURBIDITY INCREASE

Figure 3-3. Occurrence of increasing turbidity in bottom waters as the transmissometer approaches the water sediment interface.

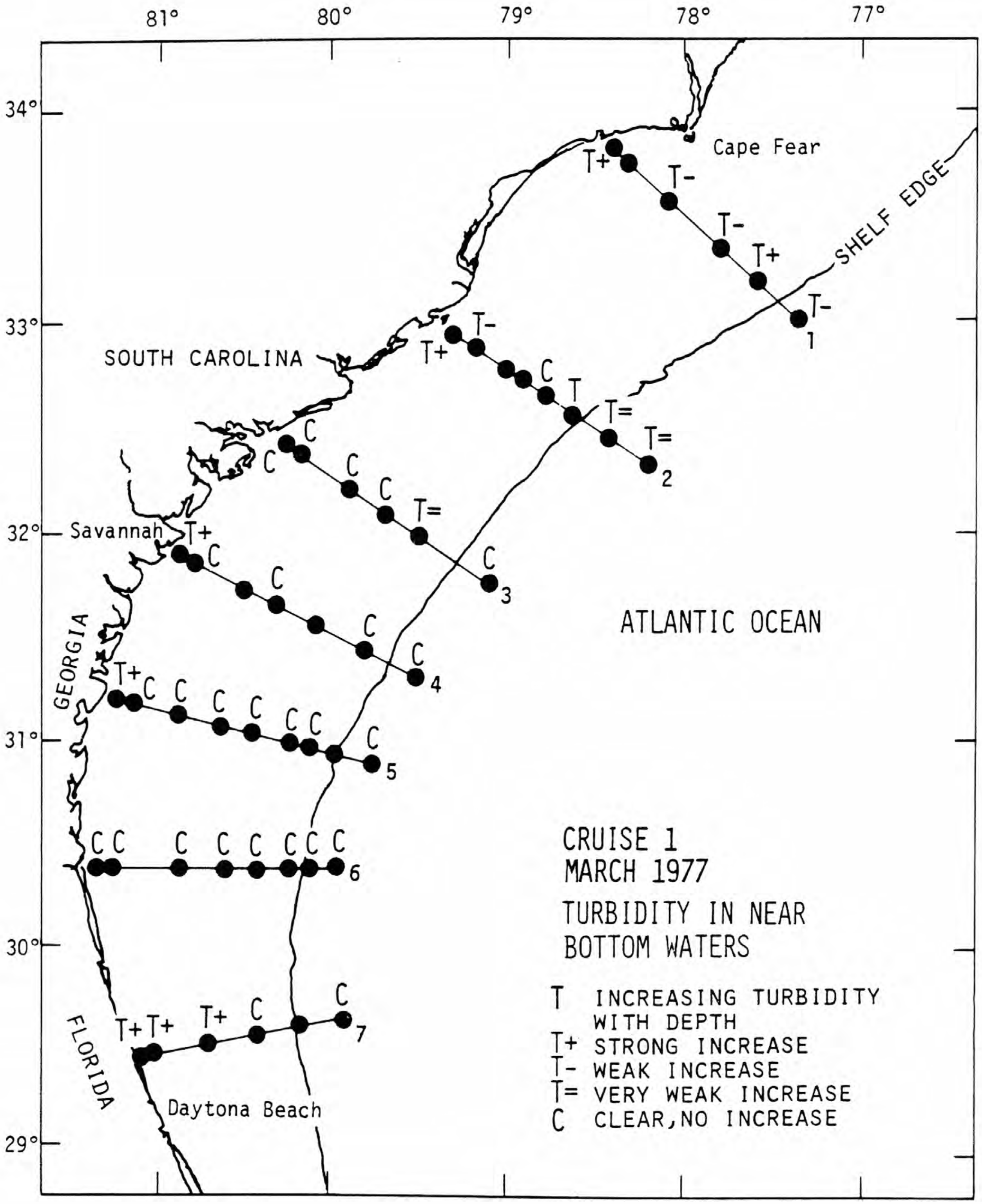
81°
80°
79°
78°
77°
34°
33°
32°
31°
30°
29°
Cape Fear
SHELF EDGE
SOUTH CAROLINA
Savannah
GEORGIA
FLORIDA
Daytona Beach
ATLANTIC OCEAN
1
2
3
4
5
6
7
CRUISE 1
MARCH 1977
TURBIDITY IN NEAR BOTTOM WATERS
T INCREASING TURBIDITY WITH DEPTH
T+ STRONG INCREASE
T- WEAK INCREASE
T= VERY WEAK INCREASE
C CLEAR, NO INCREASE

0.77 for bottom waters (Figure 3-4), which suggests a narrower compositional range with respect to transmission of light.

During the March cruise, increasing turbidity in near-bottom waters was observed at all stations across the shelf in the northern-most transect and at all but the mid-shelf stations in transect #2. Largest increases in turbidity were observed in the nearshore bottom waters and to some distance seaward in the southern-most transect. The bottom turbidity increase along the shore line is undoubtedly related to wave-generated turbulence and possibly to longshore currents. In addition to a high energy environment, the nearshore areas have finer surficial sediment (fine sand) than offshore areas (Pilkey _et al_, this volume), which may increase the effectiveness in resuspending sediments.

The explanation of the persistent bottom turbidity throughout the northern two transects awaits examination of the hydrographic data. Surficial sediments in this area are typically medium to coarse sand (Pilkey 1978).

There is a noticeable absence of a turbid bottom layer on the mid-shelf south of transect 2. This is similar to the pattern observed in the Baltimore Canyon Trough during much of the year (Milliman _et al_ 1978). The absence of the turbid bottom layer south of transect 3 at the shelf edge, however, is different from shelf edge areas of the Baltimore Canyon Trough where resuspension was a persistent feature during all seasons--possibly caused by internal waves and tides and/or by excursions of the front between shelf and slope water.

June 1977

The deck readout for transmissometer data was again available for the second cruise permitting examination of the turbidity profile in real time. A considerable amount of instrumental drift was encountered

Figure 3-4. Plot of total suspended matter concentration (mg/l) against extinction coefficient at the same depth. Equation of least squares regression line Y = 1,009X - 10, r^2 = 0.77 (*X and Y values divided by 2 to facilitate plotting).

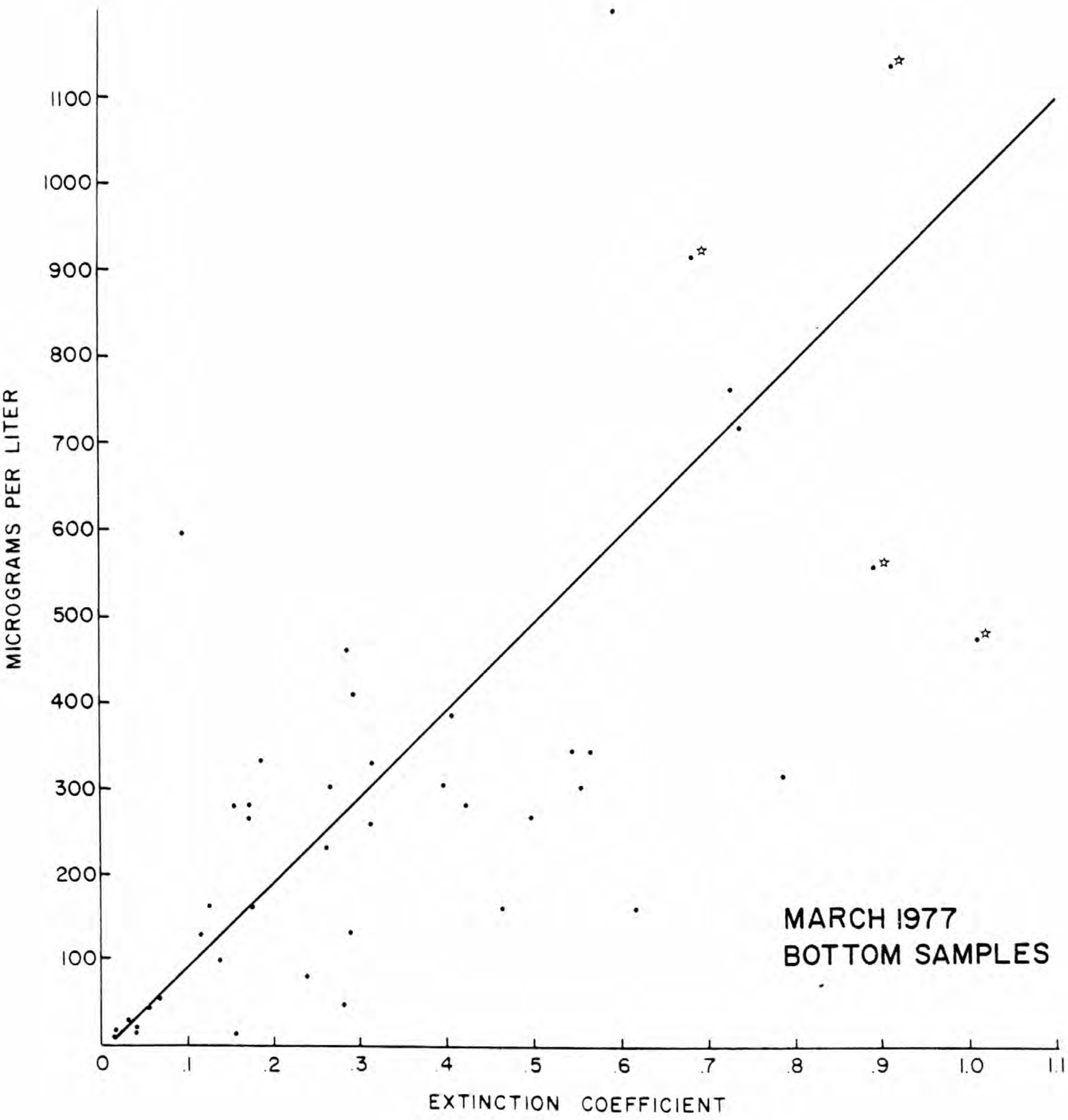
1100
1000
900
800
700
600
500
400
300
200
100
MICROGRAMS PER LITER
0
.1
.2
.3
.4
.5
.6
.7
.8
.9
1.0
1.1
EXTINCTION COEFFICIENT
MARCH 1977
BOTTOM SAMPLES

throughout the cruise. For any given station, the major features in the turbidity profiles were easily recognizable, but the instrumentation drift caused an offset in transmission values between the down and up cast. The relationship between α and the suspended matter concentration (Figure 3-5) shows considerable scatter for surface and mid-depth samples. Layers of high turbidity were observed at the surface at most nearshore and mid-shelf stations and at greater depth at or beyond the shelf edge (Figure 3-6). Perhaps due to higher consistency in the composition of the bottom suspended matter a somewhat improved relationship is observed between and total suspended matter in the near-bottom samples (Figure 3-7). Transmissometer profiles showing increasing turbidity in near-bottom waters were obtained at the stations indicated in Figure 3-6. This feature was observed in the vicinity of the shelf edge in all transects and at nearshore stations in northern and southern areas.

August 1977

Following the second cruise an effort was made to interface the transmissometer data output with the Plessey CTD system. The change was implemented because the transmission data could then be easily integrated with CTD information and because the transmissometer operation would be greatly simplified.

Modification was made by the Plessey Instrument Co. in time for the third cruise. Unfortunately, the connector box which accepts the transmissometer signal cable leaked on the first station and, as a result, real time display of the data was lost, although the data were recorded internally. The first 18 stations were successfully taped and yielded clean data. Unfortunately, during a bench check after the 18th station, the major circuit board shorted out due to a faulty reader

Figure 3-5. Plot of total suspended matter concentration (mg/l) against extinction coefficient at the same depth. Equation of least squares regression line Y = 913x - 5, $r^2 = 0.60$. (*X and Y values divided by 2).

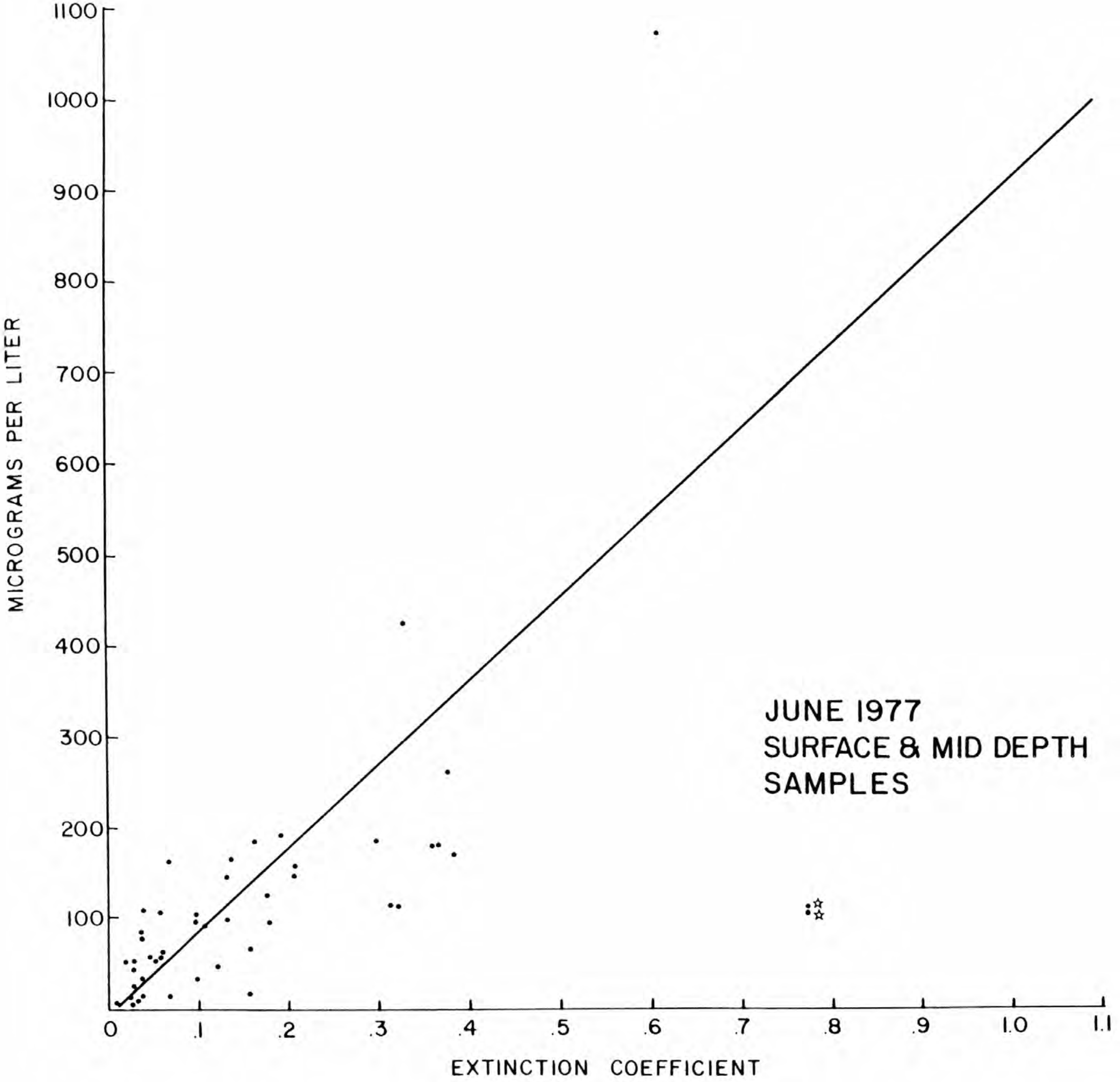

JUNE 1977
SURFACE & MID DEPTH
SAMPLES
MICROGRAMS PER LITER
1100
1000
900
800
700
600
500
400
300
200
100
EXTINCTION COEFFICIENT
0
.1
.2
.3
.4
.5
.6
.7
.8
.9
1.0
1.1

Figure 3-5

Figure 3-6. Occurrence of turbidity increases in surface or near-surface waters.

Figure 3-6

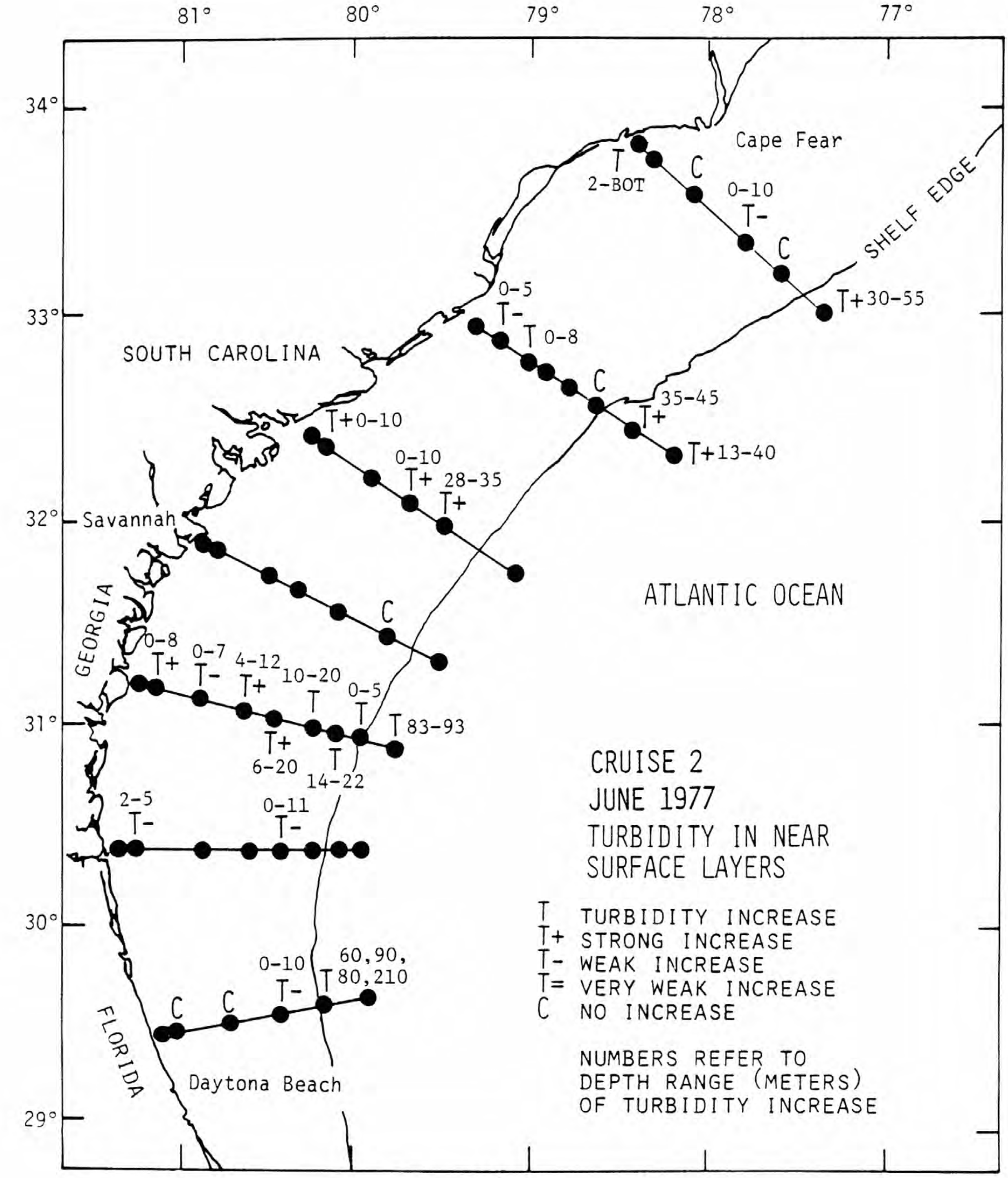
81°
80°
79°
78°
77°
34°
33°
32°
31°
30°
29°
Cape Fear
T
2-BOT
C
0-10
T-
C
SHELF EDGE
T+30-55
0-5
T-
T 0-8
C
35-45
T+
T+13-40
SOUTH CAROLINA
T+0-10
0-10
T+ 28-35
T+
Savannah
C
ATLANTIC OCEAN
GEORGIA
0-8
T+
0-7
T-
4-12
T+
10-20
T
0-5
T
T 83-93
T+
6-20
T
14-22
2-5
T-
0-11
T-
0-10
T-
60,90,
T 80,210
C
C
FLORIDA
Daytona Beach
CRUISE 2
JUNE 1977
TURBIDITY IN NEAR
SURFACE LAYERS
T TURBIDITY INCREASE
T+ STRONG INCREASE
T- WEAK INCREASE
T= VERY WEAK INCREASE
C NO INCREASE
NUMBERS REFER TO
DEPTH RANGE (METERS)
OF TURBIDITY INCREASE

Figure 3-7. Plot of total suspended matter concentration (mg/l) against extinction coefficient at the same depth. Equation of least squares regression line $Y = 634X + 17$, $r^2 = 0.70$ (*X and Y values divided by 2 to facilitate plotting).

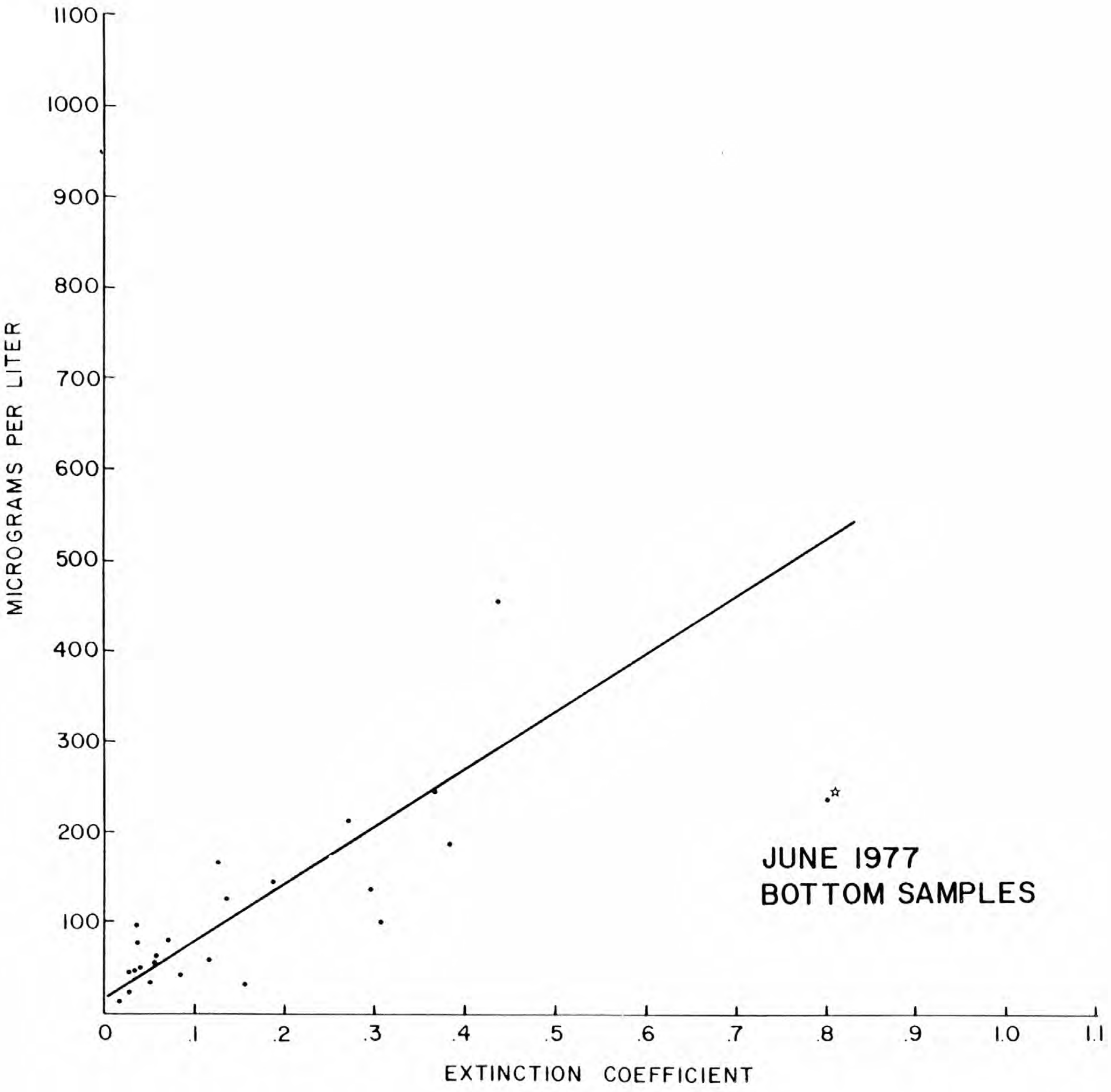
1100
1000
900
800
700
600
500
400
300
200
100
MICROGRAMS PER LITER
0
.1
.2
.3
.4
.5
.6
.7
.8
.9
1.0
1.1
EXTINCTION COEFFICIENT
JUNE 1977
BOTTOM SAMPLES

Figure 3-7

Figure 3-8. Occurrence of increasing turbidity in bottom waters as the transmissometer approaches the water sediment interface.

Figure 3-8

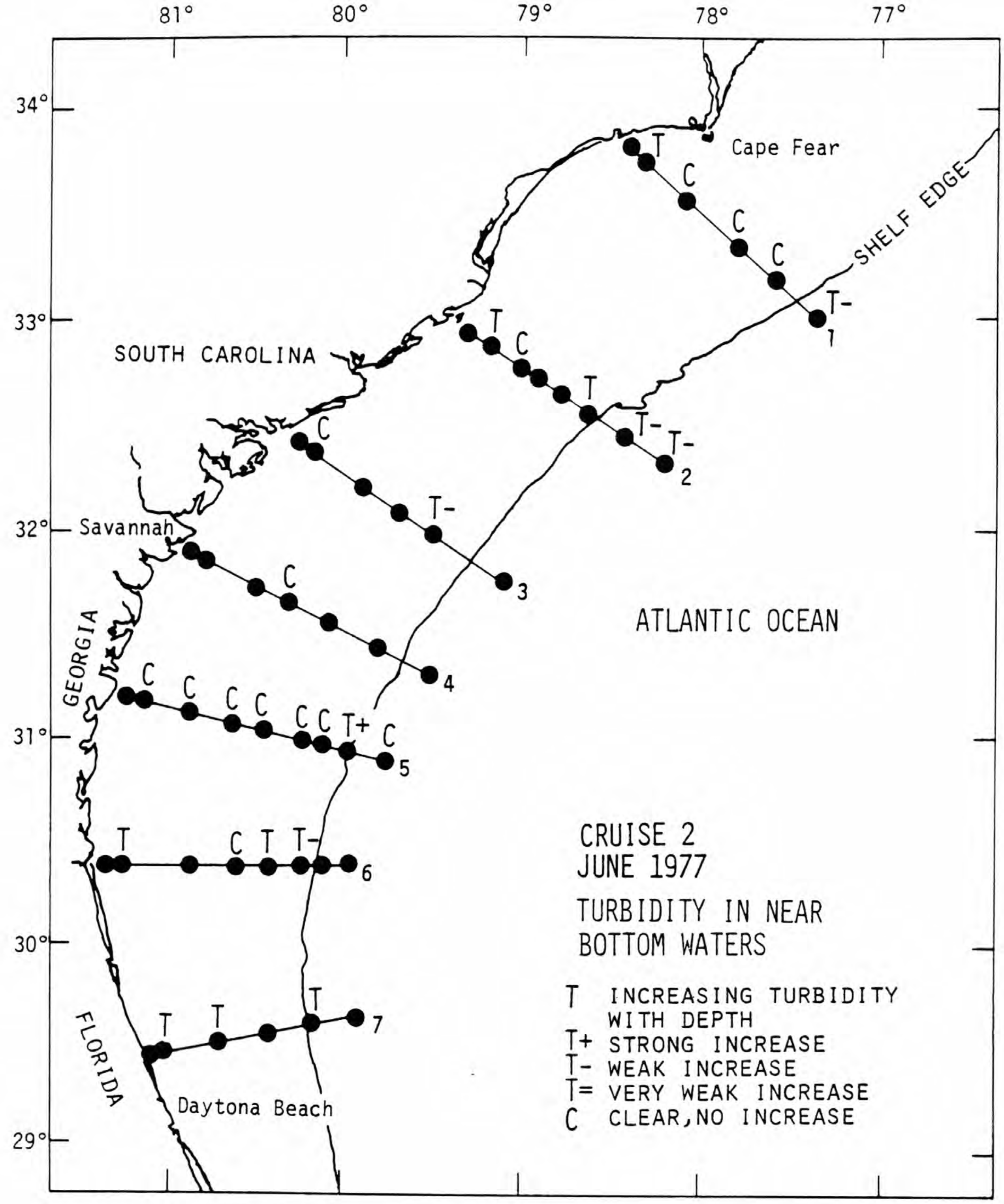
81°
80°
79°
78°
77°
34°
33°
32°
31°
30°
29°
Cape Fear
SHELF EDGE
SOUTH CAROLINA
Savannah
GEORGIA
FLORIDA
Daytona Beach
ATLANTIC OCEAN
1
2
3
4
5
6
7
T
C
T+
T-
CRUISE 2
JUNE 1977
TURBIDITY IN NEAR
BOTTOM WATERS
T INCREASING TURBIDITY WITH DEPTH
T+ STRONG INCREASE
T- WEAK INCREASE
T= VERY WEAK INCREASE
C CLEAR, NO INCREASE

card. Attempts to repair the instrument at sea were unsuccessful and tapes used after the short circuit contained no data.

For this cruise a strong linear relationship was observed between the calculated extinction coefficient and suspended matter concentration (Figures 3-9 and 3-10). The available data was collected only from the three northern transects which may have limited the compositional variability of the suspended matter. Transmissometer profiles in most cases showed a turbidity high in the surface waters, typically 5-10 m thick (Figure 3-11), and undoubtedly related to biological productivity. Increasing turbidity in near-bottom waters was observed in the mid-shelf area of transect 1 and in the mid- and inner-shelf areas of transect 3 (Figure 3-12).

November 1977

The leaking connector box had been replaced since the previous cruise and again the transmissometer was to be channelled through the Plessey CTD fish recorder and deck readout. Collection of transmissometer data during the 4th cruise, however, was plagued by two new equipment problems. First, the transmissometer signal did not stimulate the expected response from the analog recorded on deck during bench checks of the instrument. Because of problems in processing the CTD data, it is not known at this time if good data was recorded on the Plessey tape in spite of problems with the analog output. The second problem was related to the tape recorder housed inside the transmissometer which worked only sporadically during the cruise. Of the 27 stations for which tapes were collected, 11 were of poor quality and the remainder were unreadable due to noise. All the tapes have been returned to the manufacturer to see if more sophisticated tape reading equipment can retrieve the data.

Figure 3-9. Plot of total suspended matter concentration (mg/l) against extinction coefficient at the same depth. Equation of least squares regression line $Y = 822X + 47$, $r^2 = 0.64$.

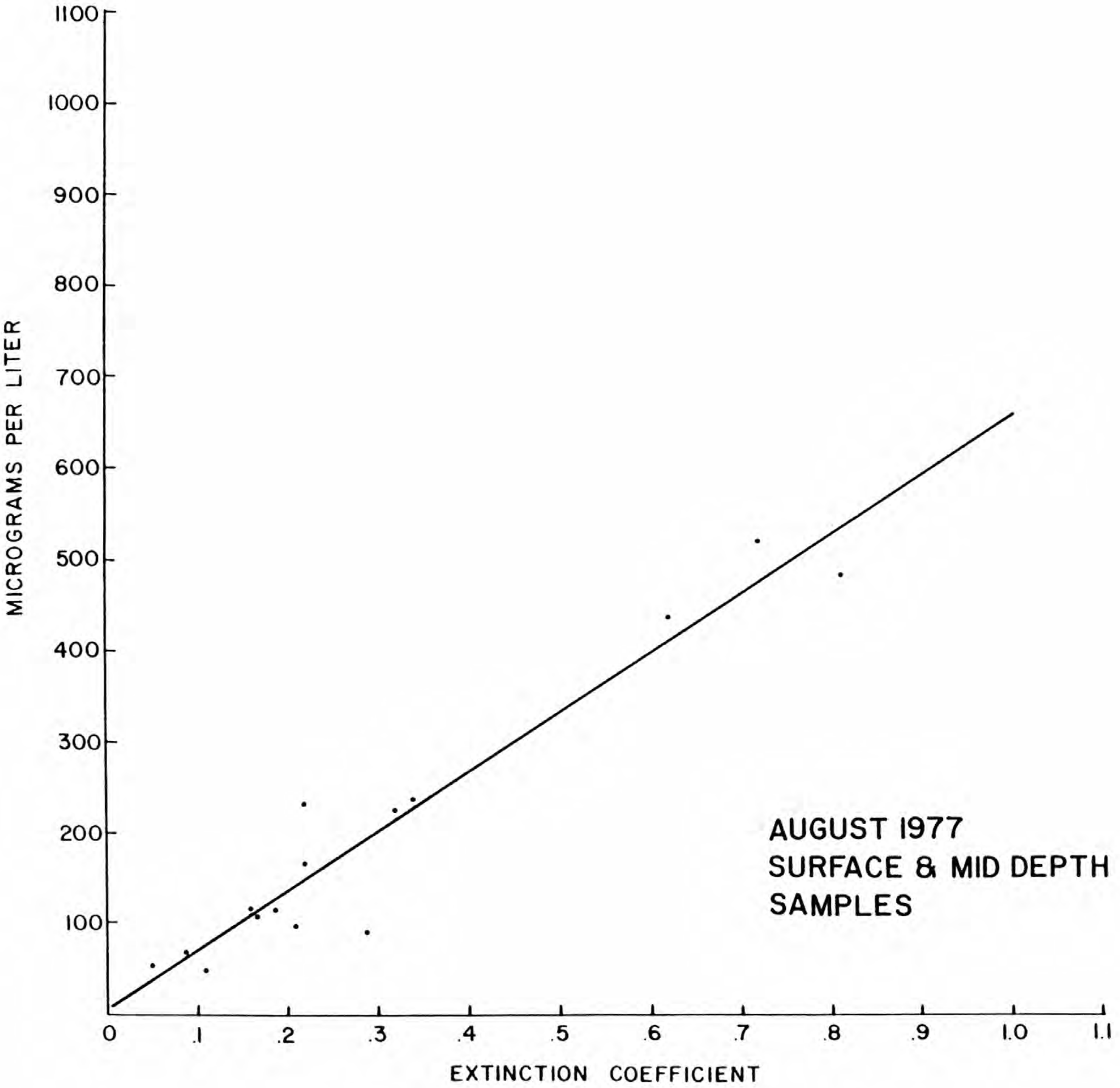

AUGUST 1977
SURFACE & MID DEPTH
SAMPLES

Figure 3-9

Figure 3-10. Plot of total suspended matter concentration (mg/l) against extinction coefficient at the same depth. Equation of least squares regression line $Y = 609X + 36$, $r^2 = 0.71$.

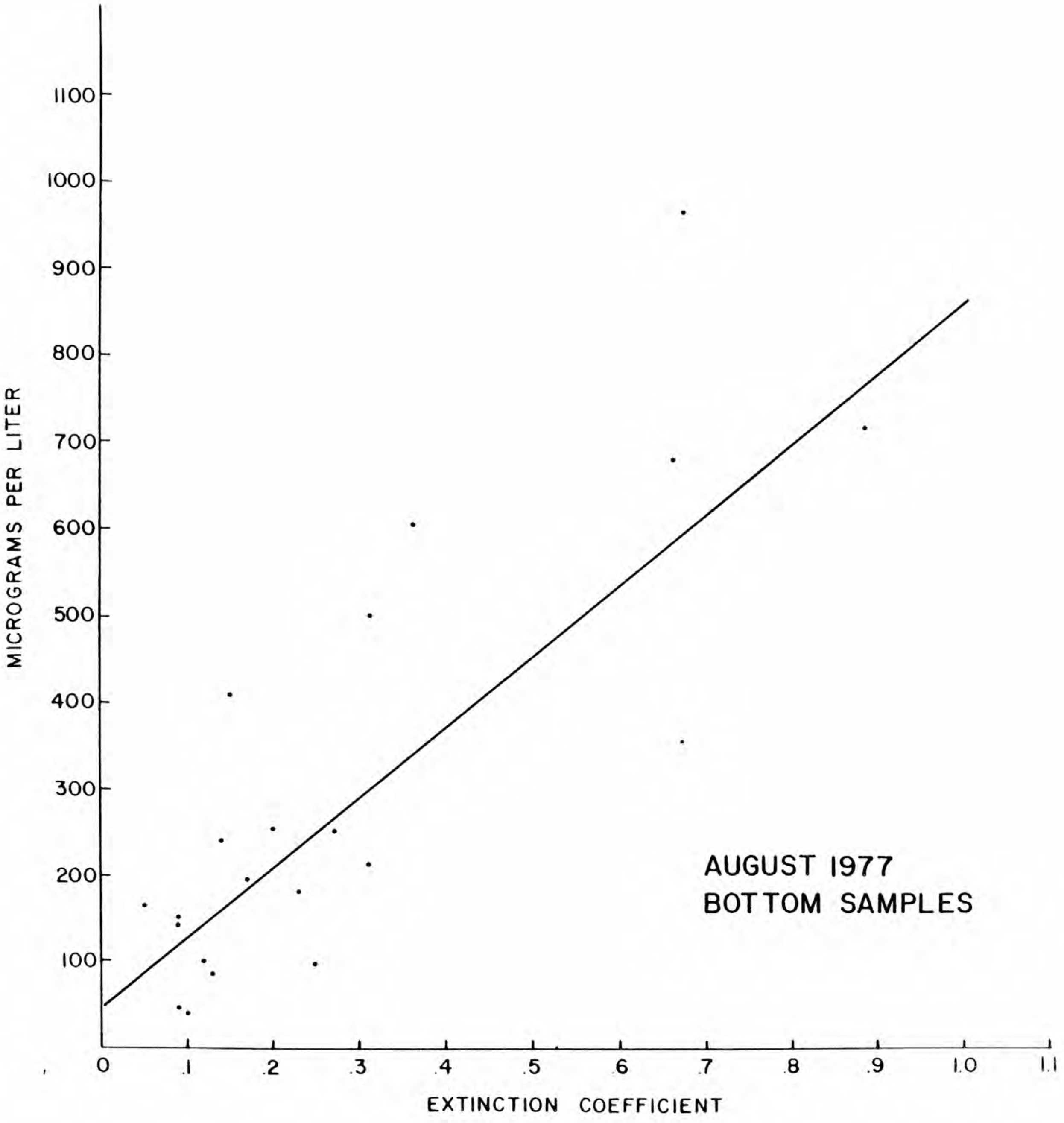
1100
1000
900
800
700
600
500
400
300
200
100
MICROGRAMS PER LITER
0
.1
.2
.3
.4
.5
.6
.7
.8
.9
1.0
1.1
EXTINCTION COEFFICIENT
AUGUST 1977
BOTTOM SAMPLES

Figure 3-10

Figure 3-11. Occurrence of turbidity increases in surface or near-surface waters.

Figure 3-11

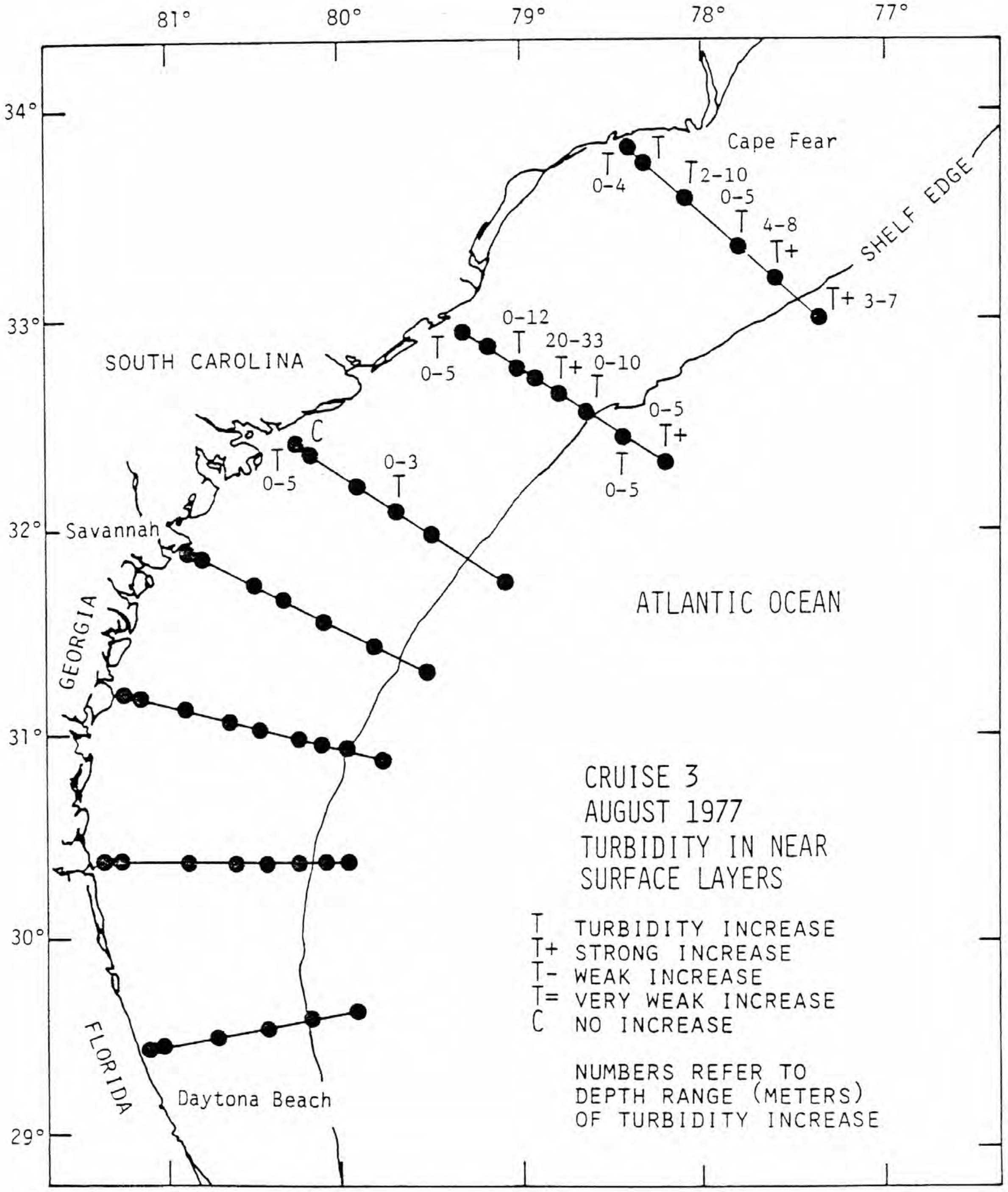
81°
80°
79°
78°
77°
34°
33°
32°
31°
30°
29°
Cape Fear
SHELF EDGE
SOUTH CAROLINA
Savannah
GEORGIA
FLORIDA
Daytona Beach
ATLANTIC OCEAN
T
T
0-4
T 2-10
0-5
T
4-8
T+
T+ 3-7
0-12
T
T
0-5
20-33
T+
0-10
T
0-5
T+
T
0-5
C
T
0-5
0-3
T
CRUISE 3
AUGUST 1977
TURBIDITY IN NEAR
SURFACE LAYERS
T TURBIDITY INCREASE
T+ STRONG INCREASE
T- WEAK INCREASE
T= VERY WEAK INCREASE
C NO INCREASE
NUMBERS REFER TO
DEPTH RANGE (METERS)
OF TURBIDITY INCREASE

Figure 3-12. Occurrence of increasing turbidity in bottom waters as the transmissometer approaches the water sediment interface.

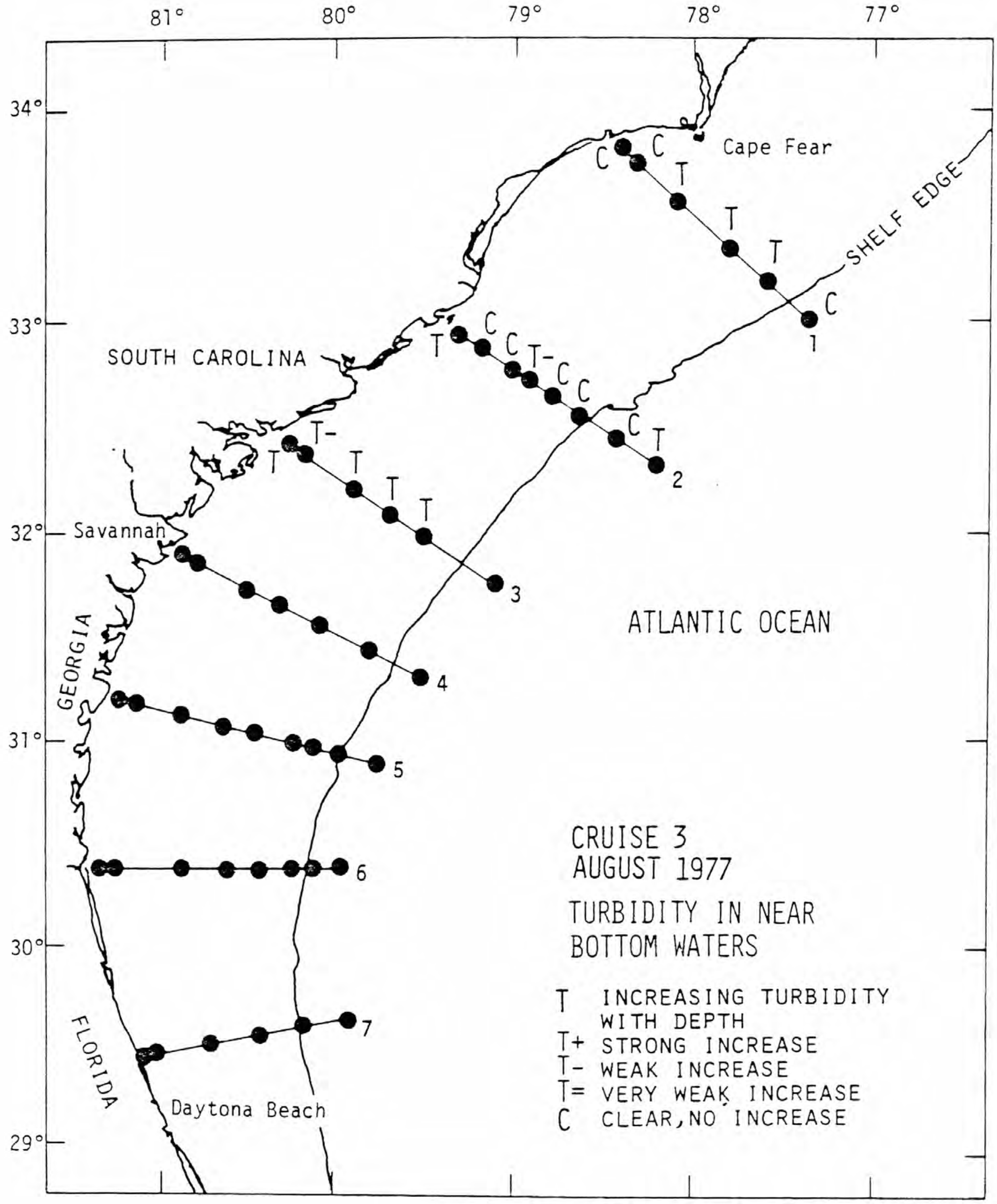
81°
80°
79°
78°
77°
34°
33°
32°
31°
30°
29°
Cape Fear
SHELF EDGE
SOUTH CAROLINA
Savannah
GEORGIA
FLORIDA
Daytona Beach
ATLANTIC OCEAN
1
2
3
4
5
6
7
C
T
T-
T=
T+

CRUISE 3
AUGUST 1977

TURBIDITY IN NEAR BOTTOM WATERS

T INCREASING TURBIDITY WITH DEPTH
T+ STRONG INCREASE
T- WEAK INCREASE
T= VERY WEAK INCREASE
C CLEAR, NO INCREASE

SUMMARY

Transmissometer data displayed on the deck contributes to the study of seston in coastal waters by giving a qualitative distribution of suspended matter concentrations with depth in real time. Maximums and minimums in the water column can then be precisely sampled and examined later with a variety of laboratory techniques to determine the composition and origin of suspended matter making up these features. The instrumental components facilitating the direct display of transmissometer data in real time were in operation during the first and second cruises. During the third and fourth cruises the transmissometer data was to be read on deck and recorded with the Plessey CTD system, but due to various instrumental failures transmission data in real time was not available.

Transmissometer profiles indicate that a surface or near surface turbidity maxima is a persistent feature during the March, June, and August sampling periods. This feature is typically 5-15 m thick and is related to higher concentrations of planktonic organisms.

The turbidity in near-bottom waters was found to correlate fairly well with suspended matter concentrations (correlation coefficients >.7). The increasing turbidity observed in bottom waters as the instrument approached the water sediment interface thus indicates increasing suspended matter concentrations, probably caused by active resuspension of bottom sediments. The occurrence of bottom sediment in suspension has implications to the study of bottom sediment transport because material in suspension will be easily transported even with gentle bottom currents.

Evidence of bottom sediment resuspension was commonly observed at stations closest to shore. In this area the processes responsible are turbulence due to waves and, perhaps, longshore currents in shallow water. In addition to a higher energy environment, the nearshore areas have finer surficial sediment than offshore areas which may increase the effectiveness of turbulence in resuspending bottom sediment.

The pattern of increasing turbidity in near-bottom waters for offshore stations varies for each cruise. Mid-shelf stations in the northern most transects (#1) show increasing turbidity in the bottom water during March and August cruises, and do not show it during the other cruises (although data is incomplete). In March, resuspension was indicated near the shelf edge in only the northern 3 transects while, in June, increasing turbidity in bottom water was observed near the shelf edge in all transects for which data are available. In the mid-shelf areas south of transect #2, most stations, during the first two cruises, are characterized by an unchanging transmission profile near the bottom, although there are a few exceptions.

The causes of sediment resuspension in the middle and outer shelf are subject to speculation. Some of the possible causes are excursions of the Gulf Stream onto the shelf, internal waves and tides, and the activities of benthic macro fauna. The frequency of events leading to resuspension is also unknown for this area but will be better defined with USGS tripod observations. Although these differences in the areas of resuspension were observed between seasonal cruises, it is doubtful that the major processes responsible are strictly controlled by seasons. There is evidence in the Baltimore Canyon Trough area that some events causing resuspension have a period of about 14 hours (Milliman _et al_ 1978).

The data obtained in the first year of study have identified areas of active sediment resuspension. This information will be useful in planning future work necessary to document the processes responsible for resuspension, their frequency of occurrence, and the magnitude of their effect in transporting bottom sediment.

LITERATURE CITED

Milliman, John D., Michael H. Bothner, and Carol M. Parmenter. 1978. Seston in Middle Atlantic Shelf and slope waters, 1976-1977 in U.S. Geological Survey Mid-Atlantic OCS Environmental Assessment, Final Report for the period 1 July 1976-30 June 1978, prepared for the Bureau of Land Management, in press.

Pilkey, Orrin H., Fred Keer, and Stephanie Keer, 1978. Surficial sediment of the U.S. Atlantic Southeastern United States Continental Shelf 1976-1977 in Final Report for the period 1 October 1976 - 30 September 1977. Geologic Studies, South Atlantic OCS Environmental Assessment, in press.

CHAPTER 4

BOTTOM CURRENTS AND BOTTOM SEDIMENT MOBILITY IN THE OFFSHORE SOUTHEAST GEORGIA EMBAYMENT

PART I

AN INSTRUMENT SYSTEM FOR LONG-TERM SEDIMENT TRANSPORT STUDIES ON THE CONTINENTAL SHELF

Bradford Butman[1] and David W. Folger[1]

PART II

OBSERVATIONS OF BOTTOM CURRENT AND BOTTOM SEDIMENT MOVEMENT IN THE SOUTHEAST GEORGIA EMBAYMENT, 1977

Bradford Butman[1] and Stephanie Pfirman[1]

[1] U. S. Geological Survey, Woods Hole, Massachusetts 02543

CHAPTER 4

Table of Contents

Page

PART I

Introduction. . . . . 4- I- 1

The Bottom Tripod Instrument System . . . . 4- I- 2

Sensors . . . . 4- I- 4

Current Speed and Direction . . . . 4- I- 4
Pressure. . . . . 4- I- 4
Turbidity . . . . 4- I- 6
Temperature . . . . 4- I- 7
Camera. . . . . 4- I- 7

Data Sampling Scheme. . . . . 4- I- 8

Electronics 4- I-14

Data Resolution and Accuracy. 4- I-14

Tripod Frame: Deployment and Recovery. 4- I-17

Data Processing and Quality Control 4- I-18

U. S. Geological Survey Sediment Transport Studies. 4- I-21

Examples of Observations. 4- I-24

Discussion. 4- I-30

Acknowledgments 4- I-33

Literature Cited. 4- I-33

PART II

Introduction. 4-II- 1

Field Program and Methods 4-II- 3

Results 4-II- 6

Bottom Currents 4-II- 6

Summer Bottom Sediment Movement 4-II-20

Summary and Conclusions 4-II-27

Acknowledgments 4-II-28

Literature Cited. 4-II-28

CHAPTER 4

BOTTOM CURRENTS AND BOTTOM SEDIMENT MOBILITY IN THE OFFSHORE SOUTHEAST GEORGIA EMBAYMENT

PART I

AN INSTRUMENT SYSTEM FOR LONG-TERM SEDIMENT TRANSPORT STUDIES ON THE CONTINENTAL SHELF

Bradford Butman and David W. Folger

INTRODUCTION

We have designed and built an instrument system to investigate processes of bottom sediment movement on the Continental Shelf. The system is intended for use in regional studies of sediment transport to determine the physical processes responsible for bottom movement and to estimate the frequency, direction, and rate of sediment transport. The system measures bottom current speed and direction, pressure, temperature, and light transmission and photographs the bottom. It consists of three major components: (1) sensors for current, pressure, temperature, light transmission, and bottom photography; (2) a data recording unit; and (3) a tripod frame to which the sensors and data recording unit are mounted for deployment.

Direct observations, acquired *in situ*, are necessary to determine the character, extent, and causes of sediment dispersal over different regions of the Continental Shelf. Measurements must resolve motions with broad time scales ranging from a few seconds for wave frequency processes to weeks and months for processes associated with meteorological and oceanic forcing. Observations must be made to assess seasonal variability and to document catastrophic events. The tripod mounted instrument package, referred to hereafter as a bottom tripod system, was designed to measure the physical parameters necessary to understand sediment transport processes. Similar systems, previously developed and used on the continental shelf, influenced our design (Sternberg _et al_ 1973; Smith and McLean 1977). Photographs are taken periodically to document the bottom response to physical forcing. The photographs remove the need to rely exclusively on empirical competency curves to determine sediment movement (for instance, Miller _et al_ 1977). The photographs also document effects of biological organisms on sediment movement. The tripod system was designed for repeated deployments of 2 to 4 months duration.

The measurement of bottom stress is of prime interest in studies of sediment transport to determine movement threshold. However, the accurate measurement and parameterization of bottom stress requires the use of sophisticated instrumentation (Smith and McLean 1977), which is not yet routine in oceanography, especially for long time periods. Measurement of the stress profile in the bottom boundary layer is required to accurately determine the stress on a sediment particle. In designing the tripod system, we chose to measure current at a single fixed height from the bottom; a single velocity measurement is adequate to monitor and define processes of sediment movement and transport. Determination of bottom stress and sediment movement thresholds can probably best be made in short term detailed experiments using other specialized instrument systems.

THE BOTTOM TRIPOD INSTRUMENT SYSTEM

The tripod system (Figure 4-I-1) measures current speed and direction, pressure, temperature, and light transmission and photographs the bottom. A data recording package samples, formats, and records the

Figure 4-I-1. U. S. Geological Survey Tripod System: (A) current sensor; (B) pressure sensor; (C) transmissometer; (D) camera (wrapped in protective plastic bag to enclose anti-fouling ring); (E) strobe light; (F) camera battery pack; (G) Sea Data electronics; (H) battery pressure housing; (I) acoustic release transponder; (J) rope canister; (K) recovery float; (L) lead anchor feet; and (M) compass and vane.

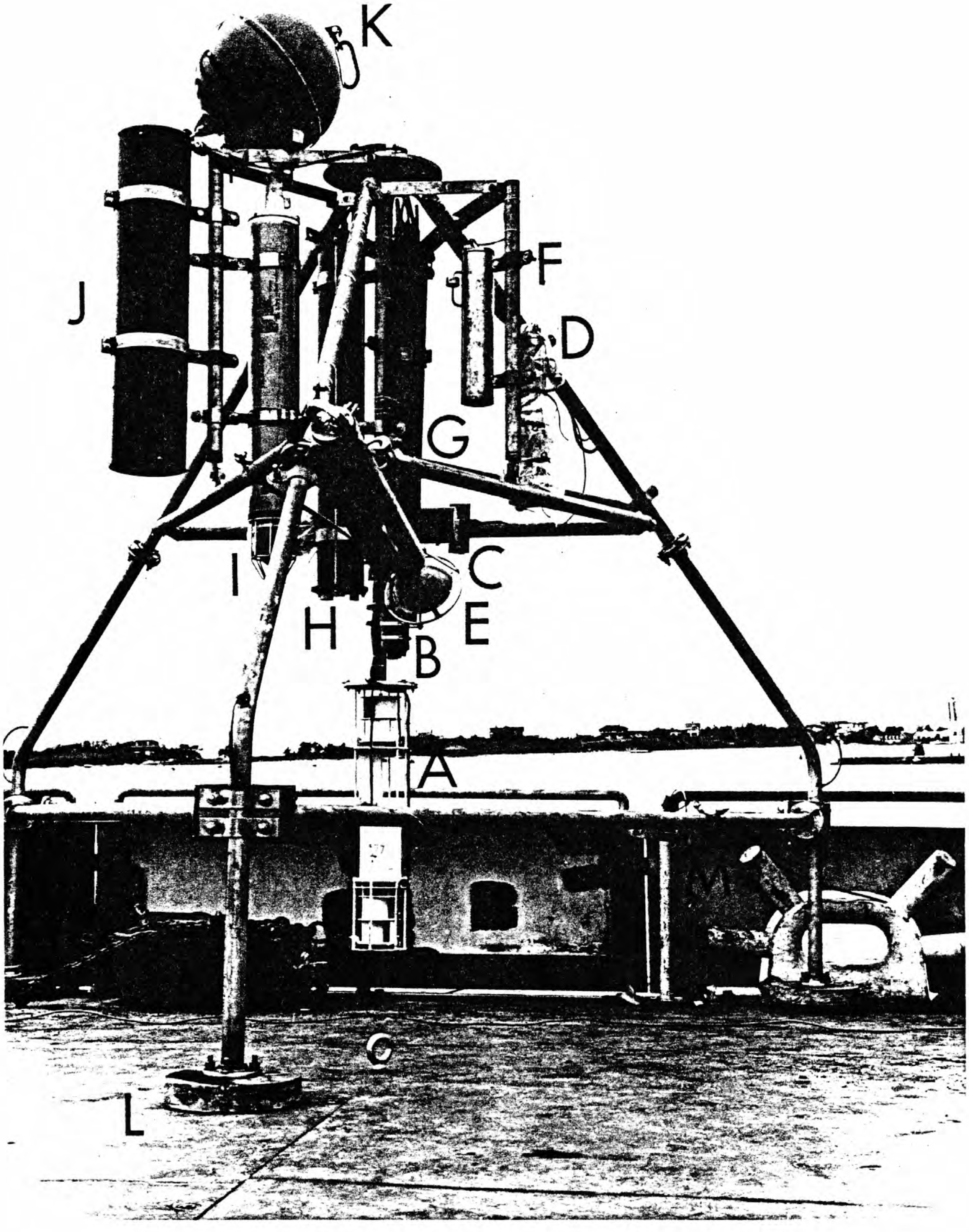
K
J
F
D
G
C
I
E
H
B
A
L

data and distributes power to all sensors. The sensors are deployed and recovered on a rigid tripod frame which causes minimal disturbance to the bottom flow while protecting the instruments from physical damage. All major tripod components and manufacturers of the components are listed in Table 4-I-1.

Sensors

Current Speed and Direction

Bottom current speed is measured by means of a savonius rotor sensor located approximately 1 m from the sea floor. Rotor motion is sensed by a reed switch which is activated by eight small magnets mounted on the rotor. A small vane directly below the rotor senses current direction; the vane is magnetically coupled with paired magnets to a magnetic compass inside an oil-filled pressure housing. Analog output from the direction sensor is 0-360° . Because the vane coupling magnets are not exactly paired the direction reading can have a systematic error of 0-5°. This error, although small and acceptable for each instantaneous direction measurement, may cause some error in the long term mean of the current records, particularly in regions having strong tidal flows. In the future, more nearly linear current sensors having faster dynamic response, such as acoustic, propeller, or electromagnetic sensors, will be incorporated into the system for shallow water measurements to better define the large high frequency wave component of bottom flow.

Pressure

Pressure is measured by means of a quartz-crystal pressure sensor mounted approximately 1.5 m from the sea floor. The sensor is available with full scale ranges of 130, 270, or 600 m. Bottom pressure is sampled to measure both wave frequency variations and lower frequency

Table 4-I-1. U. S. Geological Survey tripod components.

Component	Type and Model	Manufacturer/ Supplier*
Electronics	Digital, CMOS (651-4)	Sea Data Corp.
Tape Transport	Stepping Digital Cassette (610)	Sea Data Corp.
Sensors		
Current	Savonius Rotor and Small Vane (Q-9)	Bendix, Inc.
Pressure	Quartz Crystal (4130,4270,4600)	Paroscientific, Inc.
Temperature	Thermistor	Sea Data Corp.
Transmissometer-Nephelometer	Incandescent Lamp. Transmission and 90° Scatter (TMU-1b)	Montedoro-Whitney
Camera	35mm (372,382,391)	Benthos, Inc.
Release	Acoustic Release - Transponder (325)	AMF Sea-Link
Frame	Tripod. Type 316 Stainless Steel	USGS/WHOI
Pressure Cases	Aluminum, hard anodized	Oceanic Industries
Penetrators, Connectors		Electro-Oceanics
Anti-Fouling	Porous bronze, impregnated with CeCAP (tri-butyl tin oxide and fluoride)	Miami Marine Research, Inc.

---

*Specification of manufacturer does not imply endorsement by U. S. Geological Survey or the Bureau of Land Management.

changes in sea level due to tides and storms.

Turbidity

A transmissometer is used to monitor changes in the suspended matter concentration of bottom water. The sensor is mounted approximately 2 m from the sea floor. It uses a wide-spectrum incandescent light source regulated by a photocell. The light beam travels a folded path of 1 m length; a 180° prism is at one end of the path. To obtain a percent transmission measurement, the sensor output is normalized by the lamp output in clear water which is determined in the laboratory before and after deployments, using a calibration tank in which distilled water is continuously filtered to remove particulates. The sensor is also empirically calibrated in the field to determine the relationship between percent transmission and naturally occurring suspended matter. However, particle size and composition affect light transmission, and any absolute calibration of the transmissometer is qualitative. Also, many major near-bottom changes in transmission are due to resuspension of bottom material which may have different transmission characteristics than samples obtained in the field in calm weather. Biological growth on the transmissometer prism and windows also limits the long term stability of the sensor calibration. Growth is retarded by using porous bronze plates impregnated with tri-butyl tin oxide; the plates fit closely around the exposed surfaces and gradually release the tin oxide into the water during deployment, inhibiting growth. Despite calibration difficulties and problems with biological fouling, the transmissometer provides a good measure of the relative changes in bottom sediment concentration as a function of time.

The transmissometer sensor also incorporates a 90° scattering nephelometer, which shares the regulated incandescent light source. The nephelometer is extremely sensitive to scattered light, making laboratory calibration difficult. The sensor is not sensitive to the low concentrations of suspended sediment typical of the mid-Continental Shelf. The sensor may be more useful in areas where suspended sediment concentrations are high.

Temperature

Water temperature is measured by a thermistor mounted inside the aluminum electronics pressure housing on the lower end cap. The time constant of the end cap is several minutes.

Camera

Bottom photographs are obtained by means of a 35 mm deep-sea camera system; color or black and white film can be used. Quantitative estimates of changes in bottom microtopography (ripple size, ripple migration rates, etc.) associated with various forcing mechanisms such as storms and waves, and the effects of biological activity on the sediments can be determined from the photographs. Qualitative estimates of changes in the suspended matter concentration can also be made from the photographs to verify the transmissometer observations. In addition, the photographs provide information on benthic biological populations, variability in populations, and behavior patterns.

Data identification, date, and time are recorded directly on each 35 mm frame for reference in data analysis. A total of 750 frames are available for each deployment. The camera is mounted approximately 2 m from the sea floor; the $42^{o} \times 54^{o}$ lens opening gives a 1.5 x 2 m viewing area on the bottom. The camera strobe is mounted at an angle to give some side lighting for good definition of the bottom microtopography. A magnetic compass and current vane is fixed in the camera field of view to provide frame orientation and a simple current direction measurement.

Biological growth is inhibited by means of a porous bronze ring impregnated with tri-butyl tin oxide fitted around the camera window.

Data Sampling Scheme

The tripod system samples the output from the sensors in two modes: interval mode and burst mode (Figures 4-I-2a through 4-I-2c). The sampling scheme allows resolution of high frequency processes without storing excessive data (Webster 1967). In the interval mode, pressure and rotor speed are averaged for a time period called the basic sampling interval, typically several minutes in length (in the present system 3.75, 7.5, 15.0, or 30.0 minutes can easily be selected). In the center of the basic sampling interval, a single sample of temperature, light transmission, and turbidity is made. The transmissometer has a warmup period to allow the incandescent lamp to stabilize (Figure 4-I-2c). A sample of transmissometer and nephelometer sensor output with lamp on and off is made to measure the ambient light level. Housekeeping variables such as instrument identification, sampling scheme, and time are also recorded in the interval record.

In the burst sampling mode, a sequence of rotor speed, vane direction, and pressure measurements are taken at relatively short intervals (a "burst" of samples). The beginning of the burst sequence is centered in the basic sampling interval and is repeated at the basic interval (Figure 4-I-2b). The time between samples in the burst (burst rate) is typically several seconds (adjustable to 2, 4, 8, or 16 seconds). The number of sample cycles within a burst (number of strobes in a burst) is adjustable from 6 to 90 strobes. Vector averaging electronics is not used for current measurements; the high frequency motions are of interest and are thus recorded.

For a typical four month deployment in 60-80 m of water, the basic

Figure 4.2.2. U. S. Geological Survey Tripod System Data Sampling Scheme (see text for further discussion).

a. Interval and burst sampling scheme. The time at which data is written on the tape transport is indicated by I (record interval) or B (record burst).

b. Burst sampling scheme. Six measurement sets of rotor speed, pressure, and vane orientation are recorded in each burst record. The spacing between the burst samples is 2, 4, 8 or 16 sec. and 1-15 records (6-90 sample sets) comprise a burst.

c. Transmissometer-nephelometer sampling scheme.

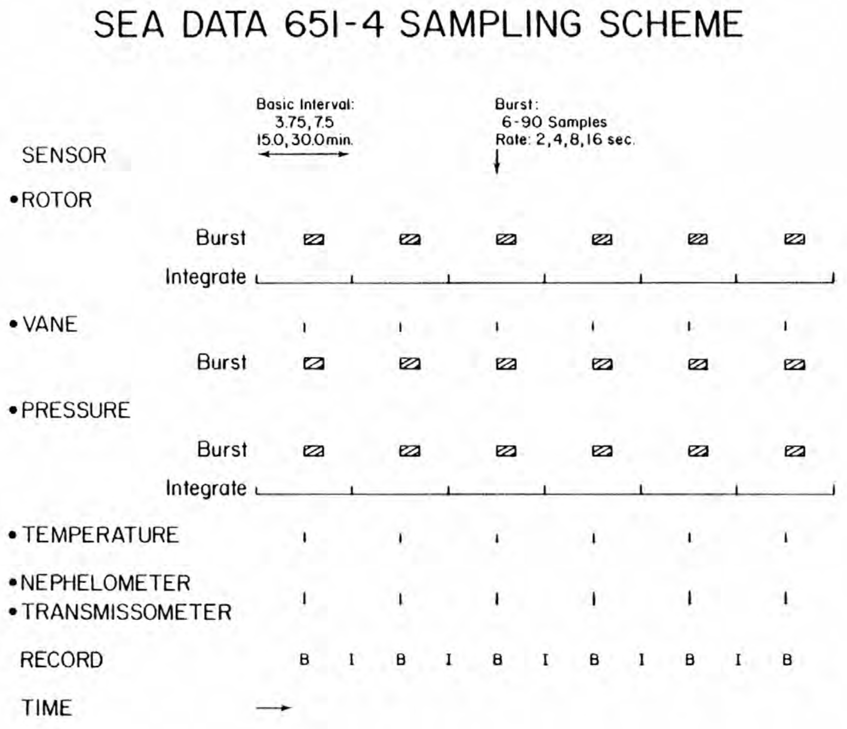
SEA DATA 651-4 SAMPLING SCHEME
Basic Interval:
3.75, 7.5
15.0, 30.0 min.
Burst:
6-90 Samples
Rate: 2, 4, 8, 16 sec.
SENSOR
• ROTOR
Burst
Integrate
• VANE
Burst
• PRESSURE
Burst
Integrate
• TEMPERATURE
• NEPHELOMETER
• TRANSMISSOMETER
RECORD
B I B I B I B I B I B
TIME

Figure 4-I-2a

SEA DATA 651-4 BURST SAMPLING SCHEME

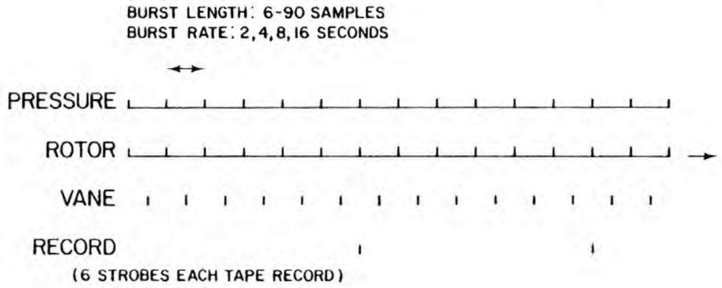
BURST LENGTH: 6-90 SAMPLES
BURST RATE: 2,4,8,16 SECONDS
PRESSURE
ROTOR
VANE
RECORD
(6 STROBES EACH TAPE RECORD)

Figure 4-I-2b

SEA DATA 651-4
TRANSMISSOMETER SAMPLING SCHEME

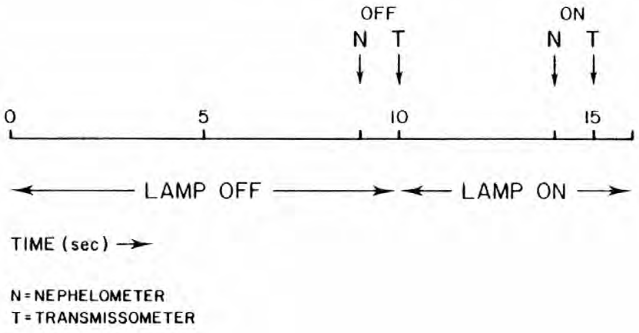
OFF
N T
ON
N T
0
5
10
15
LAMP OFF
LAMP ON
TIME (sec) →
N = NEPHELOMETER
T = TRANSMISSOMETER

Figure 4-I-2c

sampling interval is 7.5 min, the burst rate is 4 seconds, and 12 samples (strobes) are made in a burst. The selection of the number of samples in a burst and of the burst rate for a deployment are primarily determined by water depth and experiment duration. Data record length for typical sampling selections are listed in Table 4-I-2. A larger number of data strobes and a faster burst rate are used in shallow water where the high frequency water waves reach the bottom. The basic sampling interval is selected to resolve the physical processes of interest; because the current meter is not vector averaging, the sampling interval must be rapid enough to prevent serious aliasing from motions that have time scales between wave periods and twice the basic sampling interval. Generally 7.5 minutes is adequate in winter when the water column is well mixed and the Brunt Vaisala period is long. In summer, when the Brunt frequency may be 10-15 minutes, a basic sampling interval of 3.75 minutes is selected.

The 35 mm camera is programmed to photograph the bottom at a fixed time interval, typically 2 or 4 hours for a 2 or 4 month deployment. In addition, logic circuitry has been developed to trigger the camera according to current speed, mainly to document bottom changes associated with high speed current events. In the present configuration, this conditional photographic sampling allows bursts of pictures. The photographic threshold (current speed above which a sequence of pictures is initiated), the number of pictures in a burst sequence, and the picture rate are adjustable within wide limits. The camera logic contains two provisions to avoid repetitious conditional picture taking and to insure that sufficient camera shots will be available for the evenly spaced time series; the total number of pictures triggered conditionally in a deployment may be specified, and the frequency at

Table 4-I-2. Data capacity of Sea Data 651-4 data logger (with single tape transport) for a basic sampling interval of 3.75 min (A) and 7.5 min (B)

Strobes in Burst	Capacity (days)	
	A	B
6	104	208
12	69	138
18	52	104
24	41	82
30	34	68
36	29	58
etc.		

which the conditional logic is activated to examine current threshold may be fixed at a multiple of the basic instrument sampling interval.

Electronics

The data recording package utilizes low-power digital circuitry (Figure 4-I-3). The circular electronics rack fits inside a 15.5 cm (inner diameter) pressure housing; penetrators in the upper end-cap connect the data logger to the various sensors mounted on the tripod frame. Power is provided from stacks of alkaline batteries, arranged to give a 21 v 50 amp-hr supply. Two battery packs are used for a tripod deployment, one in the electronics pressure case and one in a separate battery pressure housing. The quiescent current drain of the data logger is approximately 5 ma; the 100 amp-hr supply is approximately twice as much as required for a typical deployment.

The incremental stepping digital cassette recorder writes four bits across the tape at a longitudinal density of 800 bits per inch. A longitudinal parity bit is written with each cassette record. Total cassette data capacity is 1.8×10^7 bits, or 10^5 data records of interval or burst type (interval and burst data records are of equal bit length). A burst record contains six samples of rotor speed, pressure, and vane direction. A second cassette recorder is planned to increase system data capacity.

Data Resolution and Accuracy

The resolution and estimated accuracy of the tripod measurements are summarized in Table 4-I-3. The accuracy has been determined from manufacturers' specifications and a limited inhouse calibration program. The resolution for current speed and pressure depends on the time for which the measurements are averaged. In Table 4-I-3, the interval measurement resolution is for an averaging period of 225 seconds, and

Figure 4-I-3. (A) Sea Data Electronics; (B) Battery Pack; (C) Pressure Case; and (D) End Cap.

Figure 4-I-3

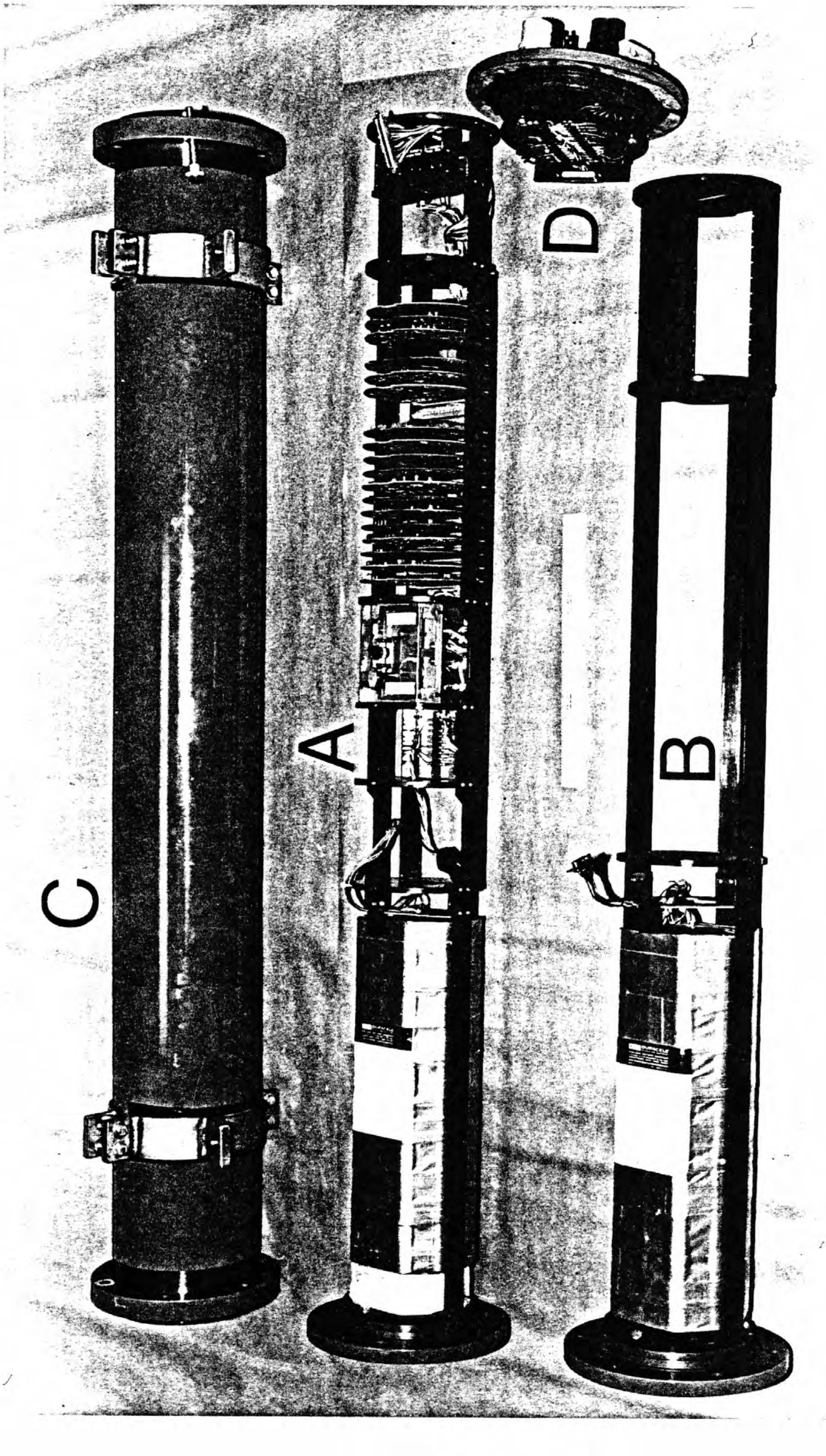

Table 4-I-3. Resolution and estimated accuracy of tripod measurements

Variable	Resolution	Accuracy*
Current speed (cm sec^{-1})[1]		±2.5
Burst (single sample)	1.2	
Burst (12 samples)	.1	
Interval	.02	
Current direction (degrees)	1.41	±5
Pressure (millibars)		±3
Burst (single sample)	∿ 1	
Interval	∿ .04	
Temperature (degrees centigrade)	.02	.1
Transmission (% full scale)	.05	∿ 5
Time (seconds)	56.25	1 in 10^5
Bottom photographs (cm)	.1 to 150	

---

*Accuracy from manufacturer's specifications. Accuracy of transmissometer estimated from laboratory experiments. Current sensor accuracy is for steady conditions. Accuracy will be less under dynamic conditions (for instance, waves) (McCullough, 1975).

[1] Assumes burst rate of 4 seconds, interval period of 225 seconds.

the burst measurement resolution is for a burst rate of 4 seconds. For current direction, temperature, and light transmission, the resolution is determined by the number of bits used to represent the parameter digitally.

Tripod Frame: Deployment and Recovery

The tripod components are deployed and recovered attached to a rigid tripod frame (Figure 4-I-1) designed to cause minimum disturbance to the current flow and still be durable enough to withstand repeated deployments and harsh treatment at sea. The frame is 3.4 m high, 3.4 m on a base, and is constructed entirely of type 316 stainless steel; the major structural members are 6.03 cm (outer diameter) schedule 40 or 80 pipe. All components are bolted together; thus the frame can be dismantled and shipped easily. Instruments are mounted by means of clamshell-like brackets so that placement can be easily changed and adjusted, and so that additional instruments for specific studies can be attached and removed as required. All dissimilar metals are completely insulated from the frame by neoprene rubber or PVC blocks, and sacrificial zinc anodes are mounted at several places on the frame as well as on the instruments to minimize corrosion. A tripod with anchor pads and all instruments weighs approximately 950 kg (2100 lbs.) in air, and 600 kg (1300 lbs.) in water. Each lead anchor pad weighs 91 kg (200 lbs.) in air. On the basis of static calculations, the tripod is probably stable in steady currents as fast as 150 cm sec^{-1} (3 knots).

For deployment, the tripod is lowered to the bottom on a braided polypropylene slip line; once the system is on the bottom, the deployment line is retrieved. The acoustic-release transponder in the system is fitted with a tilt switch which, when interrogated from the surface, modifies a reply code if the unit is tipped at an angle greater than 30° from the vertical. The release is interrogated immediately after deployment and before recovery to determine that the tripod is upright.

For recovery, a coded acoustic command from the surface actuates the release; a float pulls one end of a 100 m long, 1.6 cm (5/8") diameter nylon line from a rope canister on the tripod to the surface. A radio transmitter and strobe light are mounted on the float to enable it to be located on the surface. The entire tripod frame is recovered with the nylon line.

We deploy one to four large lighted buoys (Figure 4-I-4) around the tripod site so that fishermen can identify the instrument location and avoid fouling their nets.

DATA PROCESSING AND QUALITY CONTROL

Once a tripod is recovered, the data are decoded, reviewed, and edited prior to scientific analysis and display. They are first transcribed from the digital cassette to a nine track tape. The clock values are examined for erroneous sequencing, and the sequence of interval and burst records is checked. Sections of the data are dumped in binary, in decimal, or in engineering units and are reviewed to assess sensor performance and general data quality. The entire data record is then decoded, applying appropriate sensor calibrations, and is placed on nine track tape in a convenient format (Maltais 1969).

The decoding program computes and stores 16 data variables derived from the burst and interval measurements (Table 4-I-4). East current, north current, current direction, and current speed are computed from the burst measurements of current speed and direction. The ratio of burst vector current speed to average burst rotor speed (called burst

Figure 4-I-4. Surface buoy used to mark tripod locations.

Figure 4-I-4

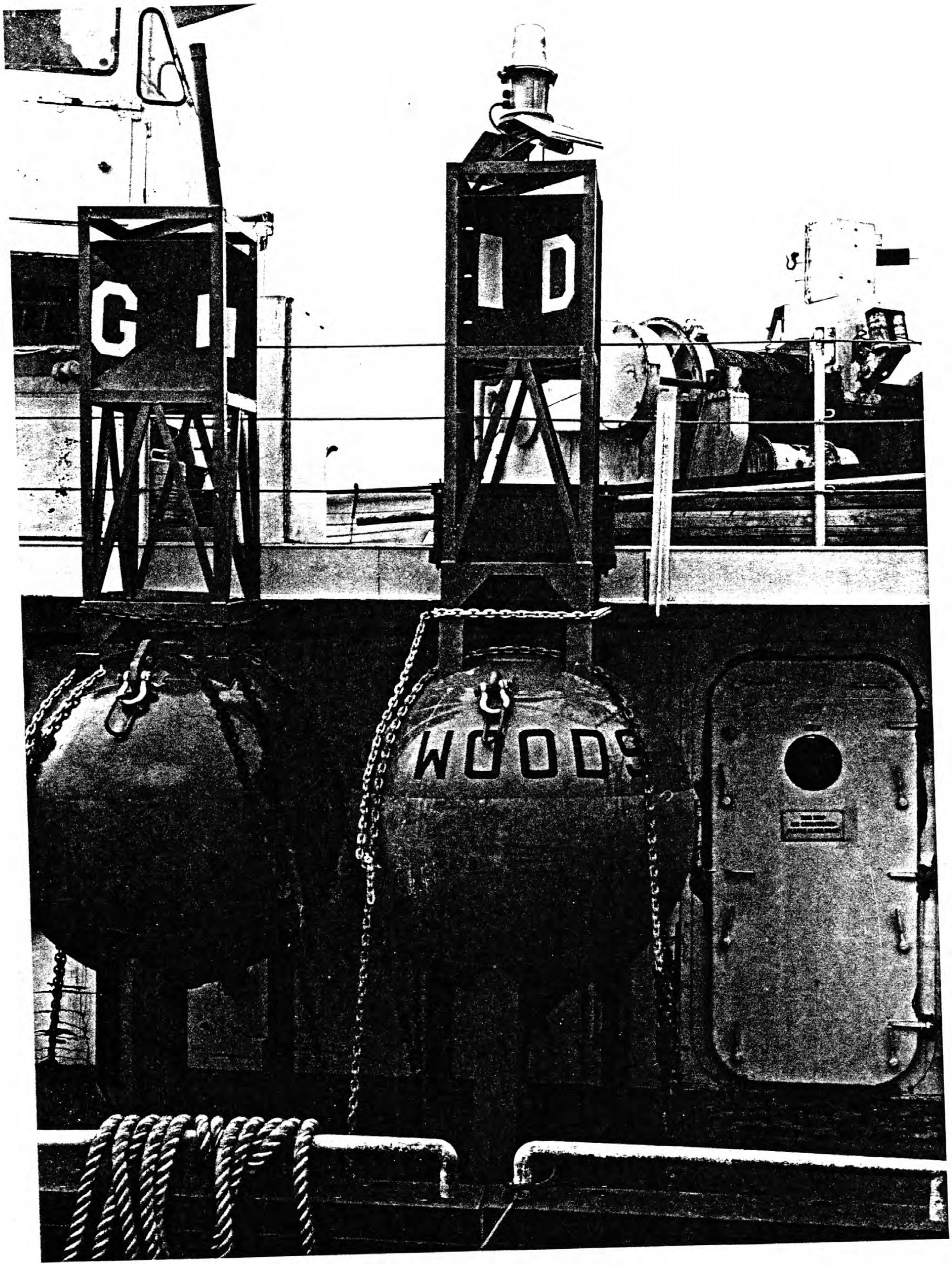

Table 4-I-4. U. S. Geological Survey tripod system - measured and derived parameters

Variable	Units	Definition
1. East current	cm sec^{-1}	computed from burst speed and direction pairs
2. North current	cm sec^{-1}	same as variable 1
3. Current speed	cm sec^{-1}	computed from variables 1 and 2
4. Current direction	degrees	computed from variables 1 and 2
5. Interval rotor	cm sec^{-1}	average rotor speed over basic interval
6. Interval pressure	mb	average bottom pressure during basic interval
7. Temperature	^{o}C	temperature inside instrument pressure case endcap
8. Average burst - interval pressure	mb	average burst pressure - variable 6
9. Burst pressure standard deviation	mb	standard deviation of burst pressure
10. Burst rotor speed/ interval rotor speed	non-dimensional (ratio)	average rotor speed in burst ÷ variable 5
11. Burst normalized unit vector	non-dimensional (ratio)	vector current speed ÷ scalar current speed
12. Transmissometer (trans.) off	relative units	trans. output with lamp off
13. Transmissometer on	relative units	trans. output with lamp on
14. Nephelometer (neph.) off	relative units	neph. output with lamp off
15. Nephelometer on	relative units	neph. output with lamp on
16. Time	sec.	internal digital quartz clock

normalized unit vector, BNUV) is computed as a measure of the current variability within a burst. The ratio of average burst rotor speed to interval rotor speed (called BROTOR/IROTOR) is also computed as a measure of the variability of current flow between burst and interval measurement periods. The standard deviation of the burst pressure measurements is computed as a first order indicator of wave-induced pressure fluctuations. Spectra of the burst pressure measurements can be calculated to resolve frequency and amplitude of the high frequency pressure field. Finally, the difference between average burst pressure and interval pressure is computed as a crude measure of the pressure variability between burst and interval time scales and as an instrumental check.

After decoding, the data are displayed in a time histogram format which is convenient for rapid review of data quality and for identification of erroneous data points. Bad values are replaced by linearly interpolated data points. After editing, the data are again displayed to verify that the improper points have been replaced. This extensive editing procedure is necessary to insure that the data set used for scientific analysis is free of erroneous data points. Typically fewer than 50 points in 2 x 10^5 (0.02%) require editing.

Once the data are edited and stored at the basic sampling interval, many programs are available to time-average, manipulate, and display the data. The programs are part of the extensive Woods Hole Oceanographic Institution Buoy Group library used to process time series data.

U.S. GEOLOGICAL SURVEY SEDIMENT TRANSPORT STUDIES

We have constructed nine bottom tripod systems for a cooperative program with the U.S. Bureau of Land Management (BLM); this program is designed to investigate processes of sediment mobility in the three major petroleum lease areas on the Continental Shelf of the United States East Coast. Observations have been made on Georges Bank, in the Middle Atlantic Bight, and in the South Atlantic Bight (Figure 4-I-5). These areas differ widely in factors that affect sediment movement, for example, meteorological and oceanic forcing, depth, topography, tidal range, river input, and biological populations.

In each area, one tripod is maintained continuously at a selected location to provide long-term observations of sediment movement. If possible, the long-term station is located where meteorological observations are also made so that correlations between atmospheric forcing and sediment movement can be made. The BLM environmental studies have supported U. S. Department of Commerce National Data Buoy Office (NDBO) meteorological buoys in all the lease areas; the buoys provide wind, atmospheric pressure, sea surface temperature and, in several locations, surface wave observations. Shorter term measurements of the cross-shelf and alongshelf variability of the processes of sediment resuspension and transport are made by means of a second tripod system. At present, measurements have been made primarily in mid-shelf regions where tracts have been leased or nominated for leasing. Nearshore measurements to study sediment movement in shallow water and to address specific pipeline corridor problems as well as measurements on the Continental Slope are planned.

In areas where the regional circulation pattern is not well understood, tripod measurements are coordinated with ongoing physical oceanographic programs. Limited studies of the near-bottom currents and the regional circulation are also conducted by means of conventional instruments where additional observations are needed. Hydrographic

Figure 4-I-5. Locations of U. S. Geological Survey tripod deployments on U.S. East Coast Continental Shelf. (LTMS (▲) = long term monitoring station; STS (O) (■) = occupied short-term monitoring station; STS (P) (●) = proposed short-term monitoring station; NDBO (*) = environmental buoys). The three major petroleum lease areas on the East Coast shelf are located on Georges Bank (GB), in the Middle Atlantic Bight (MAB), and in the South Atlantic Bight (SAB).

Figure 4-I-5

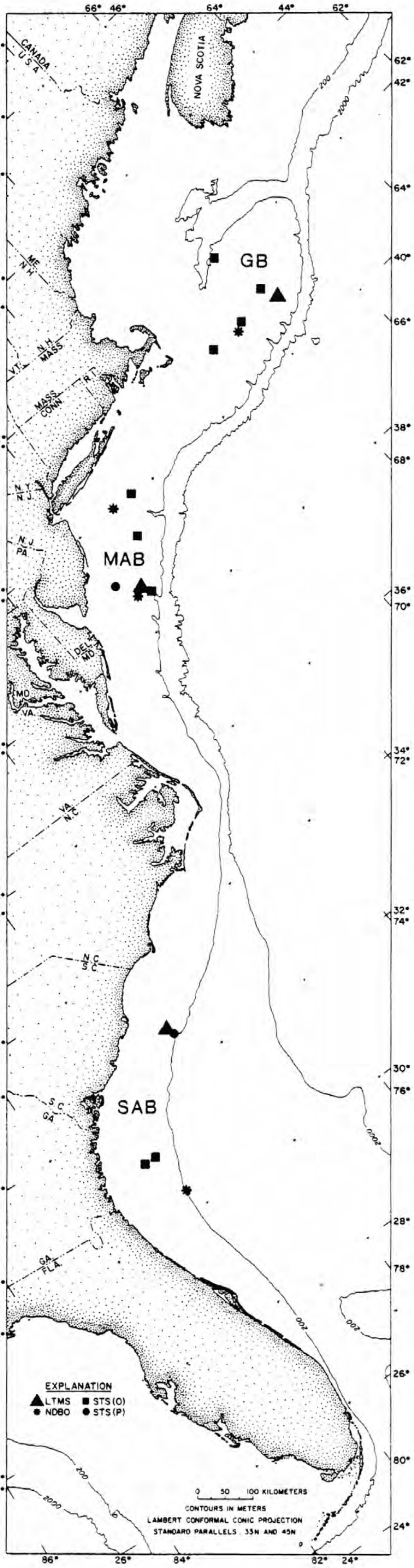

USGS TRIPOD LOCATIONS

CANADA
U.S.A.
NOVA SCOTIA
ME
N.H.
VT.
N.H.
MASS
MASS
CONN
R.I.
N.Y.
N.J.
N.J.
PA
DEL
MD
MD
VA
VA
N.C.
N.C.
S.C.
S.C.
GA
GA
FLA
GB
MAB
SAB
200
2000
EXPLANATION
LTMS
STS (O)
NDBO
STS (P)
0 50 100 KILOMETERS
CONTOURS IN METERS
LAMBERT CONFORMAL CONIC PROJECTION
STANDARD PARALLELS 33N AND 45N
66°
46°
64°
44°
62°
68°
62°
42°
46°
70°
64°
40°
44°
72°
66°
42°
74°
38°
68°
40°
76°
36°
70°
38°
78°
34°
72°
36°
80°
32°
74°
34°
30°
82°
76°
32°
28°
84°
78°
30°
26°
80°
28°
86°
24°
86°
26°
84°
82°
24°

observations are made on each instrument deployment and recovery cruise to determine the position of the tripod with respect to the various coastal and oceanic water masses.

EXAMPLES OF OBSERVATIONS

Observations made during the winter of 1976-1977 by means of a tripod system on the southern side of Georges Bank near the mean position of the shelf-slope water front showed frequent resuspension of the surficial bottom material (Figures 4-I-5 through 4-I-7) and are typical of measurements made to date. The current and pressure signals were dominated by the semidiurnal tide. The semidiurnal tidal current rotated clockwise; the major axis of the tidal ellipse was oriented approximately 20° west of north. The magnitude of the major and minor axes was 21 cm sec^{-1} and 13 cm sec^{-1} respectively. During the first month of the deployment, the bottom temperature gradually decreased from 16° to 6^oC, as the shelf-slope water front apparently moved offshore. The temperature signal was also modulated by the semidiurnal tide. Short periods of steady flow having magnitude greater than the tidal current to the west and east were observed (30-31 December 1976, and 8 January 1977, for example).

The transmissometer indicated changes in suspended sediment concentrations caused by several processes (Figure 4-I-6). The cold shelf water is generally more turbid than slope water (Milliman and Bothner 1977). Gradual movement of slope water offshore at the tripod location and a corresponding decrease in transmission took place during the first month of the deployment. A rapid temperature decrease on 25 December 1976, indicating offshore movement of the front, was associated with a drop in relative transmission; conversely, a temperature increase

Figure 4-I-6. Tripod observations from southern flank of Georges Bank, winter 1967-1977.

a. Bottom pressure, north-south current, east-west current, current direction and current speed.

b. Temperature, relative light transmission (normalized by maximum observed value), pressure standard deviation, interval rotor speed, burst normalized unit vector, and burst rotor/interval rotor. Calibration from field observations made in calm weather suggest that a relative transmission of 1.0 = .5 mg 1^{-1}, and .5 = 1.0 mg 1^{-1}.

TRIPOD OBSERVATIONS GEORGES BANK STA.A
5 DEC. 1976 - 18 MAR. 1977

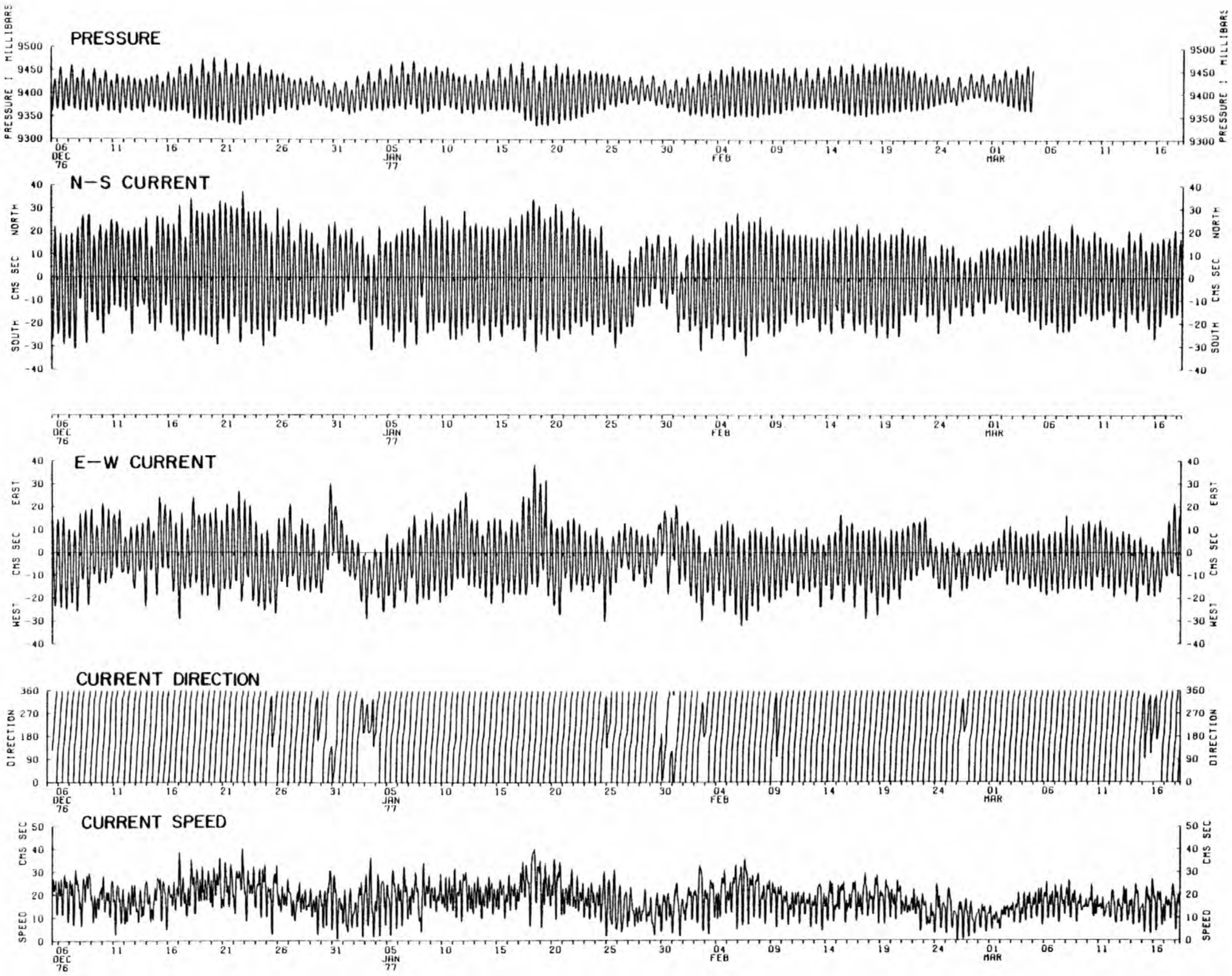

Figure 4-I-6a

Figure 4-I-6b

TRIPOD OBSERVATIONS GEORGES BANK STA. A
5 DEC. 1976 - 23 FEB. 1977

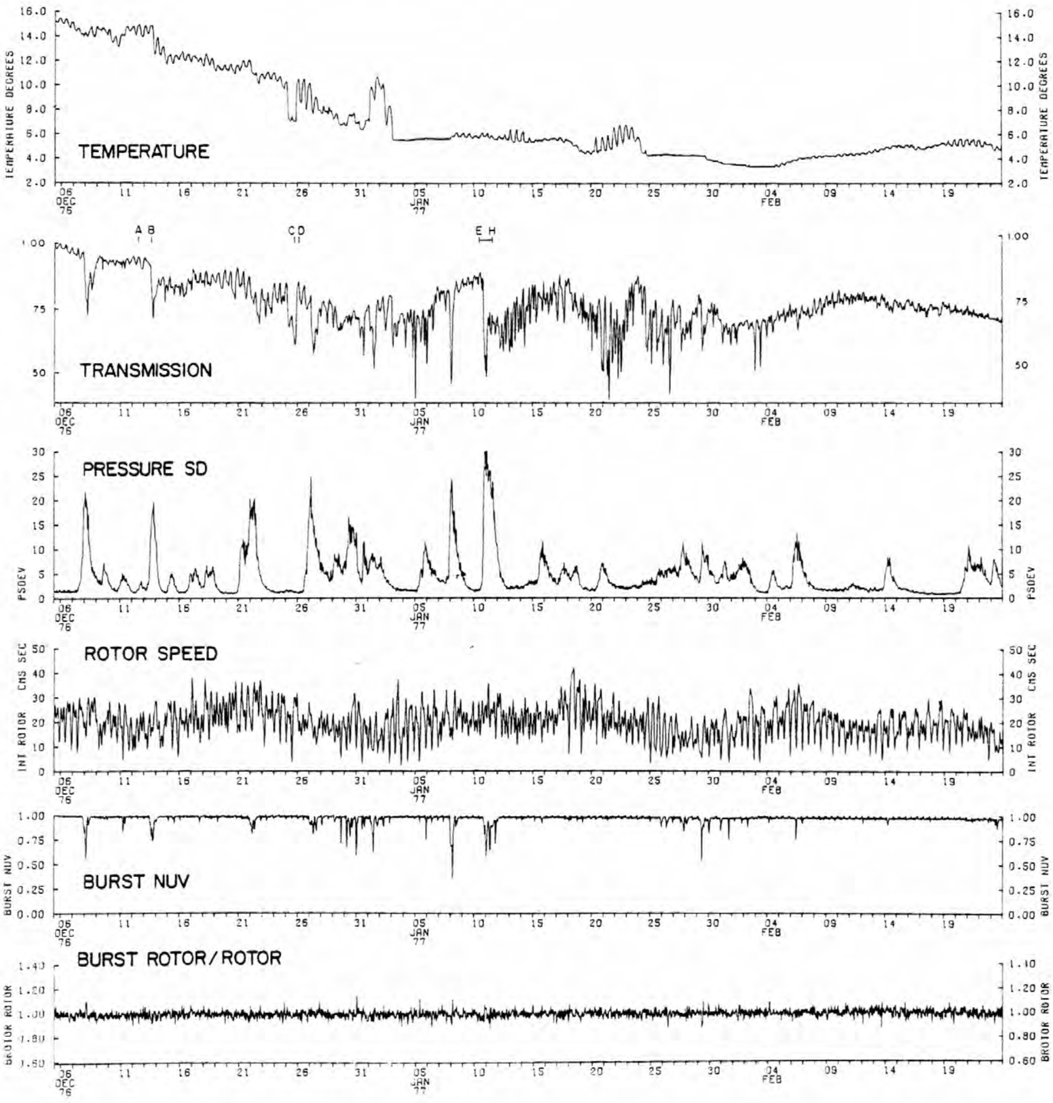

Figure 4-I-7. Typical bottom photographs from Georges Bank tripod deployment December 1976-February 1977 (water depth = 85 m). North is at 1 o'clock. The total viewing area is approximately 2.3 x 1.6 m.

a. 1205 Dec. 12, 1976
b. 1929 Dec. 13, 1976
c. 2141 Dec. 25, 1976
d. 0137 Dec. 26, 1976
e. 1336 Jan. 10, 1977
f. 1731 Jan. 10, 1977
g. 0120 Jan. 11, 1977
h. 1305 Jan. 11, 1977

Date and time when bottom photographs were taken are indicated in upper left hand corner of photograph. Scale in lower right corner is 0-20 cm.

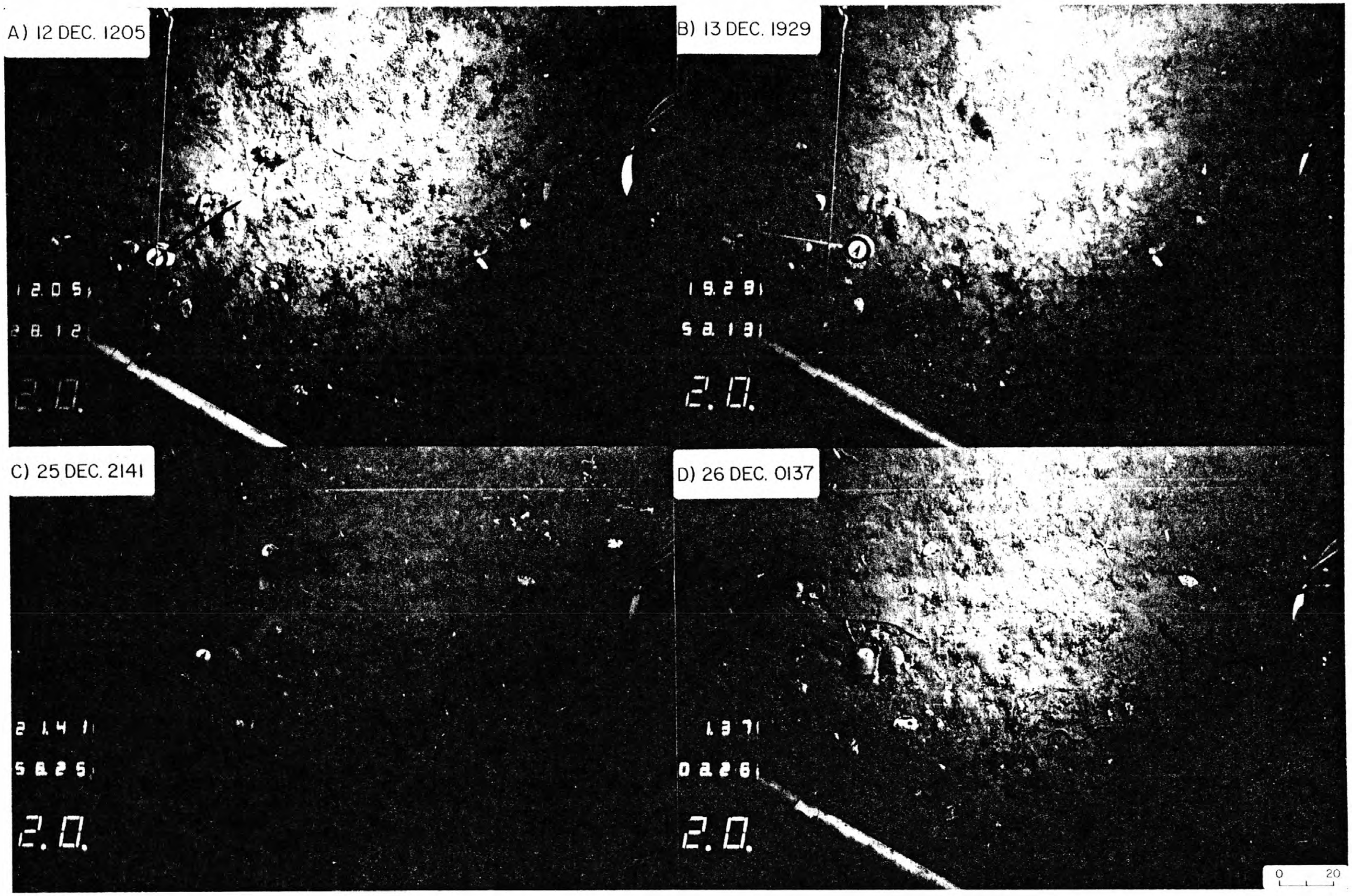
A) 12 DEC. 1205
B) 13 DEC. 1929
C) 25 DEC. 2141
D) 26 DEC. 0137
2.0.
0
20

Figure 4-I-7a-d

Figure 4-I-7e-h

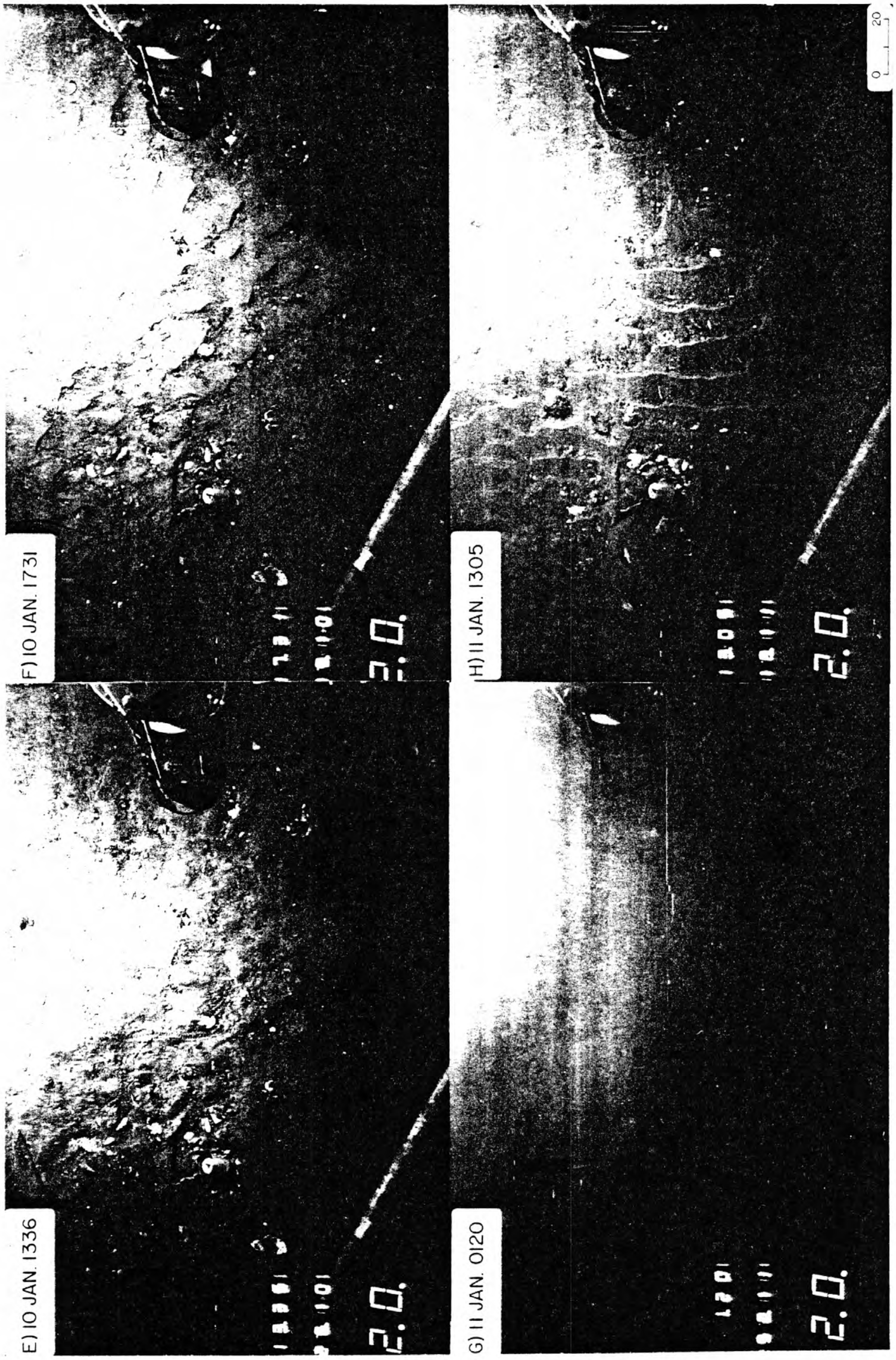
E) 10 JAN. 1336
F) 10 JAN. 1731
G) 11 JAN. 0120
H) 11 JAN. 1305
2.0
0
20

on 1-2 January was associated with an increase in relative transmission, suggesting onshore movement of the front.

The peaks in PSDEV (pressure standard deviation) and slight drops in BNUV (burst normalized unit vector) in December and January indicate periods when surface waves were large (Figure 4-I-6). The storm on 21-22 December in which the ARGO MERCHANT broke apart is clearly shown. Increases in PSDEV on 8, 13, 22, 27 December, 8, 11, 28, 29 January, and 7 February are correlated with a marked decrease in transmission. For scale, the amplitude of bottom pressure fluctuations associated with an 11-sec wave having a 2 m peak-to-trough amplitude in 85 m of water is 14 mb, and maximum bottom current speed is 8 cm sec^{-1}. Superimposed on the wave resuspension events and low frequency variations in transmission (attributed to movements of the shelf-slope water front) were variations in suspended concentration at the tidal period and at harmonics of the tidal period.

Bottom photographs taken on Georges Bank illustrate scour and other changes in bottom microtopography. They also show, qualitatively, changes in suspended sediment concentrations caused by tidal currents, surface waves, and water mass variability (Figure 4-I-7). The clarity of photographs taken in the warm slope water at mooring site A early in December 1976 indicates a low level of suspended sediment (see photograph taken on 12 December, Figure 4-I-7a). On 13 December (Figure 4-I-7b), apparently in response to an increase in surface waves (Figure 4-I-6, see pressure standard deviation), small ripples formed, and suspended matter in the water increased. An intrusion of cool turbid shelf water occurred at the mooring site on 25 December (Figure 4-I-7c); the photographs appear underexposed because of the increase in suspended material. A return to clearer water took place on 26 December (Figure

4-I-7d). Bottom sediments were resuspended sufficiently on 11 January to entirely obscure the bottom from view; this resuspension was associated with large surface waves (Figures 4-I-7e through 4-I-7h).

Observations off the New Jersey coast during winter were similar to those acquired on Georges Bank, but tidal currents were weaker. However, during summer, turbidity was observed when no storms or large waves were present. Bottom photographs (Figures 4-I-8a through 4-I-8d) made in July and August 1977 on the Outer Continental Shelf off New Jersey showed resuspension of the surficial sediments, probably due to bottom trawling. The sea floor on 7 August 1977 was tranquil and was covered by a thin layer of fluffy material (Figure 4-I-8a). Resuspension of bottom sediments or advection of turbid water past the tripod site obscured the bottom from view (Figure 4-I-8b). The tripod orientation with respect to north shifted between 7 and 8 August, and again on 9 August. Bottom current records show no large bottom flow; we suspect that the tripod movement and the observed sediment resuspension were due to bottom trawling. Many hake were at the tripod site.

DISCUSSION

Knowledge of the frequency, direction, and extent of bottom sediment movement on the sea floor of the Continental Shelf is important to assess the environmental consequences of many potential uses of the shelf area. For example, decisions on disposal of drilling muds, drill cuttings, dredge spoil, or industrial wastes on the sea floor require information on the expected patterns and extent of dispersal of dumped material. Information on sediment stability and anticipated scour around structures is necessary for offshore petroleum exploration and development, particularly for planning and constructing offshore

Figure 4-I-8. Typical bottom photographs from summer tripod deployment off New Jersey July-September 1977 (water depth = 65 m). The tripod moved twice during this picture sequence with respect to north. Total picture viewing area is approximately 2 x 1.4 m.

a. 0435 Aug. 7, 1977
c. 1927 Aug. 8, 1977
b. 0735 Aug. 7, 1977
d. 1237 Aug.17, 1977

Date and time when bottom photographs were taken are indicated in upper left corner of photographs. Scale is 0-20 cm. The tripod movement was probably caused by bottom trawlers (see text).

Figure 4-I-8a-d

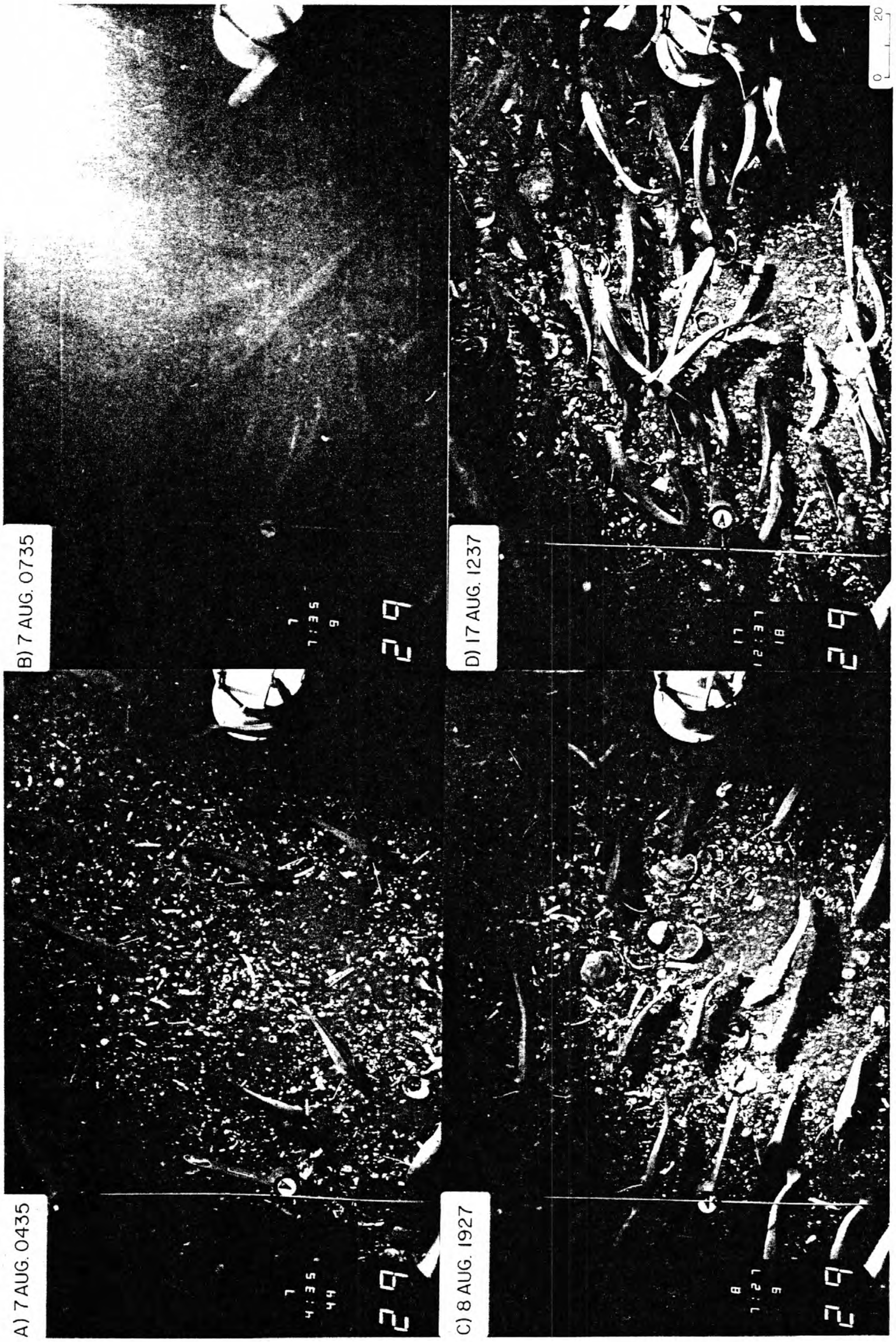
A) 7 AUG. 0435
B) 7 AUG. 0735
C) 8 AUG. 1927
D) 17 AUG. 1237
0
20

pipelines. Dispersal and distribution of sediments, particularly the finer material which may accumulate the most toxic pollutants from offshore activity, is important to determine the effects of these materials on the unusually productive biological communities of the shelf region. Spatial and temporal variability of bottom stress on the Continental Shelf may also significantly affect shelf circulation.

Deployments of the bottom tripod systems on Georges Bank and on the New Jersey Continental Shelf have shown bottom sediment resuspension and transport caused by surface waves, tidal currents, and storms. The fine sediments can be transported 10-20 km alongshore in the mid-shelf region during one winter storm; thus fine material could be distributed over significant areas of the shelf in several years.

The intermittent and seasonal nature of sediment movement on the shelf indicates the absolute necessity of continuous long-term monitoring of bottom conditions to adequately define the frequency and processes of bottom sediment transport. Short-term measurements have been misleading. Several months of observation appear adequate to determine the typical influence of surface waves, internal waves, tides and storms on the bottom at one location during a particular season. Several years of observation are probably required to assess seasonal variability, whereas many years of continuous observation (or different measurement techniques) may be necessary to determine the influence of catastrophic events. Simultaneous observations from tripod arrays and in the water column are required to determine the large scale regional sediment transport patterns and the variability of processes on the shelf. The diversity of transport mechanisms also indicates the need for multisensor instrument packages that measure the appropriate physical parameters. For example, interpretation of the transmission record presented in this paper would be extremely difficult without simultaneous current, wave, temperature, and visual observations. The sensor sampling scheme must resolve both low frequency and high frequency processes.

Future deployments of the instrument systems should continue to increase and refine our rather crude understanding of local bottom processes and of regional sediment transport on the Continental Shelf.

ACKNOWLEDGMENTS

Winfield Hill (Sea Data Corporation) designed and constructed the data recording package used on the tripod to U. S. Geological Survey specifications and provided invaluable assistance throughout the program. Marlene Noble and William Strahle (U.S.G.S.), and Dave Hosom, Woods Hole Oceanographic Institution (WHOI), have made substantial contributions to the engineering design, and construction of the systems. John West, Charles Deadmon, Stephanie Pfirman, and Gary Prisby (all of U.S.G.S.) assisted in tripod deployment, maintenance, construction, and data processing. The Woods Hole Oceanographic Institution assisted in design, construction and maintenance of the tripod systems. The use of the WHOI Buoy Group data processing program library is gratefully acknowledged. A similar tripod system has been constructed by U.S.G.S., Office of Marine Geology, Pacific Arctic Branch, which utilizes four electromagnetic current sensors to obtain a current profile in the bottom 2 m.

LITERATURE CITED

Maltais, J. A. 1969. A nine channel digital magnetic tape format for storing oceanographic data. Woods Hole Oceanographic Institution, Ref. 69-5, 13 p. (unpublished manuscript).

McCullough, J. R. 1975. Vector averaging current meter speed calibration and recording technique. Woods Hole Oceanographic Institution, Ref. 75-44, 35 p. (unpublished manuscript).

Miller, M. L., I. N. McCave, and P. D. Komar. 1977. Threshold of sediment movement under unidirectional currents. Sedimentology 24:507-527.

Milliman, J. and M. Bothner. 1977. Suspended particulate matter along the shelf slope front, Northeastern U. S. (abs). EOS 58(9):889.

Smith, J. D. and S. R. McLean. 1977. Spatially averaged flow over a wavy surface. Journal of Geophysical Research 82:1735-1746.

Sternberg, R. W., D. R. Morrison, and J. A. Trimble. 1973. An instrument system to measure near-bottom conditions on the continental shelf. Marine Geology 15:181-189.

Webster, F. 1967. A scheme for sampling deep-sea currents from moored buoys. Pages 419-431 in 2nd International Buoy Technology Symposium, Marine Technology Society.

CHAPTER 4

BOTTOM CURRENTS AND BOTTOM SEDIMENT MOBILITY IN THE OFFSHORE SOUTHEAST GEORGIA EMBAYMENT

PART II

OBSERVATIONS OF BOTTOM CURRENT AND BOTTOM SEDIMENT MOVEMENT IN THE SOUTHEAST GEORGIA EMBAYMENT, 1977

Bradford Butman and Stephanie Pfirman

INTRODUCTION

During the first year South Atlantic OCS environmental program, long term *in situ* observations were initiated to determine the frequency and direction of bottom sediment movement, and the processes responsible for bottom sediment motion in the mid-shelf region. The studies were undertaken to assess possible environmental hazards, caused by sediment movement, to petroleum exploration and development on the Continental Shelf. Information on the frequency and extent of surface sediment reworking by physical processes, such as surface and internal waves, tides, storm-driven currents, and the Gulf Stream as well as by epibenthic organisms is important for the engineering design of structures for use on the Continental Shelf. In addition, such information will help to predict the distribution of material deposited on the shelf (for instance, drilling muds), and the fate of pollutants associated with suspended material or incorporated into the bottom sediments.

The currents on the South Atlantic OCS are strongly influenced by the Gulf Stream which flows northward along the eastern edge of the shelf, with surface current speeds in excess of 100 cm sec^{-1} (2 knots). Meanders and spin-off eddies may also cause strong southerly flow however. Drift bottle observations (Bumpus 1973) show a variable but generally northerly surface flow between Miami and Cape Fear of approximately 10 km day^{-1}; nearshore the net flow is southerly. Bottom drift is weak (less than 2 km day^{-1}) with both southwesterly and northerly flow observed. Superimposed on this weak mean circulation are large, primarily longshelf, fluctuations in current due to wind forcing and intrusion of the Gulf Stream onto the shelf (Lee and Brooks 1979). Strong semidiurnal tidal currents are also present.

The nearshore surface sediments on the South Atlantic OCS, north of Cape Canaveral and south of Cape Romain, are primarily fine sand. In the mid-shelf region the surface sediments are medium sand with some small patches of coarse sand. Offshore at the shelf break, the surface sediments are again fine sand (Chapter 5, this volume, Surficial Sediments of the U. S. Atlantic Southeastern United States Continental Shelf). North of Cape Romain to Cape Hatteras, the distribution of surficial sediments is similar, but there is more coarse sand in the mid-shelf region, and the distribution is more patchy. There is little silt and clay size material in the surface sediments.

Although grain size is relatively uniform, the sediment lithofacies are patchy which indicates no major longshelf or cross-shelf transport and mixing on the Georgia Shelf. Vibracore observations however, suggest that the surficial sediments are mixed to depths of 1-3 m (Chapter 6, this volume, Vibracore Investigations). The sediment texture and surface stratigraphy thus indicate active reworking of the surface sediments but little major transport.

FIELD PROGRAM AND METHODS

In situ observations of bottom processes were made with an instrument system which measured bottom current speed and direction, temperature, light transmission, bottom pressure, and waves (bottom pressure), and photographed the bottom (Butman and Folger 1979). All instrument sensors are attached to a rigid tripod frame which sits on the bottom. The instrument system and the U. S. Geological Survey-Bureau of Land Management sediment transport studies are described in detail in Part I of this chapter (An Instrument System for Long-Term Sediment Transport Studies on the Continental Shelf).

The bottom sediment mobility studies in the South Atlantic OCS region were initially funded by the Bureau of Land Management in 1977. The major effort for 1977 was construction of two instrument systems to be used in the South Atlantic OCS region in 1978. However, a pilot field study was conducted in August-September 1977 and the results are presented in this report. The objectives of the short deployment were to:

1. Begin to assess the frequency and direction of bottom sediment motion and the major processes causing movement at a representative mid-shelf location.
2. Determine the feasibility of *in situ* bottom observations on the South Atlantic OCS, particularly to identify any logistic or system problems associated with shallow water and the semi-tropical environment.

A tripod was deployed at Station B (Figure 4-II-1, Table 4-II-1) from 6 August to 8 September 1977 in water 30 m deep. The instrument sampled average current speed and direction (24 samples at a 2 second rate), and temperature every 3.75 minutes. Average 3.75 minute values

Figure 4-II-1. Location of U. S. Geological Survey tripod deployments on the South Atlantic Continental Shelf, 1977-1978.

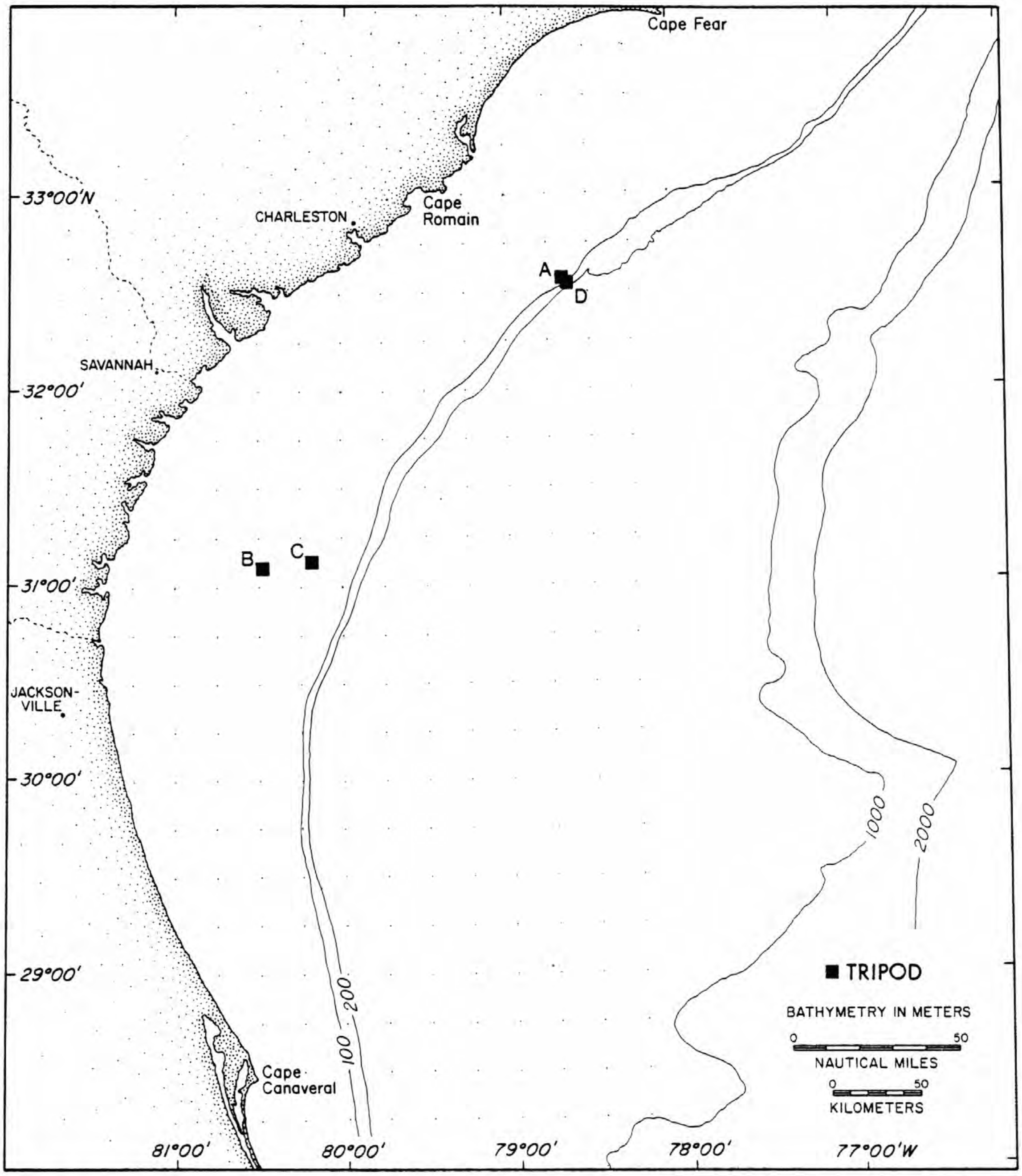
Cape Fear
33°00'N
CHARLESTON
Cape Romain
A
D
SAVANNAH
32°00'
B
C
31°00'
JACKSON-VILLE
30°00'
1000
2000
29°00'
■ TRIPOD
BATHYMETRY IN METERS
0
50
NAUTICAL MILES
0
50
KILOMETERS
200
100
Cape Canaveral
81°00'
80°00'
79°00'
78°00'
77°00'W

Table 4-II-1. Location and dates of U. S. Geological Survey tripod deployments on South Atlantic Continental Shelf, 1977-1978.

Sta.	Type[1]	Water Depth	Latitude	Longitude	Deployment	Recovery	Record ID[2]
A	T	44	32°33.7′N	78°39.5′W	5 Feb. 78	13 April 78	142
					13 April 78	13 July 78	147
					13 July 78	15 Nov. 78	152
B	T	30	31°05.3′N	80°28.8′W	6 Aug. 77	8 Sept. 77	134
C	T	47	31°06.8′N	80°10.6′W	5 Feb. 78	11 April 78	143
D	T	86	32°32.5′N	78°37.5′W	13 July 78	13 Dec. 78	153

---

[1] T = Tripod

[2] All USGS current and tripod moorings are assigned a sequential mooring number. Data from these moorings are referenced by this number.

of current speed and direction were obtained by vector-averaging the burst samples. The 3.75 minute sampling rate was selected to resolve the expected high frequency motions associated with internal waves. The camera system photographed the bottom every 2 hours. Unfortunately, transmission and pressure sensors failed at launch.

Additional deployments of the tripod systems have been made in 1978 (Figures 4-II-1 and 4-II-2, Table 4-II-1); results of these observations will be presented in the 1978 Final Report. The sampling philosophy of the field program was to maintain one instrument at a selected location continuously (Station A) to monitor long term variability and seasonal changes. Measurement of the longshelf and cross-shelf variability of the processes of sediment movement were made with shorter term deployments of two element cross-shelf (Stations A and D) and longshelf (Stations A and C) arrays.

RESULTS

Bottom Currents

The bottom currents at Station B in summer can be conveniently separated by frequency into low frequency fluctuations (motions with periods of 2-10 days), the tidal currents (periods of 12-24 hours), and high frequency currents with periods shorter than the tides. The currents were dominated by the semidiurnal tide (Figure 4-II-3). The major axis of the tidal ellipse was oriented approximately cross-shelf with amplitude of 25 cm sec^{-1} (Table 4-II-2). The tidal current rotated clockwise. The average near-bottom current speed was 19 cm sec^{-1} and current speeds exceeded 30 cm sec^{-1} approximately 10% of the time (Figure 4-II-4a). The strongest currents tended to cluster in the onshore-offshore direction (Figure 4-II-4b) reflecting the cross-shelf

Figure 4-II-2. Sequence of U. S. Geological Survey tripod deployments on the South Atlantic Continental Shelf, 1977-1978. The number indicates a U. S. Geological Survey sequential mooring identification number. Data is referenced by this number. Letters show the ships used to conduct cross-shelf hydrographic sections at deployment and recovery of the tripods (AD = ADVANCE II; O = OCEANUS; I = ISELIN; W = WHITEFOOT).

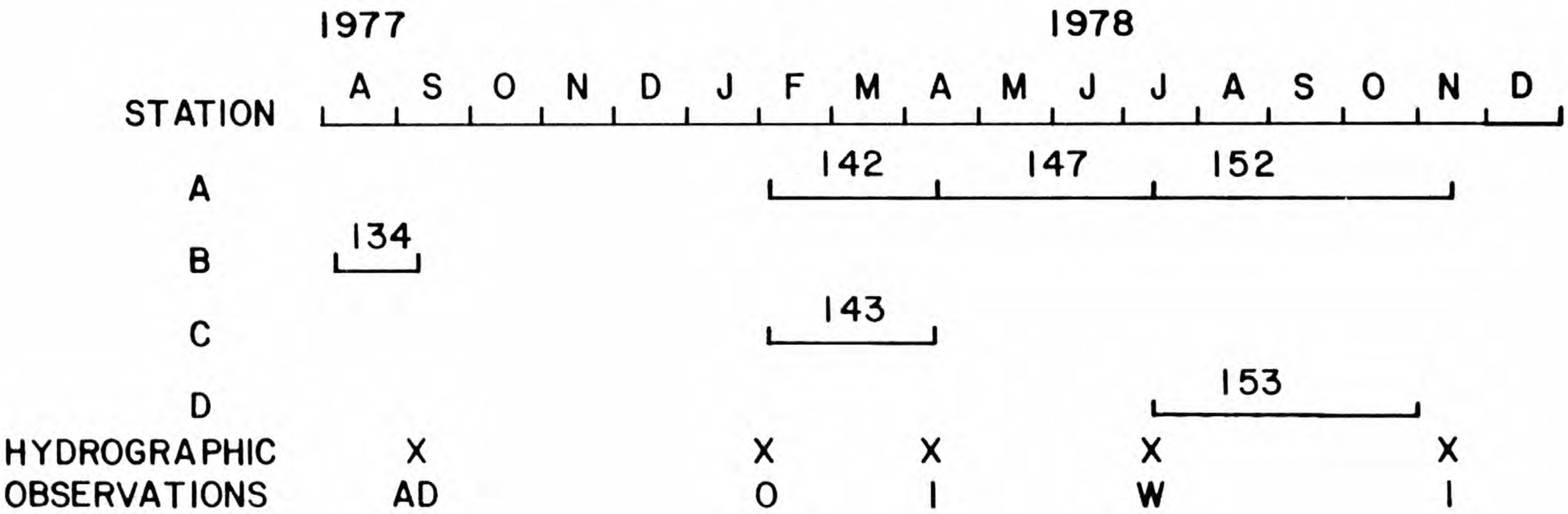

SOUTH ATLANTIC BIGHT
USGS TRIPOD OBSERVATIONS

Figure 4-II-2

Figure 4-II-3. Bottom observations from Station B, August-September 1977 (Record 134).

a. North-south current, east-west current, current direction and current speed. All plots are of hour-averaged data.

b. Temperature (hour-averaged), speed (every 3.75 minutes), and standard deviation of rotor speed (hour-averaged).

c. High-passed bottom temperature and bottom current speed (every 3.75 minutes). (High pass gaussian filter essentially removed all motions with periods longer than 2 hours.)

d. Low-passed bottom current. (Low pass filter essentially removed all motions with periods shorter than 33 hours, Flagg 1977.)

Figure 4-II-3a

STATION B (RECORD 134)

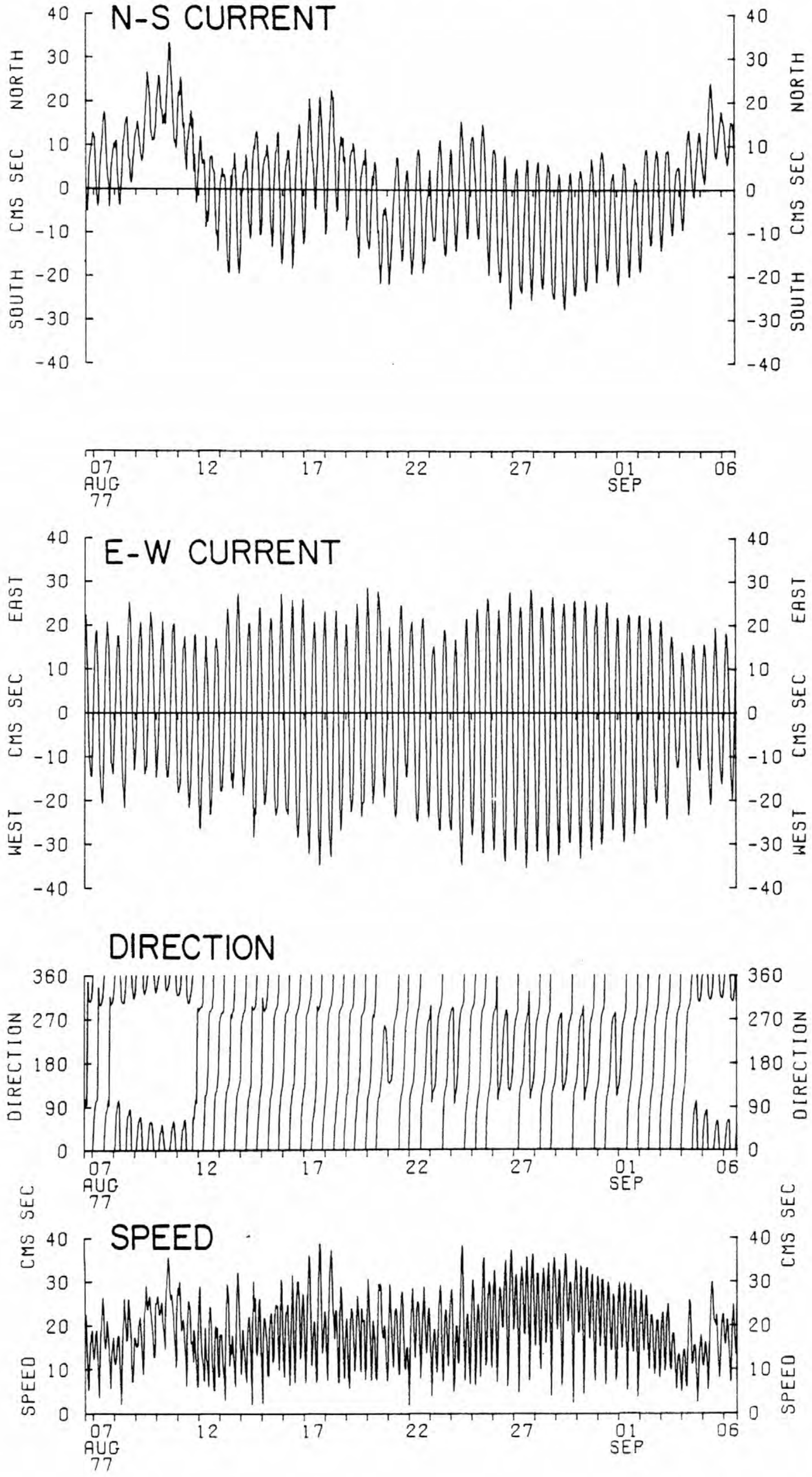

Figure 4-II-3b

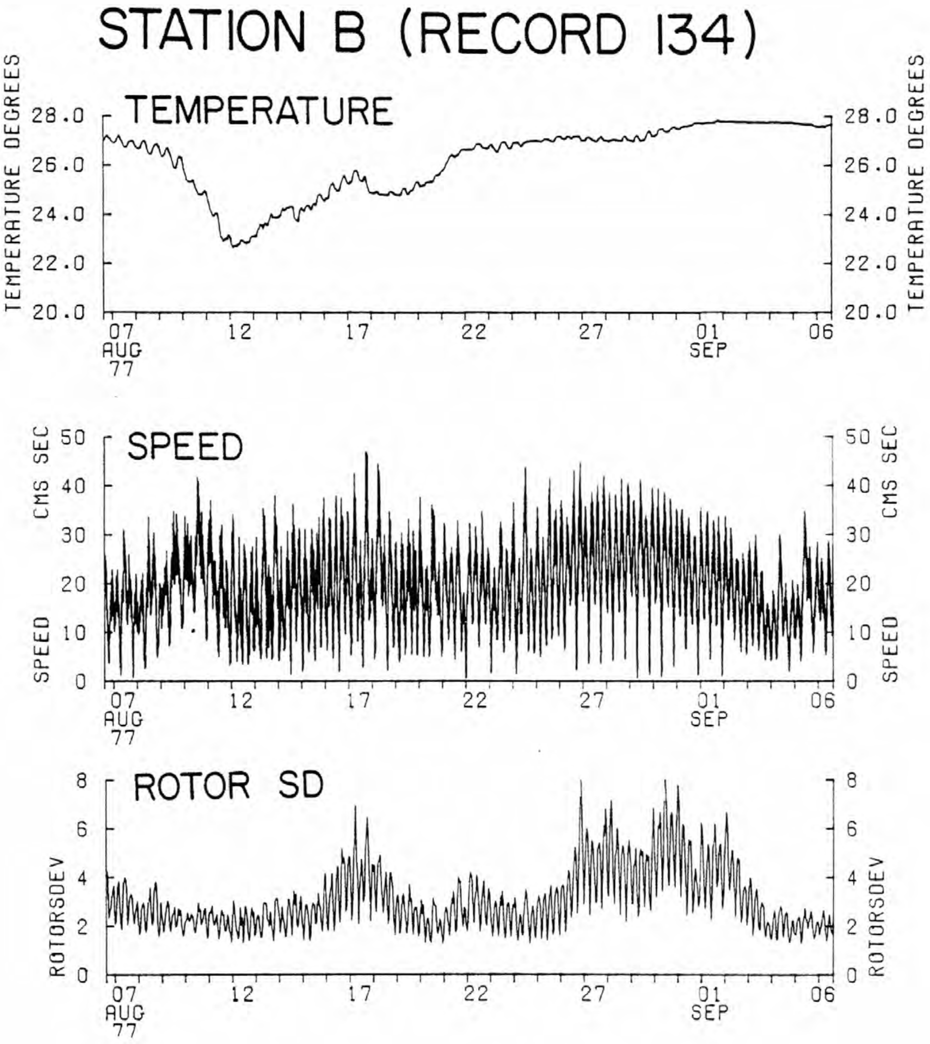

Figure 4-II-3c

STATION B (RECORD 134)

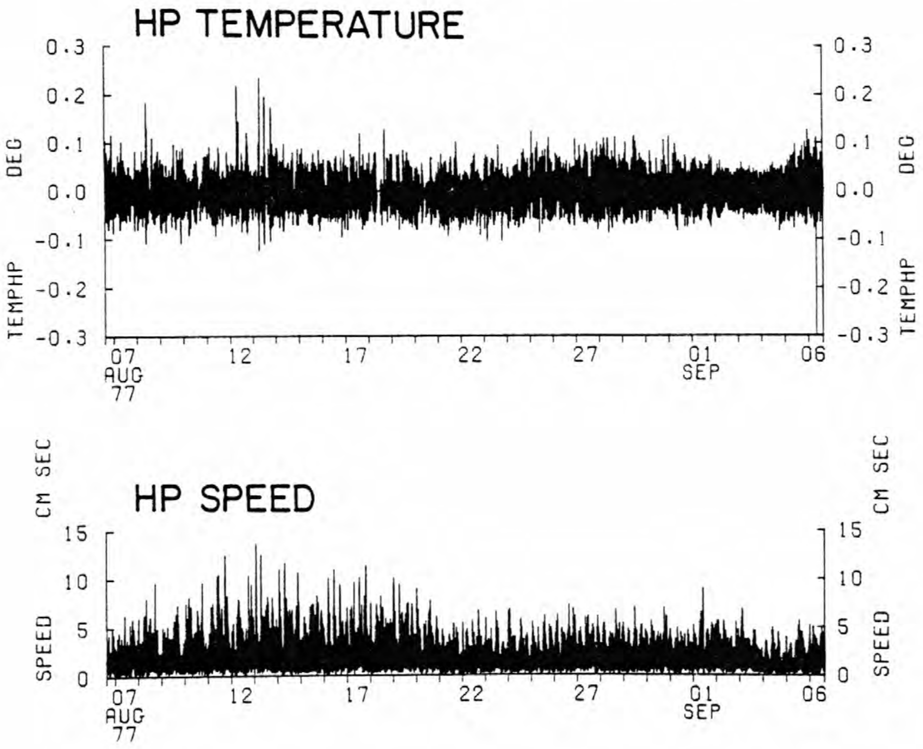

Figure 4-II-3d

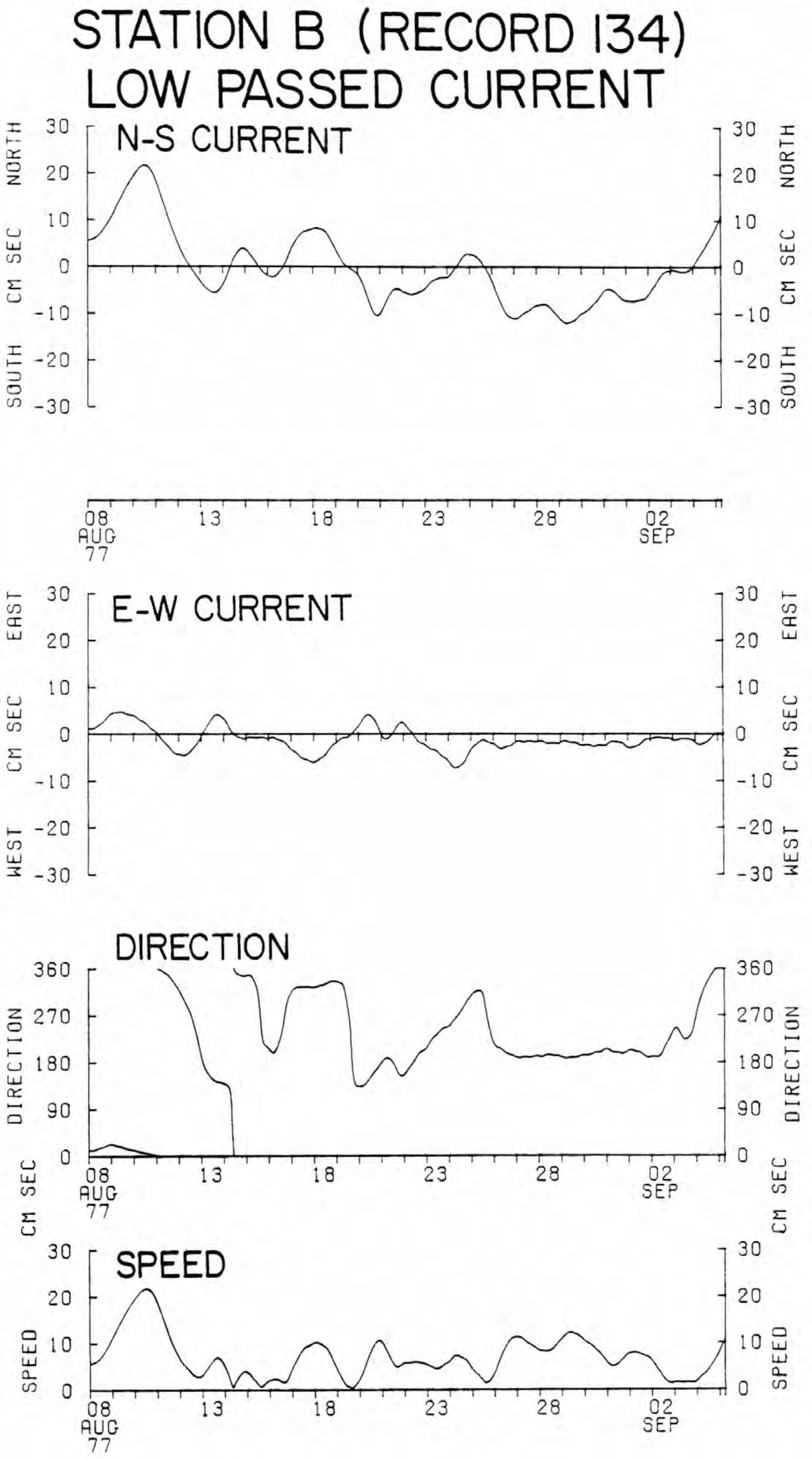

Table 4-II-2. Current Statistics[1] South Atlantic Bight

Sta.	Record	Water Depth (m)	Length (days)	Speed			Mean Current[2]		SD, LP[3]		Tide[4]		
				Mean	SD	Max.	S	D	E	N	Maj.	Min.	Orien.
B	134	30	31	19	8	39	1.2	251°	3	8	25	7	291°

---

[1] All current data in cm sec^{-1} and were computed from hour-averages of original data series.

[2] Mean current computed from low-passed data series (S = speed, D = direction).

[3] Standard deviation of East-West and North-South low-passed current components.

[4] Semidiurnal tidal ellipse. Major and minor axis, and ellipse orientation.

Figure 4-II-4. a. Percent occurrence of bottom current speed in 10 cm sec^{-1} intervals (Record 134). For example, approximately 40% of all speeds observed were between 10 and 20 cm sec^{-1}. The sum of all percentages is 100%. The histogram was constructed with the 3.75 minute observations.

b. Percent occurrence of bottom current speed in 10 cm sec^{-1} intervals and 45° intervals of direction (Record 134). The sum of the occurrence for all directions in one speed category is equivalent to the occurrence in that speed category shown in Figure 4-II-4a. The sum of all percentages is 100%. The histogram was constructed with 3.75 minute observations.

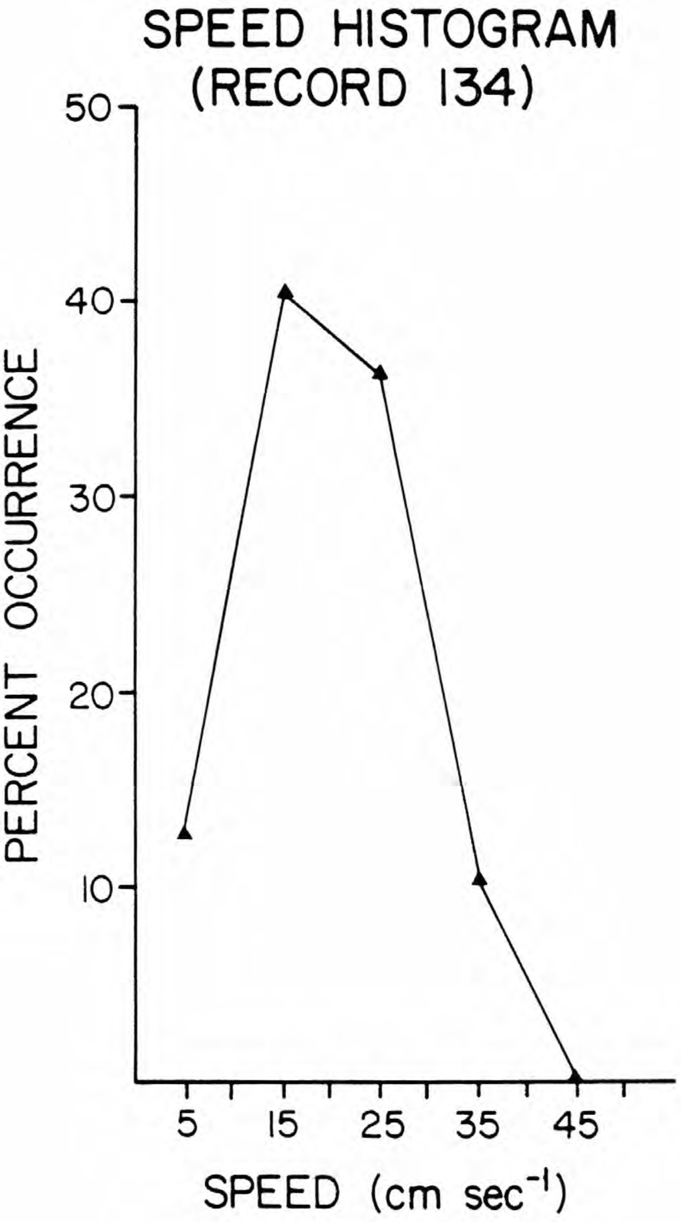
SPEED HISTOGRAM
(RECORD 134)
PERCENT OCCURRENCE
50
40
30
20
10
5
15
25
35
45
SPEED (cm sec⁻¹)

Figure 4-II-4b

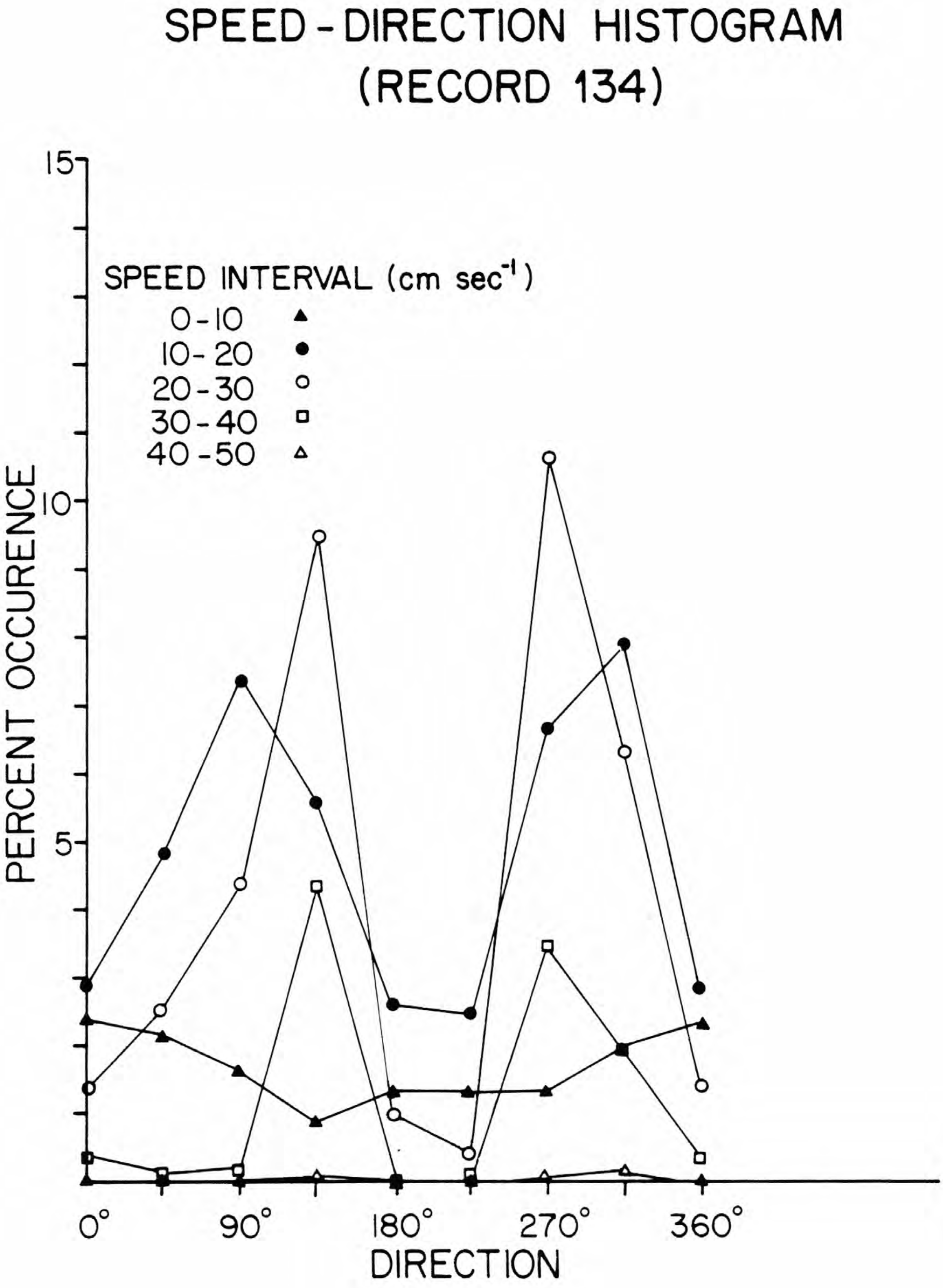

orientation of the semidiurnal tidal current. In the 30-40 cm sec^{-1} speed range there was a slight preference for onshore (toward 270° and 315°) rather than offshore (toward 135°) flow.

The bottom water temperature varied between 23° and 28°C (Figure 4-II-3b). The decrease in bottom water temperature between 9 and 16 August suggests an intrusion of cooler shelf water. The small temperature fluctuations at the semidiurnal tidal period indicate the presence of a weak cross-shelf temperature gradient which was advected past the instrument location by the tidal current. A cross-shelf temperature section made 8 September 1977 showed a large body of warm, well-mixed, 27.7°C water to the west of the instrument location, and a cooler bottom intrusion with a core temperature of 24.4°C to the east (Figure 4-II-5). Atkinson (1977) shows that 24°C Gulf Stream water is sufficiently heavy to intrude along the bottom in the summer months; we suggest that the 24°C water is of Gulf Stream origin.

Because the pressure sensor failed on mooring 134, no direct wave measurements were made. However, the standard deviation of the rotor speed within the burst measurements is a crude indicator of the high frequency energy (Figure 4-II-3b). Two periods of surface waves are indicated, 16-18 August and 27 August-1 September. During the first period, winds were toward the northeast, parallel to the coast (Figure 4-II-6). During the second period winds were onshore.

High frequency current fluctuations were observed throughout the observation period (Figure 4-II-3c), probably associated with internal waves. The high frequency current and temperature fluctuations were largest between 8-18 August, reaching 10-15 cm sec^{-1} and 0.2°C, respectively. This period coincided with the intrusion of cooler Gulf Stream water at the mooring site, and presumably an increased density

Figure 4-II-5. Cross-shelf temperature section, 8 September 1977. Surface salinity (SS) and surface temperature (ST) are shown for each station.

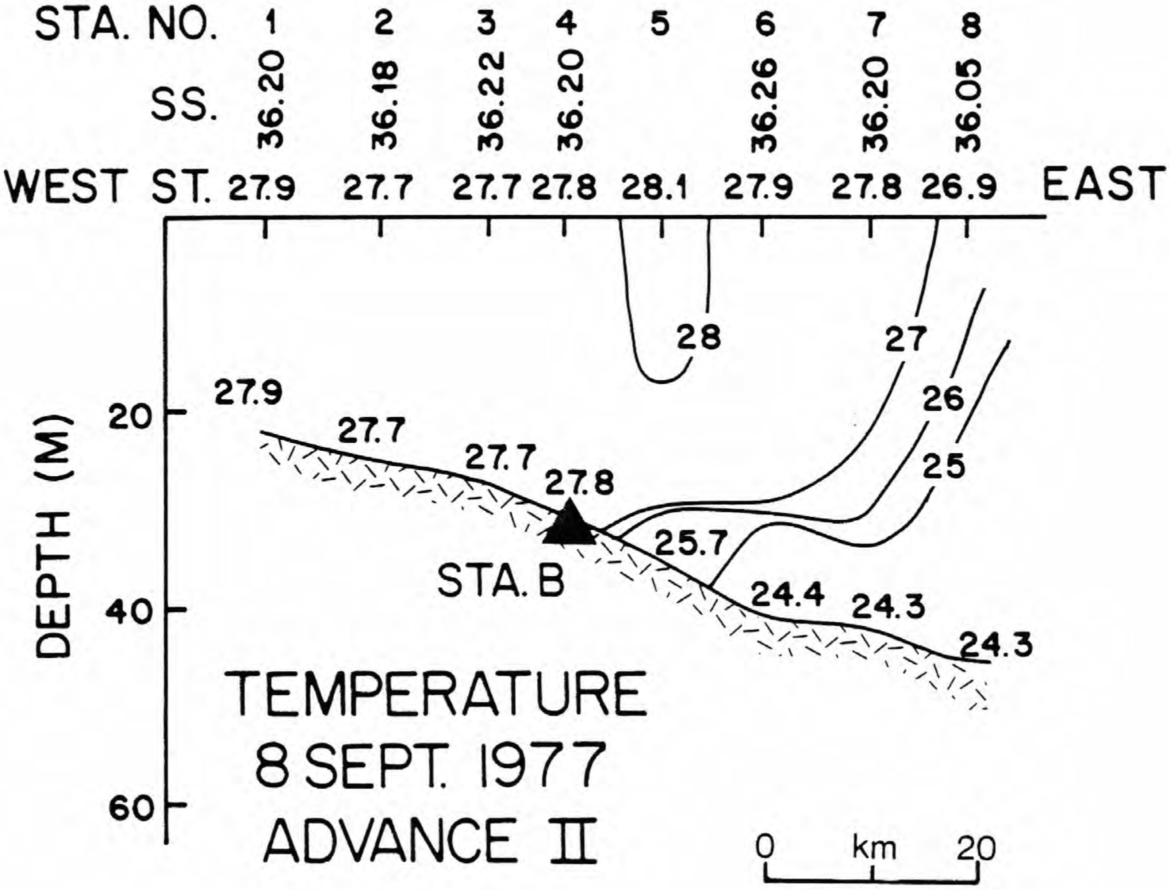
STA. NO.
1
2
3
4
5
6
7
8
SS.
36.20
36.18
36.22
36.20
36.26
36.20
36.05
WEST
ST.
27.9
27.7
27.7
27.8
28.1
27.9
27.8
26.9
EAST
DEPTH (M)
20
40
60
28
27
26
25
27.9
27.7
27.7
27.8
25.7
24.4
24.3
24.3
STA. B
TEMPERATURE
8 SEPT. 1977
ADVANCE II
0
km
20

Figure 4-II-6. Wind and air temperature at Savannah, Georgia August-September, 1977. Wind direction uses oceanographic convention and is the direction toward which the wind is blowing.

Figure 4-II-6

SAVANNAH

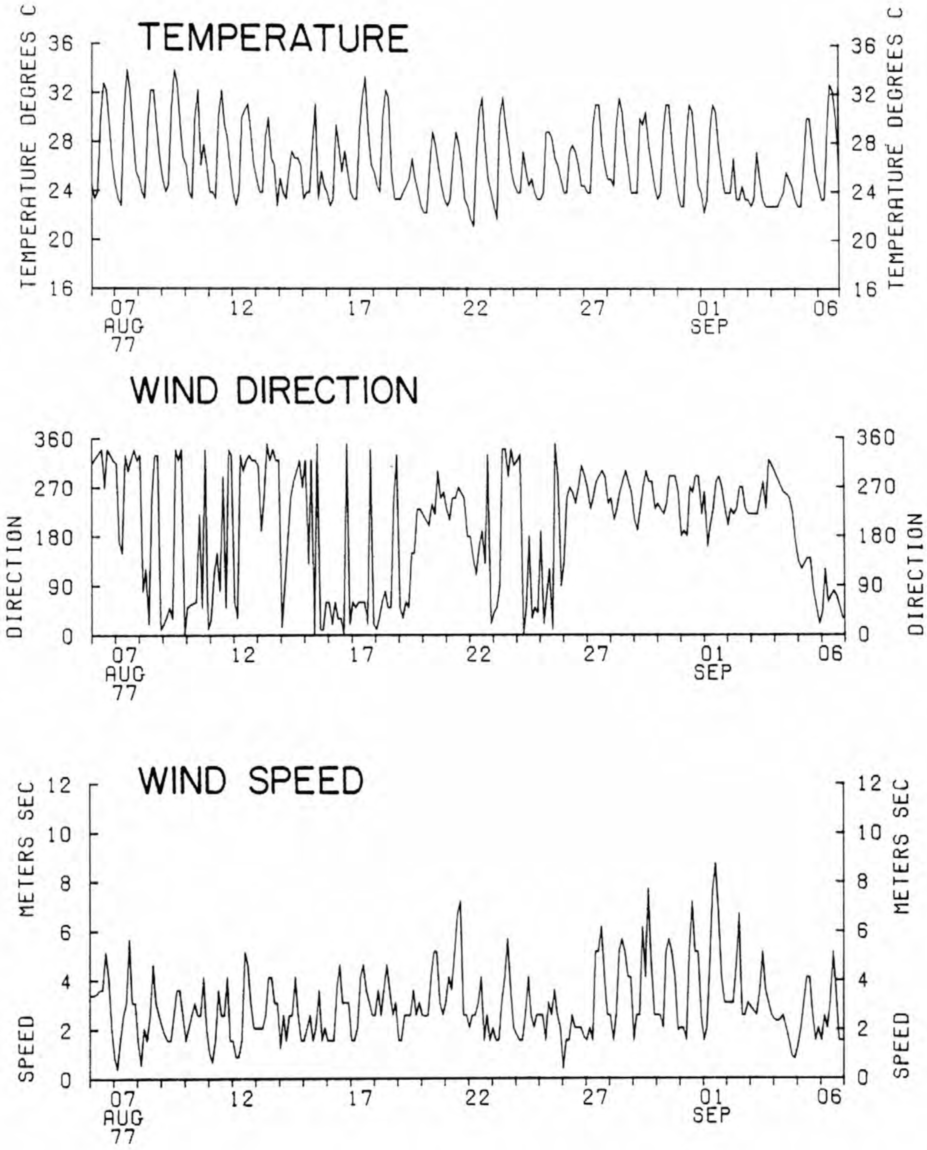

stratification. Otherwise the high frequency current and temperature fluctuations were typically less than 5 cm sec^{-1} and $0.1^{o}C$. The high frequency motions were oriented onshore-offshore.

The mean flow computed over the entire current record was 1.3 cm sec^{-1} toward 251° (Table 4-II-2). The low-passed currents were generally less than 10 cm sec^{-1} (Figure 4-II-3d). Low frequency current fluctuations were larger in the longshelf direction (north-south) than in the cross-shelf direction (Table 4-II-2). A period of strong northward flow occurred between 8-11 August, and again at the end of the deployment. A southerly drift of approximately 10 cm sec^{-1} occurred between 26 August and 1 September.

The water particle displacements caused by the mean flow, the low frequency currents and the tidal flow are summarized in Figure 4-II-7. The tidal currents cause continual cross-shelf near-bottom excursions of approximately 4 km, and longshelf excursions of 1 km. The low frequency currents cause longshelf excursions of approximately 15 km and cross-shelf excursions of 4 km. The excursions for the low frequency currents were calculated as the displacement due to a sinusoidal current with an amplitude of the standard deviation of the low-passed current components and a typical time scale of 5 or 3 days for the longshore and cross-shore current, respectively. The mean net displacement due to the mean current was approximately 12 km for a 10 day period. The mean flow is small compared to the low frequency current fluctuations, and thus the estimate of the mean from the relatively short data series (3 days) is probably not a good measure of the direction of the very long term net flow.

Figure 4-II-7. Typical water particle displacement associated with the mean current (M, computed for 10 days), the low frequency current (LF), and the semidiurnal tidal currents (T). The low frequency excursions were calculated as the displacement due to a sinusoidal current with an amplitude of the standard deviation of the low-passed current components and a typical time scale of 5 or 3 days for the longshore and cross-shore current, respectively. Note that the displacement scale is five times the map scale and thus the displacements are actually small compared to shelf dimensions.

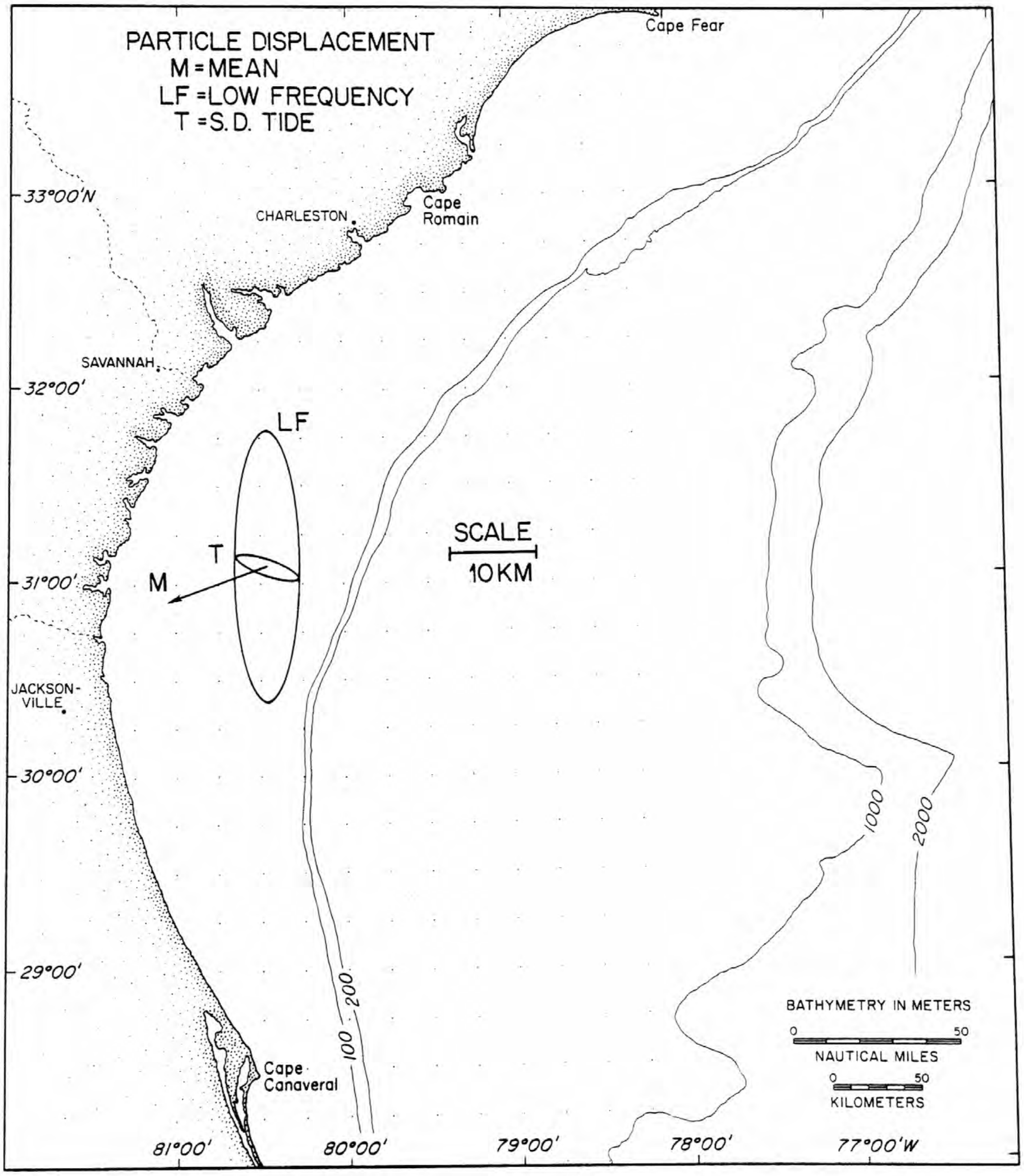
PARTICLE DISPLACEMENT
M = MEAN
LF = LOW FREQUENCY
T = S.D. TIDE
Cape Fear
Cape Romain
CHARLESTON
SAVANNAH
JACKSON-VILLE
Cape Canaveral
33°00'N
32°00'
31°00'
30°00'
29°00'
81°00'
80°00'
79°00'
78°00'
77°00'W
LF
T
M
SCALE
10 KM
100
200
1000
2000
BATHYMETRY IN METERS
0
50
NAUTICAL MILES
0
50
KILOMETERS

Summer Bottom Sediment Movement

The bottom photographs showed that the upper 5-10 cm of the bottom sediments were reworked by organisms, bottom currents, and surface waves during the summer deployment (Figure 4-II-8). On 6-8 August the bottom was generally tranquil but there was active burrowing by bottom organisms (Figure 4-II-9a, b). On 11-12 August there was an increase of suspended sediment in the water. This increase was associated with a decrease in water temperature (Figure 4-II-3c) as a small front moved past the instrument, and suggests an accumulation of suspended material in frontal regions. The turbidity increase also occurred just after a maximum bottom current speed of approximately 40 cm sec^{-1} on 10 August and 35 cm sec^{-1} on 11 August, due to superposition of a mean northward current, the tidal current, and high frequency internal waves (Figure 4-II-3b through 4-II-3d).

On 11-13 August there was intense biological reworking of the surface sediments; the sediments appeared rippled and scoured but the features were not those commonly associated with physical forcing (Figure 4-II-9d). The features disappeared within several hours (Figure 4-II-9e). A small fish was observed on 15 August, apparently forming a trough in the surface sediments (Figure 4-II-9f); similar activity may have caused the surface reworking observed on 13 August.

On 16 August very small ripples were observed orientated north-south, and on 17 August surface scour indicating flow to the north-northwest was apparent (Figure 4-II-9g). Maximum bottom currents greater than 40 cm sec^{-1}, a slight increase in surface wave activity, and a mean low-passed current to the northwest were observed during this period.

From 18-30 August the camera system did not function properly and

Figure 4-II-8. Summary of bottom conditions observed at Station B August-September 1977. The black line indicates periods during which the bottom camera failed to function. The approximate wavelength and symmetry of the ripple marks is indicated. A qualitative assessment of relative water clarity is indicated by shaded circles (more shading means higher turbidity).

Figure 4-II-8

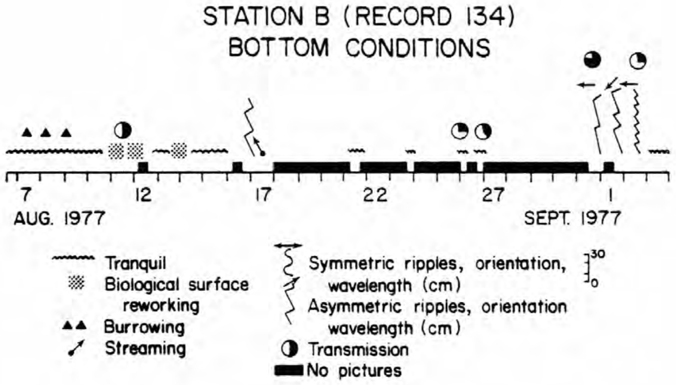
STATION B (RECORD 134)
BOTTOM CONDITIONS
7
12
17
22
27
1
AUG. 1977
SEPT. 1977
Tranquil
Biological surface reworking
Burrowing
Streaming
Symmetric ripples, orientation, wavelength (cm)
Asymmetric ripples, orientation wavelength (cm)
30
0
Transmission
No pictures

Figure 4-II-9. Bottom photographs from Station B August-September, 1977. In all photographs north is toward the upper left corner (arrow in compass indicates magnetic north). The light spots in the picture of 17 August are the early indications of biological fouling on the camera window. By 31 August the camera window was heavily fouled; the ripple marks can be clearly distinguished however.

a. 6 August
b. 8 August
c. 11 August
d. 13 August
e. 14 August (2 hours after previous picture. Greener appearance is due to daylight.)
f. 15 August
g. 17 August
h. 31 August
i. 2 September

Figure 4-II-9a-b

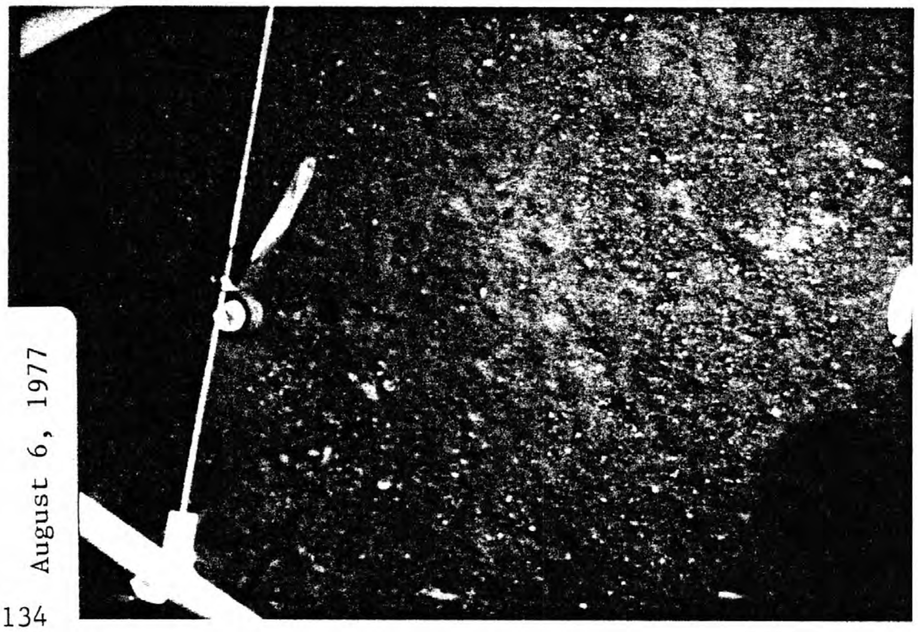
August 6, 1977
134

A

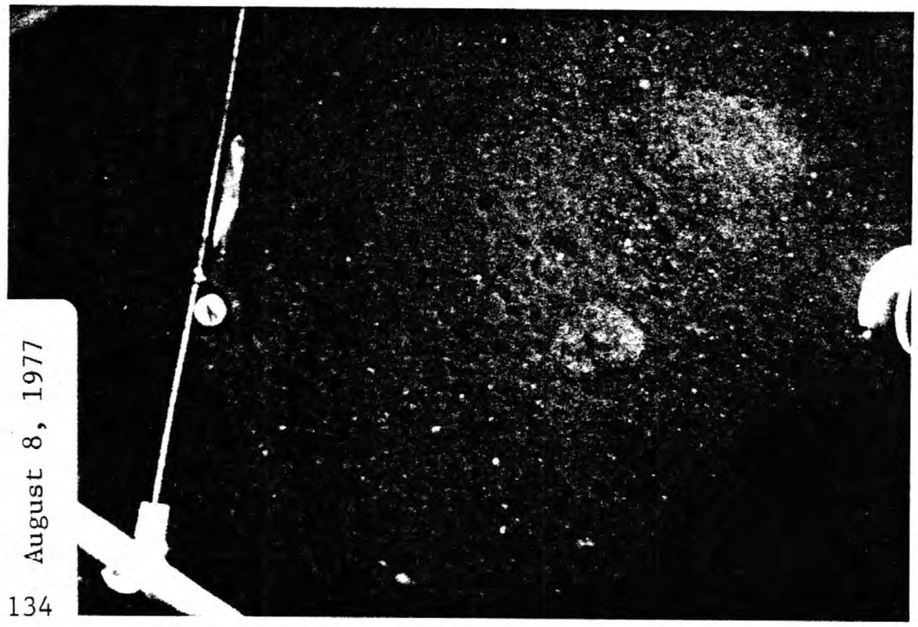
August 8, 1977
134

B

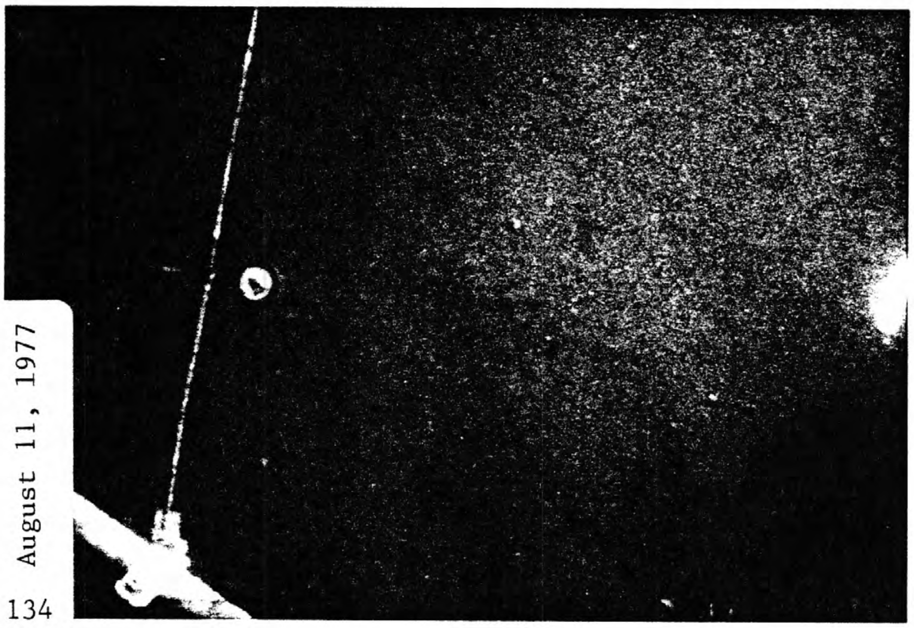

August 11, 1977
134

C

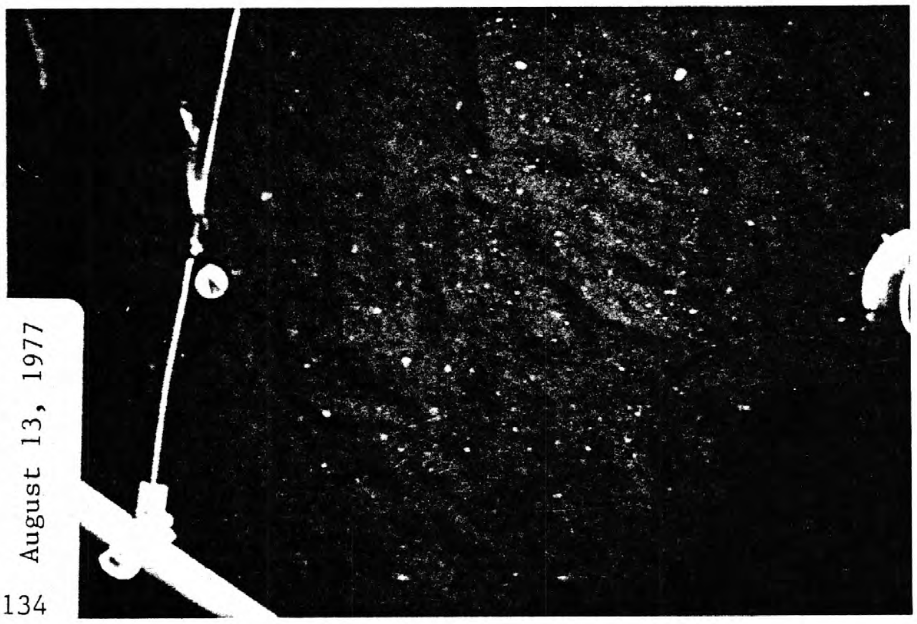

August 13, 1977
134

D

Figure 4-II-9e-f

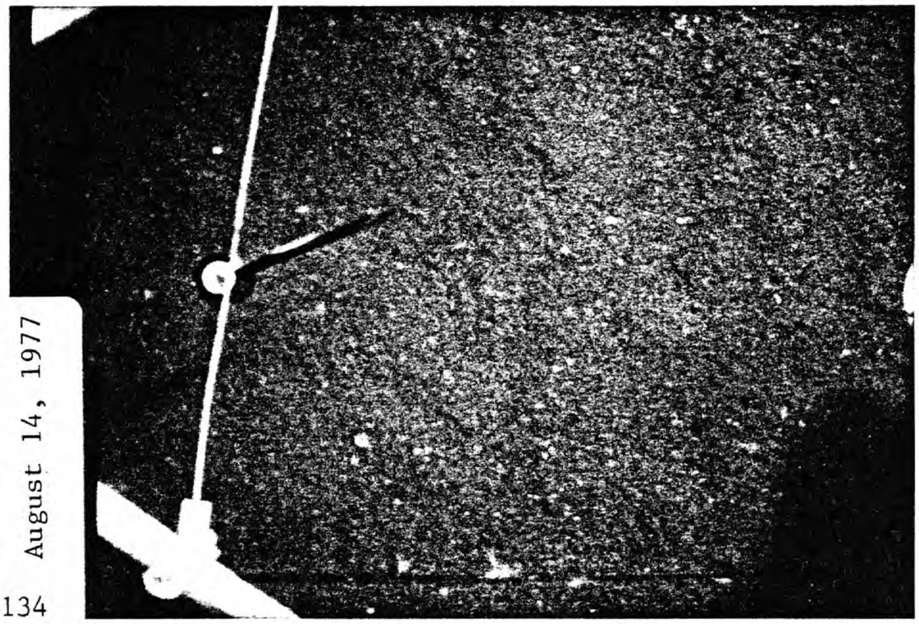
134
August 14, 1977

E

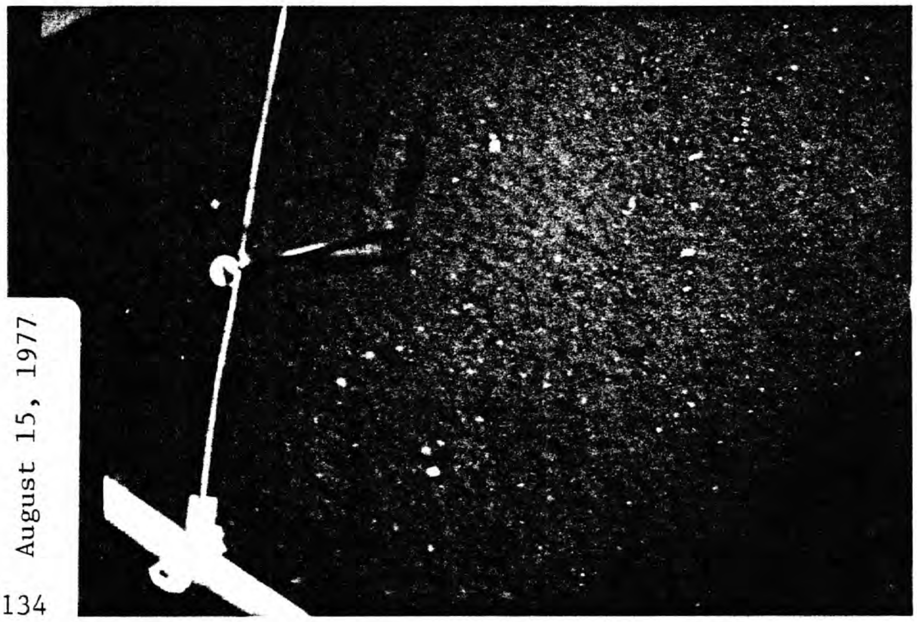
134
August 15, 1977

F

Figure 4-II-9g-h

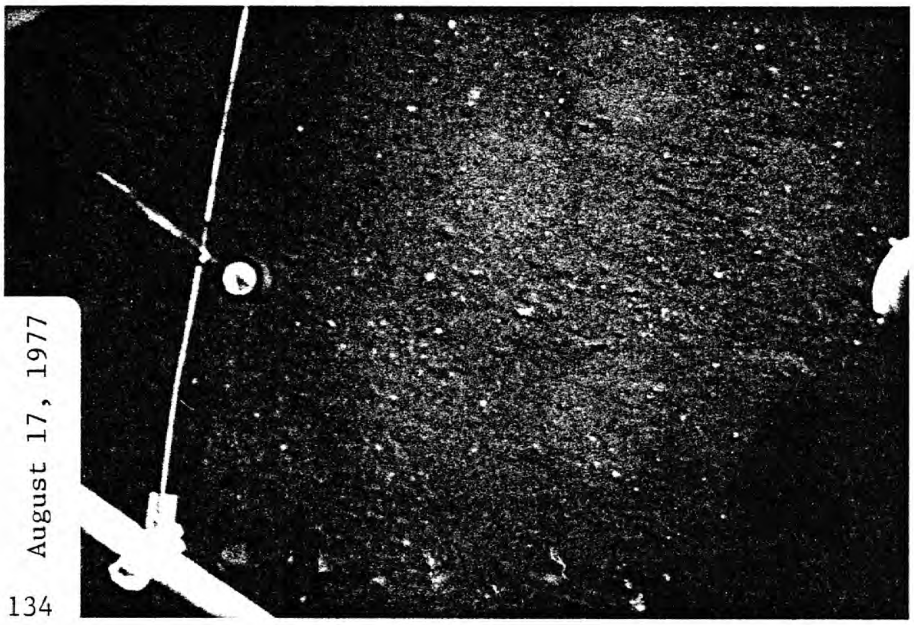
134
August 17, 1977

G

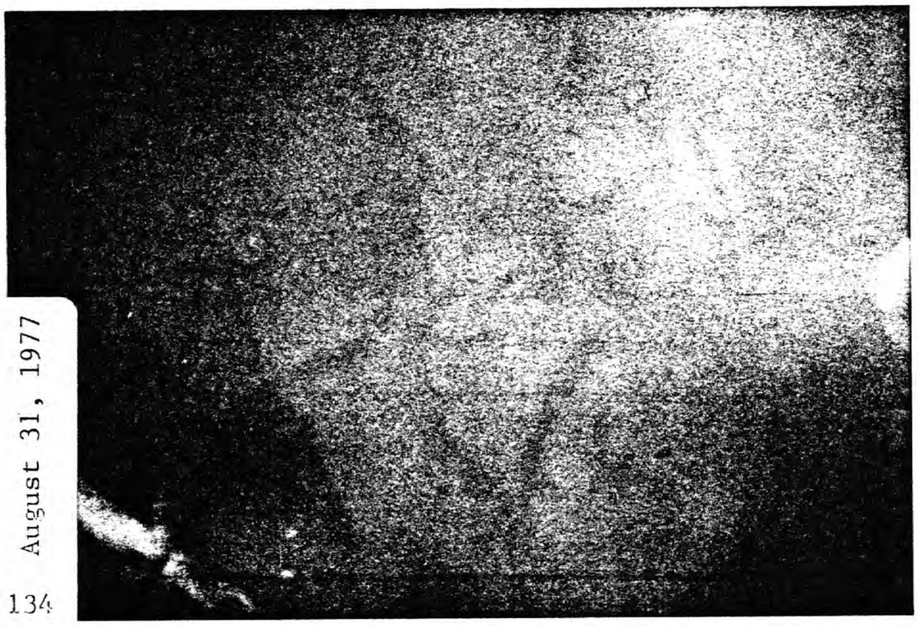
134
August 31, 1977

H

Figure 4-II-9i

September 2, 1977
134

no photographs were obtained. On 1-3 September asymmetric ripples with steep faces toward the west and wavelengths of approximately 30 cm were observed (Figure 4-II-9h). These ripples were observed at the end of a period of large surface wave activity and probably existed throughout the period of surface waves and onshore wind, 27 August-2 September (Figure 4-II-3b). The ripples decreased in wavelength by 2 September but retained the north-south orientation with steep faces toward the west (Figure 4-II-9i). Biological growth on the camera window limited further observations of the bottom after 3 September.

SUMMARY AND CONCLUSIONS

In summary, the summer observations from the short pilot tripod experiment at Station B shows:

1. The bottom currents on the middle part of the South Atlantic Shelf were typically 20 cm sec^{-1} and were dominated by the semidiurnal tide. Superimposed on the tidal currents were low frequency fluctuations of 5-10 cm sec^{-1} probably caused by Gulf Stream intrusions or wind stress and high frequency motions of 5-15 cm sec^{-1} probably associated with internal waves. The mean flow was less than 2 cm sec^{-1}.
2. Maximum currents observed 1 m from the bottom at Station B were approximately 40 cm sec^{-1}.
3. The surficial bottom sediments were reworked by benthic organisms, and occasionally by the near-bottom currents. Asymmetric ripples and surface scour were observed. Bottom features associated with surface reworking disappeared rapidly, typically within one day.
4. No major resuspension of the bottom sediments into the water

column was observed, although an increase in suspended material associated with a near-bottom intrusion of Gulf Stream water was suggested.

These conclusions are based on a relatively short observation period during the tranquil summer months but do show that there was continual reworking of the surficial sediments. The data suggests that any fine material deposited on the sea floor in this region would be dispersed over a wide area quite rapidly. The lack of heavy resuspension of sediments into the water column suggests that no long distance transport of bottom sediments occurred during the observation period. The results are consistent with the surface texture and vibracore observations which suggested reworking of surface sediments but little transport; the medium grained sand in the mid-shelf region is apparently in equilibrium with the typical summer physical forcing. Future observations made in the more eventful winter season or at locations closer to the energetic Gulf Stream may show more frequent and more significant bottom sediment motion as has been observed on the New England Continental Shelf (Butman, Noble and Folger 1979).

ACKNOWLEDGMENTS

W. Strahle and J. West prepared, deployed and recovered the instrument system from the R/V ADVANCE II. M. Noble and S. Conley assisted in the preparation of this report.

LITERATURE CITED

Atkinson, L.P., 1977. Modes of Gulf Stream intrusion into the South Atlantic Bight Shelf waters: Geophysical Research Letters, 4(12), pp. 583-586.

Butman, B., M. Noble, and D.W. Folger, 1979. Long term observations of bottom current and bottom sediment motion on the mid-Atlantic Continental Shelf: Journal of Geophysical Research, in press.

Butman, Bradford and David W. Folger, 1979. An instrument system for long term sediment transport studies on the Continental Shelf: Journal of Geophysical Research, in press.

Bumpus, D.F., 1973. A description of the circulation on the Continental Shelf of the East Coast of the United States: Progress in Oceanography, vol. 6, pp. 111-158.

Flagg, C.N., 1977. The kinematics and dynamics of the New England Continental Shelf and shelf/slope front, Doctoral dissertation: Woods Hole Oceanographic Institution and Massachusetts Institute of Technology. WHOI Ref. No. 77-67, 207 p.

Lee, T. and D.A. Brooks, 1979. Initial observations of current, temperature and coastal sea level response to atmospheric and Gulf Stream forcing on the Georgia Shelf. Submitted to Geophysical Research Letters.

CHAPTER 5

SURFICIAL SEDIMENTS OF THE U.S. ATLANTIC SOUTHEASTERN UNITED STATES CONTINENTAL SHELF

Orrin H. Pilkey[1], Fred Keer[1], and Stephanie Keer[1]

---

[1] U. S. Geological Survey, Duke University, Durham, North Carolina 27708

Chapter 5

Table of Contents

Page

Abstract 5- 1

Introduction 5- 1

  Sample Locations 5- 2

Results 5- 6

  Mean Grain Size 5- 6

  Total Sediment Color 5-10

  Carbonate Color 5-17

  Non-Carbonate Color 5-24

  Sediment Lithofacies 5-29

Summary of Conclusions 5-38

Literature Cited 5-40

CHAPTER 5

SURFICIAL SEDIMENTS OF THE U.S. ATLANTIC SOUTHEASTERN UNITED STATES CONTINENTAL SHELF

Orrin H. Pilkey, Fred Keer, and Stephanie Keer

ABSTRACT

Over 1,500 surficial sediment samples from the Florida-Hatteras Shelf and upper slope were examined to furnish baseline information on surficial sediment properties. Parameters such as mean grain size, total sediment color, carbonate color, non-carbonate color, and sediment lithofacies were recorded and surficial maps were made showing their distribution.

The distribution of surficial sediment parameters suggests the following general conclusions: although patchiness occurs, nearshore sediments tend to be fine-grained sand whereas central and outer shelf tend to be coarse grained. Slope sediments are also fine-grained. These areas of fine-grained materials may mark locations where deposition exceeds winnowing; the patchiness of carbonate and non-carbonate color suggests that long distance lateral transport and regional mixing of surficial sediments are not important processes. Similarly, the overall picture of surficial sedimentation suggests that little material is being added to the shelf at the present time.

INTRODUCTION

The following discussion is based on an investigation of over 1,500 continental shelf samples collected mainly by Duke University and also by the University of Georgia Marine Institute and by the Woods Hole Oceanographic Institution-U.S. Geological Survey program. This represents the most densely sampled large continental shelf area in the world and provides at least in a relative sense, a firm basis to speculate on sedimentary processes.

The ultimate purposes of this regional investigation are to furnish baseline information concerning shelf surficial sediment properties and to determine what processes of sedimentation are going on at the present time. Of a specific interest are sedimentation activities that could affect future continental shelf development activities. This investigation is made in the context of perhaps 30 technical papers concerned with sediments in this area, published in scientific journals during the last decade.

Surficial sediments are only part of the story and observations such as those discussed here must be reinforced by third dimension studies (cores) and by measurements of in situ physical properties of shelf waters.

Sample Locations

Sample locations are shown in Figures 5-1 through 5-3. Most of these are from the Duke University sample collection. Georgia shelf samples were collected using the University of Georgia Marine Institute facilities. They were obtained by a variety of means, but primarily by a Pierce box dredge. This is a non-quantitative sampler; i.e., it is dragged along the bottom and area or sediment depth sampled is unknown. Maximum sediment depth sampled is likely to be about 10 cm. In areas of sparse samples in the Duke Collection, additional samples were obtained from the Woods Hole Oceanographic Institution-U.S. Geological Survey sample collection. These are mostly from the South Carolina and North Florida shelf. The very detailed linear transects off Georgia and Florida were carried out in order to best observe expected linear trends in sediment properties paralleling the present shoreline (Late

Figure 5-1. Sample locations; Cape Hatteras vicinity and north. Letters and arrows on right side designate latitudinal bands used in averaging regional trends.

Figure 5-1

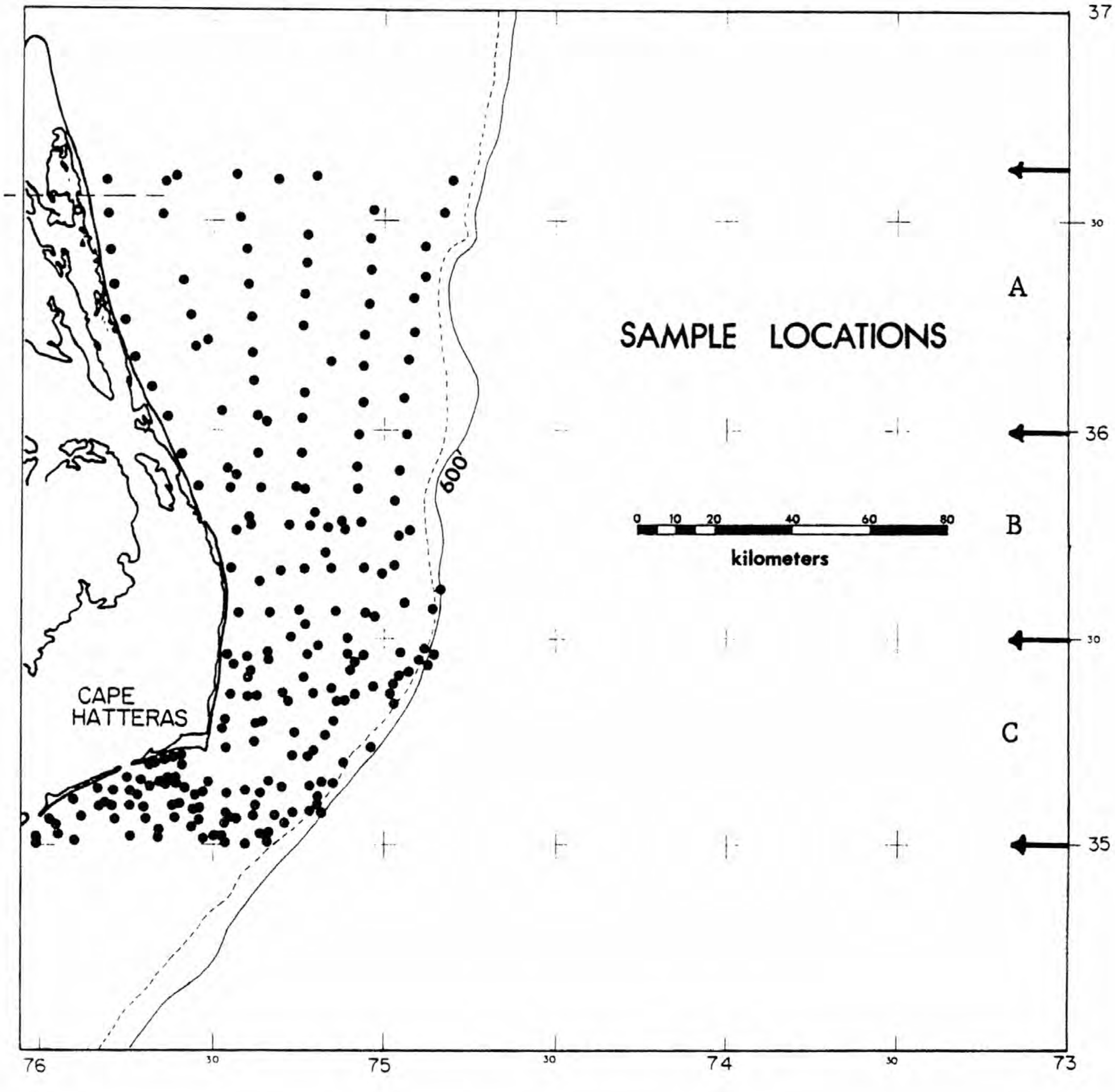
SAMPLE LOCATIONS
CAPE HATTERAS
600
0
10
20
40
60
80
kilometers
A
B
C
37
30
36
30
35
76
30
75
30
74
30
73

Figure 5-2. Sample locations on the North Carolina Shelf.

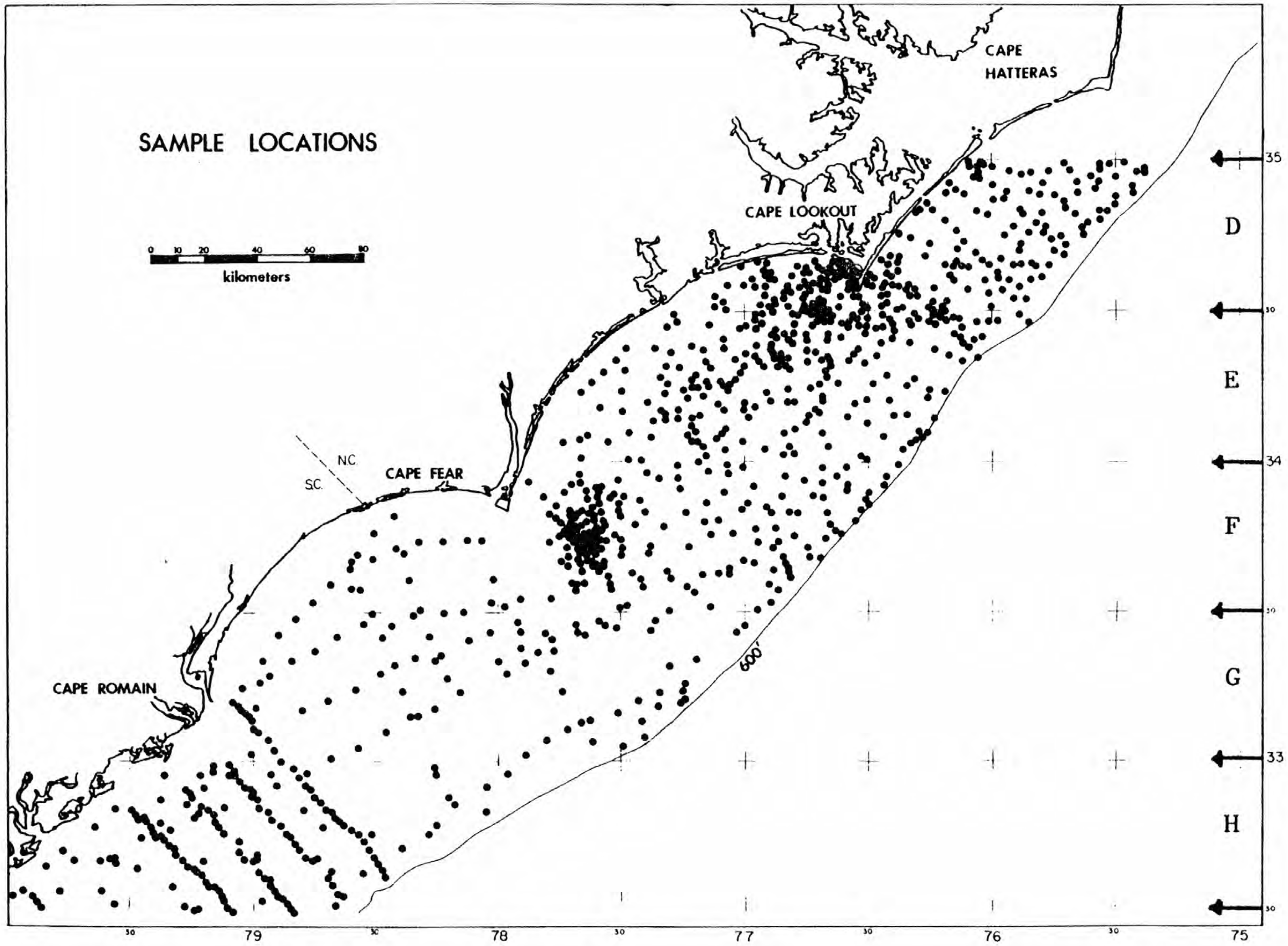
SAMPLE LOCATIONS
CAPE HATTERAS
CAPE LOOKOUT
CAPE FEAR
CAPE ROMAIN
N.C.
S.C.
0 10 20 40 60 80
kilometers
600'
D
E
F
G
H
35
30
34
30
33
30
30
79
30
78
30
77
30
76
30
75

Figure 5-2

Figure 5-3. Sample locations on the continental shelf off Georgia, South Carolina, and north Florida.

Figure 5-3

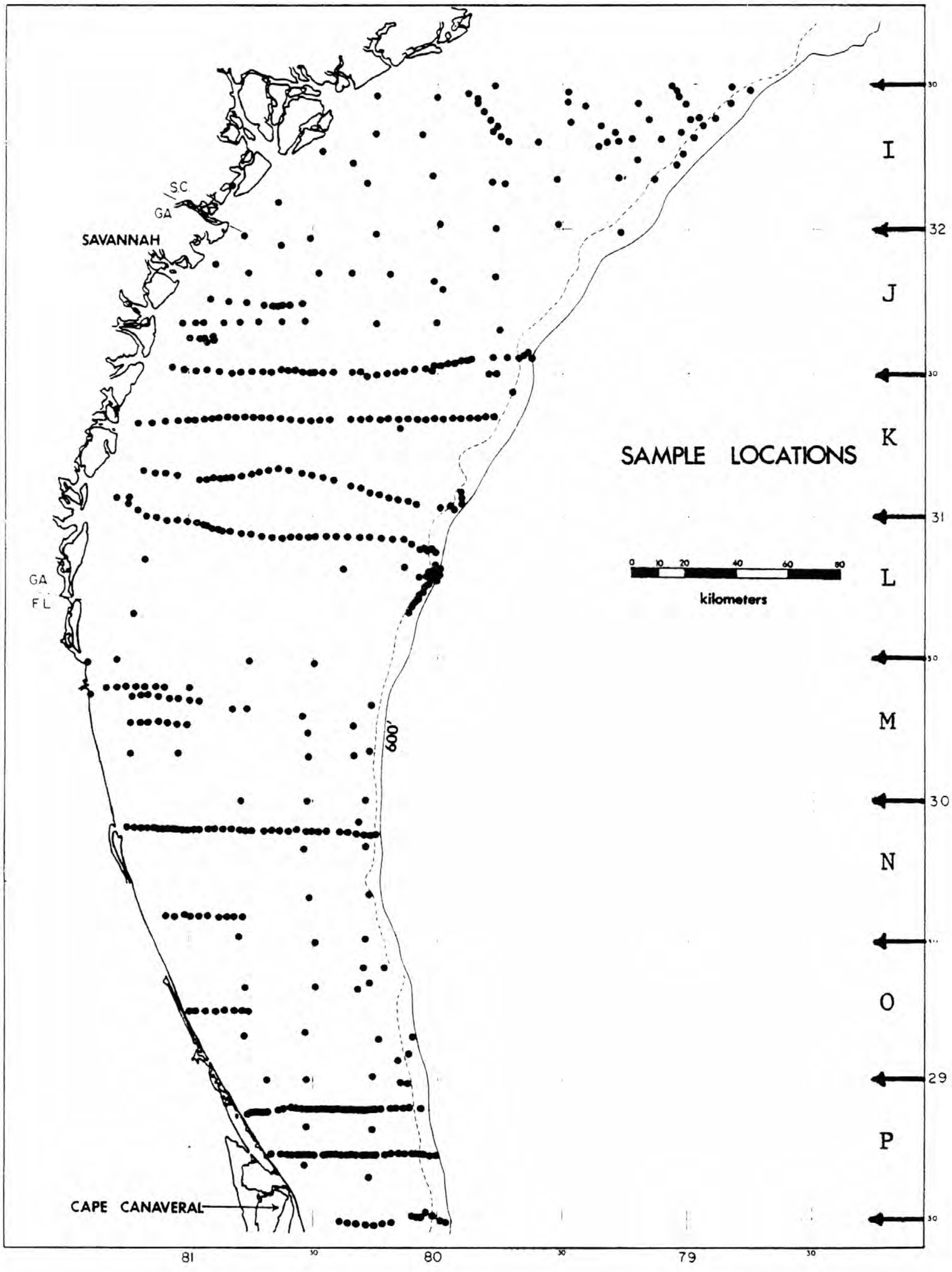
SAMPLE LOCATIONS
SC
GA
SAVANNAH
GA
FL
CAPE CANAVERAL
600'
0 10 20 40 60 80
kilometers
I
J
K
L
M
N
O
P
30
32
30
31
30
30
29
30
81
30
80
30
79
30

Pleistocene-Early Holocene shoreline features).

Navigation used in sample collection ranged from Loran A to Loran C to satellite navigation for the most recently collected samples. Taken as a whole, however, navigation control can be considered to be no better than the poorest method used, which is Loran A.

On the right hand margins the letters and arrows delineate the latitudinal bands used to illustrate regional trends of various sediment properties in Figures 5-8, 5-12, 5-16, and 5-20. That is, certain sediment characteristics such as color and lithofacies designations were averaged along these strips in order to more clearly delineate north-south trends. Letter designations in the right hand column are shown adjacent to the appropriate column illustrating percentages in Figures 5-8, 5-12, 5-16, and 5-20.

RESULTS

Mean Grain Size

Mean grain size of surficial shelf sediments is illustrated in Figures 5-4 and 5-5. This is mean grain size of total samples.

Grain size of the surficial shelf sediment cover is a highly variable parameter with rapid local changes over short distances. This was first noted by Gorsline (1963) in his investigation of the Southeastern U.S. shelf. He observed that multiple samples from the same location, within limits of navigational accuracy, were quite different. Thus, we know the grain size of sediments of this area can be characterized as being "patchy." By choosing the rather broad categories of coarse, medium, and fine sand, the patchiness is reduced (Figures 5-4 and 5-5). Broad categories such as this also minimize the possibility of finding artificial differences in sediment type

Figure 5-4. Areal distribution of mean grain size; Cape Hatteras to Cape Romain.

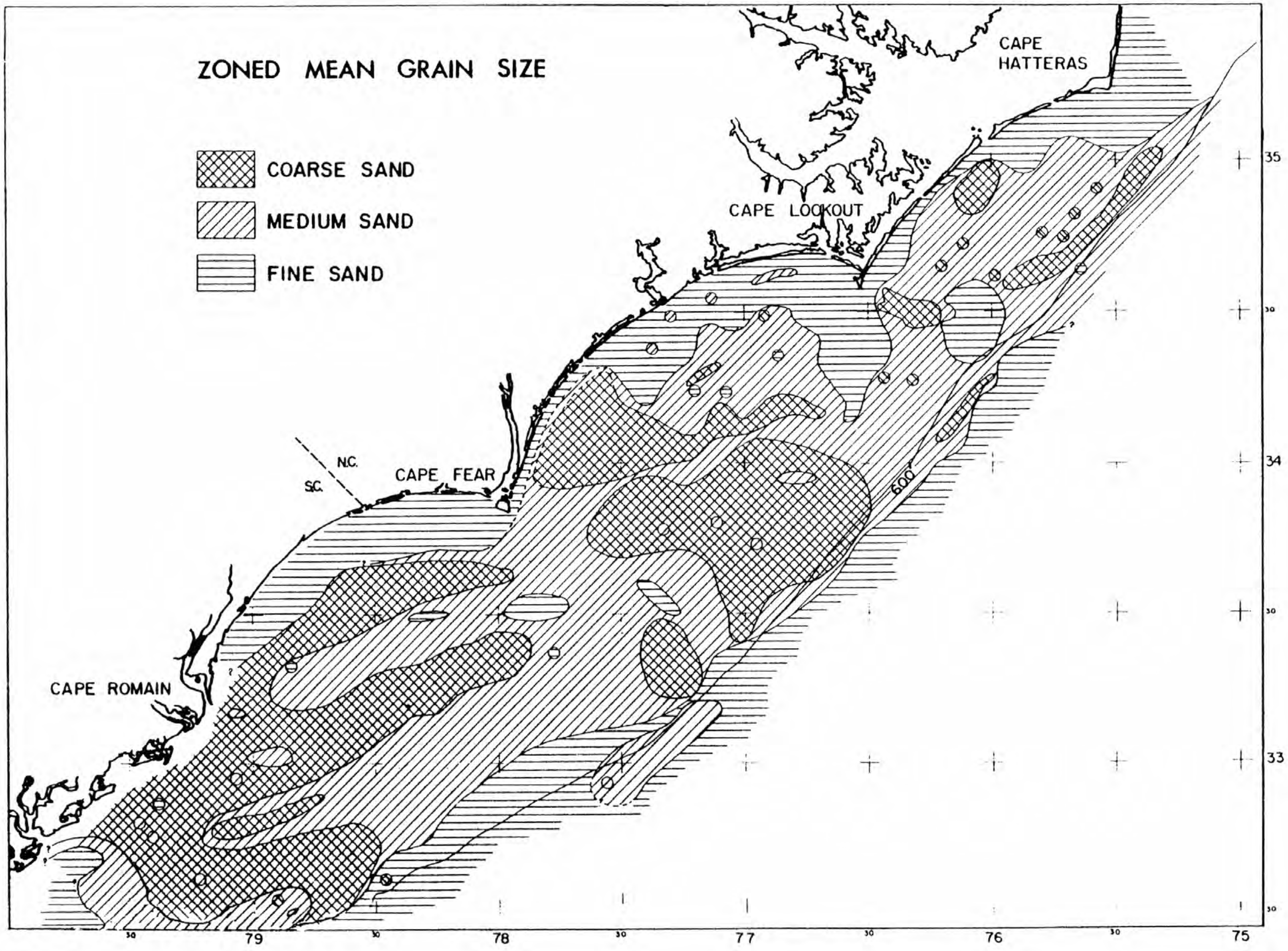
ZONED MEAN GRAIN SIZE

COARSE SAND
MEDIUM SAND
FINE SAND
CAPE HATTERAS
CAPE LOOKOUT
CAPE FEAR
CAPE ROMAIN
N.C.
S.C.
600
35
30
34
30
33
30
30
79
30
78
30
77
30
76
30
75

Figure 5-4

Figure 5-5. Areal distribution of mean grain size; Cape Romain to Cape Canaveral.

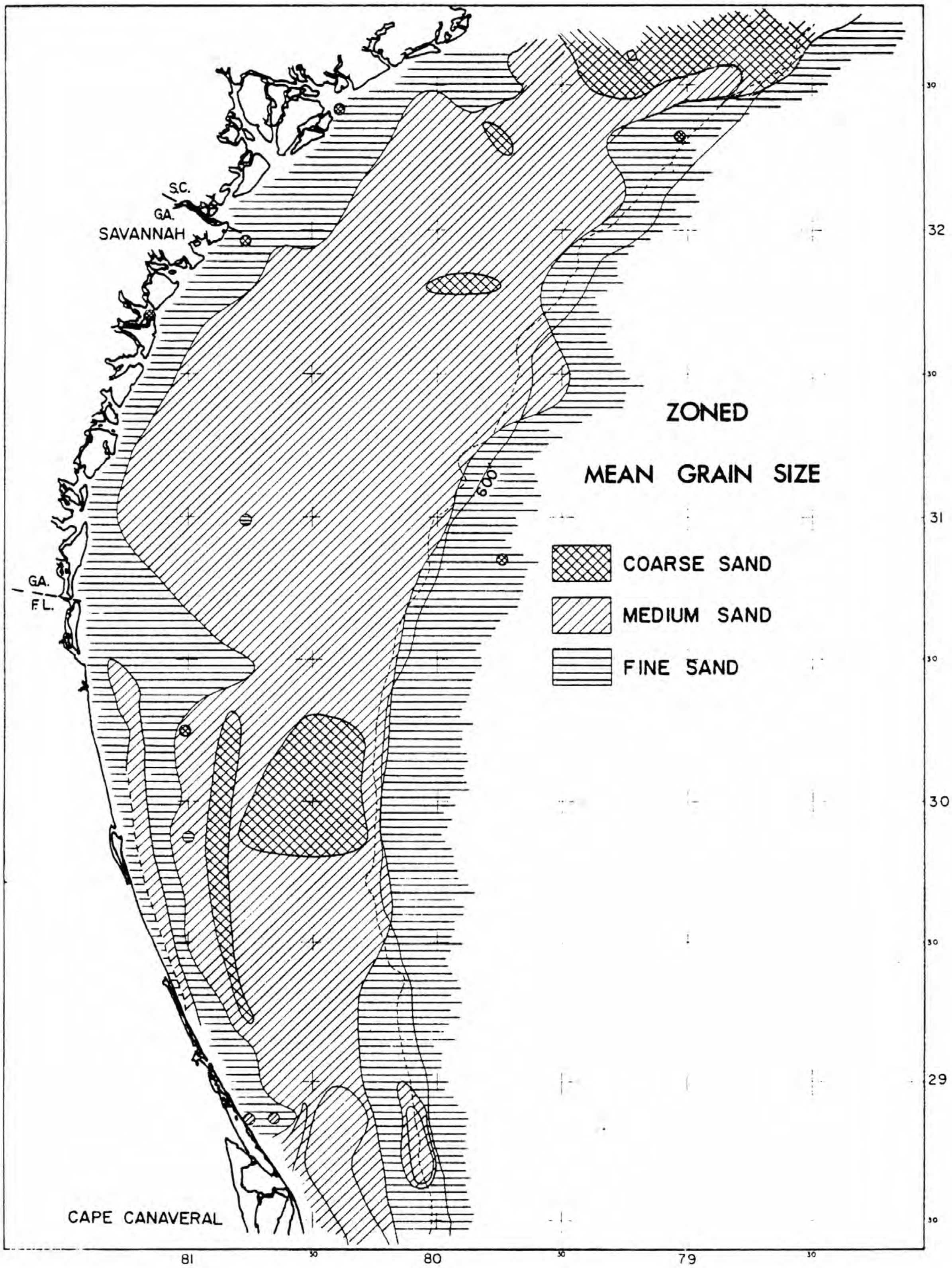
S.C.
GA.
SAVANNAH
GA.
F.L.
CAPE CANAVERAL
ZONED
MEAN GRAIN SIZE
COARSE SAND
MEDIUM SAND
FINE SAND
600
32
31
30
29
81
80
79

distribution due to: (1) different techniques of grain size analysis, and (2) inter-institution differences in instrumentation.

In interpretation of Figures 5-4 and 5-5, it is important to compare them with Figures 5-1 through 5-3, showing the distribution of sample locations. Some grain size attributes, particularly patchiness, might be related to sample density. Obviously, heavily sampled areas (such as Onslow Bay, North Carolina) are more likely to show patchiness than sparsely sampled areas (such as the South Carolina shelf).

In general terms, the grain size distribution of surficial sediments on the Southeastern U.S. shelf is as follows: nearshore grain size tends to be in the fine sand range; on the central and outer shelf grain size tends to be in the medium to coarse range; and, immediately over the shelf break grain size again is in the fine sand range. The nearshore fine sand band includes the shoals extending off Cape Hatteras and Cape Lookout (Figure 5-4). Although this cannot be determined from Figures 5-4 and 5-5, the nearshore fine sand band is particularly well developed off North Florida, Georgia and Southern South Carolina.

There are also general north to south trends as well. The South Carolina, Georgia and North Florida shelves are covered with medium sand with the exception of a couple of major patches of coarse sand off North Florida. From Cape Romain shoals north, patches of coarse sand become very important. Frequently such patches are shell hashes or at least have high $CaCO_3$ concentrations.

The transition from medium or coarse sand to fine sand and silt on the uppermost slope occurs rapidly. Depth of the abrupt change ranges from 100 to 300 m and in all cases is at greater depths than the shelf break.

Patchiness is greatest to the north, particularly in Onslow Bay, between Capes Lookout and Fear. Although sample density is highest in this area, which would naturally increase the likelihood of patchiness, nonetheless it is believed the north-south differences in patchiness are real.

It was observed that fine sands were almost always micaceous with some exceptions off North Florida. Occasionally medium sands were micaceous. Since fine sand size mica is hydraulically equivalent to mud, it has been suggested that the mica content of sediment should be an accurate indicator of areas of deposition (Doyle _et al_ 1968). Abundant mica would indicate a given shelf area to be a potential sink for fine grained size pollutants. This is an area of research well worth pursuing.

Total Sediment Color

Total or general sediment color refers to the overall color of the sediment sample. This is based on the megascopic appearance of dried samples residing in small plastic boxes. This is a difficult parameter to judge as a great deal of gradation exists between the color classification types shown in Table 5-1. Because of the complexity of classification, only the densely sampled shelf areas between Cape Romain, South Carolina, and the Virginia State Line were studied in this regard.

Table 5-1 lists some very generalized attributes of the major color groupings. It is likely that no two investigators would choose the same groups or number of groupings. Basically, four color groupings are used. The green and the gray groups and the reddish brown and the multicolor groups are combined for illustration in Figures 5-6 through 5-8. A fifth group, termed undifferentiated, was used to collect everything that did not fall into other classifications. To have

Table 5-1. Generalized attributes of the various groupings based on color appearance of total samples. Areal distribution of these groups is shown in Figures 5-6 through 5-8.

Group Name	Descriptive Color	Carbonate Content	Noncarbonate Content	Primary Reason for Color	Grain Size Tendency
salt and pepper	white with black specks	less than 10%	almost pure quartz	white quartz sand with phosphorite, manganese, black shells	fine to medium sand
green**	medium to dark greenish grey	less than 5%	quartz, mica, clays	presence of clays and mica; fine grain size	silt
grey**	dirty white to grey	0% to 25%	quartz	greyish quartz and grey-stained shells	fine to medium sand
reddish brown*	dark reddish brown and brown	5% to 30%	mostly quartz; up to 10% phosphorite	iron-staining and presence of phosphorite	medium to coarse sand
multicolor*	mixture of brown, grey, black, and white grains	5% to 30%	quartz and phosphorite	phosphorite; black and iron-staining of carbonate and quartz	medium to coarse sand
orange-yellow	dirty yellow to dirty orange-brown	less than 1%	quartz	iron-staining of quartz	fine to medium to coarse sand
undifferentiated	did not satisfactorily fall into any one color group	5% to 30%	quartz and phosphorite	all or any of the above reasons for color	

*These two groups plotted as one group.
**These two groups plotted as one group.

reasonably classified every sample into a pigeon hole might have resulted in another six to eight group names.

It is apparent from Table 5-1 that the presence or absence of iron staining of quartz, feldspar, and carbonate grains is usually the main factor determining sediment color. Oxidized iron oxide, generally limonite or goethite, produces a yellow stain which gives the sediment an overall yellow or brown color (groups 4, 5, and 6, Table 5-1). In groups 1, 2, and 3 the quartz and feldspar is generally unstained; hence the more typical gray appearance of these samples. Usually of secondary importance in determining overall sediment color is the carbonate fraction and phosphorite grains. Locally, however, these can be of critical importance. For example, the "pepper" in the salt and pepper group can be either black shells or phosphorite, and occasionally both. Phosphorite is generally most important in Georgia shelf sediments. Elsewhere, the dark colored specks are typically black shell fragments. Shell material can also impart a brown or grayish color to sediments. Phosphorite is usually black, but locally is brown colored, most notably in an area of unusually abundant phosphorite northeast of Cape Fear, North Carolina in Onslow Bay.

Typically the feldspar content of Southeastern U.S. shelf sediments is of the order of 5 to 15% of the total carbonate-free sediment (Field and Pilkey 1969).

Figure 5-6 shows the areal distribution of total or general sediment color north of Cape Hatteras. Relative to areas to the south, the pattern is simple. It consists of two sediment types: those with a gray green color and those with an orange yellow aspect.

To the south, the distribution of total sediment color becomes more patchy and complex (Figure 5-7). This is especially true in Onslow Bay,

Figure 5-6. Areal distribution of total sediment color north of Cape Hatteras.

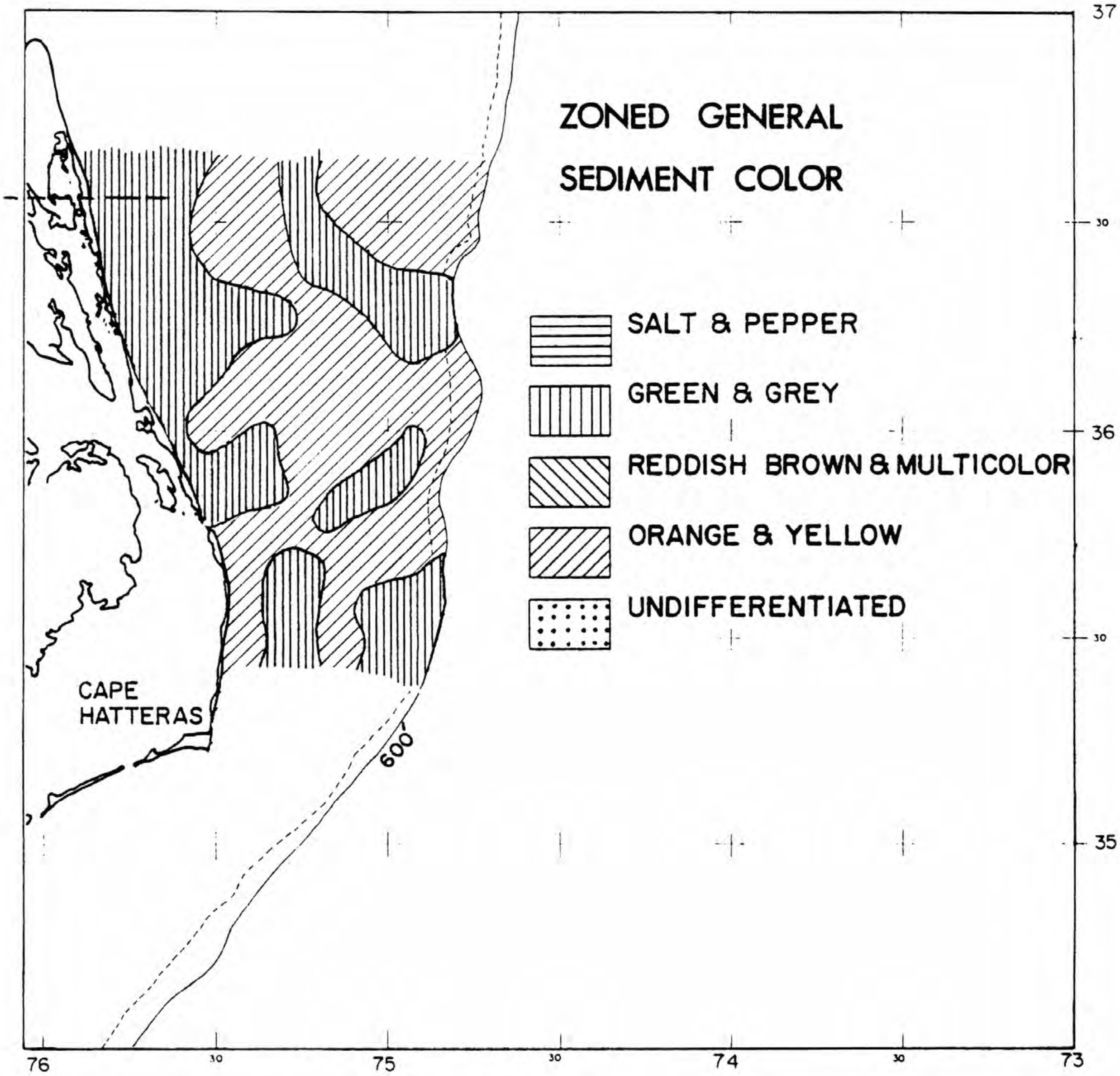
ZONED GENERAL SEDIMENT COLOR
SALT & PEPPER
GREEN & GREY
REDDISH BROWN & MULTICOLOR
ORANGE & YELLOW
UNDIFFERENTIATED
CAPE HATTERAS
600
37
30
36
30
35
76
30
75
30
74
30
73

Figure 5-7. Areal distribution of total sediment color; Cape Hatteras to Cape Romain.

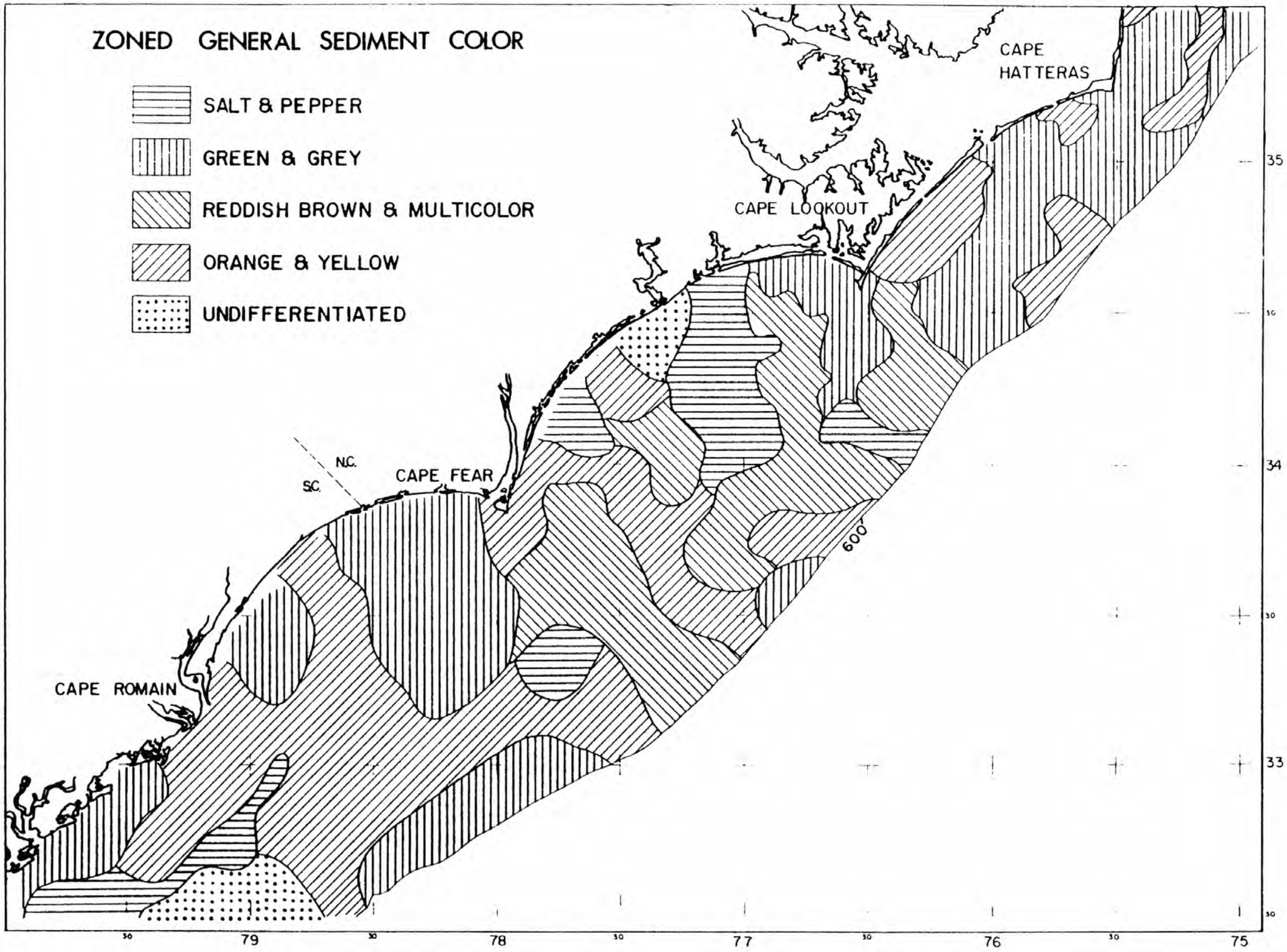
ZONED GENERAL SEDIMENT COLOR
SALT & PEPPER
GREEN & GREY
REDDISH BROWN & MULTICOLOR
ORANGE & YELLOW
UNDIFFERENTIATED
CAPE HATTERAS
CAPE LOOKOUT
CAPE FEAR
N.C.
S.C.
CAPE ROMAIN
600
35
34
33
30
79
78
77
76
75

Figure 5-7

the shelf segment between Cape Lookout and Cape Fear. This must reflect the fact that Onslow Bay is a unique shelf area relative to other areas on the southeastern U.S. shelf (Cleary and Pilkey 1967). No Piedmont rivers empty into the shelf here and as a consequence, rate of sedimentation on the shelf during sea level fluctuations has been very low. Tertiary and Pleistocene rock outcrops abound because of the low rate of sedimentation and these furnish much sediment to the shelf sea floor. This variety of sources most likely is responsible for the patchy color type distribution. Raleigh Bay (between Capes Hatteras and Lookout) and Long Bay (between Capes Lookout and Romain) generally exhibit a color distribution similar to the shelf north of Cape Hatteras (Figure 5-6).

Figure 5-8 is a series of bar graphs which better show regional trends of total sediment color of continental shelf sediments. Letters on the right side of the bar graphs refer to the latitudinal bands shown in Figures 5-1 and 5-2. Averages of all samples within a given band are used to construct the bar graph adjacent to each letter on Figure 5-8. Unfortunately, the northeast-southwest trend of the Hatteras-Romain shoreline of North and South Carolina causes some of the bands to cut across the shelf "bays". The overall importance of the green and gray and reddish brown-multi color sediment color groups is apparent as these dominate the bar graphs. Bar graph E includes most of the Onslow Bay shelf and it clearly illustrates the complexity of that shelf area. Subdivisions exhibiting regional trends include the gray and green sediment color group, which tends to become less important in a southerly direction and the reddish brown-multi color group, which is restricted to the central portion of the area of investigation.

Environmental conclusions based on the total sediment color are

Figure 5-8. Bar graphs showing latitudinal averages of total sediment color. Latitudinal bands are labelled on Figures 5-1 and 5-2.

TOTAL SEDIMENT COLOR

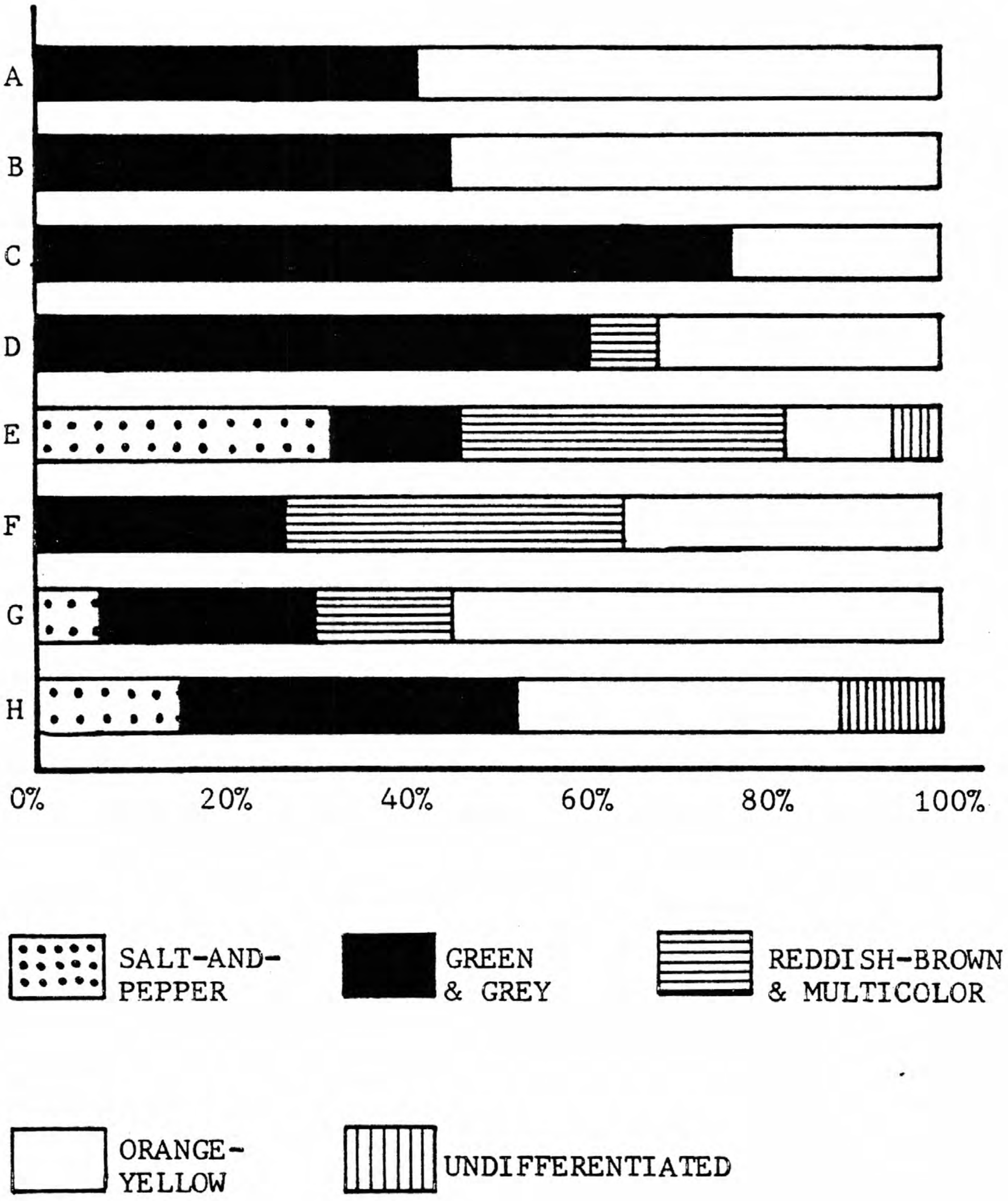

very generalized at best because of the many avenues by which a sediment obtains its overall color (Table 5-1). The general patchiness of this attribute, however, does indicate that regional sediment mixing may not be important. That is, long distance lateral transport and consequent homogenization is minimal.

Carbonate Color

Carbonate and non-carbonate color involve properties of individual grains rather than of entire samples. Individual grains of calcareous material were observed under 30x power with a binocular microscope and were classified into three color groups. These are white ("unstained"), brown, and grey-black. Each total sample was classified according to the most abundant carbonate fraction color class.

Each of these color types has some environmental significance and can be an important indicator of both past history and present processes (Doyle 1967; Pilkey _et al_ 1969). More research is needed to quantify the environmental significance of carbonate staining.

White unstained shells are those with either original coloration or "shiny white" appearance, indicating probably original color. Original coloration does not necessarily mean the shells are newly produced and deposited. For example, some 7,000-9,000 year old shells on North Carolina's beaches apparently have original coloration. Time required for "bleaching", aging, or staining under subaqueous conditions is not precisely known.

One statement that can be made with some degree of certainty is that a sediment dominated by unstained shells has not undergone previous storage as a beach or lagoon sediment.

Brown shells are believed to owe their color to limonite filling of microborings made by sponges, algae, and fungi. This is assumed to occur principally under subaerial conditions, hence the brown color of most southeastern U.S. beaches with high carbonate content. If the foregoing assumption is true, the presence of brown shells indicates some or all of the carbonate fraction has been left behind from a pre-existing beach environment. Thus, the carbonate fraction owes its presence to conditions no longer in existence; again the sediment must be relict.

Black shells are stained by burial in mud, a process that may take only weeks. The black coloration is probably due to pyrite formation, perhaps in conjunction with alteration of the organic matrix. Since for all practical purposes, there is no mud on the shelf, it can be assumed that a blackened shell fragment went through the estuarine or lagoonal environment at one time in its history. If the shell fragment is presently located on the open shelf, it must be relict.

Grey shell fragments are "bleached" and appear to have "aged" on the sea floor. Since both black and grey denote old material, they are classified together.

Figures 5-9 through 5-11 show the areal distribution of the color of the carbonate fraction in southeastern U.S. shelf sediments. It is important to again emphasize that this is based on examination of total samples, not individual size fractions. Thus, most particles involved in the statistical count are sand size particles, not the occasional large whole shell which in terms of particle abundance, is a rarity on the shelf.

There are clearcut regional differences in the color of carbonate materials. North of Cape Hatteras unstained and white shell fragments predominate. The Raleigh and Onslow Bay shelf sectors are dominated by grey-black shells. In Onslow Bay are found the only large patches of

Figure 5-9. Areal distribution of color of the carbonate fraction north of Cape Hatteras.

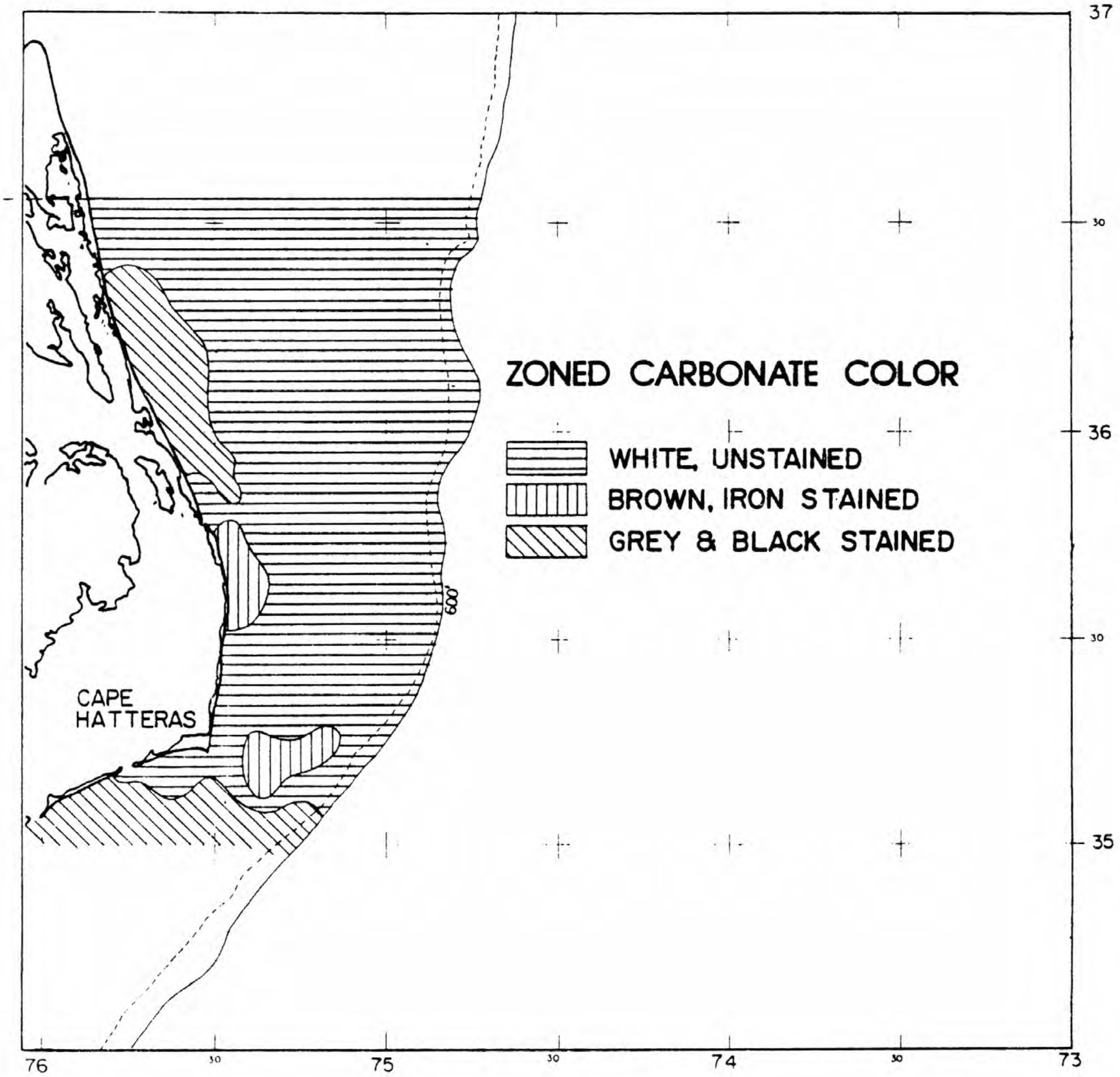
ZONED CARBONATE COLOR
WHITE, UNSTAINED
BROWN, IRON STAINED
GREY & BLACK STAINED
CAPE HATTERAS
600'
37
30
36
30
35
76
30
75
30
74
30
73

Figure 5-10. Areal distribution of color of the carbonate fraction; Cape Hatteras to Cape Romain.

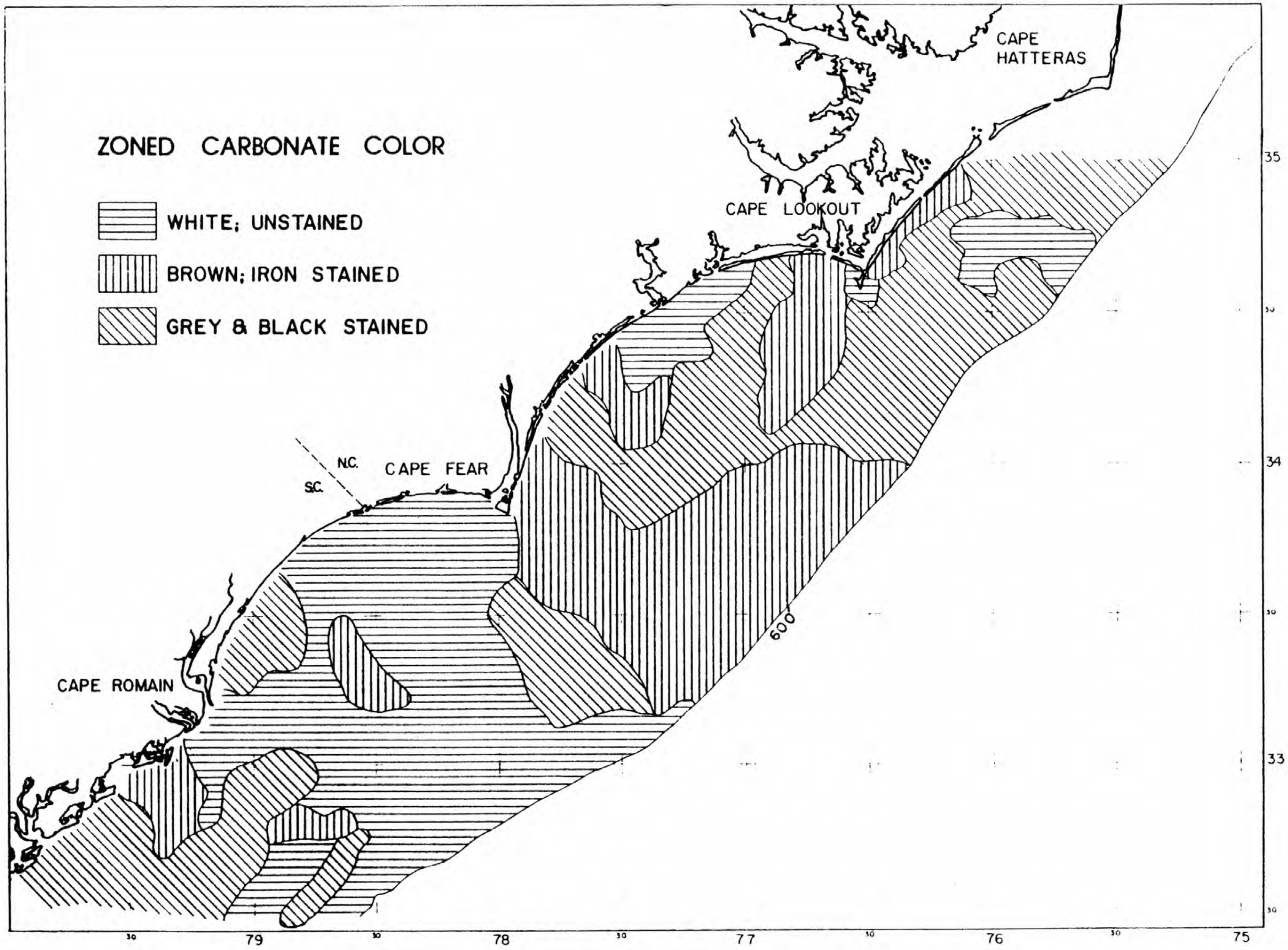
ZONED CARBONATE COLOR
WHITE; UNSTAINED
BROWN; IRON STAINED
GREY & BLACK STAINED
CAPE HATTERAS
CAPE LOOKOUT
CAPE FEAR
N.C.
S.C.
CAPE ROMAIN
600
35
34
33
30
79
78
77
76
75

Figure 5-10

Figure 5-11. Areal distribution of color of the carbonate fraction; Cape Romain to Cape Canaveral.

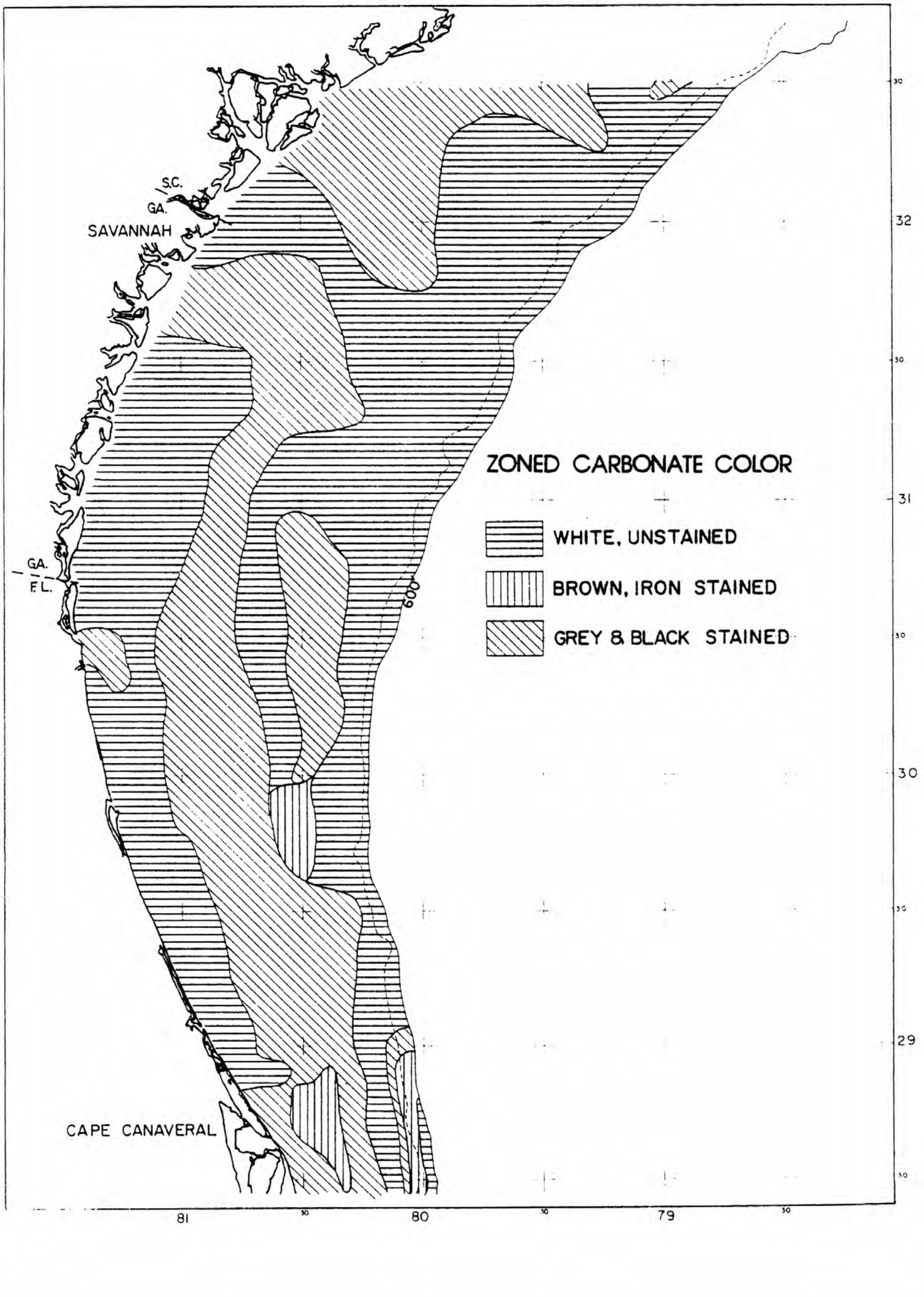
ZONED CARBONATE COLOR
WHITE, UNSTAINED
BROWN, IRON STAINED
GREY & BLACK STAINED
S.C.
GA.
SAVANNAH
GA.
FL.
CAPE CANAVERAL
600
32
31
30
29
81
80
79

brown shells observed anywhere on the southeastern U.S. study area. From Cape Fear south, white-unstained shells dominate with large areas of black shell occurrences, particularly off Cape Romain and on the central shelf of South Carolina, Georgia, and North Florida.

Figure 5-12 shows regional abundance differences along the latitudinal bands shown in Figures 5-1 through 5-3. Latitudinally, grey-black shells can be seen to be bimodaly distributed with a high in Onslow Bay and a second area of abundant grey-black shells off North Florida. Brown shell abundance is clearly anomalously high off North Carolina. Also samples with carbonate fractions dominated by brown shells are overall much less abundant than those with grey-black or unstained-white shell fragments.

One interpretation of Figure 5-12 is as follows: shelf areas north of Hatteras and the Georgia, South Carolina shelf have had relatively high rates of sedimentation during the last sea level rise compared to North Carolina (Raleigh and Onslow Bay) and North Florida. That is, the abundance of brown and black shells in the latter shelf areas indicates that carbonate fraction was relatively undiluted by fluvial sediment as the shoreline moved across the shelf. Thus, shell fragments with coloration reflecting beach, lagoon, and shelf environments are mixed together. Off Georgia and South Carolina and north of Hatteras, beach and lagoon-derived shell fragments were slightly more diluted by fluvial material during the last transgression and a shelf-derived carbonate fraction predominates. Presumably, the Holocene-Pleistocene sediment cover should be regionally thickest in areas where the carbonate fraction coloration reflects shelf derivation.

Shell coloration or staining could possibly be used locally as a simple means to delineate areas where virtually no sedimentation is

Figure 5-12. Bar graphs showing latitudinal averages of color of the carbonate fraction. Latitudinal bands are labelled on Figures 5-1 through 5-3.

Figure 5-12

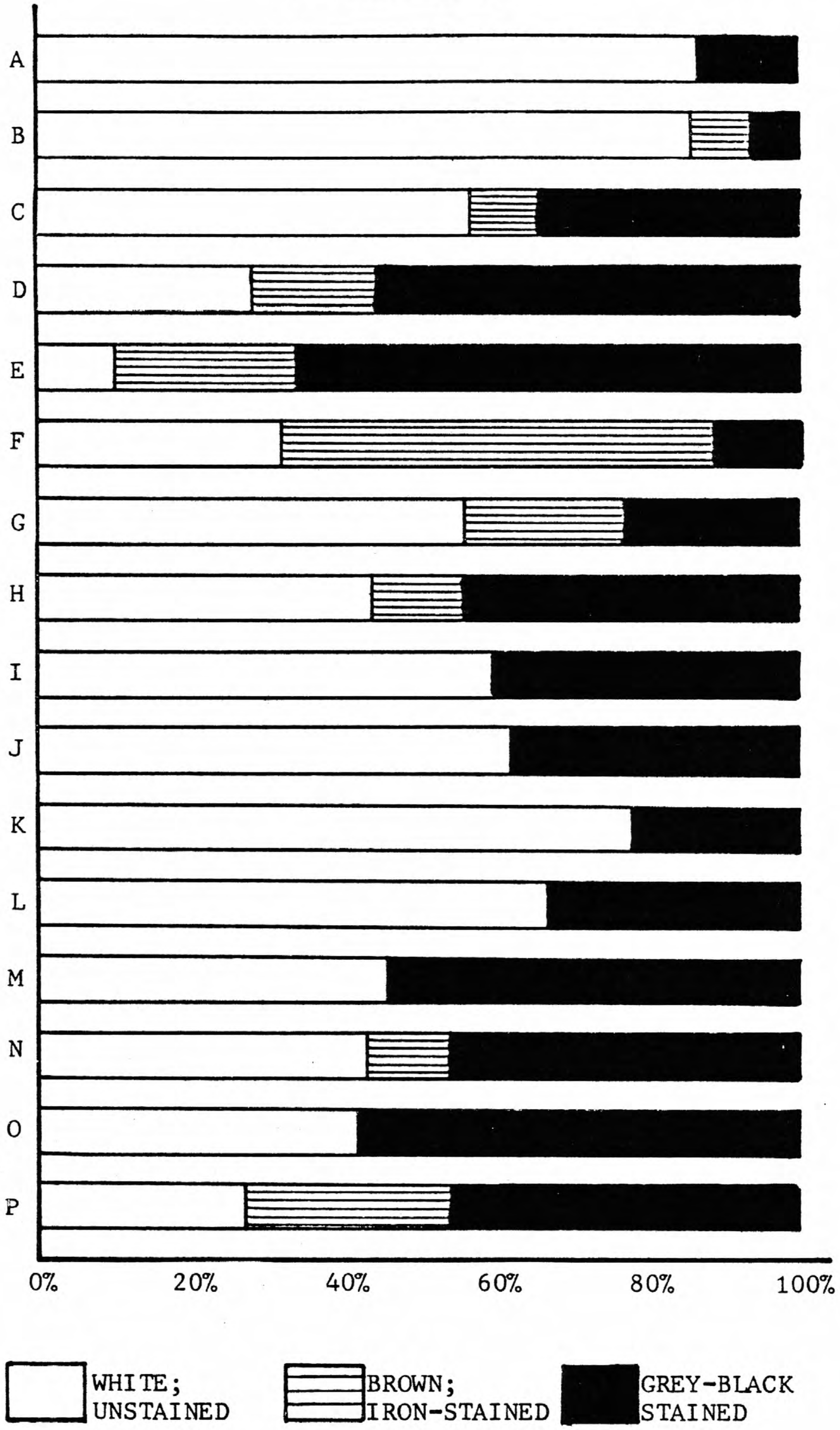

CARBONATE COLOR

going on at present. The presence of abundant grey-black or brown shells would immediately furnish a solid basis for such an assumption. If coupled with observations of the mica content, previously discussed in the grain size section, an idea of the winnowing potential of the area can be gained as well. If white-stained shells dominate the carbonate fraction of an area, interpretation is more difficult. Conceivably, it may mean that some material is locally accumulating in the area, perhaps by shifting about by storm activity. However, since it appears that shell fragments may retain their original coloration for thousands of years, they may also be present in areas of low sedimentation rate. If unstained shells are found in conjunction with high mica content, there is strong reason to suspect deposition is locally going on.

Obviously, delineation of areas of deposition and non-deposition is important in understanding the paths of future pollutant dispersal.

Non-Carbonate Color

This parameter is based on counts of individual quartz-feldspar grains. Both the degree of staining and color of stain was observed and counted. Classification into the four color groups of Figures 5-13 through 5-15 is based on the most abundant color group in the sample. Distinction between yellow, brown, and yellow-brown transitional is somewhat subjective. Figures 5-13 through 5-16 are best interpreted by considering white-unstained grains as one category and by lumping all other groups into a second category.

Iron staining of quartz-feldspar grains is not well understood. Earlier workers have suggested that abundant iron stained grains indicate relict sediments and that the stain is derived by long exposure to oxidizing conditions on the sea floor (Judd et al 1970). However,

Figure 5-13. Areal distribution of color of the non-carbonate fraction north of Cape Hatteras.

Figure 5-13

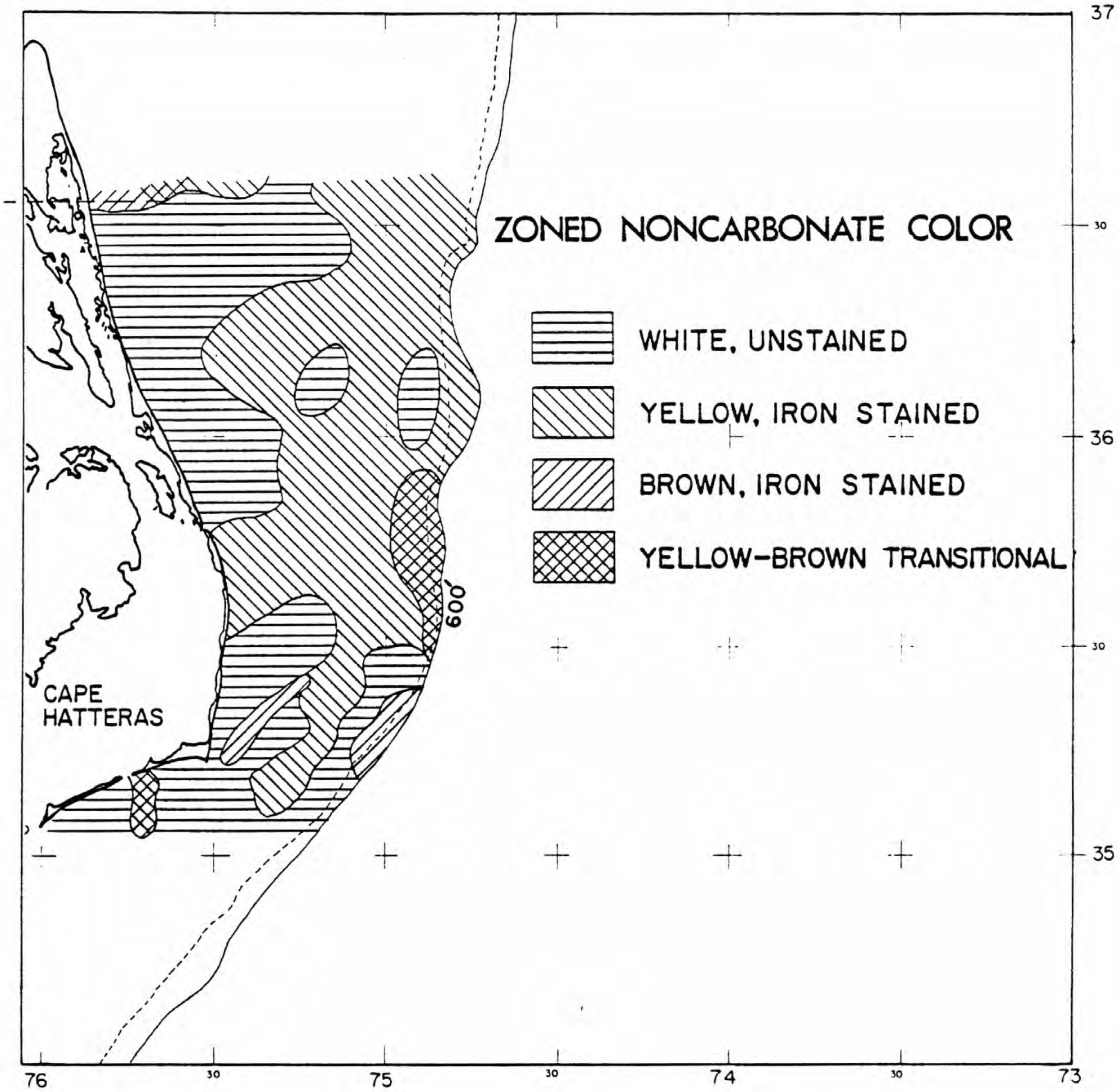
ZONED NONCARBONATE COLOR
WHITE, UNSTAINED
YELLOW, IRON STAINED
BROWN, IRON STAINED
YELLOW-BROWN TRANSITIONAL
CAPE HATTERAS
600
37
30
36
30
35
76
30
75
30
74
30
73

Figure 5-14. Areal distribution of color of the non-carbonate fraction; Cape Hatteras to Cape Romain.

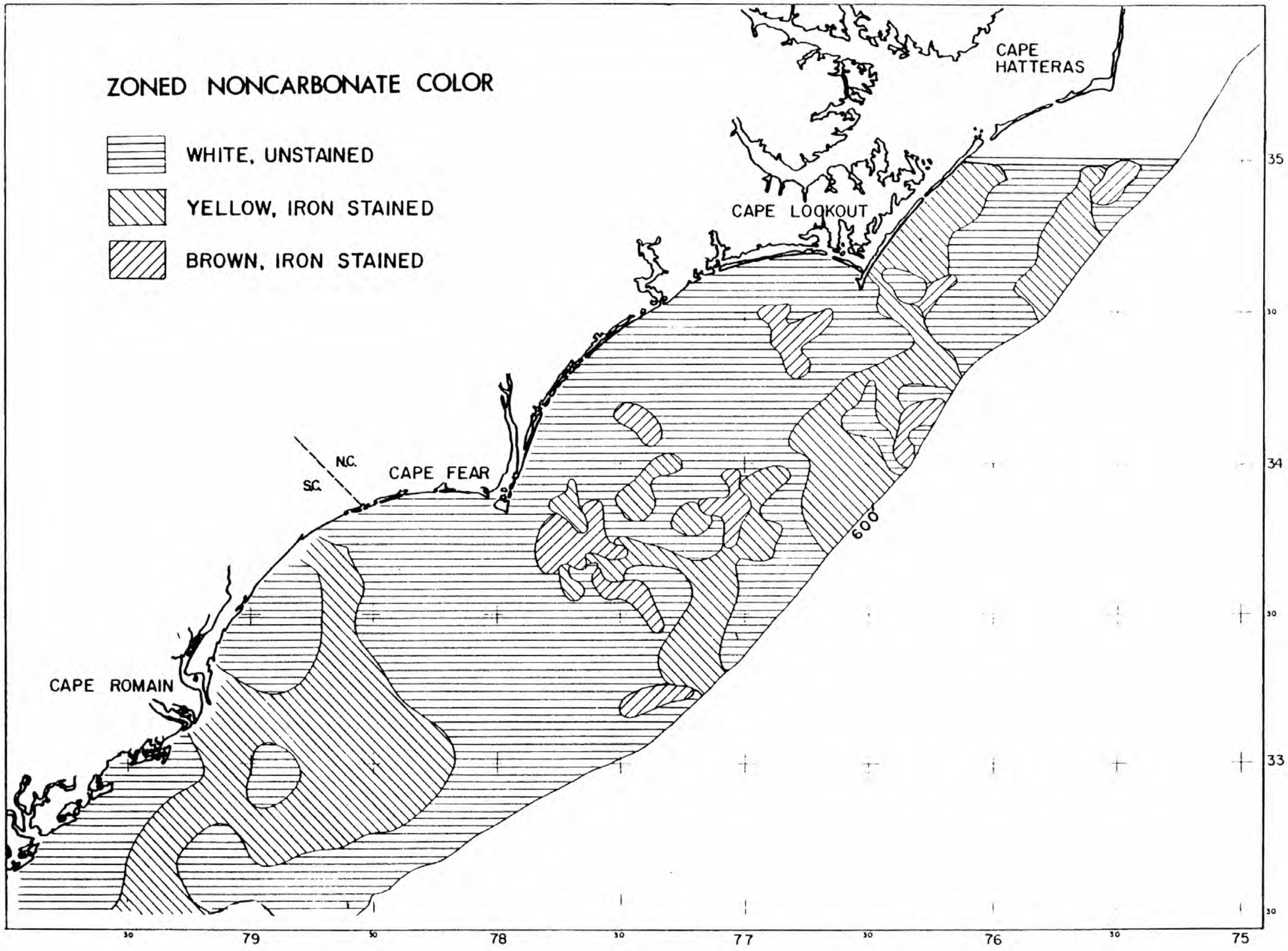
ZONED NONCARBONATE COLOR
WHITE, UNSTAINED
YELLOW, IRON STAINED
BROWN, IRON STAINED
CAPE HATTERAS
CAPE LOOKOUT
N.C.
S.C.
CAPE FEAR
CAPE ROMAIN
600
35
30
34
30
33
30
30
79
30
78
30
77
30
76
30
75

Figure 5-14

Figure 5-15. Areal distribution of color of the non-carbonate fraction; Cape Romain to Cape Canaveral.

Figure 5-15

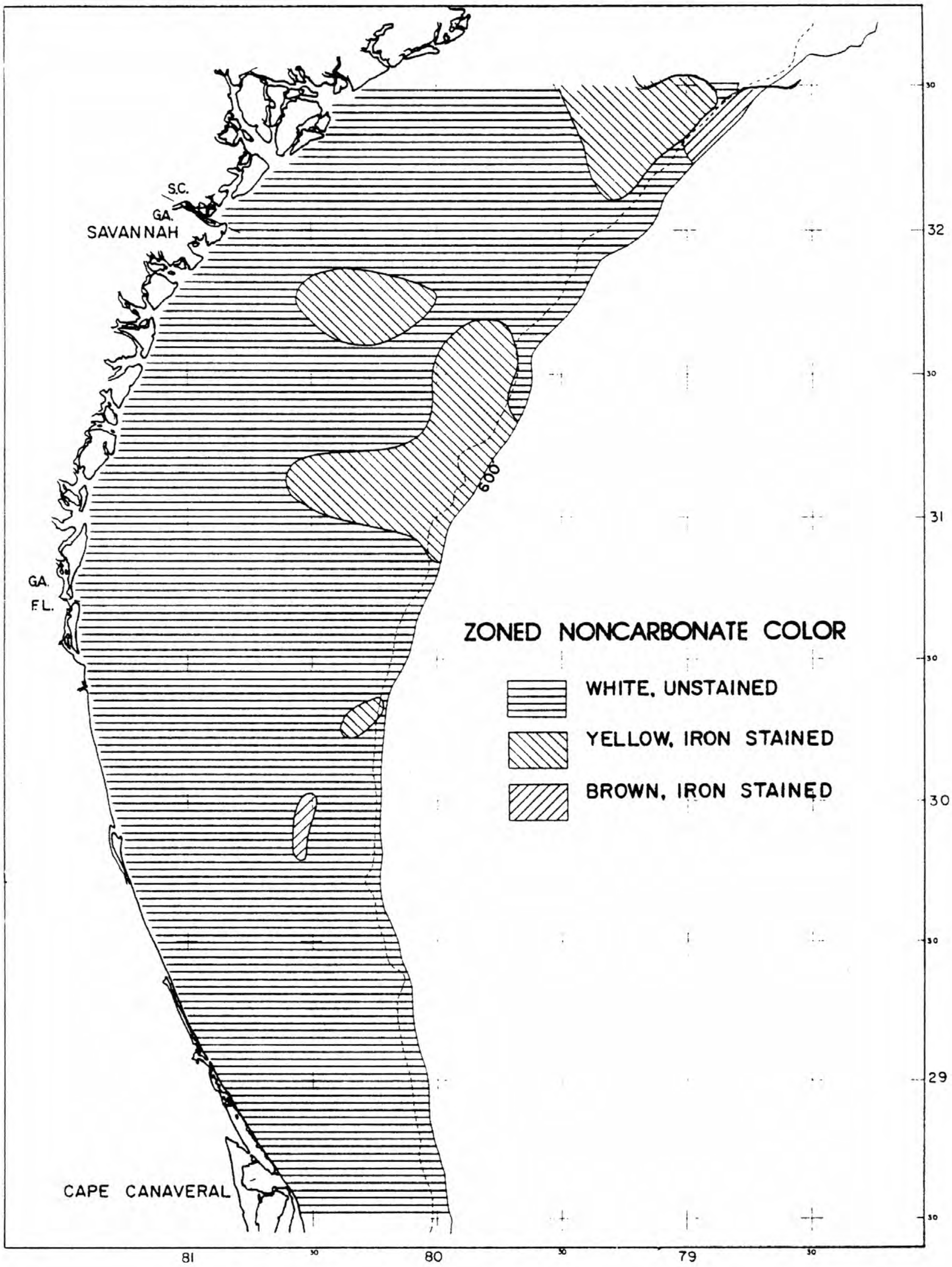
ZONED NONCARBONATE COLOR
WHITE, UNSTAINED
YELLOW, IRON STAINED
BROWN, IRON STAINED
S.C.
GA.
SAVANNAH
GA.
FL.
CAPE CANAVERAL
600
32
31
30
29
81
80
79
30

quartz-feldspar grains that ultimately make it to the shelf from Piedmont and Coastal Plain rivers are heavily iron stained. It also has been frequently observed that much staining occurs in sandy coastal plain soils by dissolution of iron-bearing heavy minerals in the zone of areation and deposition of the iron on the grains below. This is an important process to consider when concerned with the evolution of shelf sediments, because such soil zone material is eventually contributed to the shelf by shoreline migrating in response to sea level rise.

The situation is made complex by the fact that quartz-feldspar grains in estuarine environments are almost always devoid of oxidized iron stain due to widespread reducing conditions. Thus, most likely fluvial sands may lose their iron stain at most southeast U.S. river mouths before reaching the sea (?). On the other hand, iron stained beach and dune sediment may be contributed directly to the shelf as the rising sea level pushes islands back. One final observation is important to the interpretation of iron stained grains. Vibracores taken for the BLM studies as well as earlier investigations have revealed that in general only surficial sediment is iron stained. Usually quartz-feldspar grains below about 1 m sediment depth would be classified as white-unstained. Apparently the typical very shallow subsurface of the shelf is sufficiently reducing to remove staining. Thus, one reason for widespread unstained grains in a given shelf area might be a high degree of bottom sediment movement during storms.

From Figures 5-13 through 5-15, it is apparent that iron stained quartz-feldspar is of relatively little importance south of Cape Romain. It is important to point out, however, that iron stained grains are usually present at least in small amounts. The patch of iron stained sediment off Cape Romain conceivably may be linked to the Santee-PeeDee river mouths. Here, the influence of the estuaries and lagoon environment on quartz grain staining may be minimal since this is the only river system of the study area which empties almost directly into the sea. Regional trends are even more strikingly evident in Figure 5-16, which shows the latitude averages for bands delineated in Figures 5-1 through 5-3. Clearly iron staining of quartz-feldspar grains diminishes in a southerly direction. North of Cape Hatteras, samples with iron stained quartz-feldspar dominate. The Cape and associated shoals mark a very sharp boundary with regard to this sediment parameter.

Because quartz-feldspar grain iron staining (and stain removal) can come about in several ways (river sediment, soil zone, shelf subaqueous surface), it is difficult to interpret the significance of the regional distribution shown in Figures 5-13 through 5-16. It is suggested, however, that iron staining of grains may be of local importance in determining areas of recent scour versus areas of high sediment cover stability. That is, if iron staining can occur subaqueously on the shelf surface as has been suggested by previous studies and if only shallow burial is required to remove the stain, then local variations in the degree of staining in surface sediment should reflect the amount of contribution from scour into the reduced zone.

Sediment Lithofacies

Lithofacies of shelf sediments can also be referred to as sediment types. Their classification is based on megascopic subdivisions of sediments into look-alike groupings. While distinction of lithofacies is subjective in the sense that no two investigators would come up with exactly the same classification niches or numbers of niches, it is a useful means of observing sediment variability and patchiness, and even

Figure 5-16. Bar graphs showing latitudinal averages of color of the non-carbonate fraction. Latitudinal bands are labelled in Figures 5-1 through 5-3.

Figure 5-16

NONCARBONATE COLOR

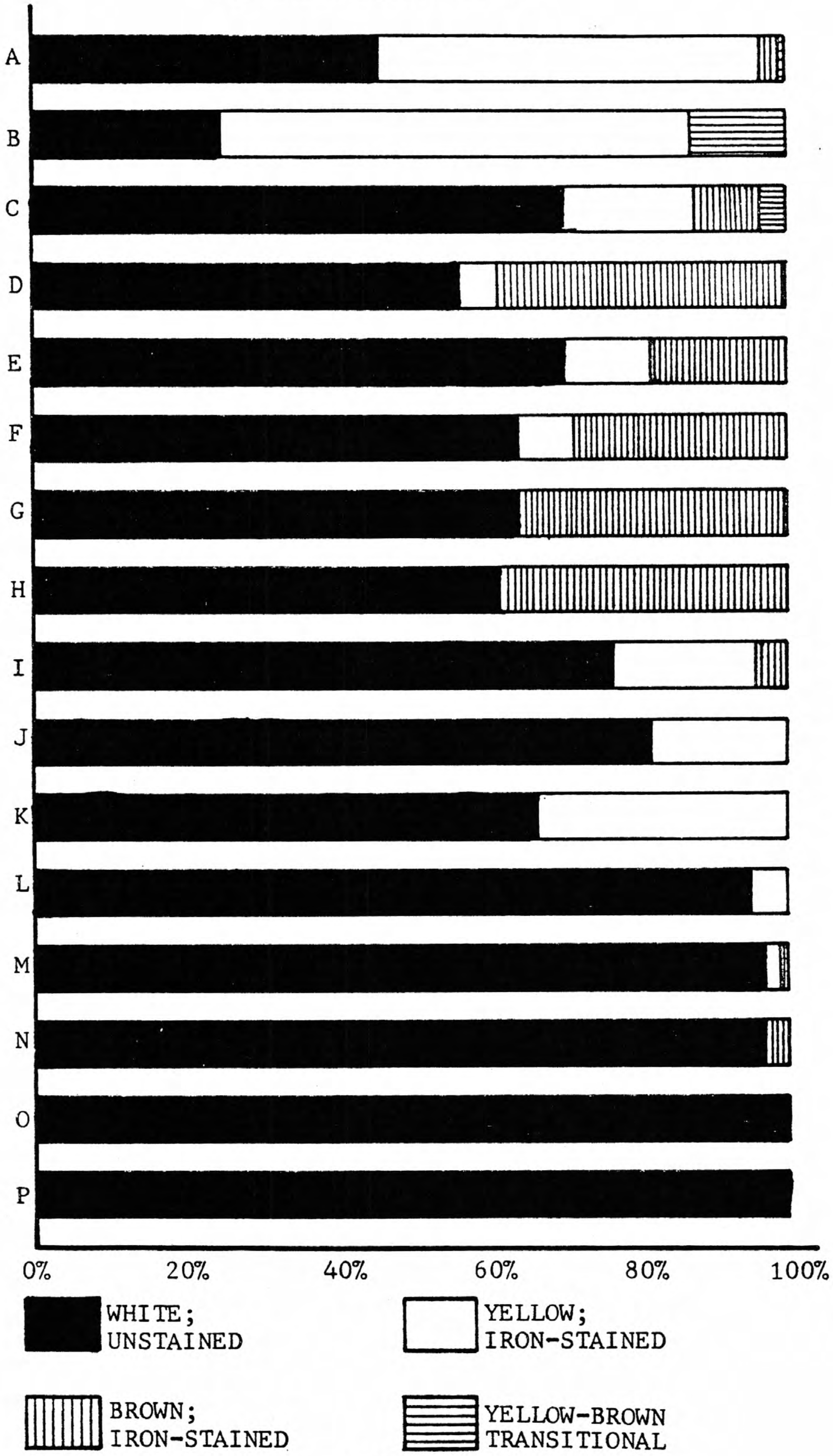

origin. Lithofacies groupings are based on a combination of grain size, color and constituent make up. Table 5-2 summarizes the major characteristics of each of the seven lithofacies.

Figures 5-17 through 5-19 show the areal distribution of lithofacies. The dominant sediment type north of Cape Hatteras is fine terrigenous sand; reflecting a low carbonate content and either or both low carbonate productivity and a high rate of sedimentation, relatively speaking. South of Cape Hatteras and north of Cape Romain the dominant sediment types are fine calcareous sand and terrigenous sand. In Onslow Bay fine calcareous sand predominates, which is a reflection of the lack of important rivers emptying onto the shelf here; hence, lack of dilution of calcareous materials (Cleary and Pilkey 1967). South of Cape Romain the lithofacies are dominated by medium to coarse terrigenous sand off Georgia and South Carolina. Off North Florida a shelf segment with no important river mouths, fine calcareous sand again is dominant, again because of the lack of dilution by terrigenous fluvial material. South of Cape Romain the nearshore zone is dominated by either fine terrigenous sand or mud (muddy sand). Patches of almost purely carbonate sand (also related to lack of a terrigenous source) appear at the shelf edge and on the central shelf near Cape Canaveral. In some cases, at the shelf edge carbonate content is also high because of very high, local carbonate productivity.

Figure 5-20 illustrates the frequency of occurrence of the various lithofacies in the latitudinal bands shown in Figures 5-1 through 5-3. The bar graphs illustrate clearly the major trend of increasingly calcareous sediment south of Cape Hatteras, relative to sediments north of Cape Hatteras. Fine calcareous sand, one of the two most common sediment types, shown in solid black in Figure 5-20, has a regional

Table 5-2. Generalized attributes of the various sediment lithofacies shown in Figures 5-16 through 5-19.

Sediment Lithofacies	Grain Size	Carbonate Content	Noncarbonate Content	Color Tendency	Appearance	Other Characteristics
terrigenous medium to coarse sand and gravel	0.5mm to 4.0mm (1φ to -2φ)	< 5%	quartz, some phosphorite >95%	white to orange to brown	moderately clean	phosphorite and manganese locally important
fine terrigenous sand	0.0625mm to 0.5mm (4φ to 1φ)	< 5%	quartz >95%	white or lt. grey; some orange samples	very clean	
coarse calcareous sand and gravel	0.5mm to 4.0mm (1φ to -2φ)	10%-50%	quartz; some phosphorite 50%-90%	grey to brown	moderately dirty	phosphorite and manganese locally; carbonate grains >mean
fine calcareous sand	0.0625mm to 0.5mm (4φ to 1φ)	10%-50%	quartz 50%-90%	white to lt. and med.grey	moderately clean	carbonate grains may be >mean grain size
coarse carbonate sand and gravel	0.5mm to 3.0mm (1φ to -3φ)	some ooids >50%	quartz; some phosphorite <50%	white or dirty brown	moderately clean	carbonate grains may be >mean grain size
fine carbonate sand	0.0625mm to 0.5mm (4φ to 1φ)	some ooids >50%	quartz <50%	white to lt. grey to tan	moderately clean	ooids and foraminifera locally important
mud	0.0156mm to 0.0625mm (6φ to 4φ)	< 5%	quartz, clays and mica >95%	dark greenish grey to dark grey	dirty	carbonate grains >mean grain size

Figure 5-17. Areal distribution of sediment lithofacies north of Cape Hatteras.

Figure 5-17

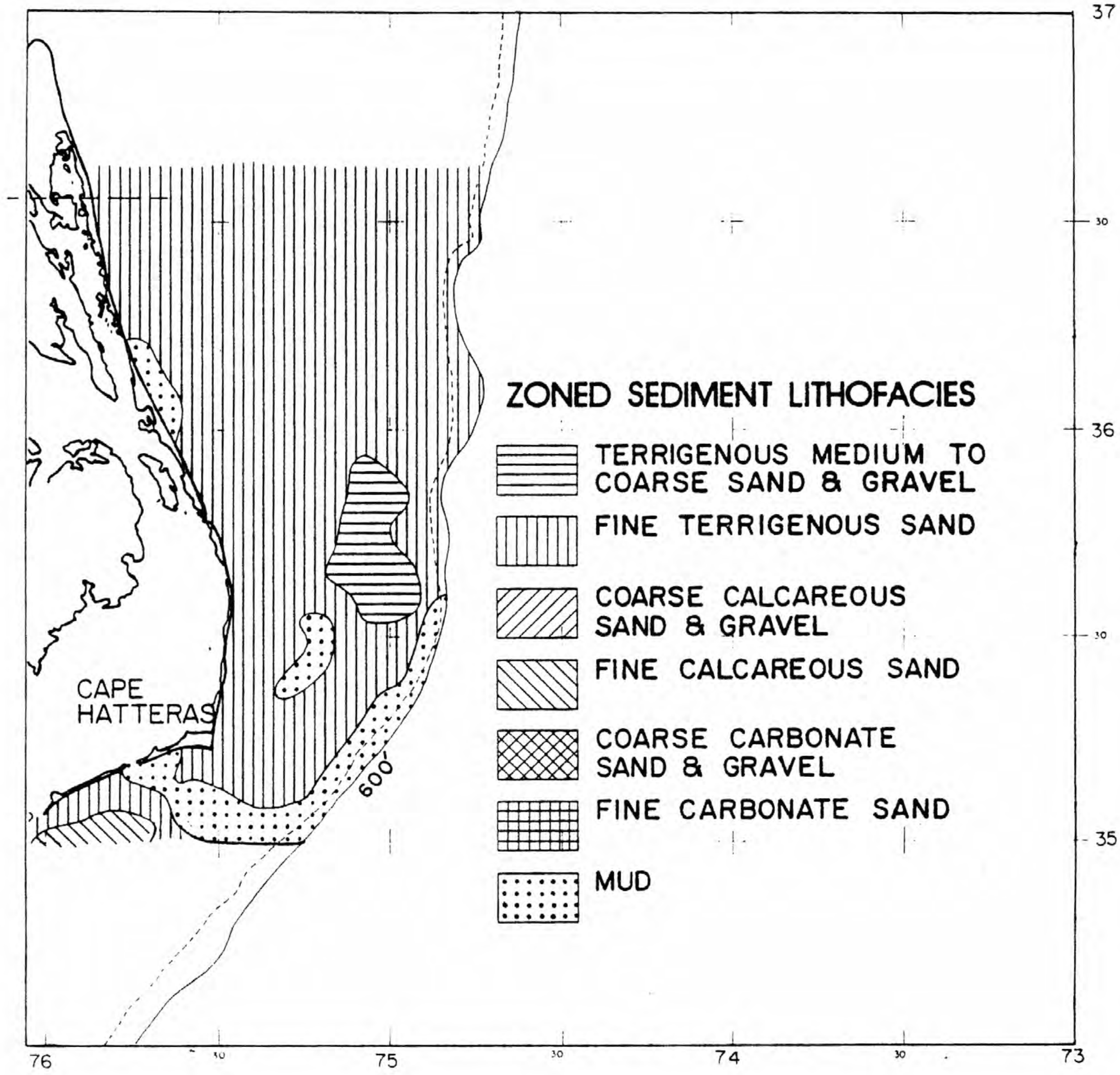
ZONED SEDIMENT LITHOFACIES
TERRIGENOUS MEDIUM TO COARSE SAND & GRAVEL
FINE TERRIGENOUS SAND
COARSE CALCAREOUS SAND & GRAVEL
FINE CALCAREOUS SAND
COARSE CARBONATE SAND & GRAVEL
FINE CARBONATE SAND
MUD
CAPE HATTERAS
600
37
30
36
30
35
76
30
75
30
74
30
73

Figure 5-18. Areal distribution of sediment lithofacies; Cape Hatteras to Cape Romain.

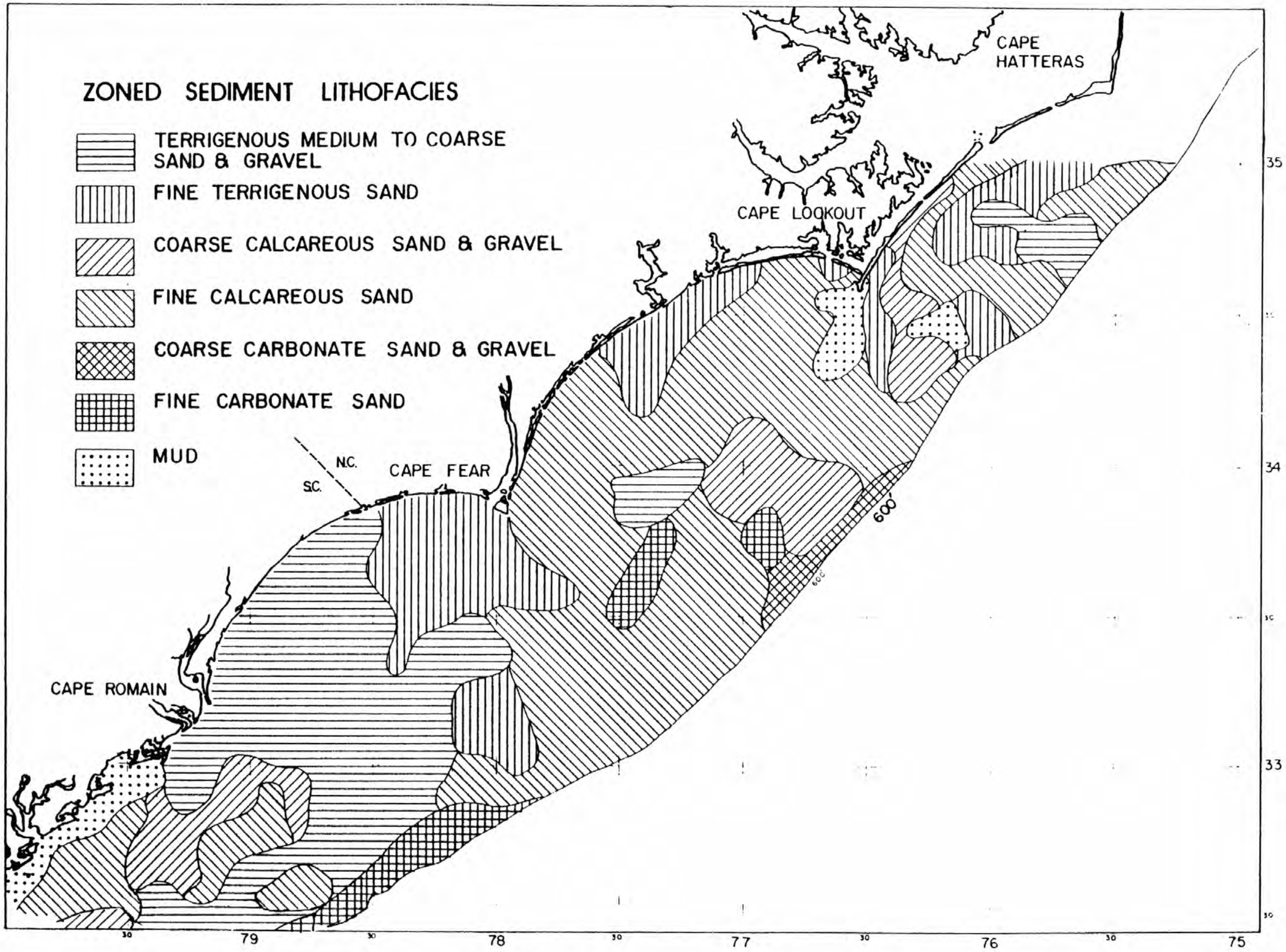
ZONED SEDIMENT LITHOFACIES
TERRIGENOUS MEDIUM TO COARSE SAND & GRAVEL
FINE TERRIGENOUS SAND
COARSE CALCAREOUS SAND & GRAVEL
FINE CALCAREOUS SAND
COARSE CARBONATE SAND & GRAVEL
FINE CARBONATE SAND
MUD
CAPE HATTERAS
CAPE LOOKOUT
CAPE FEAR
CAPE ROMAIN
N.C.
S.C.
600
600
35
34
33
79
78
77
76
75
30
30
30
30
30

Figure 5-18

Figure 5-19. Areal distribution of sediment lithofacies; Cape Romain to Cape Canaveral.

Figure 5-19

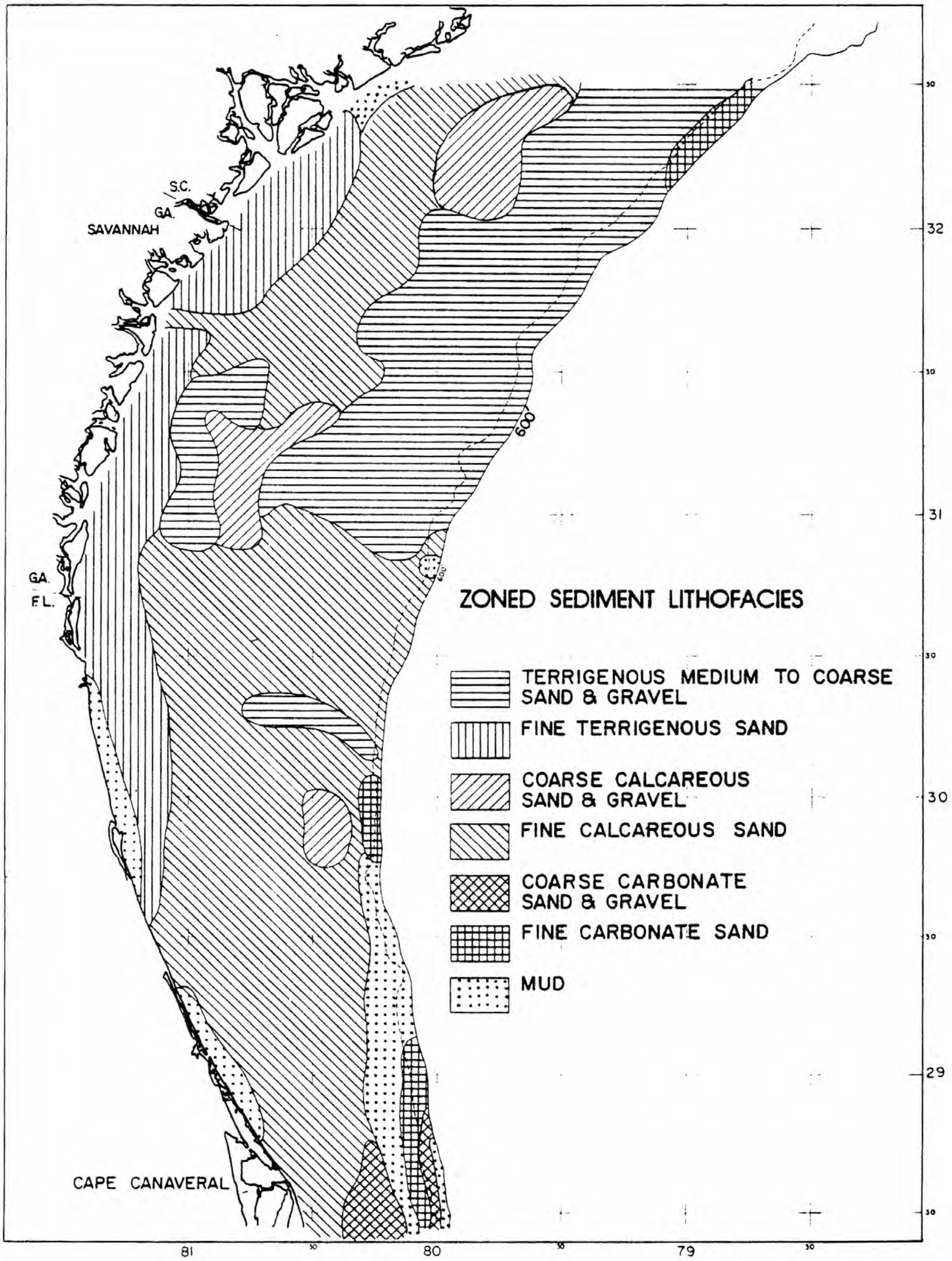
S.C.
GA.
SAVANNAH
GA.
F.L.
CAPE CANAVERAL
600
600
ZONED SEDIMENT LITHOFACIES
TERRIGENOUS MEDIUM TO COARSE SAND & GRAVEL
FINE TERRIGENOUS SAND
COARSE CALCAREOUS SAND & GRAVEL
FINE CALCAREOUS SAND
COARSE CARBONATE SAND & GRAVEL
FINE CARBONATE SAND
MUD
30
32
30
31
30
30
30
29
30
81
30
80
30
79
30

Figure 5-20. Bar graphs showing latitudinal distribution of sediment lithofacies. Latitudinal bands are labelled on Figures 5-1 through 5-3.

SEDIMENT LITHOFACIES

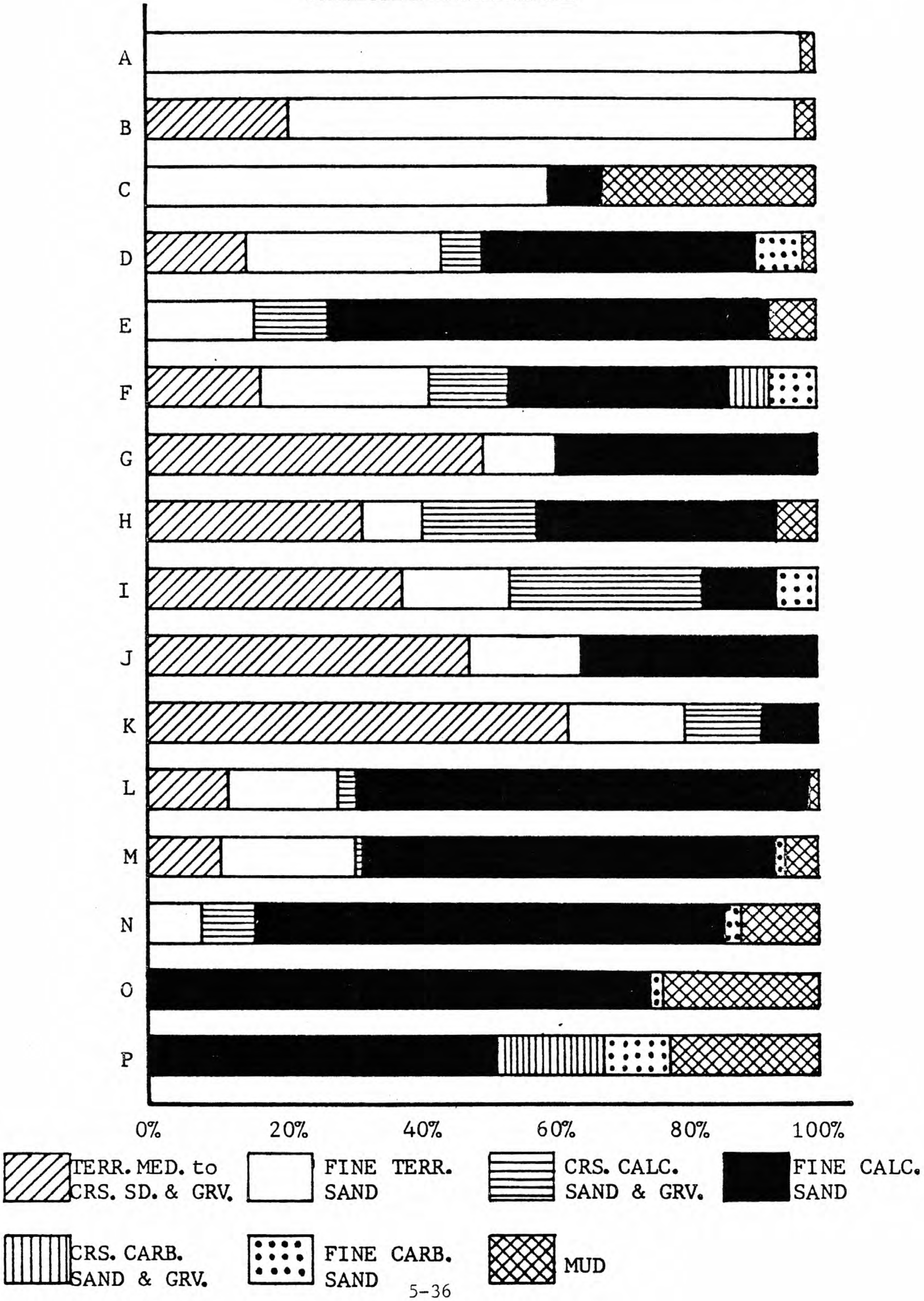

bimodal distribution. Highs on the Central North Carolina shelf (Onslow Bay) and on the North Florida shelf both reflect low fluvial input at present and probably during the last rise in sea level as well. The second important sediment type, medium to coarse terrigenous sand and gravel, follows a mirror image distribution relative to fine calcareous sand. Its major area of occurrence is on the South Carolina and Georgia shelf, where fluvial terrigenous input has been relatively large.

Lithofacies distribution throughout the study area is quite patchy, possibly giving some indication of the lack of mixing and lateral transport on the shelf. However, if the number of lithofacies or sediment type categories was increased, the resultant areal distribution would appear much patchier than indicated in Figures 5-17 through 5-19. Thus, this parameter is not a good measure of shelf activity and mixing processes.

Lithofacies maps probably are best used to show areas of the region where deposition rate during the last transgression was low (highly calcareous sediments) and also areas where accumulation of fines is presently occurring (muddy sediments). As a first crude approximation, it could be assumed that particulate pollutants are most likely going to end up being deposited in areas designated as mud or fine terrigenous sand on Figures 5-17 through 5-19 and least likely to end up in areas of coarse calcareous sediments. Such lithofacies comparisons could be applied to local areas of environmental concern by detailed local sampling.

In carrying out local sampling, care must be taken to have precise bathymetric control. Preliminary observations on the Georgia shelf indicate that topographic control by features with as little as 1 m relief may play a major role in determining local shelf processes and depositional versus winnowing regimes.

SUMMARY OF CONCLUSIONS

The following are very generalized conclusions based on the areal distribution of sediment parameters determined from surficial grab samples. The density of sampling in this investigation is by far the highest ever used in a regional shelf investigation (Figures 5-1 through 5-3).

1. Grain size offers an important indication of possible dispersal paths of various sized particulate pollutants. In particular, areas of muddy or micaceous sediment are locations where deposition may exceed winnowing.
2. Nearshore sediments tend to be fine sand size, and the central and outer shelf is largely covered by medium or coarse sand. Patches of coarse sand become increasingly important north of Cape Romain. The upper slope is covered by muds and muddy sands. Locally, grain size may be controlled by minor shelf topographic features.
3. Patchiness of carbonate and non-carbonate grain color as well as total sediment color all indicate that regional sediment mixing and long distance lateral transport are not important processes.
4. The type of staining, or the lack thereof, of the carbonate fraction along with lithofacies distribution all indicate that the Georgia-South Carolina shelf along with the North Carolina shelf north of Cape Hatteras have had relatively high rates of sedimentation during the last sea level rise compared to North Florida and the remainder of the North Carolina shelf.

5. The presence of fresh shells in a micaceous sediment is a likely indicator of an active depositional site. The presence of brown and black stained shells, respectively, indicating beach and lagoon derivation point to areas of non-deposition.

6. The areal distribution of lithofacies broadly reflects the rate of deposition on the shelf during the last transgression. Calcareous sediments denote low rates of deposition due to lack of dilution by terrigenous grains. Low carbonate content of sediments indicates the opposite situation. It is likely that the Holocene-Pleistocene sediment cover is slightly thicker in areas of low carbonate sediments.

7. Apparently quartz-feldspar grains can be iron stained in the subaqueous shelf environment. Shallow burial usually removes the stain, however. Thus, detailed local studies of iron staining could furnish a basis for determining the extent of sea floor scour by waves and currents.

8. The overall picture of surficial shelf sedimentation activity on the southeastern U.S. shelf is as follows: little material is being added to the shelf at the present time except that $CaCO_3$ from organisms and sediment eroded or weathered from underlying rocks. Modern river sands and most muds are being trapped in estuaries. Locally, however, patchy depositional regions may occur and must be considered in planning development activities on the shelf. Probably most fine material produced on the southeastern U.S. Atlantic shelf either returns to the estuaries or is ultimately deposited on the upper slope off Cape Hatteras.

LITERATURE CITED

Cleary, W.J., and Pilkey, O.H. 1967. Sedimentation in Onslow Bay: Southeastern Geol. Spec. Paper 1, pp. 1-17.

Doyle, L.J. 1967. Black shells. Unpublished M.S. Thesis, Duke University, Durham, N.C., 69 p.

Doyle, L.J., Cleary, W.J., and Pilkey, O.H. 1969. Mica, its use in determining shelf deposition regimes: Marine Geology, vol. 6, pp. 381-389.

Field, M.E., and Pilkey, O.H. 1969. Feldspar in Atlantic continental margin sand off the southeastern United States: Geol. Soc. America Bull., vol. 80, pp. 2097-2102.

Gorsline, D.S. 1963. Bottom sediments of the Atlantic shelf and slope off the southern United States: Jour. of Geol., vol. 71, pp. 423-440.

Judd, J.B., Smith, W.C., and Pilkey, O.H. 1970. The environmental significance of iron-stained quartz grains on the southeastern United States continental shelf: Marine Geology, vol. 8, pp. 355-362.

Pilkey, O.H., Blackwelder, B.W., Doyle, L.J., Estes, E.L., and Terlecky, P.M. 1969. Aspects of carbonate sedimentation of the Atlantic continental shelf of the southern United States: Jour. of Sed. Pet., vol. 39, pp. 744-768.

CHAPTER 6

VIBRACORE STUDIES: GEORGIA EMBAYMENT SHELF

Mark Ayers[1], Blake W. Blackwelder[2], James D. Howard[3],
Fred Keer[1], Harley Knebel[4], and Orrin H. Pilkey[1]

[1] U. S. Geological Survey, Duke University, Durham, North Carolina 27708
[2] U. S. Geological Survey, Reston, Virginia 22092
[3] University of Georgia, Skidaway Institute, Savannah, Georgia 31406
[4] U. S. Geological Survey, Woods Hole, Massachusetts 02543

Chapter 6

Table of Contents

Page

Abstract 6- 1

Introduction 6- 2

Methods. 6- 9

Subbottom Profiles 6-18

Core Descriptions. 6-19

  Sediment Type. 6-19

  Sedimentary Structures 6-24

  Texture of Vibracore Sediments 6-29

  Calcium Carbonate. 6-29

  Organic Carbon 6-46

  Mollusk Assemblages. 6-55

    Late Pleistocene and Holocene. 6-56
    Waccamaw Formation 6-70

Stratigraphy of the Shelf Sediment Cover 6-71

Sea Level History. 6-80

Discussion 6-82

  Implications Regarding Barrier Island Evolution. 6-83

  Origin of the Shelf Sediment Cover 6-83

  Implications Concerning Environmental Impact of Shelf Development. . . . 6-87

Literature Cited 6-88

CHAPTER 6

VIBRACORE STUDIES: GEORGIA EMBAYMENT SHELF

Mark Ayers, Blake W. Blackwelder, James D. Howard,
Fred Keer, Harley Knebel, and Orrin H. Pilkey

ABSTRACT

Forty-two vibracores taken across the continental shelf of the Georgia Embayment have been studied in detail. Aspects studied include faunal assemblages, sediment textures, compositions, and structures. Core penetration rates and Tertiary rock recovered at the base of the cores indicate that the unconsolidated Holocene-Pleistocene sediment veneer is thin, usually less than 4 m and rarely over 6 m.

Molluscan assemblages and radiocarbon dates indicate that the shelf sediment cover has undergone extensive *in situ* "mixing" during the Holocene. The "mixing" has occurred under the shelf energy regimes prevailing today and is probably largely the result of alternate scouring and filling during storms. The high percentage of bioturbation which occurs throughout 90% of the sediment column indicates that such sand movement must occur in relatively small surges. The lack of Tertiary fossils eroded from underlying sediments and the general thinness of the sediment cover indicate that shoreface erosion and mixing during a rising sea level affects only the upper few meters of sediment on the shelf.

In spite of the various ice age sea level transgressions, only Late Pleistocene-Holocene fossils are present in the shelf sediment cover. Therefore, most of the shelf sediment cover is not strictly relict as previously assumed. The shelf sediments must be viewed as a two-component system of non-carbonate and carbonate fractions. The

non-carbonate materials have been repeatedly reworked by succeeding transgressions and regressions, whereas the carbonate fraction is subaerially removed during each regression and then is recharged within the sand body during each transgression.

INTRODUCTION

This report presents the results of the detailed investigation of 22 vibracores obtained in two linear transects across the southeastern U.S. Atlantic continental shelf and of 18 vibracores obtained in two proposed lease areas in the Georgia Embayment Shelf Area (Figures 6-1 and 6-2 and Table 6-1). The northern transect consists of 10 cores, roughly evenly spaced across the shelf of Long Bay between Cape Romain, South Carolina, and Cape Fear, North Carolina. Depths of the cores range from 24 to 64 m. The southern transect consists of 12 cores from water depths of 26 to 130 m. Eight cores were recovered in the proposed northern lease area and 10 cores were recovered in the proposed southern lease area. Seismic data were obtained on an initial run down the proposed transect lines before coring stations along the transects were chosen. Because of navigational error (LORAN C) and ship drift on station, it cannot be assumed that the cores were taken precisely on the line of the sections shown in Figures 6-3 and 6-4.

These are the first vibracore transects across any continental shelf. They provide a basis for looking at the big picture of shelf sedimentation history and shelf sedimentation processes. The cores from the lease areas, taken from a much smaller area, allow a more detailed examination of shelf sedimentation.

Figure 6-1. Locations of vibracores used in this study.

Figure 6-1

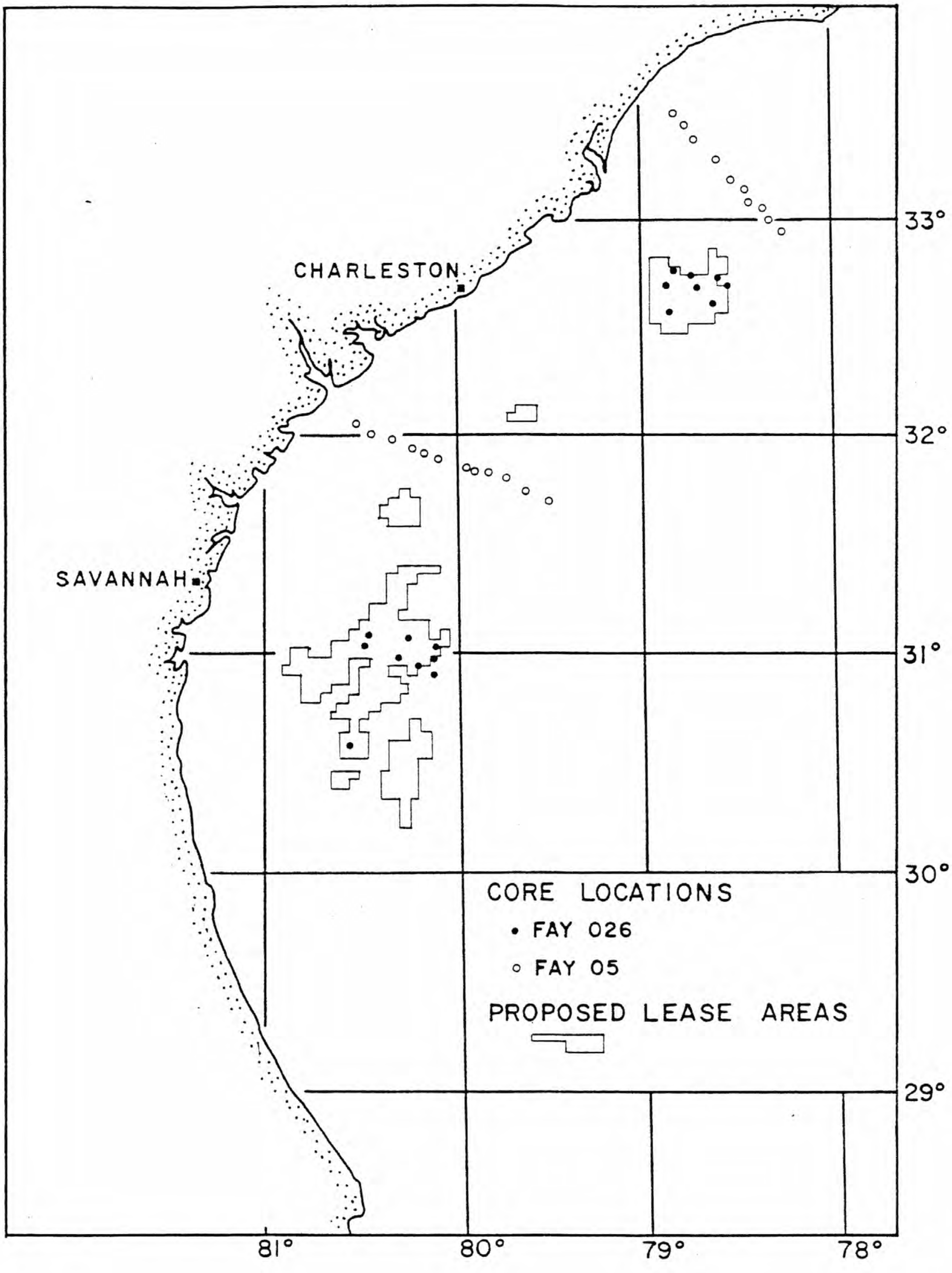
CHARLESTON
SAVANNAH
33°
32°
31°
30°
29°
81°
80°
79°
78°
CORE LOCATIONS
• FAY 026
○ FAY 05
PROPOSED LEASE AREAS

Figure 6-2. Index map showing the locations of the two cross-shelf transects the individual core stations, and the seismic profiles. Letters along the seismic profiles denote sections presented in Figures 6-3 and 6-4. Bathymetry after Uchupi (1965).

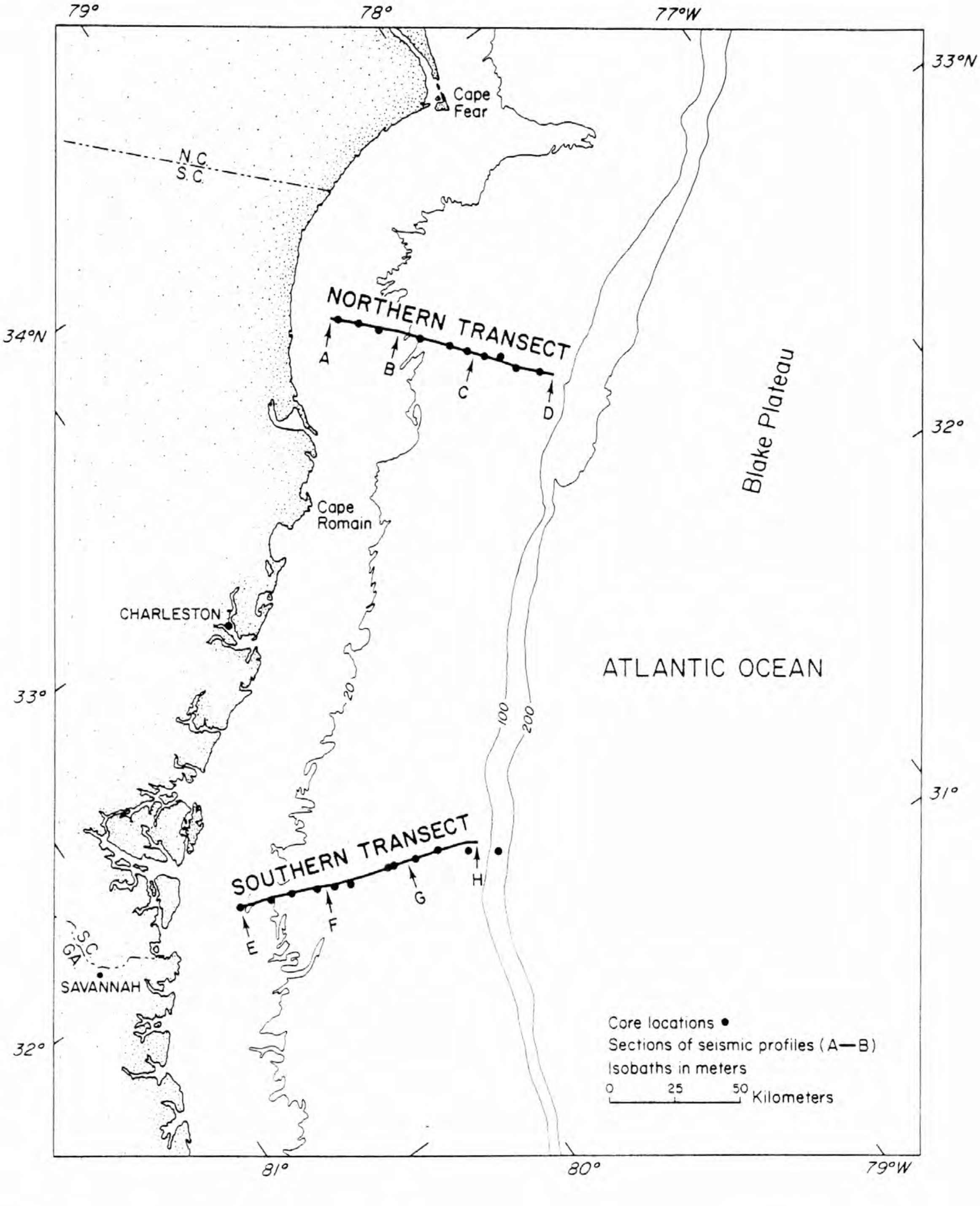
79°
78°
77°W
33°N
34°N
32°
33°
31°
32°
81°
80°
79°W
Cape Fear
N.C.
S.C.
NORTHERN TRANSECT
A
B
C
D
Blake Plateau
Cape Romain
CHARLESTON
ATLANTIC OCEAN
20
100
200
SOUTHERN TRANSECT
E
F
G
H
S.C.
GA.
SAVANNAH
Core locations ●
Sections of seismic profiles (A—B)
Isobaths in meters
0 25 50 Kilometers

Table 6-1. Location, water depth, and core length data for the vibracores used in this investigation.

Northern Cross-Shelf Transect

Core No.	Latitude	Longitude	Water Depth (meters)	Core Length (meters)
4525	33°29.27'N	78°50.27'W	13	2.68
4526	33°25.76'N	78°46.76'W	17	1.69
4527	33°22.68'N	78°43.85'W	15	3.37
4528	33°16.14'N	78°36.93'W	21	2.79
4529	33°11.37'N	78°31.71'W	24	2.30
4530	33°08.37'N	78°28.66'W	25	6.01
4531	33°05.39'N	78°26.37'W	27	3.26
4532	33°03.40'N	78°22.99'W	27	4.63
4533	32°59.61'N	78°21.77'W	31	5.16
4534	32°56.16'N	78°17.48'W	35	3.12
Southern Cross-Shelf Transect				
4535	32°02.19'N	80°30.14'W	14	3.79
4536	31°59.66'N	80°24.95'W	20	4.53
4537	31°58.25'N	80°19.75'W	24	1.19
4538	31°56.03'N	80°14.16'W	26	6.01
4539	31°54.49'N	80°10.13'W	27	5.08
4540	31°52.97'N	80°06.70'W	26	3.29
4541	31°51.30'N	79°57.06'W	31	4.74
4542	31°50.99'N	79°55.72'W	34	1.97
4543	31°49.49'N	79°50.43'W	43	5.95
4544	31°48.42'N	79°44.85'W	34	6.08
4545	31°44.94'N	79°38.96'W	53-55	5.12
4546	31°41.02'N	79°32.88'W	71	4.70

Table 6-1. Location, water depth, and core length data for the vibracores used in this investigation (continued).

Core No.	Latitude	Longitude	Water Depth (meters)	Core Length (meters)
Northern Lease Area				
4610	32°34.4'N	78°51.4'W	36	3.90
4612	32°47.2'N	78°50.7'W	31	3.00
4613	32°43.8'N	78°45.0'W	33	2.10
4614	32°40.4'N	78°43.8'W	38	3.00
4615	32°43.0'N	78°36.5'W	36	2.25
4616	32°41.4'N	78°34.5'W	38	3.05
4617	32°37.5'N	78°38.3'W	35	2.70
4618	32°41.1'N	78°52.5'W	38	1.82
Southern Lease Area				
4600	31°18.0'N	80°17.0'W	NA	2.50
4601	31°05.2'N	80°29.2'W	NA	2.05
4602	31°02.2'N	80°29.6'W	29	4.77
4605	31°04.4'N	80°17.3'W	37	4.15
4606	30°58.4'N	80°19.1'W	37	3.35
4607	30°56.6'N	80°13.7'W	37	2.80
4608	30°54.5'N	80°08.3'W	38	4.05
4609	30°57.7'N	80°08.4'W	38	1.50
4620	31°00.5'N	80°07.9'W	46	5.80
4622	30°34.7'N	80°34.5'W	31	0.60

Figure 6-3. Line drawing of the high-resolution (3.5 kHz) seismic profile from the northern transect. Locations of individual sections are shown in Figure 6-2. Core locations near or along the profile are also noted. Sound velocity in the sediments is assumed to be that of water (1,500 m/sec).

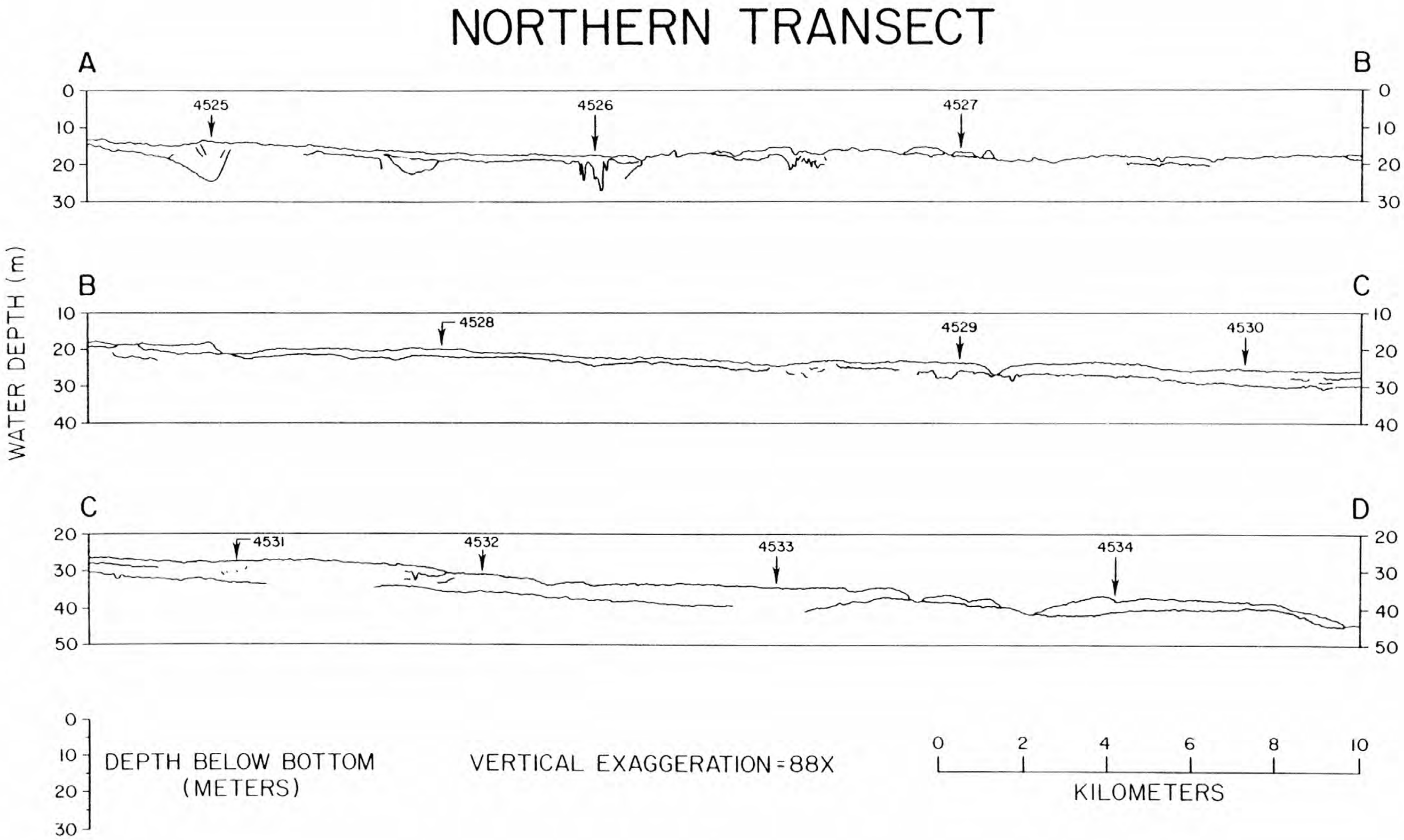
NORTHERN TRANSECT
A
B
0
10
20
30
4525
4526
4527
WATER DEPTH (m)
B
C
10
20
30
40
4528
4529
4530
C
D
20
30
40
50
4531
4532
4533
4534
0
10
20
30
DEPTH BELOW BOTTOM
(METERS)
VERTICAL EXAGGERATION = 88X
0
2
4
6
8
10
KILOMETERS

Figure 6-3

Figure 6-4. Line drawing of the high-resolution (3.5 kHz) seismic profile from the southern transect. Locations of individual sections are shown in Figure 6-2. Core locations near or along the profile are also noted. Sound velocity in the sediments is assumed to be that of water (1,500 m/sec).

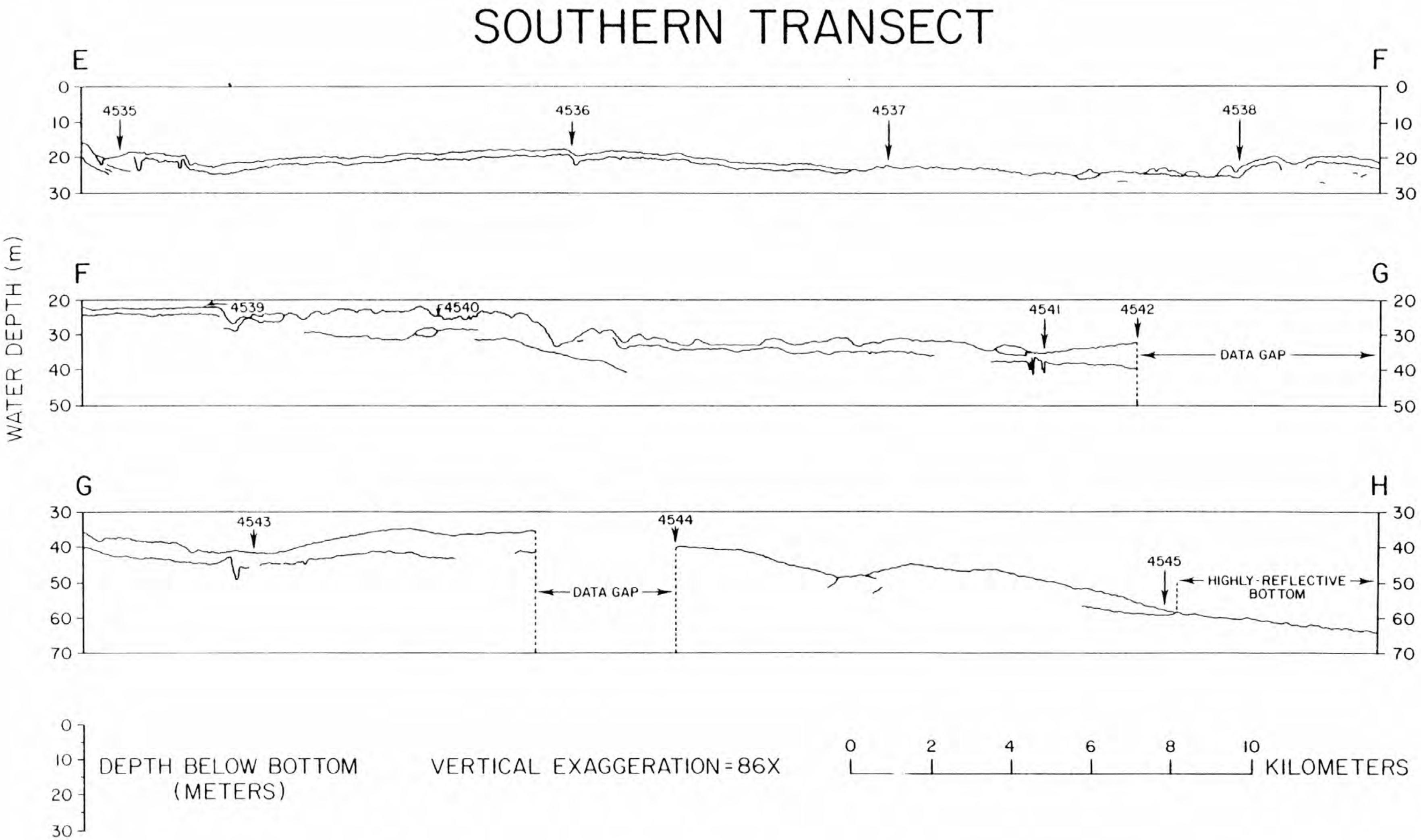

SOUTHERN TRANSECT
E
F
G
H
WATER DEPTH (m)
4535
4536
4537
4538
4539
4540
4541
4542
4543
4544
4545
DATA GAP
DATA GAP
HIGHLY-REFLECTIVE BOTTOM
0
10
20
30
40
50
60
70
DEPTH BELOW BOTTOM (METERS)
VERTICAL EXAGGERATION = 86X
0 2 4 6 8 10 KILOMETERS

Figure 6-4

METHODS

The suite of 40 vibracores was carefully examined and described in shore-based laboratories. Whole cores were X-rayed in their liners to determine sedimentary structures and split into halves. One half was selectively subsampled to determine: (1) the percent $CaCO_3$, (2) the percent organic carbon, (3) the clay mineralogy, (4) light mineralogy, (5) heavy mineralogy, and (6) sediment texture. Resin peels taken of the unsampled core halves facilitated visual description of the sediment types in the cores.

Samples used for textural analysis were dried, weighed, dispersed using a 10% calgon solution, and wet-sieved to determine the percentages of silt and clay (<63 u), sand (>63 u - <2 mm), and gravel (>2 mm). Samples containing greater than 10% mud were also analyzed for percent silt and clay using a pipette technique (Folk 1974). Sand texture was determined with a modified Woods Hole settling tube (described by Felix 1968); mean grain size, sorting, skewness and kurtosis values were calculated using Folk's (1974) graphic statistics and cumulative weight percentages measured at 1/2 phi intervals. Errors of this type of grain size analysis have been studied by Cook (1969). Additionally, four replicate grain size analyses of a single sand sample were performed here in order to document the reproducibility of the results (Table 6-2). Variation in the results of the replicate analyses was greatest at 1.00 phi with a 4.5 weight percent difference between the minimum and maximum values. In the replicate analyses the mean variation for all seven size intervals was much lower; equaling 1.6 weight percent.

Tetrabromoethane was used to separate the light and heavy minerals of the 125 to 250 micron (fine sand) fraction following treatment with 10% HCl to remove the carbonate fraction. The composition of the light

Table 6-2. Reproducibility of settling tube data. Four splits of a single sand sample where analyzed for grain size. Data from the replicate analyses are shown here at 0.50 phi intervals and are expressed in cumulative weight percentage.

Phi Size	Run				$\overline{X}$	Sd
	1	2	3	4		
0.00	0.0	0.0	0.0	0.0	0.0	0.0
0.50	7.9	7.0	8.5	7.5	7.7	0.6
1.00	29.5	30.7	34.0	31.0	31.3	1.9
1.50	75.0	77.5	75.6	76.0	76.0	1.1
2.00	97.9	98.0	97.0	96.0	97.2	0.9
2.50	99.5	99.7	99.1	99.0	99.3	0.3
3.00	100.0	100.0	100.0	100.0	100.0	0.0

and heavy mineral fractions was determined by petrographic analysis of grain mounts. Three hundred heavy mineral grains were counted and identified for each sample. Light mineralogy was determined by identifying 200 grains on slides stained for plagioclase and potassium feldspar (Bailey and Stevens 1960). The results are presented in Tables 6-3 through 6-5. Several samples were also analyzed to determine the total weight percent of heavy minerals contained in the sand fraction (Table 6-6). A Leco Induction Furnace and a Dietert Two Minute Carbon Analyzer were used to determine the weight percent organic carbon in the $CaCO_3$-free samples. To estimate error and determine reproducibility of the analytical procedures, five blanks and five known standards were analyzed for percent carbon (Table 6-7). The minimum detectable difference in the response of an analytical instrument is defined by Kaiser and Specker (1955) as $K\ 2S_b$, where S_b is the standard deviation of the blank determination and K equals 1.96 (at the 95% confidence level). Given the results of the blank determinations (Table 6-7) the carbon analyzer used in this study has a minimum detectable difference in response of 0.18 g. Maximum variation in the data obtained by analyzing the known samples was .08%.

The clay mineralogy of 13 vibracore samples was determined using X-ray diffraction techniques (Table 6-8) following preparations described by Carroll (1970). After dispersion in a 10% calgon solution, the <2 micron fraction was separated from the rest of the sample by centrifuge and pre-treated with a 10% hydrochloric acid solution to remove the $CaCO_3$ fraction. This fraction was also treated with an 1N solution of magnesium acetate to saturate the expandable minerals with magnesium ions. Dissolved salts and excess acetate were removed from the samples by washing the clays with deionized water. After drying

Table 6-3. Light mineral content of selected vibracore samples.

Core No.	Depth in Meters	% Quartz	% Plagioclase	% K-Feldspar
4525	1.05-1.25	88.7	5.8	5.5
4525	2.48-2.68	85.1	6.5	8.4
4526	1.10-1.30	93.7	3.0	3.3
4528	1.08-1.28	91.6	4.2	4.2
4530	1.26-1.46	83.9	5.7	10.4
4530	3.25-3.45	86.7	1.6	11.7
4530	4.30-4.50	88.7	4.3	7.0
4530	5.34-5.54	94.7	0.9	4.4
4532	3.30-3.50	86.1	5.4	8.5
4532	4.28-4.48	80.1	8.7	11.2
4533	5.02-5.22	87.3	7.8	4.9
4534	2.89-3.09	85.3	7.2	7.5
4536	1.00-1.20	84.8	8.7	6.5
4536	2.50-2.70	91.5	5.2	3.3
4536	4.25-4.45	92.2	3.1	4.7
4539	1.00-1.20	90.4	7.1	2.5
4539	1.88-2.08	91.4	6.6	2.0
4539	2.70-2.90	92.2	3.1	4.7
4544	1.30-1.50	90.1	6.2	3.7
4544	4.10-4.30	82.0	11.7	6.3
4544	5.87-6.07	82.8	9.3	7.9
4545	0.80-1.00	90.8	5.8	3.4
4545	3.80-4.00	85.9	6.3	7.8
4545	4.80-5.00	85.5	6.9	7.6
4602	2.10-2.30	90.5	5.6	3.9
4602	4.80-5.00	91.2	4.6	4.3
4608	2.10-2.30	94.8	3.2	2.0
4608	3.90-4.10	88.8	4.9	6.3

Table 6-4. Heavy mineral content of selected subsamples of vibracores from the northern transect.

Core No.	4525	4525	4526	4528	4530	4530	4530	4530	4532	4532	4533	4533	4534
Core Interval in Meters	1.05-1.25	2.48-2.68	1.10-1.30	1.08-1.28	1.26-1.46	3.25-3.45	4.30-4.50	5.34-5.54	3.30-3.50	4.28-4.48	1.45-1.65	5.02-5.22	2.89-3.09
Non-Opaques (percent)													
Amphibole	25	24	28	29	40	40	42	33	29	41	35	47	34
Epidote	24	34	13	35	30	35	33	32	38	29	33	24	26
Zircon	9	8	8	6	7	4	5	5	5	6	7	5	10
Tourmaline	8	8	15	6	3	6	6	6	8	6	7	6	5
Staurolite	9	5	6	7	5	2	4	6	4	5	5	3	5
Sillmanite	9	2	4	1	3	2	3	5	4	P	3	4	3
Kyanite	1	4	6	5	4	3	2	3	2	3	3	4	2
Garnet	3	4	3	1	3	P	1	4	3	P	3	P	4
Rutile	2	2	--	1	P	P	P	2	2	P	1	1	1
Apatite	--	P	--	P	--	--	--	--	--	--	--	--	--
Sphene	--	--	--	--	P	--	P	--	--	--	--	--	--
Sphinel	--	--	--	--	--	P	--	--	--	--	--	P	--
Other	8	8	16	8	5	6	4	5	4	8	3	6	10
Opaques	31	47	59	42	33	22	28	37	25	21	22	14	23
ZTR[1]	19	18	23	13	10	11	11	13	16	11	15	12	16
EG[2]	27	38	16	36	33	35	34	36	41	29	36	24	30
$\frac{ZTR}{EG}$	0.70	0.47	1.43	0.36	0.30	0.31	0.32	0.36	0.39	0.38	0.42	0.50	0.53

[1] Zircon + Tourmaline + Rutile

[2] Epidote + Garnet

P = <1% present

Table 6-5. Heavy mineral content of selected subsamples of vibracores from the southern lease area.

Core No.	4602	4602	4602	4606	4606	4606	4607	4607	4607	4608	4608	4608
Core Interval in Meters	0.00-0.20	2.40-2.60	4.50-5.00	0.00-0.20	1.80-2.00	3.30-3.50	0.00-0.20	1.20-1.40	2.70-2.90	0.00-0.20	1.80-2.00	3.90-4.10
Non-Opaques (percent)												
Epidote	20	23	13	25	26	27	21	22	31	18	27	29
Hornblende	13	28	13	17	22	23	9	16	16	18	16	15
Staurolite	6	2	5	6	6	6	3	4	6	11	5	9
Garnet	5	2	5	1	2	1	3	8	5	7	4	4
Kyanite	2	2	5	6	6	5	--	--	--	2	1	--
Sillmarite	3	6	1	2	1	1	2	6	4	3	3	1
Zircon	6	7	13	7	7	7	6	13	5	6	9	4
Tourmaline	6	5	9	7	6	10	2	1	4	2	1	3
Rutile	3	5	2	8	1	6	4	6	2	1	3	--
Monazite	2	1	--	1	3	2	--	1	1	1	1	--
Apatite	--	2	3	--	--	--	--	--	1	1	--	--
Mica	2	2	--	2	1	1	3	--	1	2	1	2
Other	4	1	2	5	3	4	3	5	3	2	1	1
Opaques	28	13	29	13	16	7	43	18	22	26	26	33
ZTR[1]	15	17	24	22	14	23	12	20	11	9	13	7
EG[2]	25	25	18	26	28	28	24	30	26	25	31	33
$\frac{ZTR}{EG}$	0.60	0.68	1.33	0.85	0.50	0.82	0.50	0.66	0.30	0.36	0.42	0.2

[1] Zircon + Tourmaline + Rutile

[2] Epidote + Garnet

Table 6-6. Weight percent heavy minerals in selected vibracore subsamples.

Core No.	Core Interval in Meters	% Heavies in Subsamples
4602	0.00-0.20	1.9
	2.40-2.60	0.8
	4.80-5.00	2.1
4606	0.00-0.20	1.3
	1.80-2.00	2.1
	3.30-3.50	1.7
4607	0.00-0.20	5.2
	1.20-1.40	2.0
	2.70-2.90	0.8
4608	0.00-0.20	0.9
	1.80-2.00	0.4
	3.90-4.10	1.4

Table 6-7. Reproducibility of organic carbon data. Five blanks and five samples containing a known percentage of carbon (0.403% ± 0.009%) were analyzed.

Blank Samples

	Run						
	1	2	3	4	5	$\overline{X}$	Sd
% Carbon	0.00	0.01	0.01	0.01	0.01	0.01	.004

Known Samples (0.403% carbon ± 0.009%)

	Run						
	1	2	3	4	5	$\overline{X}$	Sd
% Carbon	0.37	0.37	0.33	0.41	0.37	0.37	±0.03

Table 6-8. Clay mineralogy of selected vibracore subsamples.

Core No.	Core Interval in Meters	Peak Area[1]				Y or N		Weight %			
		14[2]	10[2]	7.15[2]	4.85[2]	Mixed Layer	Chlorite	Smectite	Illite	Kaolinite	Gibbsite
4525	1.55-1.75	132	36	229	6	N	Y	26	29	44	1
4525	1.05-1.25	123	20	189	4	N	Y	31	20	48	1
4526	0.47-0.77	71	8	44	0	N	N	48	23	29	0
4526	0.40-0.43	132	15	112	10	N	N	42	19	36	3
4530	3.25-3.45	23	12	139	21	N	N	9	21	60	10
4530	2.65-2.85	80	10	252	12	N	N	21	10	65	3
4530	1.96-2.16	16	2	57	2	N	N	19	10	69	2
4530	1.26-1.46	192	22	299	14	N	N	32	15	51	2
4531	3.00-3.20	50	9	162	10	N	N	19	14	63	4
4531	1.51-1.71	57	13	156	15	N	N	20	19	56	5
4532	2.29-2.49	60	9	153	8	N	N	23	14	60	3
4544	4.10-4.30	178	25	267	8	N	N	32	18	48	2
4545	3.80-4.00	42	8	30	0	N	N	40	31	29	0

[1] Expressed in mm^2

[2] d- values

N = not contained in sample

Y = present but not quantified

overnight, sedimentation slides made from the clay fraction were X-rayed from $2^{\circ}20$ to $40^{\circ}20$ at a scan rate of $2^{\circ}20$ per minute using a Phillips X-ray diffractometer equipped with Ni-filtered copper K-alpha radiation. Several slides were treated with ethylene glycol to test for dioctahedral vermiculite, with negative results. Peak areas of the basal reflections (001) were determined from X-ray patterns of untreated samples, multiplied by the appropriate weighting factors suggested by Pevear (1968), and the results normalized to 100%. The results (Table 6-8) are, at best, semi-quantitative (±5%).

The radiocarbon age determinations used in the study were made at the Radiocarbon Dating Laboratory of the University of Miami. All shell material was etched with 10% HCl prior to analysis. Apparent ages were calculated relative to 0.95 x the NBS Oxalic acid radiocarbon dating standard. The laboratory's quoted precision is one-standard deviation; this includes only the counting errors on the unknown sample, background, and modern standard. The ages were calculated, without any age corrections, using a C-14 half-life of 5,568 years.

High-resolution, seismic-reflection profiles were obtained along the cross-shelf transects with a 3.5 kHz transceiver that was towed 7 m below the sea surface from the R/V H.J.W. FAY during 2-6 November 1975. While profiling, the ship's speed was 10-13 km/hr. Navigational control for the track lines and station locations was provided by Loran-C.

SUBBOTTOM PROFILES

The characteristics of the shallow subbottom profiles (Figure 6-2) change across the continental shelf. Beneath the inner shelf (water depth <19 m) the acoustic reflectors define numerous subbottom depressions (Figure 6-3, section AB; Figure 6-4, westernmost section

EF). Although some of these depressions are small, others have as much as 8 m of relief. Generally, the depressions are devoid of internal structure.

Between water depths of 19 amd 24 m, on the other hand, the subbottom is characterized by a shallow (<4 m deep) flat-lying reflector (Figure 6-3, section BC; Figure 6-4, section EF). In several places, this reflector approaches or forms the sea floor and appears to be the horizontal base upon which some of the small topographic ridges have been built. In the southern profile, this reflector can be traced (in the subsurface) for more than 18 km.

Across the outer shelf (>24 m water depth), we find a deeper, flat-lying reflector (Figure 6-3, section CD; Figure 6-4, section GH). At depth, this horizon becomes discontinuous owing to the small output of energy from the acoustic transducer. The reflector appears to crop out on the sea floor near the eastern ends of both profiles. Along the southern transect this exposure was marked by a noticeable increase in the reflectivity of the bottom.

CORE DESCRIPTIONS

Sediment Type

By far the dominant sediment type in these cores is a medium to coarse shelly sand, represented by sediment types E anf F in Figures 6-5, 6-6, and 6-7. Type E is dusky yellow to pale olive brown to brown in color due to iron staining on quartz grains. Type F is differentiated from Type E solely on the basis of color. The various shades of olive gray reflect the more reducing conditions of burial and consequent loss of iron stain on quartz-feldspar grains. The uppermost sediment in most cores is type E, reflecting the stirring effect of wave

Figure 6-5. Sediment types in the vibracores from the cross-shelf transects shown with descriptions of their textures, based on megascopic core descriptions. The terminology used in the textural descriptions is taken from Folk (1974). Subscripts denote the presence of prominent sediment components which conceivably are of importance in interpreting the origin of the various units.

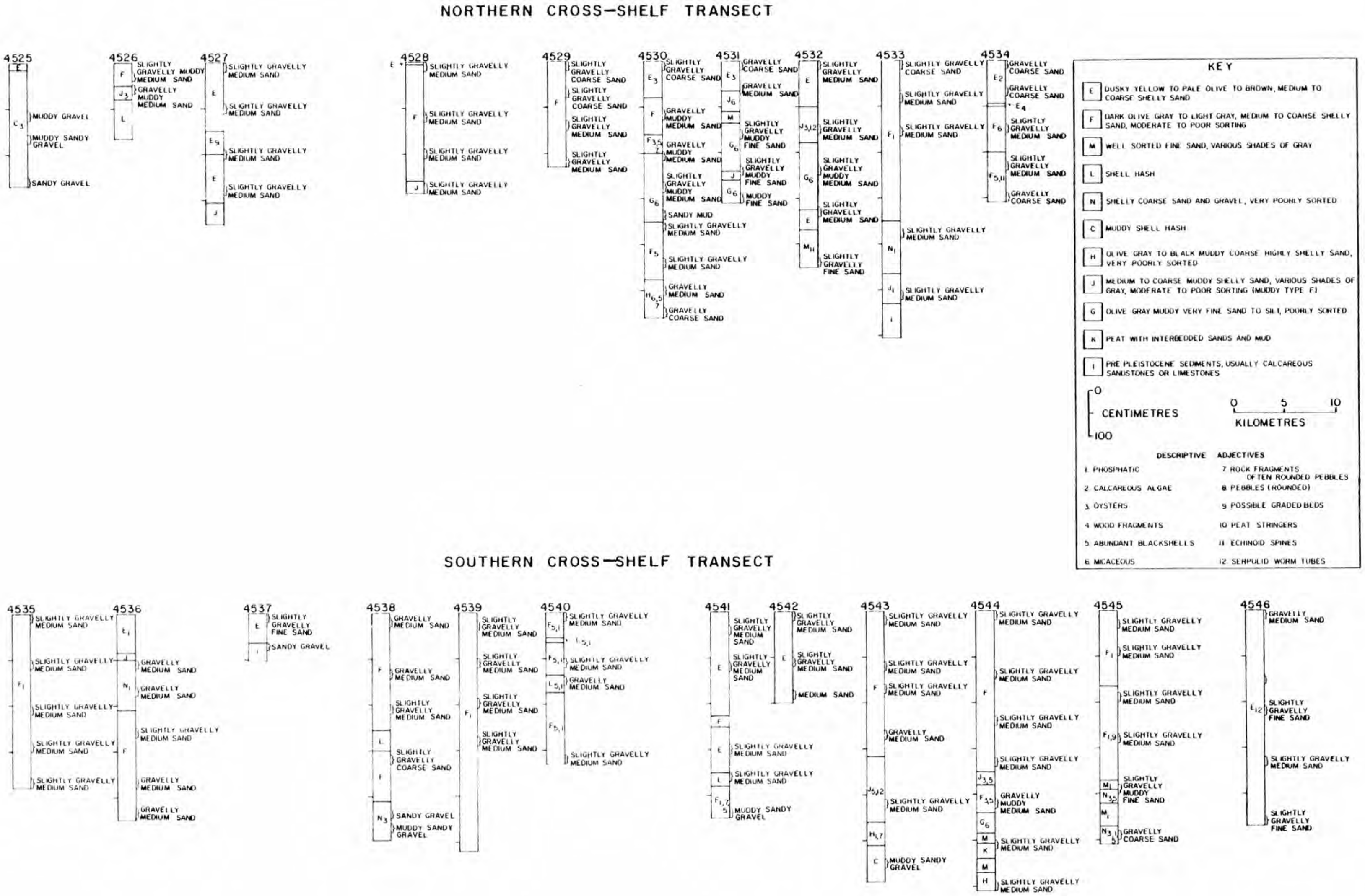
NORTHERN CROSS–SHELF TRANSECT
4525
E
C3
MUDDY GRAVEL
MUDDY SANDY GRAVEL
SANDY GRAVEL
4526
F
SLIGHTLY GRAVELLY MUDDY MEDIUM SAND
J3
GRAVELLY MUDDY MEDIUM SAND
L
4527
E
SLIGHTLY GRAVELLY MEDIUM SAND
SLIGHTLY GRAVELLY MEDIUM SAND
E9
SLIGHTLY GRAVELLY MEDIUM SAND
E
SLIGHTLY GRAVELLY MEDIUM SAND
J
4528
E
SLIGHTLY GRAVELLY MEDIUM SAND
F
SLIGHTLY GRAVELLY MEDIUM SAND
SLIGHTLY GRAVELLY MEDIUM SAND
J
SLIGHTLY GRAVELLY MEDIUM SAND
4529
F
SLIGHTLY GRAVELLY COARSE SAND
SLIGHTLY GRAVELLY COARSE SAND
SLIGHTLY GRAVELLY MEDIUM SAND
SLIGHTLY GRAVELLY MEDIUM SAND
4530
E3
SLIGHTLY GRAVELLY COARSE SAND
F
GRAVELLY MUDDY MEDIUM SAND
F3,5,7
GRAVELLY MUDDY MEDIUM SAND
G6
SLIGHTLY GRAVELLY MUDDY MEDIUM SAND
SANDY MUD
SLIGHTLY GRAVELLY MEDIUM SAND
F5
SLIGHTLY GRAVELLY MEDIUM SAND
H6,5,7
GRAVELLY MEDIUM SAND
GRAVELLY COARSE SAND
4531
E3
GRAVELLY COARSE SAND
GRAVELLY MEDIUM SAND
J6
M
G6
SLIGHTLY GRAVELLY MUDDY FINE SAND
SLIGHTLY GRAVELLY MUDDY FINE SAND
J
G6
MUDDY FINE SAND
4532
E
SLIGHTLY GRAVELLY MEDIUM SAND
J3,12
SLIGHTLY GRAVELLY MEDIUM SAND
G6
SLIGHTLY GRAVELLY MUDDY MEDIUM SAND
E
SLIGHTLY GRAVELLY MEDIUM SAND
M11
SLIGHTLY GRAVELLY FINE SAND
4533
F1
SLIGHTLY GRAVELLY COARSE SAND
SLIGHTLY GRAVELLY MEDIUM SAND
SLIGHTLY GRAVELLY MEDIUM SAND
N1
SLIGHTLY GRAVELLY MEDIUM SAND
J1
SLIGHTLY GRAVELLY MEDIUM SAND
I
4534
E2
GRAVELLY COARSE SAND
GRAVELLY COARSE SAND
E4
F6
SLIGHTLY GRAVELLY MEDIUM SAND
F5,11
SLIGHTLY GRAVELLY MEDIUM SAND
GRAVELLY COARSE SAND
KEY
E DUSKY YELLOW TO PALE OLIVE TO BROWN, MEDIUM TO COARSE SHELLY SAND
F DARK OLIVE GRAY TO LIGHT GRAY, MEDIUM TO COARSE SHELLY SAND, MODERATE TO POOR SORTING
M WELL SORTED FINE SAND, VARIOUS SHADES OF GRAY
L SHELL HASH
N SHELLY COARSE SAND AND GRAVEL, VERY POORLY SORTED
C MUDDY SHELL HASH
H OLIVE GRAY TO BLACK MUDDY COARSE HIGHLY SHELLY SAND, VERY POORLY SORTED
J MEDIUM TO COARSE MUDDY SHELLY SAND, VARIOUS SHADES OF GRAY, MODERATE TO POOR SORTING (MUDDY TYPE F)
G OLIVE GRAY MUDDY VERY FINE SAND TO SILT, POORLY SORTED
K PEAT WITH INTERBEDDED SANDS AND MUD
I PRE PLEISTOCENE SEDIMENTS, USUALLY CALCAREOUS SANDSTONES OR LIMESTONES
0
CENTIMETRES
100
0 5 10
KILOMETRES
DESCRIPTIVE ADJECTIVES
1 PHOSPHATIC
2 CALCAREOUS ALGAE
3 OYSTERS
4 WOOD FRAGMENTS
5 ABUNDANT BLACKSHELLS
6 MICACEOUS
7 ROCK FRAGMENTS OFTEN ROUNDED PEBBLES
8 PEBBLES (ROUNDED)
9 POSSIBLE GRADED BEDS
10 PEAT STRINGERS
11 ECHINOID SPINES
12 SERPULID WORM TUBES
SOUTHERN CROSS–SHELF TRANSECT
4535
F1
SLIGHTLY GRAVELLY MEDIUM SAND
SLIGHTLY GRAVELLY MEDIUM SAND
SLIGHTLY GRAVELLY MEDIUM SAND
SLIGHTLY GRAVELLY MEDIUM SAND
SLIGHTLY GRAVELLY MEDIUM SAND
4536
E1
J
N1
GRAVELLY MEDIUM SAND
GRAVELLY MEDIUM SAND
F
SLIGHTLY GRAVELLY MEDIUM SAND
GRAVELLY MEDIUM SAND
GRAVELLY MEDIUM SAND
4537
E
SLIGHTLY GRAVELLY FINE SAND
I
SANDY GRAVEL
4538
F
GRAVELLY MEDIUM SAND
GRAVELLY MEDIUM SAND
SLIGHTLY GRAVELLY MEDIUM SAND
L
F
SLIGHTLY GRAVELLY COARSE SAND
N3
SANDY GRAVEL
MUDDY SANDY GRAVEL
4539
F1
SLIGHTLY GRAVELLY MEDIUM SAND
SLIGHTLY GRAVELLY MEDIUM SAND
SLIGHTLY GRAVELLY MEDIUM SAND
SLIGHTLY GRAVELLY MEDIUM SAND
4540
F5,1
SLIGHTLY GRAVELLY MEDIUM SAND
L5,1
F5,1
SLIGHTLY GRAVELLY MEDIUM SAND
L5,1
GRAVELLY MEDIUM SAND
F5,1
SLIGHTLY GRAVELLY MEDIUM SAND
4541
E
SLIGHTLY GRAVELLY MEDIUM SAND
SLIGHTLY GRAVELLY MEDIUM SAND
F
E
SLIGHTLY GRAVELLY MEDIUM SAND
L
SLIGHTLY GRAVELLY MEDIUM SAND
F1,7,5
MUDDY SANDY GRAVEL
4542
E
SLIGHTLY GRAVELLY MEDIUM SAND
SLIGHTLY GRAVELLY MEDIUM SAND
MEDIUM SAND
4543
F
SLIGHTLY GRAVELLY MEDIUM SAND
SLIGHTLY GRAVELLY MEDIUM SAND
SLIGHTLY GRAVELLY MEDIUM SAND
GRAVELLY MEDIUM SAND
J5,12
SLIGHTLY GRAVELLY MEDIUM SAND
H1,7
C
MUDDY SANDY GRAVEL
4544
F
SLIGHTLY GRAVELLY MEDIUM SAND
SLIGHTLY GRAVELLY MEDIUM SAND
SLIGHTLY GRAVELLY MEDIUM SAND
SLIGHTLY GRAVELLY MEDIUM SAND
J3,5
F3,5
GRAVELLY MUDDY MEDIUM SAND
G6
M
K
M
H
SLIGHTLY GRAVELLY MEDIUM SAND
SLIGHTLY GRAVELLY MEDIUM SAND
4545
F1
SLIGHTLY GRAVELLY MEDIUM SAND
SLIGHTLY GRAVELLY MEDIUM SAND
F1,9
SLIGHTLY GRAVELLY MEDIUM SAND
SLIGHTLY GRAVELLY MEDIUM SAND
M1
N3,5
SLIGHTLY GRAVELLY MUDDY FINE SAND
M1
N3,1,5
GRAVELLY COARSE SAND
4546
E12
GRAVELLY MEDIUM SAND
SLIGHTLY GRAVELLY FINE SAND
SLIGHTLY GRAVELLY MEDIUM SAND
SLIGHTLY GRAVELLY FINE SAND

Figure 6-5

Figure 6-6. Sediment types in the vibracores from the northern lease area with descriptions of their textures, based on megascopic core descriptions. The terminology used in the textural descriptions is taken from Folk (1974). Subscripts denote the presence of prominent sediment components which conceivably are of importance in the interpretation of the origin of the various units.

SEDIMENT TEXTURE: NORTHERN AREA

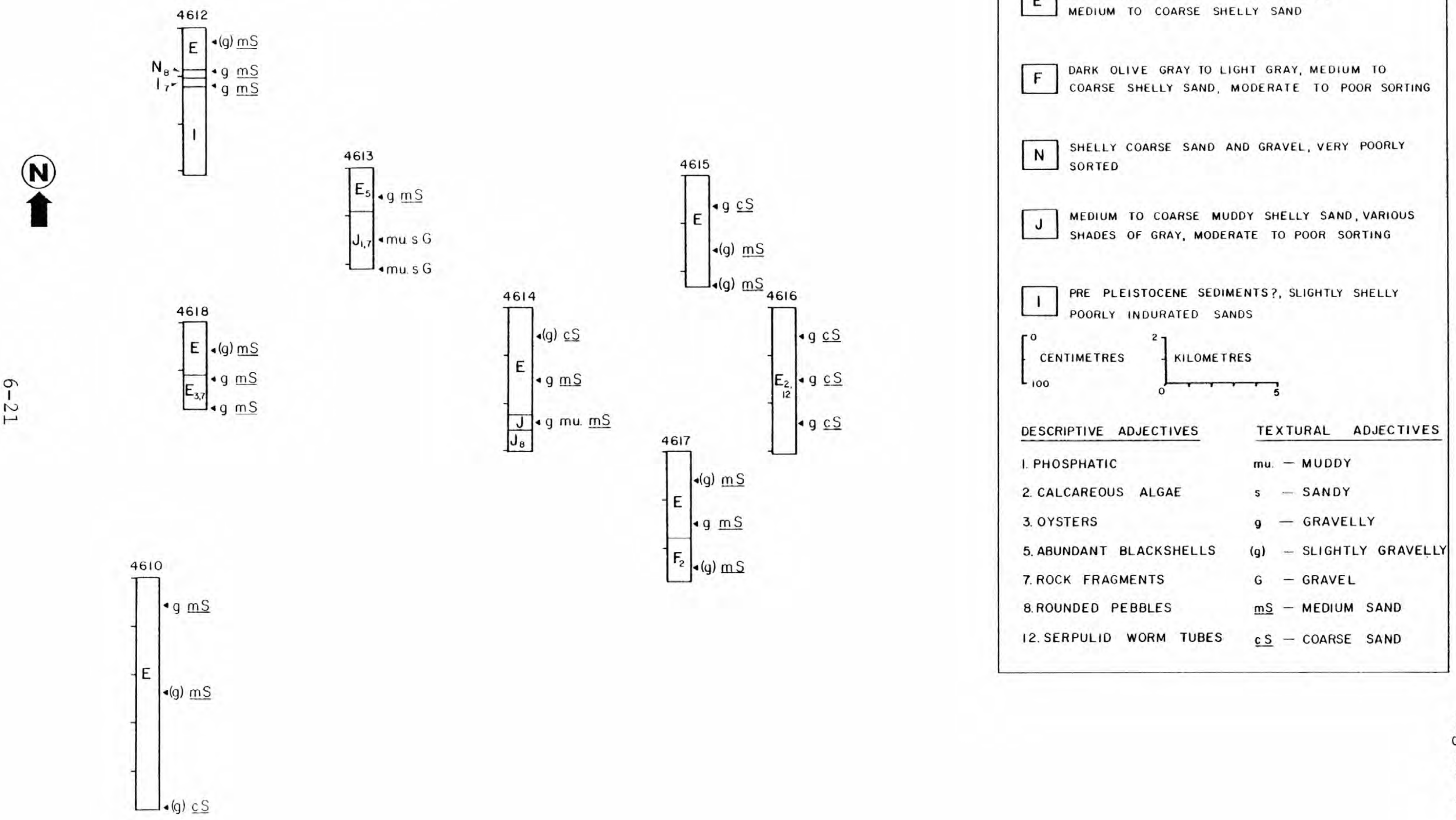

N
4612
E
(g) mS
N8
g mS
I7
g mS
I
4613
E5
g mS
J1,7
mu. s G
mu. s G
4615
E
g cS
(g) mS
(g) mS
4618
E
(g) mS
E3,7
g mS
g mS
4614
E
(g) cS
g mS
J
g mu. mS
J8
4616
E2,12
g cS
g cS
g cS
4617
E
(g) mS
g mS
F2
(g) mS
4610
E
g mS
(g) mS
(g) cS
KEY
E DUSKY YELLOW TO PALE OLIVE TO BROWN, MEDIUM TO COARSE SHELLY SAND
F DARK OLIVE GRAY TO LIGHT GRAY, MEDIUM TO COARSE SHELLY SAND, MODERATE TO POOR SORTING
N SHELLY COARSE SAND AND GRAVEL, VERY POORLY SORTED
J MEDIUM TO COARSE MUDDY SHELLY SAND, VARIOUS SHADES OF GRAY, MODERATE TO POOR SORTING
I PRE PLEISTOCENE SEDIMENTS?, SLIGHTLY SHELLY POORLY INDURATED SANDS
0
CENTIMETRES
100
2
KILOMETRES
0
5
DESCRIPTIVE ADJECTIVES
1. PHOSPHATIC
2. CALCAREOUS ALGAE
3. OYSTERS
5. ABUNDANT BLACKSHELLS
7. ROCK FRAGMENTS
8. ROUNDED PEBBLES
12. SERPULID WORM TUBES
TEXTURAL ADJECTIVES
mu. — MUDDY
s — SANDY
g — GRAVELLY
(g) — SLIGHTLY GRAVELLY
G — GRAVEL
mS — MEDIUM SAND
cS — COARSE SAND

Figure 6-6

Figure 6-7. Sediment types in the vibracores from the southern lease area shown with descriptions of their textures, based on megascopic core descriptions. See Figure 6-6 for additional explanation of this figure.

SEDIMENT TEXTURE: SOUTHERN AREA

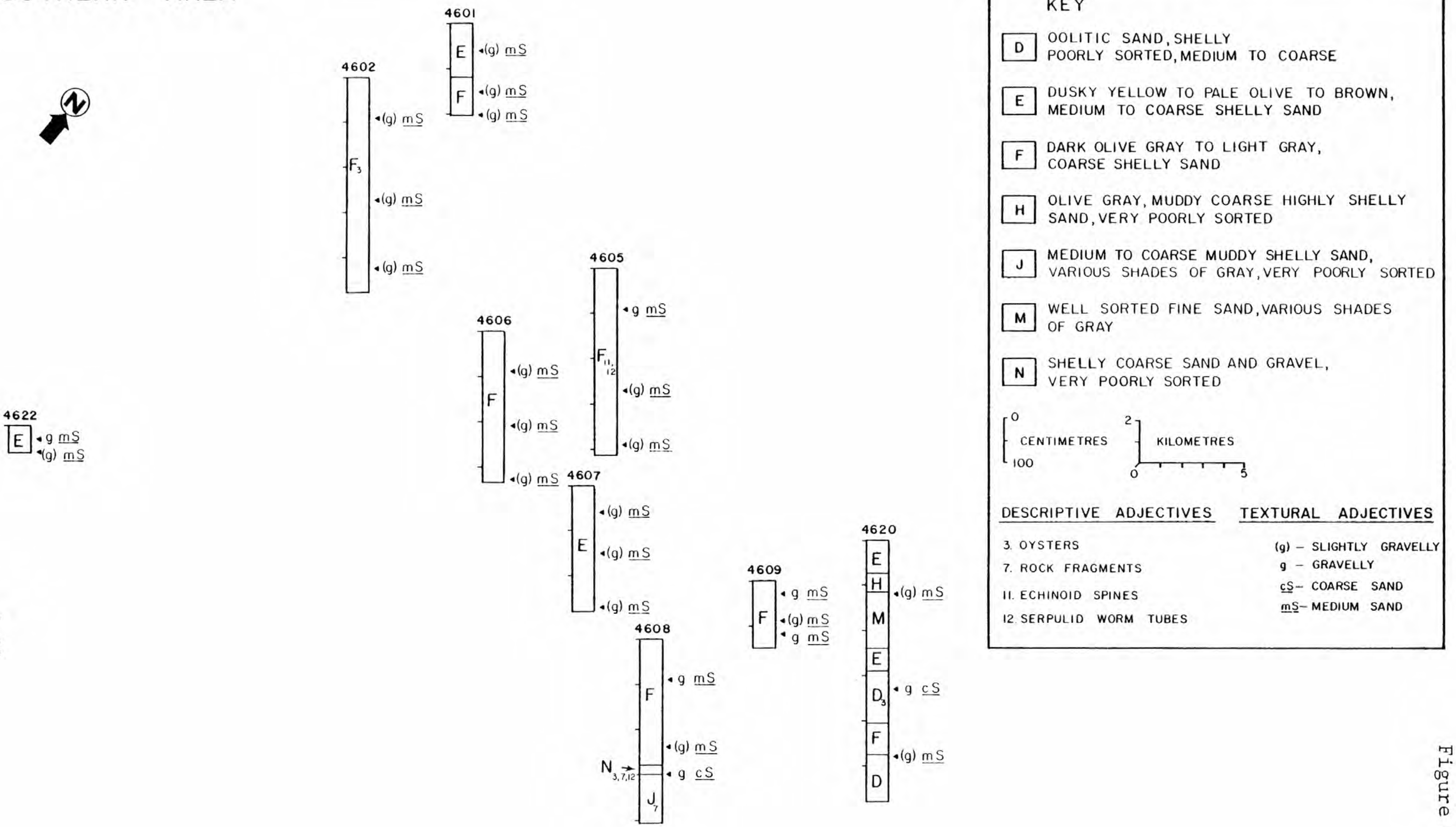
N
4601
E
(g) mS
F
(g) mS
(g) mS
4602
F_3
(g) mS
(g) mS
(g) mS
4605
g mS
$F_{11,12}$
(g) mS
(g) mS
4606
F
(g) mS
(g) mS
(g) mS
4607
E
(g) mS
(g) mS
(g) mS
4608
F
g mS
(g) mS
$N_{3,7,12}$
g cS
J_7
4609
F
g mS
(g) mS
g mS
4620
E
H
M
E
D_3
F
D
(g) mS
g cS
(g) mS
4622
E
g mS
(g) mS
0
CENTIMETRES
100
2
KILOMETRES
0
5

KEY

D	OOLITIC SAND, SHELLY POORLY SORTED, MEDIUM TO COARSE
E	DUSKY YELLOW TO PALE OLIVE TO BROWN, MEDIUM TO COARSE SHELLY SAND
F	DARK OLIVE GRAY TO LIGHT GRAY, COARSE SHELLY SAND
H	OLIVE GRAY, MUDDY COARSE HIGHLY SHELLY SAND, VERY POORLY SORTED
J	MEDIUM TO COARSE MUDDY SHELLY SAND, VARIOUS SHADES OF GRAY, VERY POORLY SORTED
M	WELL SORTED FINE SAND, VARIOUS SHADES OF GRAY
N	SHELLY COARSE SAND AND GRAVEL, VERY POORLY SORTED

DESCRIPTIVE ADJECTIVES

3. OYSTERS
7. ROCK FRAGMENTS
11. ECHINOID SPINES
12. SERPULID WORM TUBES

TEXTURAL ADJECTIVES

(g) – SLIGHTLY GRAVELLY
g – GRAVELLY
cS – COARSE SAND
mS – MEDIUM SAND

Figure 6-7

action, promoting oxidation of iron. Type F is the second and thickest overall unit. Occasionally, as in cores 4541 and 4532, the oxidized E unit is overlain by the reduced sand of Type F. In one core, 4546, only sediment Type E is present. Type F is the only sediment type in cores 4535, 4539, and 4529. Sediment Types E and F are megascopically identical to present day shelf surficial sediments.

Shell hashes are the next most common sediment types. Types C, H and J are muddy, resulting in extremely poor sorting. These sediments megascopically resemble nearshore sediments found in inlets or backbarrier environments. One core, 4620, contained oolitic sand in two separate units. The oolitic sediment in the upper unit was unlithified while the lower unit was lithified (Figure 6-7).

The fine and very fine sands, Types M and G, are grossly similar to the fine nearshore sands presently covering the inner shelf shoreface of Georgia and South Carolina (Pilkey and Frankenberg 1964). The presence of prominent sediment components which conceivably are of importance in interpreting the origin of the various units are also shown in Figures 6-5 through 6-7. Particularly important are calcareous algae, designating open shelf origin, and oysters, which are indicative of a lagoonal environment. Abundant mica indicates deposition either catastrophically or in a "quiet" environment such as a shelf depression. Mica flakes hydraulically equivalent to silt and clay-sized material would not be expected in an environment of gradual deposition with continual stirring and winnowing by waves and currents. Phosphate grains may be indicative of a residual source of the sediment, i.e., erosion or weathering from an underlying Tertiary rock formation.

In general, unit distinctions in these cores, as shown in Figures 6-5 through 6-7, are subtle rather than sharp. This is particularly true for the sand units. Boundaries between sand units tend to be gradational over 10 cm or so. Units with significant mud content such as C, H, J or G (Figure 6-5) tend to have sharper upper and lower boundaries than the sand units. All sediment types identified as lagoonal in origin on the basis of the microfauna are muddy. Visibly muddy shelf sediment is rare.

Sedimentary Structures

Sedimentary structures are important to this study from two standpoints. They indicate the nature or type of depositional processes on the sea floor and at the same time they afford some idea of the frequency and intensity of such processes. The most common types of sedimentary structures that are identifiable in the vibracores are interbedded sand and mud, remnant stratification, shell layers, and shell fragment layers (Figures 6-8 and 6-9). The so-called interbedded sand and mud sedimentary structure designated by closely spaced unbroken lines (Figure 6-8a) is actually more likely to be interbedded coarse and fine sand or silt.

Individual burrows are sometimes identifiable. Spreite-type burrows (Figure 6-8a) are assumed to have been formed by heart urchins, an open shelf form. The coarse sand-filled burrows are not environment or organism specific.

It is apparent from Figures 6-8 and 6-9 that most of the sedimentary column represented by these cores is highly bioturbated. In fact, most of the column is greater than 90% bioturbated. In perhaps 40-50% of the sedimentary column, identifiable sedimentary structures are not present.

This intense bioturbation suggests that sufficient time elapsed between shelf depositional events such as storms to allow complete

Figure 6-8. a. Sedimentary structures of vibracores from the northern transect based on core x-radiography (center column). The left-hand column shows sediment type (basically the same as the information in Figure 6-5) and the right-hand column shows an estimate of % bioturbation. The symbols on the right-hand side of each column represent sedimentary components; essentially the same as those illustrated by subscripts in Figure 6-5.

b. Sedimentary structures of vibracores from the southern transect based on core x-radiography (see Figure 6-8a for details and explanation of symbols).

Figure 6-3a

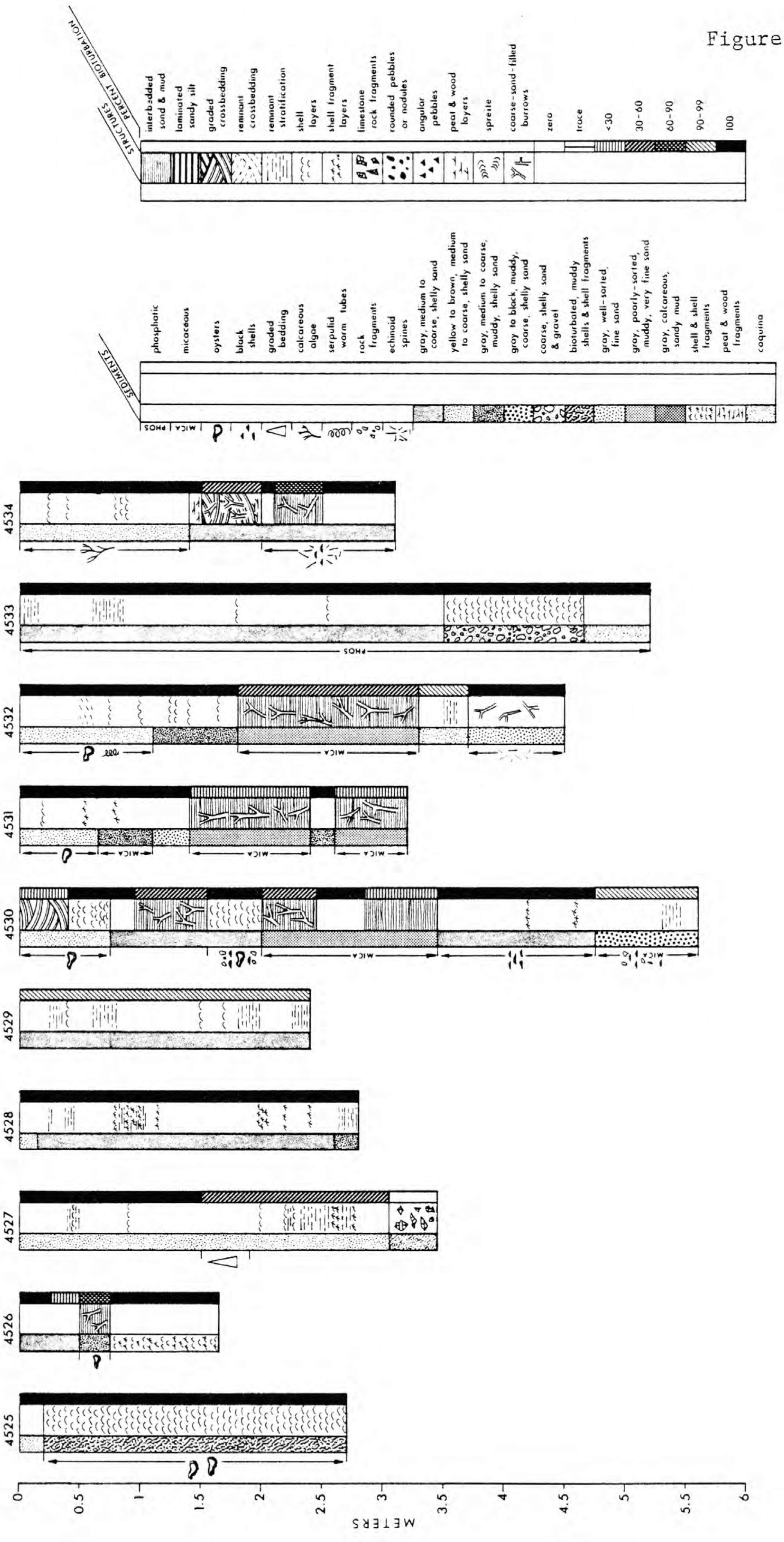
PERCENT BIOTURBATION
STRUCTURES
interbedded sand & mud
laminated sandy silt
graded crossbedding
remnant crossbedding
remnant stratification
shell layers
shell fragment layers
limestone rock fragments
rounded pebbles or nodules
angular pebbles
peat & wood layers
spreite
coarse-sand-filled burrows
zero
trace
<30
30-60
60-90
90-99
100
SEDIMENTS
phosphatic
micaceous
oysters
black shells
graded bedding
calcareous algae
serpulid worm tubes
rock fragments
echinoid spines
gray, medium to coarse, shelly sand
yellow to brown, medium to coarse, shelly sand
gray, medium to coarse, muddy, shelly sand
gray to black, muddy, coarse, shelly sand
coarse, shelly sand & gravel
bioturbated, muddy shells & shell fragments
gray, well-sorted, fine sand
gray, poorly-sorted, muddy, very fine sand
gray, calcareous, sandy mud
shell & shell fragments
peat & wood fragments
coquina
PHOS
MICA
4534
4533
4532
4531
4530
4529
4528
4527
4526
4525
0
0.5
1
1.5
2
2.5
3
3.5
4
4.5
5
5.5
6
METERS

Figure 6-8b

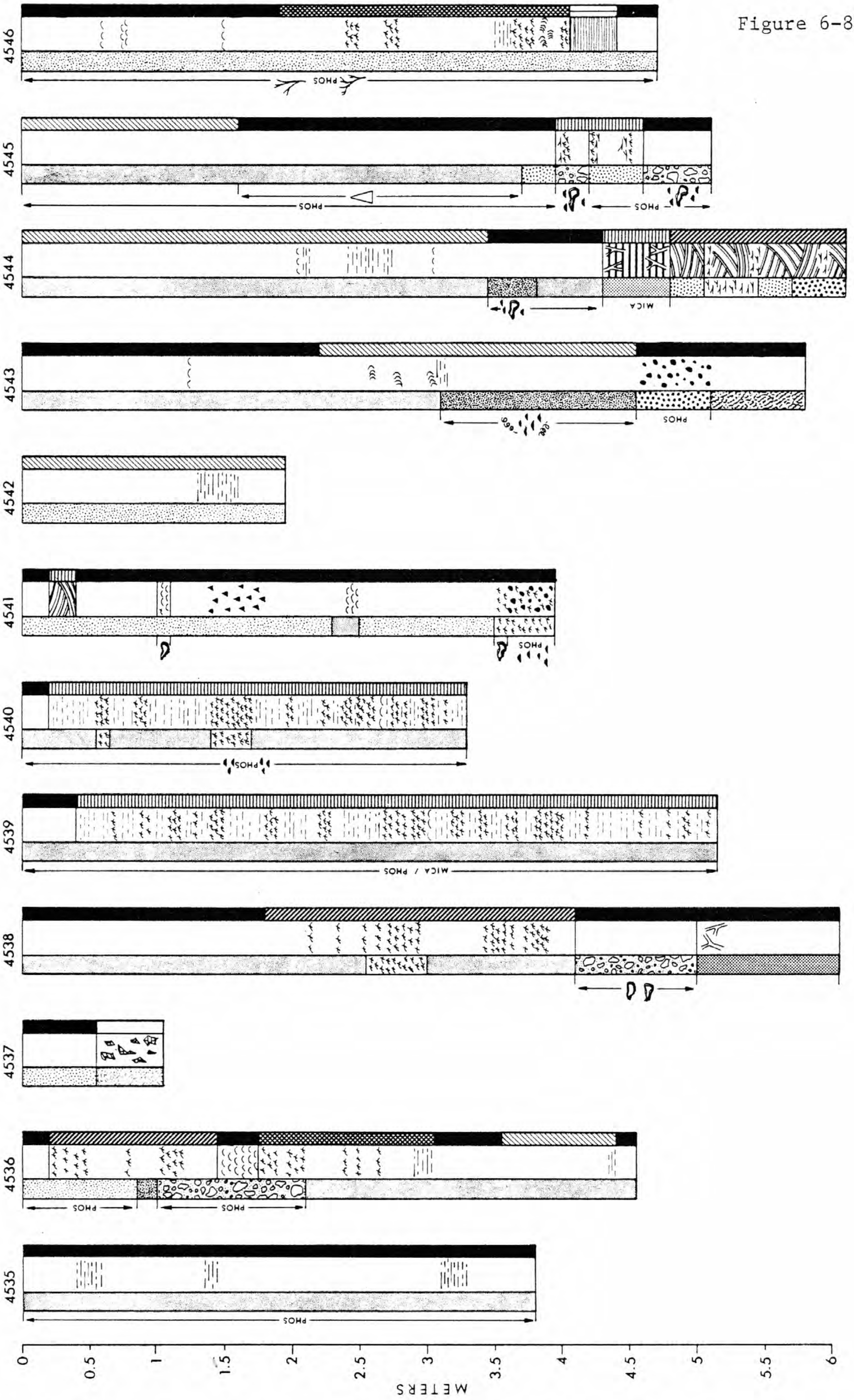
4546
PHOS
4545
PHOS
PHOS
4544
MICA
4543
PHOS
4542
4541
PHOS
4540
PHOS
4539
MICA / PHOS
4538
4537
4536
PHOS
PHOS
4535
PHOS
0
0.5
1
1.5
2
2.5
3
3.5
4
4.5
5
5.5
6
METERS

Figure 6-9. a. Sedimentary structures of vibracores from the northern and southern lease areas based on core x-radiography (center column). The left-hand column shows sediment type (basically the same as the information in Figure 6-5) and the right-hand column shows an estimate of % bioturbation. The symbols on the right-hand side of each column represent sedimentary components; essentially the same as those illustrated by subscripts in Figure 6-5.

b. Sedimentary structures of vibracores from the northern and southern lease areas based on core x-radiography (see Figure 6-9a for details and explanation of symbols).

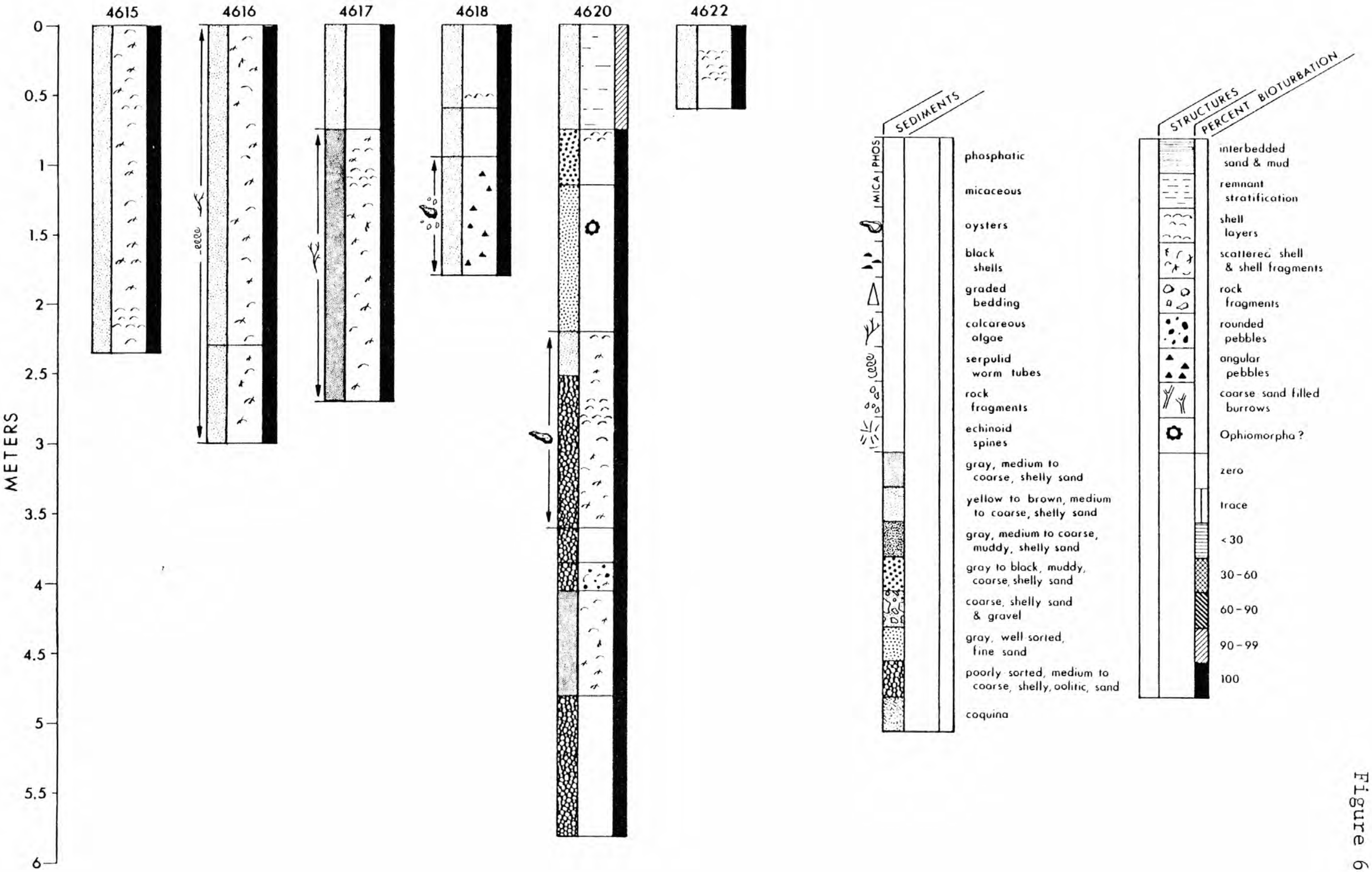
4615
4616
4617
4618
4620
4622
METERS
0
0.5
1
1.5
2
2.5
3
3.5
4
4.5
5
5.5
6
SEDIMENTS
MICA | PHOS
phosphatic
micaceous
oysters
black shells
graded bedding
calcareous algae
serpulid worm tubes
rock fragments
echinoid spines
gray, medium to coarse, shelly sand
yellow to brown, medium to coarse, shelly sand
gray, medium to coarse, muddy, shelly sand
gray to black, muddy, coarse, shelly sand
coarse, shelly sand & gravel
gray, well sorted, fine sand
poorly sorted, medium to coarse, shelly, oolitic, sand
coquina
STRUCTURES
PERCENT BIOTURBATION
interbedded sand & mud
remnant stratification
shell layers
scattered shell & shell fragments
rock fragments
rounded pebbles
angular pebbles
coarse sand filled burrows
Ophiomorpha ?
zero
trace
< 30
30 - 60
60 - 90
90 - 99
100

Figure 6-9a

Figure 6-9b

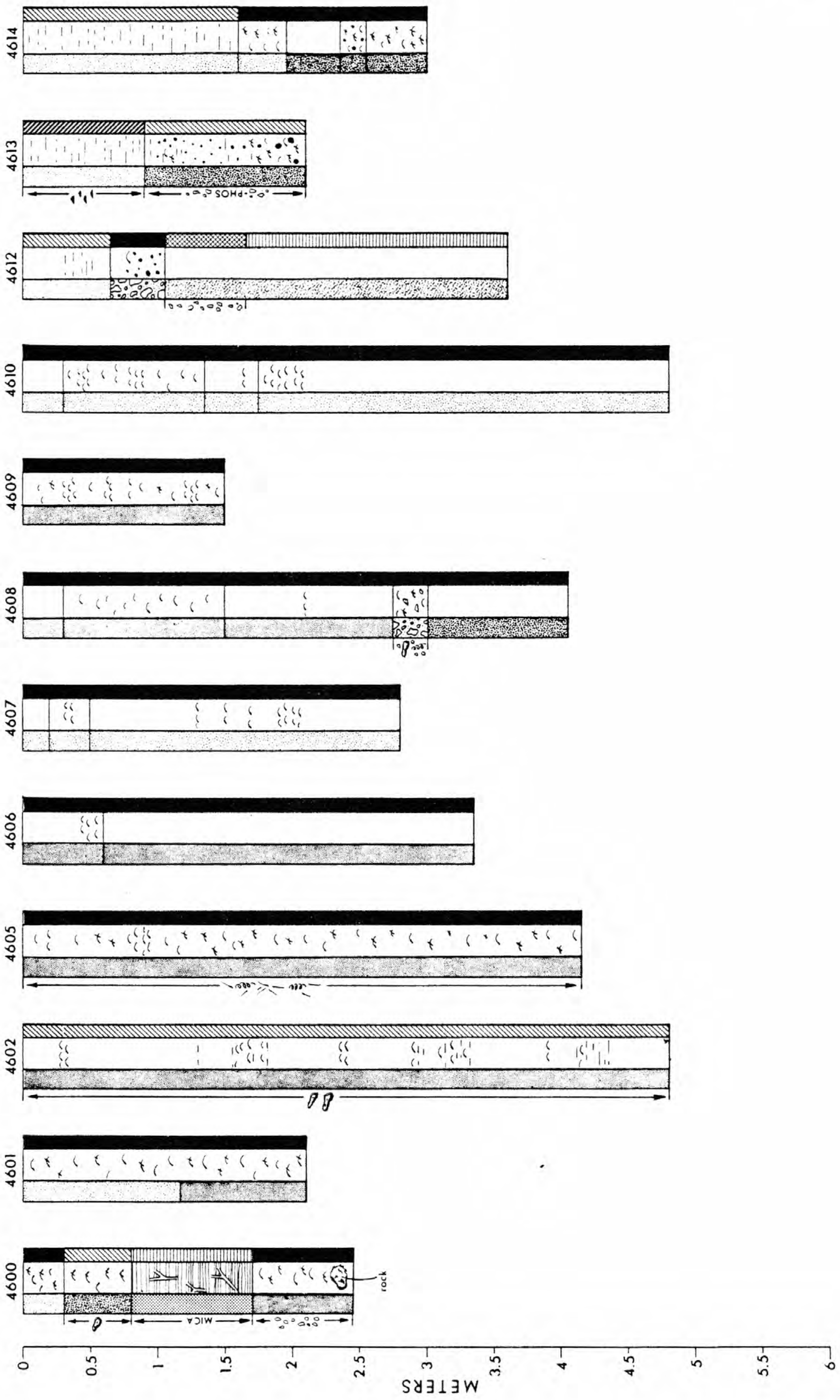

4614
4613
PHOS
4612
4610
4609
4608
4607
4606
4605
4602
4601
4600
MICA
rock
0
0.5
1
1.5
2
2.5
3
3.5
4
4.5
5
5.5
6
METERS

sediment turnover. The presence of intense bioturbation may also indicate that layers of sediment brought to the depositional site were not too thick to prevent bioturbation throughout.

Texture of Vibracore Sediments

It would be expected that the sediment cover has been extensively reworked on the U.S. Atlantic continental shelf, which has undergone several late Quaternary episodes of transgression and regression. The textural implications of such reworking under a high energy regime are apparent; fine minerals would be winnowed away leaving only the coarser fraction. The winnowed nature of surficial sediments on the southeastern U.S. shelf has been demonstrated by Doyle et al (1968). Shelf sediments were shown to have low contents of fine-grained mica (approximately 10-20 grains of mica per 10,000 insoluble grains). This contrasts sharply with the unwinnowed slope sediments that typically have much higher contents of mica (>80 grains per 10,000 insoluble grains).

Textures of most of the vibracore subsamples in this study indicate that the winnowing of shelf sediments is not restricted to the surficial deposits. The textures of the vibracore subsamples do not vary greatly (Tables 6-9 and 6-10). The majority of the samples are medium sands containing slightly different amounts of gravel (Figures 6-5 through 6-7). Only 15 of the 148 samples analyzed for texture contained greater than 10% mud, and only 2 of these contained more than 50% mud (Figure 6-10 and Table 6-11). Fine sands do occur, but like the muddy samples they are usually found below the zone of Holocene mixing.

Calcium Carbonate

The percentage of $CaCO_3$ was determined in 269 selected vibracore subsamples (Figures 6-11 through 6-13). On the southeastern U.S.

Table 6-9. Textural data of selected vibracore subsamples from the cross-shelf transects.

Core No.	Core Interval in Meters	Weight %		
		Mud <63µm	Sand <2mm >63µm	Gravel >2mm
4525	1.05-1.25	54.33	33.04	12.64
"	1.55-1.75	18.66	18.15	63.19
"	2.48-2.68	5.85	54.24	39.91
4526	0.20-0.40	48.48	50.25	1.27
"	0.47-0.67	14.65	77.01	8.34
4527	0.00-0.20	0.76	96.64	2.60
"	0.90-1.10	1.48	97.70	0.82
"	1.89-2.09	1.49	96.24	2.27
"	2.61-2.81	0.85	98.05	1.11
4528	0.00-0.20	0.52	98.59	0.89
"	1.08-1.28	0.62	98.24	1.13
"	1.90-2.10	1.28	97.54	1.17
"	2.64-2.79	6.54	90.69	2.77
4529	0.00-0.20	1.18	95.94	2.88
"	0.60-0.80	0.56	97.32	2.13
"	1.30-1.50	0.83	98.42	0.74
"	2.11-3.11	5.86	93.09	1.05
4530	0.00-0.20	1.02	96.44	2.54
"	1.26-1.46	15.60	78.65	5.75
"	1.96-2.16	27.15	67.03	5.81
"	2.65-2.85	17.53	78.82	3.65
"	3.25-3.45	60.54	39.46	0.00
"	3.50-3.70	6.38	91.10	2.52
"	4.30-4.50	4.48	94.34	1.18
"	4.90-5.10	5.91	87.74	6.34
"	5.34-5.54	5.11	78.53	16.36
4531	0.00-0.20	1.26	77.74	21.02
"	0.51-0.71	3.80	89.34	6.86
"	1.51-1.71	37.37	60.77	1.86
"	2.30-2.50	19.16	78.15	2.69
"	3.00-3.20	43.52	56.48	0.00
4532	0.00-0.20	0.96	98.61	0.43
"	1.39-1.59	5.14	91.13	3.73
"	2.29-2.49	16.92	79.76	3.32
"	3.30-3.50	6.28	92.39	1.33
"	4.28-4.48	7.51	92.24	0.25
4533	0.00-0.20	1.24	97.63	1.13
"	0.73-0.93	1.18	98.23	0.59
"	1.45-1.65	1.03	98.30	0.67
"	3.66-3.86	2.03	89.62	8.35
"	5.02-5.22	4.16	92.64	3.20
4534	0.00-0.20	1.11	92.40	6.49
"	0.60-0.80	1.58	93.95	4.47
"	1.38-1.58	4.34	93.36	2.30
"	2.20-2.40	5.86	91.65	2.49
"	2.89-3.09	5.00	79.48	15.52

Table 6-9. Textural data of selected vibracore subsamples from the cross-shelf transects (continued)

Core No.	Core Interval in Meters	Weight %		
		Mud <63µm	Sand <2mm >63µm	Gravel >2mm
4535	0.00-0.20	0.00	98.32	1.68
"	1.00-1.20	1.02	96.56	2.42
"	2.00-2.20	1.41	96.11	2.48
"	2.80-3.00	1.35	97.81	0.84
"	3.57-3.77	1.49	97.76	0.75
4536	1.00-1.20	5.58	87.91	6.52
"	1.60-1.80	6.08	76.89	17.03
"	2.50-2.70	2.22	97.02	0.76
"	3.60-3.80	3.18	88.89	7.93
"	4.25-4.45	5.43	87.03	7.54
4537	0.00-0.20	6.92	92.98	0.10
"	0.65-0.85	2.66	40.19	57.15
4538	0.10-0.30	2.44	85.08	12.48
"	1.23-1.43	4.12	88.24	7.40
"	2.00-2.20	2.16	96.70	1.14
"	3.10-3.30	2.91	94.64	2.45
"	4.30-4.50	4.67	59.39	35.94
"	4.60-4.80	6.66	57.87	35.46
4539	0.20-0.40	1.16	94.99	3.85
"	1.00-1.20	1.75	95.25	3.00
"	1.88-2.08	1.97	96.05	1.97
"	2.70-2.90	0.78	96.80	2.42
4540	0.00-0.20	1.13	93.25	5.62
"	1.00-1.20	1.02	95.87	3.11
"	1.40-1.60	5.14	80.03	14.83
"	2.20-2.40	0.59	97.09	2.32
4541	0.30-0.50	0.64	97.69	1.67
"	1.10-1.30	1.89	97.83	0.27
"	2.90-3.10	1.34	96.37	2.29
"	3.50-3.70	4.05	92.65	3.30
"	4.30-4.50	5.94	56.04	38.02
4542	0.00-0.20	0.43	98.51	1.06
"	1.00-1.20	0.58	98.66	0.76
"	1.71-1.91	0.65	99.25	0.01
4543	0.10-0.30	6.98	92.36	0.66
"	1.10-1.30	1.60	97.47	0.93
"	1.60-1.80	1.26	98.06	0.68
"	2.60-2.80	3.73	88.74	7.53
"	4.10-4.30	3.23	94.47	2.30
"	5.40-5.60	16.91	52.45	30.64
4544	0.00-0.20	0.68	97.22	2.10
"	1.30-1.50	1.56	97.71	0.73
"	2.30-2.50	1.74	95.73	2.52
"	3.20-3.40	1.79	96.51	1.69
"	4.10-4.30	19.90	72.32	7.78
"	5.00-5.20	7.20	92.75	0.05
"	5.87-6.07	8.49	86.69	4.82

Table 6-9. Textural data of selected vibracore subsamples from the cross-shelf transects (continued)

Core No.	Core Interval in Meters	Weight %		
		Mud <63µm	Sand <2mm >63µm	Gravel >2mm
4545	0.20-0.40	3.70	95.14	1.17
"	0.80-1.00	3.62	92.16	4.22
"	1.80-2.00	3.76	92.89	3.35
"	2.70-2.90	4.49	95.16	0.35
"	3.80-4.00	14.16	81.81	4.03
"	4.80-5.00	3.98	79.77	16.25
4546	0.00-0.20	2.40	83.72	13.87
"	1.42-1.62	0.90	91.38	7.72
"	2.10-2.30	1.60	96.63	1.77
"	3.20-3.40	2.61	94.58	2.81
"	4.44-4.64	3.38	96.13	0.49

Table 6-9. Textural data of selected vibracore subsamples from the proposed lease areas.

Core No.	Core Interval in Meters	Weight %		
		Mud <63µm	Sand <2mm >63µm	Gravel >2mm
4600	0.60-0.80	1.15	83.15	15.70
"	1.80-2.00	4.83	92.54	2.62
"	2.40-2.60	0.06	97.02	2.92
4601	0.60-0.80	0.15	98.00	1.85
"	1.50-1.70	0.81	97.62	1.57
"	2.40-2.60	0.43	98.47	1.10
4602	0.90-1.10	2.32	94.52	3.16
"	2.70-2.90	2.82	93.64	3.54
"	4.20-4.40	2.41	92.99	4.60
4605	0.90-1.10	3.02	83.08	13.90
"	2.70-2.90	0.18	98.14	1.41
"	3.90-4.10	2.86	96.31	0.83
4606	0.90-1.10	1.71	97.03	1.26
"	2.10-2.20	1.94	97.83	0.23
"	3.30-3.50	1.03	98.53	0.44
4607	0.60-0.80	1.24	97.30	1.46
"	1.50-1.70	1.79	97.67	0.55
"	2.70-2.90	1.49	96.68	1.82
4608	0.90-1.10	1.21	89.35	9.44
"	2.40-2.60	0.09	97.30	2.61
"	3.60-3.80	3.66	88.47	7.86
4609	0.30-0.50	3.45	83.33	7.41
"	0.09-1.10	1.14	94.46	4.39
"	1.20-1.40	0.83	93.29	5.88
4610	0.60-0.80	1.91	85.36	12.73
"	2.40-2.60	0.11	96.95	2.93
"	4.80-5.00	2.61	93.44	3.95
4612	0.30-0.50	3.08	95.75	1.18
"	0.90-1.10	3.12	73.76	23.12
"	1.20-1.40	9.74	60.99	29.27
4613	0.60-0.80	2.44	90.63	6.92
"	1.50-1.70	5.65	52.87	41.48
"	2.10-2.20	6.20	48.12	45.68
4614	0.60-0.80	8.02	87.09	4.89
"	1.50-1.70	2.44	96.31	1.25
"	2.40-2.60	7.61	79.14	13.25
4615	0.60-0.80	2.66	91.14	6.20
"	1.50-1.70	3.33	94.84	1.83
"	2.36-2.56	2.58	93.33	4.09
4616	0.60-0.80	4.28	79.75	15.97
"	1.50-1.70	3.14	81.53	15.33
"	2.40-2.60	3.10	82.64	14.26
4617	0.60-0.80	1.73	95.58	2.69
"	1.50-1.70	1.73	92.99	5.28
"	2.40-2.60	3.07	93.69	3.25

Table 6-9. Textural data of selected vibracore subsamples from the proposed lease areas, (continued)

Core No.	Core Interval in Meters	Weight %		
		Mud <63µm	Sand <2mm >63µm	Gravel >2mm
4618	0.60-0.80	2.46	98.84	3.71
"	1.20-1.40	3.24	70.09	26.67
"	1.80-2.00	4.40	80.43	15.18
4620	1.20-1.40	4.96	93.77	1.28
"	3.30-3.50	5.03	82.51	12.46
"	4.80-5.00	3.93	91.40	4.66
4622	0.30-0.50	2.18	79.70	18.13
"	0.60-0.80	1.67	96.83	1.50

Table 6-9. Vibracore subsamples - cumulative weight percent by phi size of sand fraction.

Core No.	Core Interval in Meters	-0.5	0.0	0.5	1.0	1.5	2.0	2.5	3.0	3.5	4.0
4525	1.05-1.25	0.0	3.0	9.0	21.0	41.5	56.5	77.5	93.5	99.5	100.0
"	1.55-1.75	2.0	8.0	18.5	36.0	59.0	74.5	87.5	95.0	99.0	100.0
"	2.48-2.68	5.0	27.0	43.5	60.0	77.0	87.5	96.5	99.0	99.9	100.0
4526	0.20-0.40	2.5	11.0	26.5	47.0	69.0	83.0	92.5	98.0	99.8	100.0
"	0.47-0.67	0.0	9.5	23.0	42.0	66.0	83.0	94.5	98.5	99.5	100.0
4527	0.00-0.20	0.0	2.5	9.5	26.0	50.0	79.0	96.5	99.8	100.0	
"	0.90-1.10	0.5	3.0	12.5	28.0	49.0	75.0	95.5	99.5	100.0	
"	1.89-2.09	0.0	0.0	4.5	14.0	26.5	49.0	92.0	99.0	99.8	100.0
"	2.61-2.81	0.0	0.5	4.5	13.5	25.5	45.0	91.0	99.3	99.9	100.0
4528	0.00-0.20	0.0	6.0	19.0	42.5	72.0	92.5	98.5	99.5	99.9	100.0
"	1.08-1.28	0.0	2.5	17.0	39.5	67.0	90.0	98.5	99.5	99.8	100.0
"	1.90-2.10	0.0	2.0	8.5	18.5	34.5	64.5	94.5	99.0	100.0	
"	2.64-2.79	0.0	3.0	12.0	24.5	39.5	60.0	90.0	98.0	99.5	100.0
4529	0.00-0.20	2.0	12.0	31.0	54.5	81.0	95.0	99.0	99.7	99.9	100.0
"	0.60-0.80	1.5	10.0	30.0	52.0	79.0	94.5	99.0	99.9	100.0	
"	1.30-1.50	0.0	0.0	4.0	15.5	37.5	74.0	94.0	99.2	99.5	100.0
"	2.11-3.11	0.0	1.5	5.0	14.0	32.0	68.5	94.5	98.0	99.0	100.0
4530	0.00-0.20	0.0	10.0	31.0	57.0	79.0	94.5	99.0	99.8	100.0	
"	1.26-1.46	0.0	9.0	22.0	39.5	62.0	83.0	90.0	95.5	99.5	100.0
"	1.96-2.16	0.5	15.0	28.5	39.0	51.0	62.0	69.0	86.0	97.5	100.0
"	2.65-2.85	0.5	3.5	8.5	18.5	32.5	50.5	75.0	92.5	98.5	100.0
"	3.25-3.45	0.0	0.0	0.5	6.0	18.0	31.0	57.0	79.0	93.0	100.0
"	3.50-3.70	0.0	7.0	22.5	41.5	68.0	85.0	93.5	98.5	99.7	100.0
"	4.30-4.50	0.0	1.5	9.0	24.5	54.4	80.0	93.5	99.0	99.9	100.0
"	4.90-5.10	0.0	6.0	16.5	35.5	61.5	80.5	93.5	98.5	99.9	100.0
"	5.34-5.54	0.0	10.0	28.0	48.5	78.0	93.0	97.0	98.5	99.5	100.0
4531	0.00-0.20	0.5	6.0	27.0	50.5	75.0	94.0	99.0	99.6	100.0	
"	0.51-0.71	0.0	0.0	7.5	19.5	33.5	62.0	93.0	98.0	99.8	100.0
"	1.51-1.71	0.5	3.5	9.5	19.0	28.5	38.0	53.0	83.0	96.0	100.0
"	2.30-2.50	0.0	3.0	5.0	9.5	14.5	18.5	32.5	86.5	97.0	100.0
"	3.00-3.20	0.0	0.0	0.5	2.0	3.5	6.0	30.0	78.0	95.0	100.0
4532	0.00-0.20	0.0	2.5	13.0	34.0	64.5	92.0	98.5	99.5	99.9	100.0
"	1.39-1.59	0.0	3.5	20.5	44.0	71.5	92.0	98.0	99.2	99.9	100.0
"	2.29-2.49	0.0	4.5	13.0	31.5	61.0	84.0	95.0	98.5	99.5	100.0
"	3.30-3.50	0.0	2.0	8.0	30.0	74.0	94.0	98.0	99.0	99.9	100.0
"	4.28-4.48	0.0	0.0	0.0	1.5	3.5	8.0	51.0	92.0	99.0	100.0

Table 6-9. Vibracore subsamples - cumulative weight percent by phi size of sand fraction (continued)

Core	Core Interval in Meters	-0.5	0.0	0.5	1.0	1.5	2.0	2.5	3.0	3.5	4.0
4533	0.00-0.20	0.0	5.0	22.5	50.0	78.0	93.5	99.0	99.9	99.9	100.0
"	0.73-0.93	0.0	4.0	19.0	46.0	78.5	95.0	99.4	99.8	100.0	
"	1.45-1.65	0.0	0.0	5.5	23.5	57.0	89.0	98.0	99.5	99.9	100.0
"	3.66-3.86	0.0	0.5	7.5	20.0	40.0	75.0	96.5	99.0	99.8	100.0
"	5.02-5.22	0.0	9.0	28.0	48.5	67.5	80.0	94.5	99.0	99.9	100.0
4534	0.00-0.20	2.0	9.0	31.5	53.0	74.0	91.0	99.0	99.7	99.9	100.0
"	0.60-0.80	1.0	11.5	31.5	52.0	72.0	91.0	98.0	99.5	100.0	
"	1.38-1.58	0.5	8.5	29.0	47.5	63.0	80.0	94.0	98.5	99.9	100.0
"	2.20-2.40	0.0	0.0	2.0	12.0	53.5	80.0	87.0	94.5	99.0	100.0
"	2.89-3.09	5.0	16.0	30.0	48.5	69.0	89.0	96.5	98.5	100.0	
4535	0.00-0.20	0.0	0.0	9.0	29.0	57.0	81.0	98.0	99.9	100.0	
"	1.00-1.20	0.0	4.0	16.5	42.5	68.5	88.5	98.5	99.5	99.9	100.0
"	2.00-2.20	0.0	0.0	7.5	23.5	47.5	80.0	98.0	99.8	100.0	
"	2.80-3.00	0.0	0.0	4.5	16.0	35.0	68.5	95.5	99.0	99.8	100.0
"	3.57-3.77	0.0	0.0	4.5	17.0	35.5	64.5	93.5	99.0	99.9	100.0
4536	1.00-1.20	0.0	4.0	17.0	39.5	60.5	79.5	96.5	98.5	99.6	100.0
"	1.60-1.80	0.0	5.0	16.0	33.5	56.5	80.5	97.0	98.0	99.5	100.0
"	2.50-2.70	0.0	0.0	2.0	8.0	20.5	54.5	97.0	99.5	100.0	
"	3.60-3.80	0.0	10.5	23.5	42.0	62.0	80.5	97.5	99.7	99.9	100.0
"	4.25-4.45	0.0	4.0	14.0	33.5	55.0	77.0	94.5	98.5	99.9	100.0
4537	0.00-0.20	0.0	0.0	0.0	0.5	2.5	10.0	75.0	94.5	99.0	100.0
"	0.65-0.85	0.0	3.0	11.0	21.5	31.5	41.5	85.0	97.0	99.9	100.0
4538	0.10-0.30	0.0	0.0	5.0	21.5	46.0	78.0	95.5	99.0	100.0	
"	1.23-1.43	0.0	1.5	12.0	34.0	57.5	81.5	97.0	99.2	99.8	100.0
"	2.00-2.20	0.0	0.0	4.0	20.0	43.5	76.0	94.0	99.0	99.9	100.0
"	3.10-3.30	0.0	0.5	21.0	66.0	84.5	91.5	98.0	99.5	99.9	100.0
"	4.30-4.50	1.0	10.0	23.5	46.0	63.5	84.0	96.0	98.5	99.5	100.0
"	4.60-4.80	10.0	18.0	31.5	46.0	64.0	83.5	95.5	98.5	99.9	100.0
4539	0.20-0.40	0.0	4.5	12.0	27.0	52.0	89.0	98.5	99.8	100.0	
"	1.00-1.20	0.0	3.0	10.5	24.5	45.5	79.5	98.0	99.1	99.9	100.0
"	1.88-2.08	0.0	2.0	6.5	16.0	36.0	77.0	97.5	99.2	99.8	100.0
"	2.70-2.90	0.0	0.0	4.5	14.5	34.0	73.0	97.0	99.3	99.9	100.0
4540	0.00-0.20	0.0	0.0	4.5	12.0	28.5	71.5	98.8	99.6	100.0	
"	1.00-1.20	0.0	0.0	0.5	12.5	27.0	67.5	98.0	99.5	99.9	100.0
"	1.40-1.60	0.0	1.0	6.0	18.5	39.0	70.5	97.0	99.0	100.0	
"	2.20-2.40	0.0	0.0	1.0	9.0	25.0	64.5	98.0	99.6	99.9	100.0

Table 6-9. Vibracore subsamples - cumulative weight percent by phi size of sand fraction (continued)

Core No.	Core Interval in Meters	-0.5	0.0	0.5	1.0	1.5	2.0	2.5	3.0	3.5	4.0
4541	0.30-0.50	0.0	2.0	17.0	43.0	71.5	93.5	98.5	99.0	99.9	100.0
"	1.10-1.30	0.0	3.0	8.5	25.0	46.5	86.5	99.0	99.8	99.9	100.0
"	2.90-3.10	0.0	2.0	10.0	29.0	51.0	87.5	98.5	99.5	100.0	
"	3.50-3.70	0.0	2.0	6.5	18.5	40.0	74.5	97.0	99.0	99.9	100.0
"	4.30-4.50	5.0	14.0	23.0	37.0	49.0	74.0	89.0	96.5	99.0	100.0
4542	0.00-0.20	0.0	3.5	20.5	48.5	73.5	94.0	98.8	99.5	99.8	100.0
"	1.00-1.20	0.0	4.0	17.0	45.0	76.0	96.5	99.6	99.8	99.9	100.0
"	1.71-1.91	1.0	3.0	12.0	36.5	71.0	95.0	99.5	99.9	100.0	
4543	0.10-0.30	0.0	2.0	14.0	34.5	51.5	81.0	97.0	99.0	99.6	100.0
"	1.10-1.30	0.0	0.0	2.0	14.0	29.0	67.5	96.0	99.0	99.8	100.0
"	1.60-1.80	0.0	0.0	3.0	11.0	25.0	60.0	94.5	98.5	99.9	100.0
"	2.60-2.80	0.0	2.5	7.0	21.5	35.5	60.5	93.5	98.5	99.6	100.0
"	4.10-4.30	0.0	2.0	9.5	20.0	31.0	68.5	97.0	99.5	99.9	100.0
"	5.40-5.60	3.0	9.5	25.0	43.0	65.5	81.5	93.0	97.5	99.5	100.0
4544	0.00-0.20	1.5	5.0	12.0	27.5	58.0	90.5	98.0	99.6	99.9	100.0
"	1.30-1.50	0.0	0.0	4.0	16.0	45.0	88.0	98.0	99.5	99.9	100.0
"	2.30-2.50	0.0	4.0	12.0	28.5	55.0	88.0	98.0	99.0	99.5	100.0
"	3.20-3.40	0.0	2.5	12.0	27.0	52.5	89.0	98.5	99.0	99.5	100.0
"	4.10-4.30	0.0	0.0	3.5	12.5	36.0	69.5	84.0	93.5	99.0	100.0
"	5.00-5.20	0.0	0.0	1.5	10.0	42.5	92.0	98.5	99.2	99.8	100.0
"	5.87-6.07	3.5	9.0	17.5	32.5	58.0	86.0	93.0	95.0	99.0	100.0
4545	0.20-0.40	0.0	2.0	13.0	27.0	54.5	83.0	95.0	98.5	99.9	100.0
"	0.80-1.00	0.0	0.0	4.5	20.0	46.0	79.5	95.0	98.5	99.9	100.0
"	1.80-2.00	0.0	1.0	5.5	19.0	45.0	77.5	93.0	98.0	99.8	100.0
"	2.70-2.90	0.0	0.5	4.0	14.0	36.5	57.0	72.0	94.0	99.0	100.0
"	3.80-4.00	0.0	0.0	1.5	6.0	11.5	17.5	28.0	69.0	94.0	100.0
"	4.80-5.00	11.5	18.0	42.0	77.5	87.0	94.0	97.5	99.0	99.9	100.0
4546	0.00-0.20	3.5	16.0	30.0	42.5	60.5	77.5	91.0	98.0	99.5	100.0
"	1.42-1.62	1.0	9.0	24.5	48.5	72.5	90.5	97.5	99.5	99.9	100.0
"	2.10-2.30	0.0	0.0	1.5	4.5	12.0	27.5	62.5	95.0	99.0	100.0
"	3.20-3.40	0.0	2.5	6.0	11.0	24.0	44.5	75.0	96.5	99.5	100.0
"	4.44-4.64	0.0	0.0	1.0	2.5	5.5	12.5	48.5	94.0	98.5	100.0
4600	0.60-0.80	3.0	13.2	26.0	39.2	55.0	71.0	86.5	97.5	99.9	100.0
"	1.80-2.00	0.0	1.5	20.0	48.5	72.0	90.5	98.5	99.5	99.9	100.0
"	2.40-2.60	0.0	0.0	10.5	26.5	48.0	75.3	98.0	99.9	100.0	

Table 6-9. Vibracore subsamples - cumulative weight percent by phi size of sand fraction (continued)

Core No.	Core Interval in Meters	-0.5	0.0	0.5	1.0	1.5	2.0	2.5	3.0	3.5	4.0
4601	0.60-0.80	0.0	0.0	0.0	22.0	60.0	86.8	97.5	99.3	99.8	100.0
"	1.50-1.70	0.0	3.0	12.0	26.8	52.5	84.5	98.0	99.8	100.0	
"	2.04-2.24	0.0	2.7	9.5	28.0	58.0	88.0	98.0	99.8	100.0	
4602	0.90-1.10	0.0	0.5	6.0	19.3	43.5	77.0	98.0	99.5	100.0	
"	2.70-2.90	0.0	2.5	6.5	14.0	29.5	61.0	95.5	100.0		
"	4.20-4.40	0.0	1.0	6.5	19.0	45.3	78.3	96.5	99.0	99.8	100.0
4605	0.90-1.10	0.0	2.0	11.5	21.3	41.5	70.5	96.0	99.5	99.9	100.0
"	2.70-2.90	0.0	0.0	10.5	27.0	51.5	85.0	97.0	99.5	99.9	100.0
"	3.90-4.10	0.0	0.0	3.0	10.5	34.0	76.0	97.3	99.3	99.8	100.0
4606	0.90-1.10	0.0	1.0	8.0	25.0	55.5	88.0	99.5	99.9	100.0	
"	2.10-2.30	0.0	0.0	2.2	12.5	35.0	77.5	97.0	99.8	100.0	
"	3.30-3.50	0.0	0.0	3.0	12.0	36.0	79.3	98.0	99.8	100.0	
4607	0.60-0.80	0.0	2.5	13.0	35.0	69.5	94.5	99.5	99.9	100.0	
"	1.50-1.70	0.0	1.0	14.0	36.0	67.5	92.0	99.0	99.8	100.0	
"	2.90-3.10	1.5	6.7	21.0	42.0	62.0	88.5	98.0	99.3	99.8	100.0
4608	0.90-1.10	0.0	5.5	23.0	49.0	78.0	95.0	99.0	99.5	99.9	100.0
"	2.40-2.60	0.0	0.0	10.5	34.3	69.5	92.3	99.0	99.5	100.0	
"	3.60-3.80	0.0	7.0	27.5	45.0	82.5	96.3	98.7	99.9	100.0	
4609	0.30-0.50	0.5	7.0	21.0	43.5	73.3	92.0	98.0	99.5	99.9	100.0
"	0.90-1.10	0.0	3.5	11.3	33.0	64.0	91.0	99.0	100.0		
"	1.20-1.40	0.0	4.0	17.5	39.5	69.3	92.5	99.0	99.5	99.9	100.0
4610	0.60-0.80	0.0	2.0	20.0	48.0	72.5	92.0	99.0	99.5	99.9	100.0
"	2.40-2.60	0.0	3.0	17.0	34.3	63.3	91.3	98.8	99.8	100.0	
"	4.80-5.00	0.0	3.0	21.0	54.5	73.5	90.0	99.0	100.0		
4612	0.30-0.50	0.0	0.0	0.5	11.7	32.0	65.0	96.5	99.3	99.9	100.0
"	0.90-1.10	0.0	2.0	9.5	35.0	60.0	82.0	98.3	99.9	100.0	
"	1.20-1.40	0.0	6.3	17.5	36.5	62.0	81.5	94.5	98.8	99.5	100.0
4613	0.60-0.80	0.0	1.0	6.0	21.0	62.0	92.0	99.0	99.9	100.0	
"	1.50-1.70	0.0	4.8	18.0	35.0	53.3	79.0	95.0	98.0	99.0	100.0
"	2.10-2.30	0.0	0.0	18.5	36.5	52.3	66.5	85.0	96.5	99.5	100.0
4614	0.60-0.80	0.0	7.0	25.0	55.5	80.0	93.3	98.0	99.0	99.5	100.0
"	1.50-1.70	0.0	1.0	7.0	23.0	51.5	83.3	89.0	99.8	100.0	
"	2.40-2.60	0.0	7.0	21.0	42.0	67.0	84.0	93.8	98.0	99.8	100.0
4615	0.60-0.80	0.0	11.0	34.0	63.3	86.0	97.3	99.0	100.0		
"	1.50-1.70	0.0	4.0	16.2	33.0	63.5	92.0	99.5	99.9	100.0	
"	2.36-2.56	0.0	2.5	7.0	18.0	45.0	82.0	98.0	99.3	99.8	100.0

Table 6-9. Vibracore subsamples - cumulative weight percent by phi size of sand fraction (continued)

Core No.	Core Interval in Meters	-0.5	0.0	0.5	1.0	1.5	2.0	2.5	3.0	3.5	4.0
4616	0.60-0.80	0.0	7.0	37.0	63.0	86.5	95.0	98.5	99.8	100.0	
"	1.50-1.70	0.0	10.0	30.0	57.5	86.0	97.5	99.5	99.9	100.0	
"	2.40-2.60	0.0	8.5	25.5	51.0	80.0	97.5	99.5	99.9	100.0	
4617	0.60-0.80	0.0	7.0	19.0	47.5	80.0	97.0	99.0	99.5	100.0	
"	1.50-1.70	0.0	6.0	22.5	42.0	67.0	92.5	99.0	99.8	100.0	
"	2.40-2.60	0.0	7.0	25.0	47.5	70.0	92.5	98.5	99.3	99.8	100.0
4618	0.60-0.80	0.0	3.0	13.5	34.5	65.0	90.5	98.5	99.8	100.0	
"	1.20-1.40	0.0	2.3	22.0	45.0	71.3	91.0	98.0	99.5	99.9	100.0
"	1.80-2.00	0.0	6.0	20.0	38.0	60.5	85.0	96.5	99.5	99.9	100.0
4620	1.20-1.40	0.0	0.8	9.5	33.3	65.0	89.5	97.5	99.8	100.0	
"	3.30-3.50	0.0	10.0	28.0	52.5	80.0	95.7	99.5	99.9	100.0	
"	4.80-5.00	0.0	1.8	12.8	37.5	62.5	88.0	98.0	99.5	99.9	100.0
4622	0.30-0.50	0.0	6.0	18.3	43.5	71.0	90.5	98.3	99.3	99.8	100.0
"	0.60-0.80	0.0	0.5	9.0	35.5	72.0	92.3	98.5	99.8	100.0	

Table 6-10. Summary of Folk's (1974) graphic grain size statistics for the sand fraction of selected vibracore subsamples from the cross-shelf transects.

Core No.	Core Interval in Meters	Median Φ	Mean Φ	Skewness	Kurtosis	Inclusive Standard Deviation Φ
4525	1.05-1.25	1.76	1.75	-0.04	0.86	0.89
"	1.55-1.75	1.29	1.34	0.08	0.99	0.96
"	2.48-2.68	0.68	0.75	0.14	0.79	0.94
4526	0.20-0.40	1.03	1.08	0.08	1.04	0.93
"	0.47-0.67	0.94	1.09	0.23	0.90	0.84
4527	0.00-0.20	1.50	1.44	-0.14	0.98	0.69
"	0.90-1.10	1.52	1.44	-0.16	0.86	0.74
"	1.89-2.09	2.00	1.81	-0.45	1.06	0.62
"	2.61-2.81	2.05	1.86	-0.46	0.98	0.64
4528	0.00-0.20	1.13	1.09	-0.09	0.98	0.67
"	1.08-1.28	1.21	1.19	-0.05	0.91	0.65
"	1.90-2.10	1.81	1.64	-0.37	1.08	0.69
"	2.64-2.79	1.82	1.64	-0.30	0.87	0.83
4529	0.00-0.20	0.90	0.86	-0.07	0.90	0.72
"	0.60-0.80	0.95	0.91	-0.05	0.88	0.71
"	1.30-1.50	1.70	1.60	-0.22	1.10	0.58
"	2.11-2.31	1.80	1.68	-0.30	1.19	0.59
4530	0.00-0.20	0.85	0.88	-0.05	0.91	0.70
"	1.26-1.46	1.25	1.20	-0.01	1.09	0.92
"	1.96-2.16	1.45	1.47	0.03	0.61	1.28
"	2.65-2.85	2.00	1.85	-0.22	0.94	0.90
"	3.25-3.45	2.43	2.33	-0.16	0.98	0.83
"	3.50-3.70	1.18	1.15	0.00	1.01	0.82
"	4.30-4.50	1.45	1.45	-0.01	1.05	0.69
"	4.90-5.10	1.27	1.30	0.02	1.01	0.81
"	5.34-5.54	1.03	0.94	-0.09	0.70	0.73
4531	0.00-0.20	1.00	0.98	-0.02	0.82	0.68
"	0.51-0.71	1.80	1.64	-0.29	0.95	0.68
"	1.51-1.71	2.45	2.12	-0.43	0.92	1.05
"	2.30-2.50	2.62	2.40	-0.50	2.74	0.75
"	3.00-3.20	2.65	2.70	0.11	1.33	0.45
4532	0.00-0.20	1.27	1.22	-0.11	0.99	0.61
"	1.39-1.59	1.11	1.11	0.00	0.92	0.68
"	2.29-2.49	1.35	1.31	-0.08	1.03	0.73
"	3.30-3.50	1.25	1.24	-0.06	1.18	0.50
"	4.28-4.48	2.50	2.54	0.09	2.24	0.34
4533	0.00-0.20	1.00	0.99	0.01	0.99	0.64
"	0.73-0.93	1.05	1.04	-0.03	0.98	0.60
"	1.45-1.65	1.50	1.41	-0.23	0.97	0.53
"	3.66-3.86	1.68	1.55	-0.28	1.03	0.64
"	5.02-5.22	1.02	1.11	0.14	0.76	0.89
4534	0.00-0.20	0.93	0.99	0.07	0.84	0.78
"	0.60-0.80	0.95	0.96	0.03	0.79	0.78
"	1.38-1.58	1.07	1.14	0.10	0.79	0.88
"	2.20-2.40	1.55	1.62	0.23	1.59	0.61
"	2.89-3.09	1.02	0.97	-0.08	0.86	0.90

Table 6-10. Summary of Folk's (1974) graphic grain size statistics for the sand fraction of selected vibracore subsamples from the cross-shelf transects (continued)

Core No.	Core Interval in Meters	Median Φ	Mean Φ	Skewness	Kurtosis	Inclusive Standard Deviation Φ
4535	0.00-0.20	1.41	1.42	0.08	1.01	0.69
"	1.00-1.20	1.16	1.18	0.01	0.89	0.68
"	2.00-2.20	1.55	1.47	-0.20	0.90	0.60
"	2.80-3.00	1.81	1.67	0.32	1.03	0.60
"	3.57-3.77	1.80	1.67	-0.29	0.92	0.63
4536	1.00-1.20	1.25	1.26	0.00	0.81	0.77
"	1.60-1.80	1.35	1.30	-0.12	0.90	0.75
"	2.50-2.70	1.97	1.85	-0.44	1.26	0.46
"	3.60-3.80	1.21	1.17	-0.09	0.80	0.85
"	4.25-4.45	1.40	1.37	-0.07	0.85	0.77
4537	0.00-0.20	2.39	2.36	-0.05	1.56	0.32
"	0.65-0.85	2.15	1.78	-0.58	0.88	0.83
4538	0.10-0.30	1.58	1.52	-0.12	0.91	0.62
"	1.23-1.43	1.32	1.32	-0.01	0.78	0.67
"	2.00-2.20	1.60	1.53	-0.12	0.89	0.60
"	3.10-3.30	0.92	0.93	0.17	1.40	0.56
"	4.30-4.50	1.12	1.12	0.00	0.83	0.84
"	4.60-4.80	1.10	1.01	-0.14	0.87	1.02
4539	0.20-0.40	1.45	1.34	-0.29	1.00	0.64
"	1.00-1.20	1.60	1.47	-0.31	0.92	0.66
"	1.88-2.08	1.75	1.61	-0.38	1.15	0.57
"	2.70-2.90	1.77	1.65	-0.33	1.05	0.55
4540	0.00-0.20	1.82	1.71	-0.39	1.13	0.52
"	1.00-1.20	1.88	1.72	-0.47	1.17	0.50
"	1.40-1.60	1.76	1.62	-0.34	0.87	0.61
"	2.20-2.40	1.90	1.77	-0.42	1.16	0.47
4541	0.30-0.50	1.15	1.13	-0.06	0.90	0.60
"	1.10-1.30	1.57	1.44	-0.35	0.89	0.59
"	2.90-3.10	1.48	1.38	-0.26	0.80	0.60
"	3.50-3.70	1.68	1.56	-0.17	1.21	0.68
"	4.30-4.50	1.54	1.32	-0.26	0.93	1.05
4542	0.00-0.20	1.05	1.03	-0.02	0.85	0.64
"	1.00-1.20	1.06	1.05	-0.06	0.91	0.57
"	1.71-1.91	1.22	1.19	-0.10	0.97	0.55
4543	0.10-0.30	1.46	1.36	-0.19	0.79	0.71
"	1.10-1.30	1.86	1.71	-0.36	1.13	0.54
"	1.60-1.80	1.93	1.79	-0.37	1.15	0.57
"	2.60-2.80	1.85	1.65	-0.35	0.98	0.74
"	4.10-4.30	1.91	1.63	-0.58	1.09	0.67
"	5.40-5.60	1.16	1.14	0.00	0.93	0.91
4544	0.00-0.20	1.38	1.30	-0.24	1.11	0.63
"	1.30-1.50	1.56	1.50	-0.19	1.06	0.49
"	2.30-2.50	1.43	1.34	-0.25	0.96	0.64
"	3.20-3.40	1.46	1.34	-0.28	0.97	0.63
"	4.10-4.30	1.71	1.77	0.14	1.18	0.72
"	5.00-5.20	1.57	1.55	-0.15	1.34	0.38
"	5.87-6.07	1.37	1.26	-0.11	1.38	0.89

Table 6-10. Summary of Folk's (1974) graphic grain size statistics for the sand fraction of selected vibracore subsamples from the cross-shelf transects (continued)

Core No.	Core Interval in Meters	Median Φ	Mean Φ	Skewness	Kurtosis	Inclusive Standard Deviation Φ
4545	0.20-0.40	1.44	1.37	-0.14	1.06	0.71
"	0.80-1.00	1.55	1.47	-0.11	0.97	0.62
"	1.80-2.00	1.55	1.53	-0.02	1.09	0.64
"	2.70-2.90	1.82	1.87	0.04	0.80	0.80
"	3.80-4.00	2.85	2.64	-0.48	1.52	0.73
"	4.80-5.00	0.59	0.61	-0.02	1.88	0.86
4546	0.00-0.20	1.20	1.15	-0.05	0.80	1.03
"	1.42-1.62	1.06	1.02	-0.05	0.95	0.74
"	2.10-2.30	2.37	2.26	-0.33	1.16	0.55
"	3.20-3.40	2.11	1.99	-0.32	1.07	0.73
"	4.44-4.64	2.50	2.47	-0.22	1.77	0.41
4600	0.60-0.80	1.40	1.30	-0.07	0.71	0.97
"	1.80-2.00	1.05	1.11	0.18	0.80	0.63
"	2.40-2.60	1.55	1.48	-0.20	0.88	0.67
4601	0.60-0.80	1.35	1.39	0.12	1.75	0.52
"	1.50-1.70	1.45	1.37	0.19	0.94	0.66
"	2.40-2.60	1.40	1.33	-0.18	0.94	0.60
4602	0.90-1.10	1.60	1.53	-0.18	1.12	0.59
"	2.70-2.90	1.90	1.75	-0.44	1.29	0.64
"	4.20-4.40	1.60	1.57	-0.11	1.03	0.63
4605	0.90-1.10	1.70	1.55	-0.32	0.92	0.71
"	2.70-2.90	1.46	1.38	-0.15	0.88	0.62
"	3.90-4.10	1.78	1.68	-0.30	1.12	0.51
4606	0.90-1.10	1.45	1.38	-0.21	1.03	0.57
"	2.10-2.30	1.70	1.63	-0.19	1.06	0.51
"	3.30-3.50	1.70	1.64	-0.20	1.03	0.50
4607	0.60-0.80	1.24	1.19	-0.14	1.01	0.58
"	1.50-1.70	1.25	1.22	-0.07	0.97	0.59
"	2.70-2.90	1.26	1.17	-0.17	0.82	0.74
4608	0.90-1.10	1.04	1.01	-0.05	0.91	0.63
"	2.40-2.60	1.23	1.22	-0.03	0.97	0.57
"	3.60-3.80	1.07	0.99	-0.23	1.00	0.65
4609	0.30-0.50	1.10	1.08	-0.06	1.00	0.69
"	0.90-1.10	1.30	1.27	-0.09	0.95	0.59
"	1.20-1.40	1.18	1.14	-0.07	0.89	0.63
4610	0.60-0.80	1.05	1.04	0.02	0.91	0.68
"	2.40-2.60	1.30	1.20	-0.20	0.90	0.65
"	4.80-5.00	0.95	0.90	0.05	0.84	0.51
4612	0.30-0.50	1.83	1.72	-0.28	0.92	0.52
"	0.90-1.10	1.30	1.35	0.06	0.81	0.65
"	1.20-1.40	1.25	1.59	-0.01	1.07	0.82
4613	0.60-0.80	1.37	1.35	-0.08	1.17	0.48
"	1.50-1.70	1.47	1.34	-0.18	0.43	0.77
"	2.10-2.30	1.42	1.45	0.06	0.69	0.91
4614	0.60-0.80	0.90	0.93	0.08	1.04	0.66
"	1.50-1.70	1.45	1.42	-0.09	0.94	0.59
"	2.40-2.60	1.17	1.18	0.04	1.07	0.84

Table 6-10. Summary of Folk's (1974) graphic grain size statistics for the sand fraction of selected vibracore subsamples from the cross-shelf transects (continued)

Core No.	Core Interval in Meters	Median Φ	Mean Φ	Skewness	Kurtosis	Inclusive Standard Deviation Φ
4615	0.60-0.80	0.74	0.76	0.06	0.88	0.65
"	1.50-1.70	1.32	1.21	-0.23	0.87	0.65
"	2.36-2.56	1.58	1.48	-0.25	1.18	0.63
4616	0.60-0.80	0.81	0.80	0.07	0.94	0.63
"	1.50-1.70	0.85	0.82	-0.05	0.90	0.62
"	2.40-2.60	1.00	0.95	-0.12	0.92	0.65
4617	0.60-0.80	1.03	1.02	-0.12	1.13	0.62
"	1.50-1.70	1.20	1.15	-0.14	0.82	0.69
"	2.40-2.60	1.05	1.05	-0.02	0.82	0.71
4618	0.60-0.80	1.30	1.25	-0.20	0.88	0.60
"	1.20-1.40	1.10	1.07	-0.01	0.84	0.69
"	1.80-2.00	1.30	1.23	-0.12	0.85	0.77
4620	1.20-1.40	1.28	1.27	-0.01	0.87	0.59
"	3.30-3.50	0.95	0.91	-0.08	0.87	0.68
"	4.80-5.00	1.25	1.23	-0.03	0.82	0.64
4622	0.30-0.40	1.14	1.08	-0.10	1.00	0.72
"	0.60-0.80	1.20	1.21	0.05	1.02	0.54

Figure 6-10. Triangular plot of the percentages of gravel-sand-mud in the vibracore sub-samples.

Figure 6-10

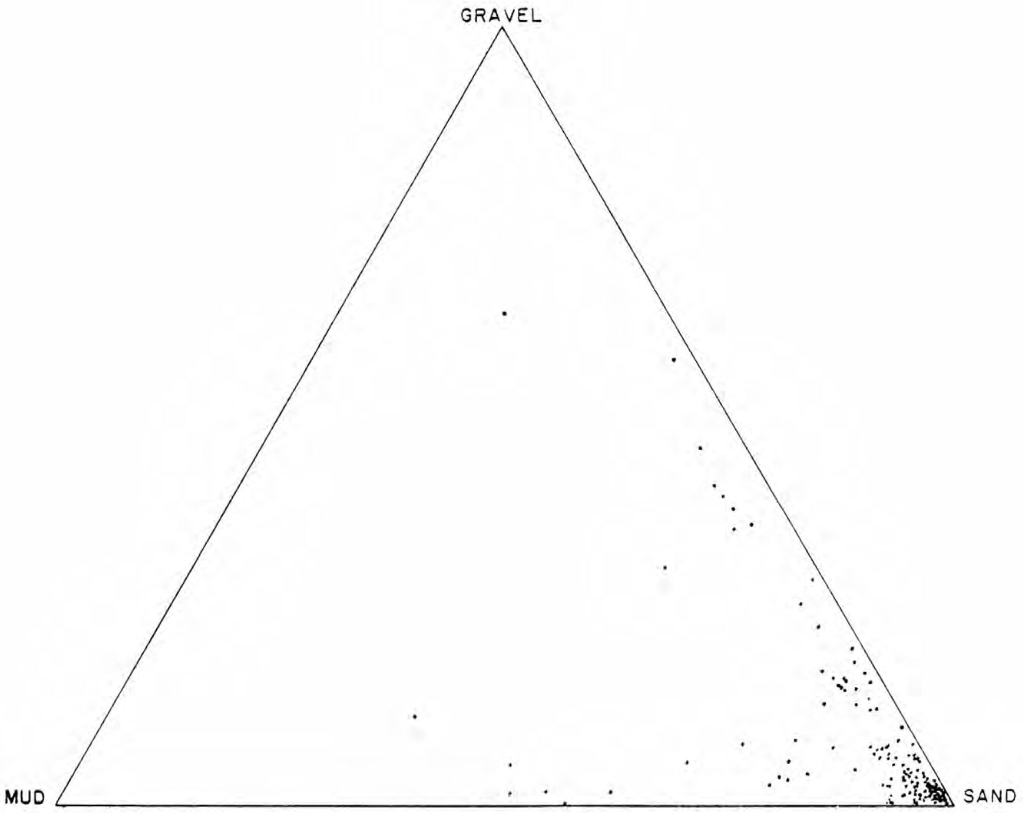

Table 6-11. Percentage of silt and clay in those selected vibracore subsamples that contain greater than 10% mud.

Core No.	Core Interval in Meters	% Mud	% Silt	% Clay
4525	1.05-1.25	54.33	25.54	28.79
"	1.55-1.75	18.66	7.45	11.21
4526	0.20-0.40	48.48	40.31	8.17
"	0.47-0.67	14.65	10.24	4.41
4530	1.26-1.46	15.60	10.02	5.58
"	1.96-2.16	27.15	14.38	12.77
"	2.65-2.85	17.53	10.85	6.68
"	3.25-3.45	60.54	3.40	26.14
4531	1.51-1.71	37.37	17.41	19.96
"	2.30-2.50	19.16	13.17	5.99
"	3.00-3.20	43.52	31.51	12.01
4532	2.29-2.49	16.92	9.06	7.86
4543	5.40-5.60	16.91	6.07	10.84
4544	4.10-4.30	19.90	10.22	9.68
4545	3.80-4.00	14.16	8.04	6.12

continental shelf, the percentage of $CaCO_3$ in the surface sediment has been shown to be a direct result of two things: (1) productivity of $CaCO_3$-secreting biota, and (2) dilution by the influx of terrigenous sediment (Milliman _et al_ 1968).

Percentage of $CaCO_3$ in the vibracore subsamples is extremely variable with values ranging from 0 to 88%. The average value of $CaCO_3$ in the subsamples was 23% (standard deviation = 18%). Values in the subsamples from the northern transect averaged 19% (standard deviation = 15%) while values from the southern transect averaged 27% (standard deviation = 20%). Given the variability of values from both transects these differences cannot be considered significantly. The higher southern average undoubtedly reflects the extremely high values of $CaCO_3$ in the core number 4546 subsamples.

It is interesting that the sediment units containing the greatest amount of shell material do not have the highest percentages of $CaCO_3$ (Table 6-12). Even the well-sorted fine sands contain significant amounts of $CaCO_3$ (15 to 43%). This suggests that much of the $CaCO_3$ is contained in the sand fraction and that non-fragmented shell material is not the principal contributor of $CaCO_3$.

Organic Carbon

The weight percentages of organic carbon in 279 select vibracore subsamples from the cross-shelf transects and the proposed lease areas are relatively low (Figures 6-14 through 6-16, and Table 6-13). Weight percent organic carbon in marine sediment is significant for several reasons. Folger (1972) has shown that organic carbon concentrations in estuarine sediments may be indicative of the quantity of pollutants introduced into the estuary. In this respect the percentage of organic carbon in these sediments serves as baseline data to be referred to at a

Figure 6-11. Percentages of calcium carbonate in selected sub-samples of vibracores from the cross-shelf transects.

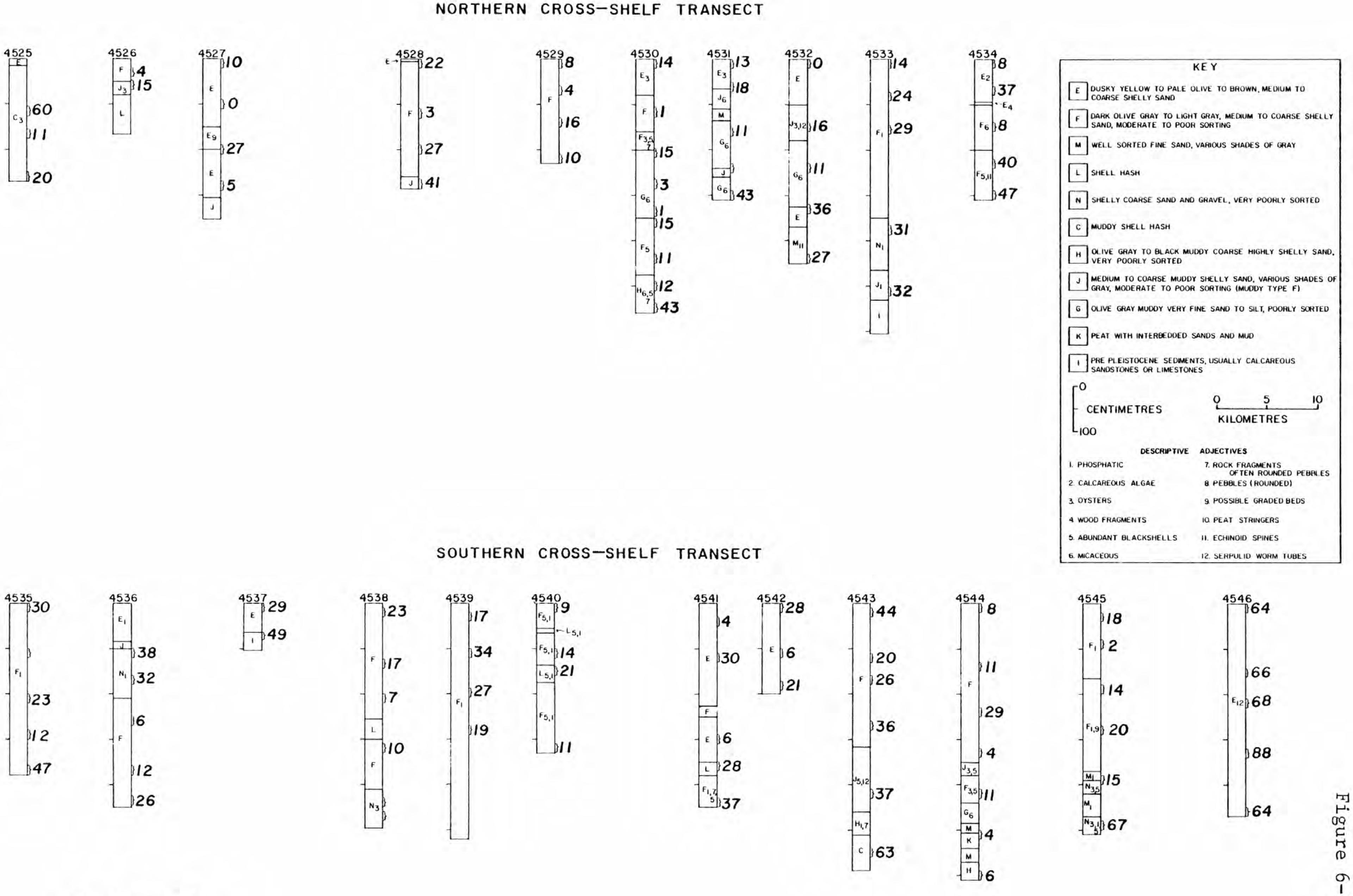
NORTHERN CROSS-SHELF TRANSECT
4525
4526
4527
4528
4529
4530
4531
4532
4533
4534
SOUTHERN CROSS-SHELF TRANSECT
4535
4536
4537
4538
4539
4540
4541
4542
4543
4544
4545
4546
KEY
E DUSKY YELLOW TO PALE OLIVE TO BROWN, MEDIUM TO COARSE SHELLY SAND
F DARK OLIVE GRAY TO LIGHT GRAY, MEDIUM TO COARSE SHELLY SAND, MODERATE TO POOR SORTING
M WELL SORTED FINE SAND, VARIOUS SHADES OF GRAY
L SHELL HASH
N SHELLY COARSE SAND AND GRAVEL, VERY POORLY SORTED
C MUDDY SHELL HASH
H OLIVE GRAY TO BLACK MUDDY COARSE HIGHLY SHELLY SAND, VERY POORLY SORTED
J MEDIUM TO COARSE MUDDY SHELLY SAND, VARIOUS SHADES OF GRAY, MODERATE TO POOR SORTING (MUDDY TYPE F)
G OLIVE GRAY MUDDY VERY FINE SAND TO SILT, POORLY SORTED
K PEAT WITH INTERBEDDED SANDS AND MUD
I PRE PLEISTOCENE SEDIMENTS, USUALLY CALCAREOUS SANDSTONES OR LIMESTONES
0
CENTIMETRES
100
0 5 10
KILOMETRES
DESCRIPTIVE ADJECTIVES
1. PHOSPHATIC
2. CALCAREOUS ALGAE
3. OYSTERS
4. WOOD FRAGMENTS
5. ABUNDANT BLACKSHELLS
6. MICACEOUS
7. ROCK FRAGMENTS OFTEN ROUNDED PEBBLES
8. PEBBLES (ROUNDED)
9. POSSIBLE GRADED BEDS
10. PEAT STRINGERS
11. ECHINOID SPINES
12. SERPULID WORM TUBES

% $CaCO_3$

Figure 6-11

Figure 6-12. Percentages of calcium carbonate in selected subsamples of vibracores from the proposed northern lease area.

NORTHERN AREA

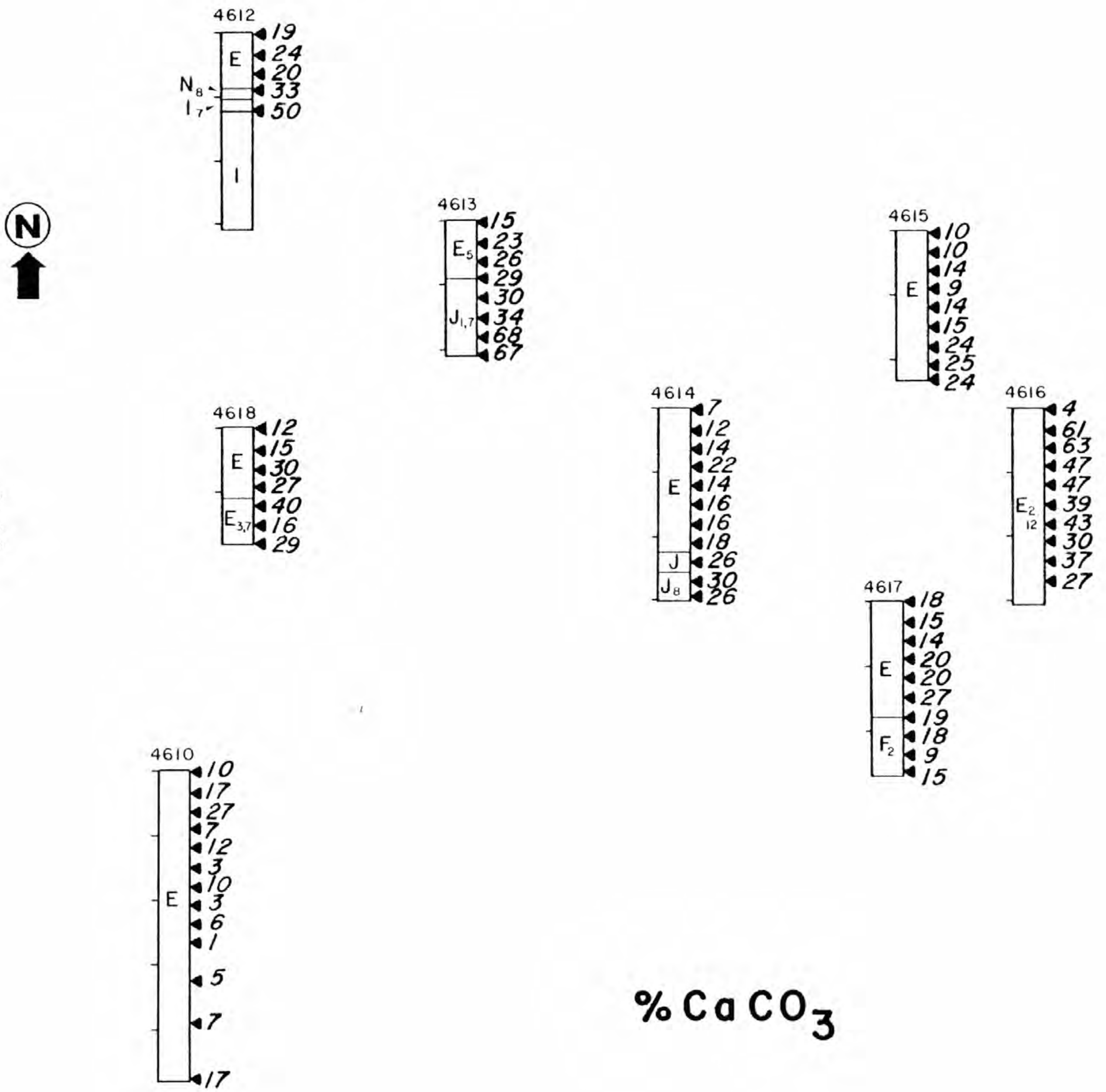
N
4612
E
N8
I7
I
19
24
20
33
50
4613
E5
J1,7
15
23
26
29
30
34
68
67
4615
E
10
10
14
9
14
15
24
25
24
4618
E
E3,7
12
15
30
27
40
16
29
4614
E
J
J8
7
12
14
22
14
16
16
18
26
30
26
4616
E2 12
4
61
63
47
47
39
43
30
37
27
4617
E
F2
18
15
14
20
20
27
19
18
9
15
4610
E
10
17
27
7
12
3
10
3
6
1
5
7
17
% Ca CO3

KEY

E	DUSKY YELLOW TO PALE OLIVE TO BROWN, MEDIUM TO COARSE SHELLY SAND
F	DARK OLIVE GRAY TO LIGHT GRAY, MEDIUM TO COARSE SHELLY SAND, MODERATE TO POOR SORTING
N	SHELLY COARSE SAND AND GRAVEL, VERY POORLY SORTED
J	MEDIUM TO COARSE MUDDY SHELLY SAND, VARIOUS SHADES OF GRAY, MODERATE TO POOR SORTING
I	PRE-PLEISTOCENE SEDIMENTS?, SLIGHTLY SHELLY POORLY INDURATED SANDS

0 CENTIMETRES 100

2 KILOMETRES 0 5

DESCRIPTIVE ADJECTIVES

1. PHOSPHATIC
2. CALCAREOUS ALGAE
3. OYSTERS
5. ABUNDANT BLACKSHELLS
7. ROCK FRAGMENTS
8. ROUNDED PEBBLES
12. SERPULID WORM TUBES

Figure 6-12

Figure 6-13. Percentages of calcium carbonate in selected subsamples of vibracores from the southern lease area.

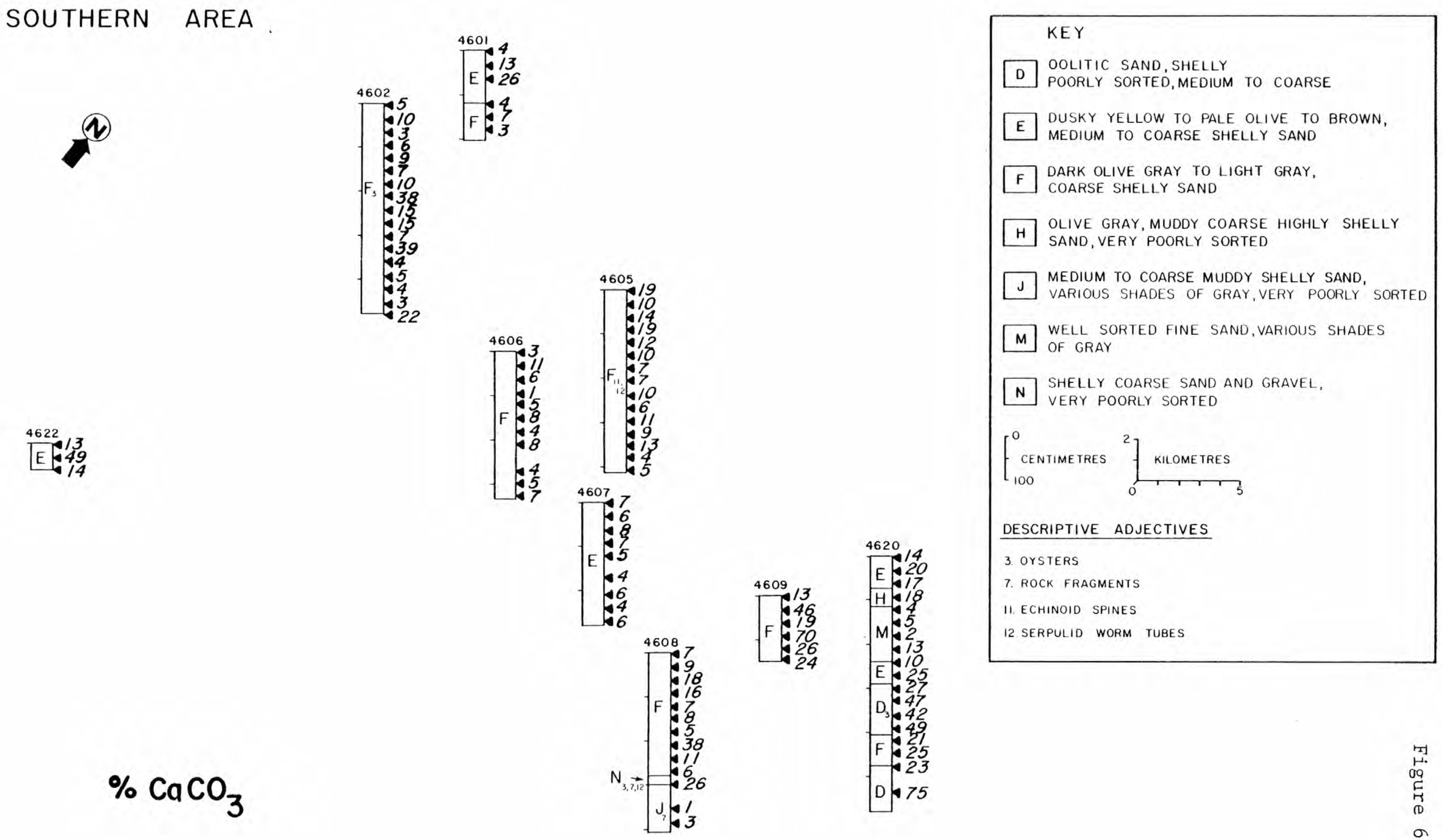
SOUTHERN AREA
N
% CaCO3
E
F
F3
F11, 12
F
E
F
N3, 7, 12
J7
F
E
H
M
E
D3
F
D
E
KEY
D OOLITIC SAND, SHELLY POORLY SORTED, MEDIUM TO COARSE
E DUSKY YELLOW TO PALE OLIVE TO BROWN, MEDIUM TO COARSE SHELLY SAND
F DARK OLIVE GRAY TO LIGHT GRAY, COARSE SHELLY SAND
H OLIVE GRAY, MUDDY COARSE HIGHLY SHELLY SAND, VERY POORLY SORTED
J MEDIUM TO COARSE MUDDY SHELLY SAND, VARIOUS SHADES OF GRAY, VERY POORLY SORTED
M WELL SORTED FINE SAND, VARIOUS SHADES OF GRAY
N SHELLY COARSE SAND AND GRAVEL, VERY POORLY SORTED
CENTIMETRES
KILOMETRES
DESCRIPTIVE ADJECTIVES
3. OYSTERS
7. ROCK FRAGMENTS
11. ECHINOID SPINES
12 SERPULID WORM TUBES

Figure 6-13

Table 6-12. Percent $CaCO_3$ in various sediment types.

Sediment types with number of measurements	Mean	Standard Deviation	Range		
			Low	→	High
E (104)	21	17	0	→	88
F (116)	15	12	1	→	47
M (7)	7	9	2	→	27
L (2)	25	5	21	→	28
N (6)	38	15	26	→	67
C (4)	39	27	11	→	63
H (3)	20	20	6	→	43
J (14)	31	19	1	→	68
G (6)	12	16	1	→	43
I (2)	50	1	49	→	50
O (5)	48	17	27	→	75

Figure 6-14. Percentages of organic carbon in selected subsamples of vibracores from the cross-shelf transects. In the figure 0 is the equivalent of 0.00.

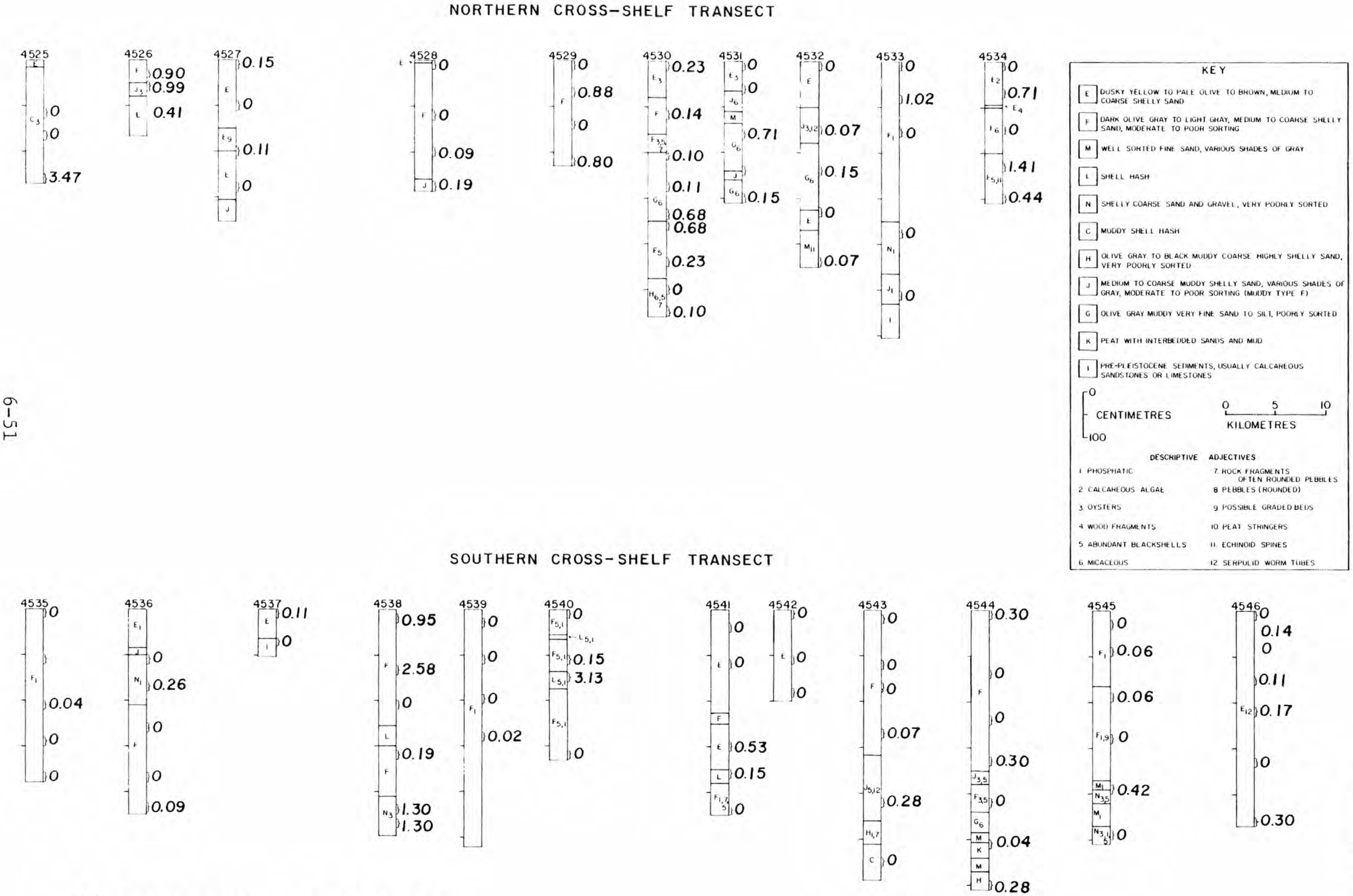
NORTHERN CROSS-SHELF TRANSECT
4525
C3
0
0
3.47
4526
F
J3
L
0.90
0.99
0.41
4527
E
E9
E
J
0.15
0
0.11
0
4528
F
J
0
0
0.09
0.19
4529
F
0
0.88
0
0.80
4530
E3
F
F3,5,7
G6
F5
H6,5,7
0.23
0.14
0.10
0.11
0.68
0.68
0.23
0
0.10
4531
E3
J6
M
G6
J
G6
0
0
0.71
0.15
4532
E
J3,12
G6
E
M11
0
0.07
0.15
0
0.07
4533
F1
N1
J1
I
0
1.02
0
0
0
4534
E2
E4
F6
F5,11
0
0.71
0
1.41
0.44
KEY
E DUSKY YELLOW TO PALE OLIVE TO BROWN, MEDIUM TO COARSE SHELLY SAND
F DARK OLIVE GRAY TO LIGHT GRAY, MEDIUM TO COARSE SHELLY SAND, MODERATE TO POOR SORTING
M WELL SORTED FINE SAND, VARIOUS SHADES OF GRAY
L SHELL HASH
N SHELLY COARSE SAND AND GRAVEL, VERY POORLY SORTED
C MUDDY SHELL HASH
H OLIVE GRAY TO BLACK MUDDY COARSE HIGHLY SHELLY SAND, VERY POORLY SORTED
J MEDIUM TO COARSE MUDDY SHELLY SAND, VARIOUS SHADES OF GRAY, MODERATE TO POOR SORTING (MUDDY TYPE F)
G OLIVE GRAY MUDDY VERY FINE SAND TO SILT, POORLY SORTED
K PEAT WITH INTERBEDDED SANDS AND MUD
I PRE-PLEISTOCENE SEDIMENTS, USUALLY CALCAREOUS SANDSTONES OR LIMESTONES
0
CENTIMETRES
100
0 5 10
KILOMETRES
DESCRIPTIVE ADJECTIVES
1 PHOSPHATIC
2 CALCAREOUS ALGAE
3 OYSTERS
4 WOOD FRAGMENTS
5 ABUNDANT BLACKSHELLS
6 MICACEOUS
7 ROCK FRAGMENTS OFTEN ROUNDED PEBBLES
8 PEBBLES (ROUNDED)
9 POSSIBLE GRADED BEDS
10 PEAT STRINGERS
11 ECHINOID SPINES
12 SERPULID WORM TUBES
SOUTHERN CROSS-SHELF TRANSECT
4535
F1
0
0.04
0
0
4536
E1
J
N1
F
0
0.26
0
0
0.09
4537
E
I
0.11
0
4538
F
L
F
N3
0.95
2.58
0
0.19
1.30
1.30
4539
F1
0
0
0
0.02
4540
F5,1
L5,1
F5,1
L5,1
F5,1
0
0.15
3.13
0
4541
E
F
E
L
F1,7,5
0
0
0.53
0.15
0
4542
E
0
0
0
4543
F
J5,12
H1,7
C
0
0
0
0.07
0.28
0
4544
F
J3,5
F3,5
G6
M
K
M
H
0.30
0
0
0.30
0
0.04
0.28
4545
F1
F1,9
M1
N3,5
M1
N3,1,5
0
0.06
0.06
0
0.42
0
4546
E12
0
0.14
0
0.11
0.17
0
0.30

% ORGANIC CARBON

Figure 6-14

Figure 6-15. Percentages of organic carbon in selected subsamples of vibracores from the proposed northern lease area. In the figure 0 is the equivalent of 0.00.

NORTHERN AREA

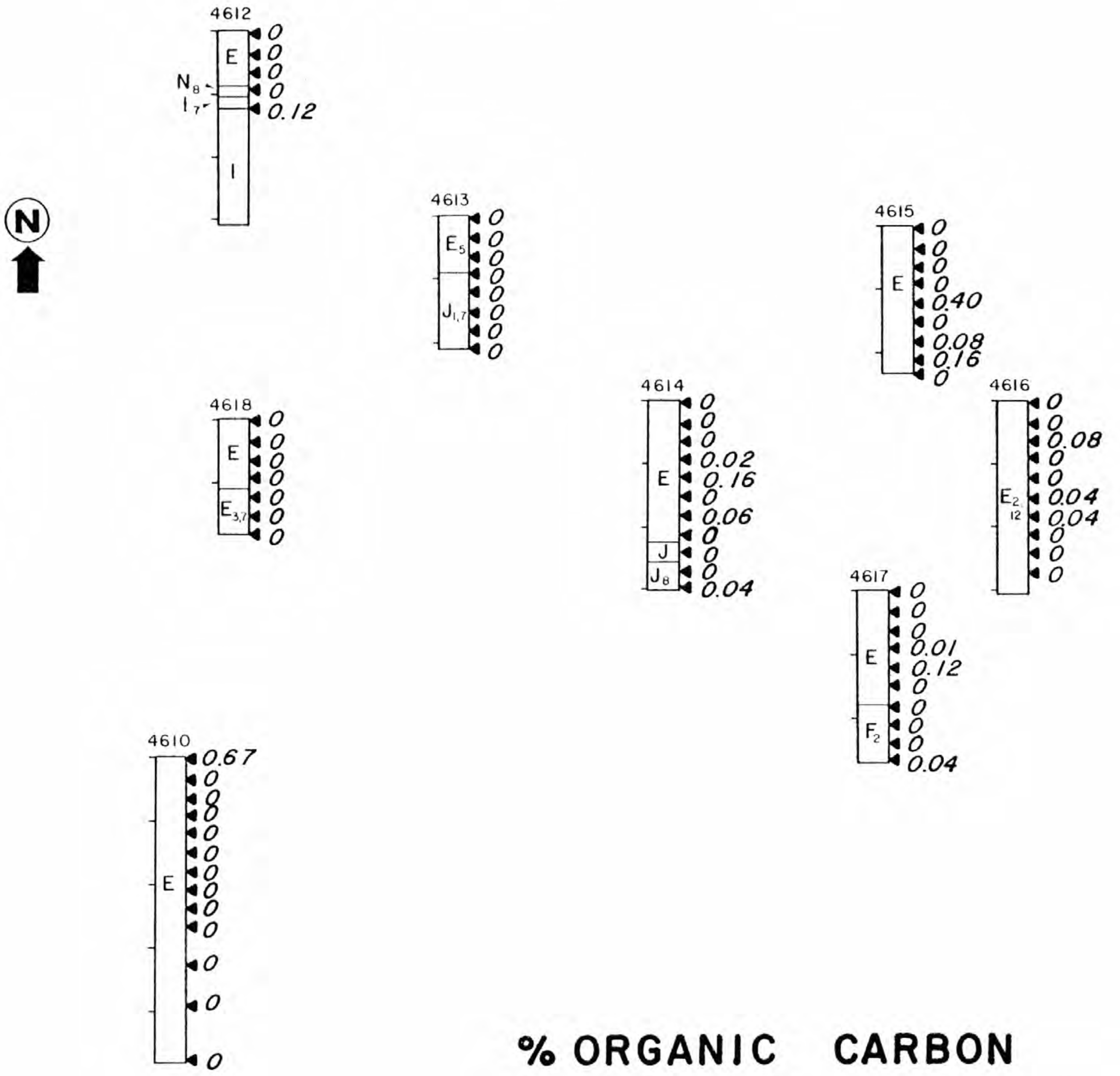
N
4612
E
N8
I7
I
0
0
0
0
0.12
4613
E5
J1,7
0
0
0
0
0
0
0
0
4615
E
0
0
0
0
0.40
0
0.08
0.16
0
4618
E
E3,7
0
0
0
0
0
0
0
4614
E
J
J8
0
0
0
0.02
0.16
0
0.06
0
0
0
0.04
4616
E2 12
0
0
0.08
0
0
0.04
0.04
0
0
0
4617
E
F2
0
0
0
0.01
0.12
0
0
0
0
0.04
4610
E
0.67
0
0
0
0
0
0
0
0
0
0
0
0

% ORGANIC CARBON

KEY

E	DUSKY YELLOW TO PALE OLIVE TO BROWN, MEDIUM TO COARSE SHELLY SAND
F	DARK OLIVE GRAY TO LIGHT GRAY, MEDIUM TO COARSE SHELLY SAND, MODERATE TO POOR SORTING
N	SHELLY COARSE SAND AND GRAVEL, VERY POORLY SORTED
J	MEDIUM TO COARSE MUDDY SHELLY SAND, VARIOUS SHADES OF GRAY, MODERATE TO POOR SORTING
I	PRE–PLEISTOCENE SEDIMENTS?, SLIGHTLY SHELLY POORLY INDURATED SANDS

0 CENTIMETRES 100

2 KILOMETRES 0 5

DESCRIPTIVE ADJECTIVES

1. PHOSPHATIC
2. CALCAREOUS ALGAE
3. OYSTERS
5. ABUNDANT BLACKSHELLS
7. ROCK FRAGMENTS
8. ROUNDED PEBBLES
12. SERPULID WORM TUBES

Figure 6-15

Figure 6-16. Percentages of organic carbon in selected subsamples of vibracores from the proposed southern lease area. In the figure 0 is the equivalent of 0.00.

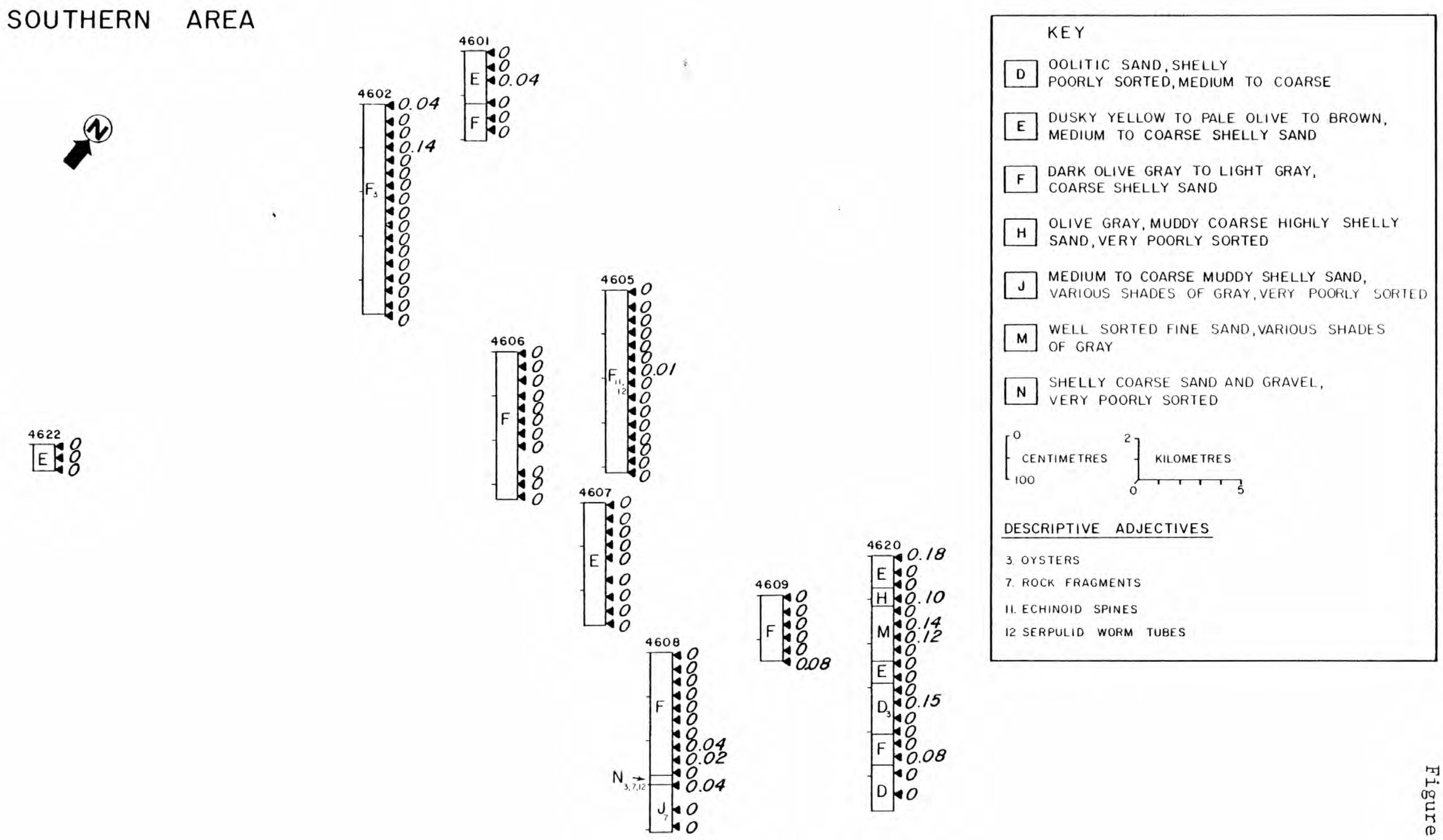
SOUTHERN AREA
N
4601
E
F
0
0
0.04
0
0
0
4602
F3
0.04
0
0
0.14
0
0
0
0
0
0
0
0
0
0
0
0
0
4605
F11,12
0
0
0
0
0
0
0.01
0
0
0
0
0
0
0
0
4606
F
0
0
0
0
0
0
0
0
0
0
0
4607
E
0
0
0
0
0
0
0
0
0
4622
E
0
0
0
4608
F
N3,7,12
J7
0
0
0
0
0
0
0
0.04
0.02
0
0.04
0
0
4609
F
0
0
0
0
0
0.08
4620
E
H
M
E
D3
F
D
0.18
0
0
0.10
0
0.14
0.12
0
0
0
0
0.15
0
0
0
0.08
0
0
KEY
D OOLITIC SAND, SHELLY POORLY SORTED, MEDIUM TO COARSE
E DUSKY YELLOW TO PALE OLIVE TO BROWN, MEDIUM TO COARSE SHELLY SAND
F DARK OLIVE GRAY TO LIGHT GRAY, COARSE SHELLY SAND
H OLIVE GRAY, MUDDY COARSE HIGHLY SHELLY SAND, VERY POORLY SORTED
J MEDIUM TO COARSE MUDDY SHELLY SAND, VARIOUS SHADES OF GRAY, VERY POORLY SORTED
M WELL SORTED FINE SAND, VARIOUS SHADES OF GRAY
N SHELLY COARSE SAND AND GRAVEL, VERY POORLY SORTED
0
CENTIMETRES
100
2
KILOMETRES
0
5
DESCRIPTIVE ADJECTIVES
3. OYSTERS
7. ROCK FRAGMENTS
11. ECHINOID SPINES
12 SERPULID WORM TUBES

% ORGANIC CARBON

Figure 6-16

Table 6-13. Percent organic carbon in various sediment types.

Sediment types with number of measurements	Mean	Standard Deviation	Range		
			Low	→	High
E (118)	0.09	0.56	0.00	→	0.70
F (118)	0.10	0.33	0.00	→	2.60
M (7)	0.11	0.14	0.00	→	0.40
L (3)	1.65	2.05	0.20	→	3.10
N (2)	0.06	0.12	0.00	→	0.30
C (4)	0.85	1.70	0.00	→	3.40
H (4)	0.13	0.13	0.00	→	0.30
J (10)	0.16	0.31	0.00	→	1.00
G (6)	0.22	0.25	0.00	→	0.70
D (6)	0.03	0.06	0.00	→	0.15

later time in order to assess future pollution. The amount of organic carbon contained in sediments has also proved to be a reliable indicator of the rate of deposition. Sediments deposited rapidly prevent oxidation of the organic constituents. Since the shelf sediments of the study area have undergone a great deal of reworking, and because they are relatively coarse, the percentage of organic carbon would be expected to be low.

The samples on the northern transect average less organic carbon (average = .20%) than those from the southern transect (average = .30%). Results of the analyses are shown in Figure 6-14. The high variation in these results suggests that the differences observed between the northern and southern transects are insignificant and are simply a function of the limited number of samples analyzed. Surprisingly, there is no clearcut correlation between the percent muds and the percent organic carbon in the samples. Perhaps this can be attributed to the extensive reworking of the samples and the transient nature (i.e., suspension and redeposition) of muds in the shelf. Possibly also, conchiolin in calcareous shell material adds significantly to organic carbon values in shelly sands.

Mollusk Assemblages

Macrofaunal studies have been perhaps the most useful tool we have used for interpreting the history of the sampled shelf sediment column. In the following discussion it is important to note that recognition of an assemblage does not indicate the total absence of components of other assemblages. Except for a few lagoonal deposits with in-place shells, no "pure" assemblages exist.

Late Pleistocene and Holocene

Examination of the late Pleistocene portion of the vibracores indicated that there were 4 different mollusk assemblages (Table 6-14); offshore, shallow shelf, inlet-backbarrier, and mixed backbarrier-shelf. These assemblages are given an ecological designation depending upon the environmental requirements of the contained species.

The offshore assemblage is found in an environment of relatively slow deposition and little sediment movement. Here such offshore mollusks as *Astarte nana* Dall, 1886, *Turritella acropora* Dall, 1899, *Laevicardium pictum* (Ravenel 1861), *Semele nucloides* (Conrad, 1841), *Varicorbula operculata* (Phillippi 1848), *Nassarium consensus* Ravenel, 1861, *Turbo castanea* (Gmelin, 1791) and *Pteromeris perplana* (Conrad, 1841) may be found in abundance. Pteropods (planktonic gastropods) are restricted to clear open marine waters and are also often found in this offshore assemblage. *Lithothamnion* algae is commonly associated with the above assemblage and indicates deposition in the photic zone in relatively clear waters.

The shallow shelf assemblage is characterized by species commonly washed up on beaches. These species are able to live under conditions of very active sand transport and deposition. Such species include *Donax variabilis* Say, 1822, *Ervilia concentrica* (Holmes, 1860), *Andara transversa* (Say, 1822), *Mulinia lateralis* (Say, 1822), and *Ensis directus* (Conrad, 1843). In addition, echinoids (sanddollars) tend to be relatively common.

The inlet and backbarrier assemblage is characterized by *Crassostrea virginica* (Gmelin, 1791), *Mulinia lateralis* (Say, 1822) [especially the thin-shelled forms], *Cyrtopleura costata* (Linné, 1786), *Mercenaria mercenaria* (Linné, 1758), *Tagelus plebeius* (Lightfoot, 1786),

Table 6-14. Summary of the faunal assemblages in vibracores.

SOUTHERN CROSS-SHELF TRANSECT

Core No.	Core Interval in Centimeters	Offshore Assemblages
4538	160-410	(some reworked? shallow elements toward base) *Pteromeris perplana* (Conrad, 1841) *Ervilia concentrica* (Holmes, 1860) *Mulinia lateralis* (Say, 1822) *Lithothamnion* algae
4539	0-140	*Turritella acropora* Dall, 1889 *Laevicardium pictum* (Ravenel, 1861) *Semele nucloides* (Conrad, 1841) *Lithothamnion* algae
	140-320	(some reworked? shallow elements) *Pteromeris perplana* (Conrad, 1841) *Glycymeris americana* (DeFrance, 1826) *Varicorbula operculata* (Philippi, 1848) *Turritella acropora* Dall, 1889 *Macrocallista maculata* (Linne, 1758) *Crassostrea* sp. (fragment, blackened) *Lithothamnion* algae
	320-517	(entirely open shelf forms) *Turritella acropora* Dall, 1889 *Chama* sp. (fragment) *Turbo castanea* Gmelin, 1791 *Lithothamnion* algae *Semele bellastriata* (Conrad, 1837) echinoderms (heart urchin plates)
4540	0-135	*Turritella acropora* Dall, 1889
	135-250	(some reworked? shallow elements) *Laevicardium pictum* (Ravenel, 1861) *Olivella mutica* (Say, 1822) *Mulinia lateralis* (Say, 1822) *Varicorbula operculata* (Philippi, 1848) *Anadara ovalis* (Bruguiere, 1789)
4541	0-100	*Chione grus* (Holmes, 1858) *Turritella acropora* Dall, 1889 *Glycymeris americana* (DeFrance, 1826) *Lithothamnion* algae
4542	0-198	*Pteromeris perplana* (Conrad, 1841) *Astarte nana* Dall, 1886 *Laevicardium pictum* (Ravenel, 1861) *Varicorbula operculata* (Philippi, 1848) *Nassarius consensus* Ravenel, 1861 *Lithothamnion* algae
4543	0-215	*Cavolinia longirostris* (Blainville, 1821) *Cadulus guadridentatus* (Dall, 1881) *Semele nucloides* (Conrad, 1841) *Chione latilirata* (Conrad, 1841) *Laevicardium pictum* (Ravenel, 1861)
	215-315	(some reworked? shallow elements; unit overlies lagoonal beds) *Dinocardium robustum* Lightfoot, 1756 *Mulinia lateralis* (Say, 1822) *Ensis directus* Conrad, 1843 *Eucrassatella speciosa* (A. Adams, 1852) *Ilyanassa obsoletus* (Say, 1822)
4544	0-345	*Astarte nana* Dall, 1886 *Turritella acropora* Dall, 1889 *Pteromeris perplana* (Conrad, 1841) branching bryozoans bryozoan balls
	345-375	(some reworked shallow elements; this unit overlies lagoonal beds) *Chione latilirata* (Conrad, 1841) *Donax* sp. (fragments) *Crassostrea virginica* (Gmelin, 1791) *Anomia simplex* d'Orbigny, 1842

Table 6-14. Summary of the faunal assemblages in vibracores (continued).

Core No.	Core Interval in Centimeters	Offshore Assemblages (continued)
4545	0-290	*Pteromeris perplana* (Conrad, 1841)
		Astarte nana Dall, 1886
		Eucrassatella speciosa (A. Adams, 1852)
		Architectonica sp. (fragment)
		Nassarius consensus Ravenel, 1861
		Lithothamnion algae
		branching bryozoans
	290-370	*Crassostrea* sp. (reworked?)
4546	0-470	*Turritella acropora* Dall, 1889
		Astarte nana Dall, 1886
		Pteromeris perplana (Conrad, 1841)
		Turbo castanea Gmelin, 1791
		Nassarius consensus Ravenel, 1861
		Lithothamnion algae

Core No.	Core Interval in Centimeters	Shallow Shelf Assemblages
4535	0-380	*Anadara transversa* (Say, 1822)
		Mulinia lateralis (Say, 1822)
		Ostrea equestris Say, 1834
		Ervilia concentrica (Holmes, 1860)
		Nassarius acutus (Say, 1822)
		(shallow reworked elements)
		Crassostrea sp. (worn)
		Abra aequalis (Say, 1822)
		Ilyanassa obsoletus (Say, 1822)
4536	0-102	*Mulinia lateralis* (Say, 1822)
		Anadara ovalis (Bruguiere, 1789)
		Ensis directus Conrad, 1843
		Ervilia concentrica (Holmes, 1860)
		Ilyanassa obsoletus (Say, 1822)
		Crassostrea sp. (worn)
		Tagelus sp. (worn)
	310-450	*Glycymeris americana* (DeFrance, 1826)
		Ensis directus Conrad, 1843
		Anadara transversa (Say, 1822)
		Ervilia concentrica (Holmes, 1860)
4537	0- 65	*Mulinia lateralis* (Say, 1822)
		Glycymeris americana (DeFrance, 1826)
4538	0-160	*Dinocardium robustum* (Lightfoot, 1756)
		Mulinia lateralis (Say, 1822)
		Anadara transversa (Say, 1822)
		Olivella mutica (Say, 1822)
		Nassarius trivittatus (Say, 1822)
4540	250-350	*Olivella mutica* (Say, 1822)
		Glycymeris americana (DeFrance, 1826)
		Anadara ovalis (Bruguiere, 1789)
		Anadara transversa (Say, 1822)
4541	140-445	*Chione latilirata* (Conrad, 1841)
		Crepidula fornicata (Linne, 1758)
		Ilyanassa obsoletus (Say, 1822)
		Mulinia lateralis (Say, 1822)
		Anadara transversa (Say, 1822)
		Olivella mutica (Say, 1822)
		Ervilia concentrica (Holmes, 1860)
		Laevicardium pictum (Ravenel, 1861)
		Eucrassatella speciosa (A. Adams, 1852)
4543	400-510	*Spisula solidissima* (Dillwyn, 1817)
		Anachis sp. (fragment)
		Ensis directus Conrad, 1843

Table 6-14. Summary of the faunal assemblages in vibracores (continued).

Core No.	Core Interval in Centimeters	Inlet-Backbarrier and Mixed (dominantly backbarrier with shelf species) Assemblages
4536	102-310	Ilyanassa obsoletus (Say, 1822) Anadara ovalis (Bruguiere, 1789) Mulinia lateralis (Say, 1822) Tagelus plebeius (Lightfoot, 1786) Mercenaria sp. (fragment) Crassostrea virginica (Gmelin, 1791) Cyrtopleura costata (Linne, 1758)
4541	100-140	Anadara ovalis (Bruguiere, 1789) Olivella mutica (Say, 1822) Crassostrea virginica (Gmelin, 1791) Nassarius trivittatus (Say, 1822) Mulinia lateralis (Say, 1822)
4543	315-410	Crassostrea virginica (Gmelin, 1791)
4544	375-608	Crassostrea virginica (Gmelin, 1791) Donax sp. (fragment) Cerithidea? sp.
4545	370-510	Noetia sp. (fragment) Crassostrea virginica (Gmelin, 1791) pulmonate snails

Core No.	Core Interval in Centimeters	Waccamaw Formation (late Pliocene to early Pleistocene)
4538	410-497	Eucrassatella sp. (fragment) Cardita tridentata Laevicardium sp. (fragment) Semele bellastriata (Conrad, 1837)
4543	510-590	see list of ostracods (listed in text under "Mollusk Assemblages") Puriana mesacostalis, Assemblage Zone of Hazel (1971)

NORTHERN SHELF TRANSECT

Core No.	Core Interval in Centimeters	Offshore Assemblages
4528	0-120	Chione intapupurea (Conrad, 1849) Turritella acropora Dall, 1889 Glycymeris sp. (fragments) Arcinella cornuta Conrad, 1866 Lucina blanda Dall and Simpson, 1901 Laevicardium pictum (Ravenel, 1861) Lithothamnion algae
	120-280	Mulinia lateralis (Say, 1822) Laevicardium pictum (Ravenel, 1861) Turritella acropora Dall, 1889 Ensis directus Conrad, 1843 Calyptraea centralis Pteromeris perplana (Conrad, 1841) Cavolinia sp. (fragment) Nassarius trivittatus (worn, black) (Say, 1822) Lithothamnion algae echinoderms (heart urchin plates)
4529	0-232	Pteromeris perplana (Conrad, 1841) Semele bellastriata (Conrad, 1837) Semele nucloides (Conrad, 1841) Tellina listeri Roding, 1798 Turritella acropora Dall, 1889 Lithothamnion algae
4530	1- 40	Glycymeris sp. Laevicardium sp. (fragment)

Table 6-14. Summary of the faunal assemblages in vibracores (continued).

Core No.	Core Interval in Centimeters	Offshore Assemblages (continued)
	40-200	(some reworked? shallow elements) Glycymeris sp. Turritella acropora Dall, 1889 Crassostrea virginica (Gmelin, 1791) Anadara ovalis (worn) (Bruguiere, 1789) Tagelus plebeius (Lightfoot, 1786) (interval 180-190 is high in proportion of bay forms) bryozoans (discoporellid type)
4531	0-140	Glycymeris sp. (fragment) Laevicardium pictum (Ravenel, 1861) Chione intapupurea (Conrad, 1849) Spisula solidissima (Dillwyn, 1817) Cavolinia sp. (fragment) Mulinia lateralis (Say, 1822) Crassostrea virginica (Gmelin, 1791) Lithothamnion algae bryozoan (discoporellid type)
4532	0-100	Glycymeris americana (DeFrance, 1826) Turritella acropora Dall, 1889 Glycymeris pectinata (Gmelin, 1791) Chione intapupurea (Conrad, 1849) bryozoan (discoporellid type)
	100-180	Turritella acropora Dall, 1889 Astarte nana Dall, 1886 Glycymeris americana (DeFrance, 1826) Glycymeris pectinata (Gmelin, 1791) Laevicardium pictum (Ravenel, 1861) Tellina listeri Roding, 1798 Semele bellastriata (Conrad, 1837) Pteromeris perplana (Conrad, 1841) Crassostrea sp. (worn) bryozoan (branching type) Lithothamnion algae
	180-320	Glycymeris pectinata (Gmelin, 1791) Mulinia lateralis (Say, 1822) Turritella acropora Dall, 1889 Lucina blanda Dall and Simpson, 1901 Crassostrea sp. pteropod (fragment) bryozoan (branching type)
	320-370	Turritella acropora Dall, 1889 Lithothamnion algae bryozoan (branching and discoporellid types)
	370-450	Ensis (silty sand, early Pleistocene?)
4533	0-350	Laevicardium pictum (Ravenel, 1861) Pteromeris perplana (Conrad, 1841) Astarte nana Dall, 1886 Chione latilirata (Conrad, 1841) Spisula sp. (blackened) Eucrassatella speciosa (A. Adams, 1852) Lithothamnion algae bryozoan (branching type) Dinocardium robustum (Lightfoot, 1756) (270 cm.)
	350-530	Eucrassatella speciosa (A. Adams, 1852) Glycymeris sp. Arcinella cornuta Conrad, 1866 Plicatula gibbosa Lamarck, 1801 Pteromeris perplana (Conrad, 1841) Cavolinia sp. (fragment) Turritella acropora Dall, 1889 Turbo castanea Gmelin, 1791 Anadara notabilis (Roding, 1798) Anadara ovalis (Bruguiere, 1789) Crassostrea sp. (fragment) Ilyanassa obsoletus (Say, 1822) Lithothamnion algae (balls)

Table 6-14. Summary of the faunal assemblages in vibracores (continued).

Core No.	Core Interval in Centimeters	Offshore Assemblages (continued)
4534	0-145	Glycymeris americana (DeFrance, 1826) Semele bellastriata (Conrad, 1837) Glycymeris pectinata Gmelin, 1791 Turbo castanea Gmelin, 1791 Semele nucloides (Conrad, 1841) Laevicardium pictum (Ravenel, 1861) Turritella acropora Dall, 1889 Chama congregata Conrad, 1833 Crassostrea sp. (fragment) Ilyanassa obsoletus (Say, 1822) Lithothamnion algae
	145-200	Olivella mutica (Say, 1822) Chione grus (Holmes, 1858) Ensis directus Conrad, 1843 Lithothamnion algae
	200-300	Anadara transversa (Say, 1822) Pteromeris perplana (Conrad, 1841) Ostrea? (fragment) Lithothamnion algae (note that 145 to 300 cm interval may contain small portions which have mostly open bay forms)

Core No.	Core Interval in Centimeters	Shallow Shelf Assemblages
4525	0- 10	Spisula solidissima (Dillwyn, 1817)
4526	0- 50	Anadara transversa (Say, 1822) Terebra dislocata (Say, 1822) Chione intapupurea (Conrad, 1849)
4527	0-307	Mulinia lateralis (Say, 1822) Laevicardium pictum (Ravenel, 1861) Spisula solidissima (Dillwyn, 1817) Nacrocallista maculata (Linne, 1758) Ervilia concentrica (Holmes, 1860) Terebra dislocata (Say, 1822) Chione latilirata (Conrad, 1841) Semele nucloides (Conrad, 1841) Chione grus (Holmes, 1858) Pleuromeris tridentata (Say, 1826)

Core No.	Core Interval in Centimeters	Inlet-Backbarrier and Mixed (dominantly backbarrier with shelf species) Assemblages
4525	10-200	Bellucina amiantus (Dall, 1901) Crassostrea virginica (Gmelin, 1791) Mulinia lateralis (Say, 1822) Anadara transversa (Say, 1822) Pteromeris perplana (Conrad, 1841)
	200-270	Mercenaria mercenaria (Linne, 1758) Crassostrea virginica (Gmelin, 1791) Mulinia lateralis (Say, 1822) Ilyanassa obsoletus (Say, 1822) Chama congregata Conrad, 1833 Chione intapupurea (Conrad, 1849) Plicatula gibbosa Lamarck, 1801
4530	200-250	Mulinia lateralis (Say, 1822) Tagelus plebeius (Lightfoot, 1786) Nassarius trivittatus (Say, 1822)
	250-290	Nucula proxima Say, 1822 Ensis directus Conrad, 1843 Argopecten sp. (fragment)
	290-350	(sediment looks lagoonal)

Table 6-14. Summary of the faunal assemblages in vibracores (continued).

Core No.	Core Interval in Centimeters	Inlet-Backbarrier and Mixed Assemblages (continued)
4530	350-560	Eupleura caudata (Say, 1822) Spisula solidissima Dillwyn, 1817 Mulinia lateralis (Say, 1822) Anadara transversa (Say, 1822) Glycymeris pectinata (Gmelin, 1791)
4531	140-240	Mulinia lateralis (Say, 1822) Ensis directus Conrad, 1843 Olivella sp. (fragment) Nucula proxima Say, 1822 echinoderm (regular urchin)
	240-310	Donax? sp. (fragment) Lithothamnion algae (fragment)

SOUTHERN LEASE AREA

Core No.	Core Interval in Centimeters	Offshore Assemblages
4610	0- 20	Discoporella, Lithothamnion (fine scattered branches), Laevicardium
	20- 40	Plicatula, Cardita perplana, Discoporella
	40- 60	branching bryozoans, Echinochama, Astarte nana, barnacles, sanddollar, Cardita perplana
	60- 80	Echinochama, sanddollar, Glycymeris pectinata, Lithothamnion (branches), Cardita perplana
	80-100	Donax, Chione intapupurea, Discoporella, Spisula, Chana, Atrina, Lithothamnion (branches)
	100-120	Crepidula, Crassostrea? (blackened, worn), Glycymeris pectinata, Chione cancellata
	120-140	Turbo castaneus, Lithothamnion, Donax? sp.
4612	0- 20	Laevicardium, Diodora
	60- 80	Angopecten, Turritella acropora
	80-100	barnacle, Echinochama, Chione grus, Chione latilirata, sanddollar
4613	20- 40	Laevicardium, Chione grus, Cardita perplana
	40- 60	Corbula, Glycymeris pectinata, Laevicardium
	60- 80	Atrina, Echinochama, Laevicardium, Discoporella
4614	0- 20	Discoporella, Cardita perplana, Glycymeris pectinata
	20- 40	Discoporella, Macrocallista, Laevicardium, Astarte nana
	40- 60	Laevicardium, Terebra, Astarte nana, Atrina, Discoporella
	60- 80	Laevicardium, Cardita perplana, Olivella (open shelf form), Astarte nana
	80-100	Astarte nana, Laevicardium, Atrina
	100-120	Natica, Eucrassatella, Laevicardium
	120-140	Discoporella (abundant), Olivella
	140-160	Cardita perplana (one, blackened), Lithothamnion (branch), Discoporella
	160-180	Echinochama, Glycymeris, Laevicardium, Cardita perplana, Marginella, Chione latilirata, Macrocallista maculata (the very shelly interval 160-200 cm contrasts to the sandier sediments above and the sandy medium coarse sediment in the 200-220 cm interval)

Table 6-14. Summary of the faunal assemblages in vibracores (continued).

Core No.	Core Interval in Centimeters	Offshore Assemblages (continued)
4614	180-200	*Glycymeris*, *Echinochama*, *Pecten*, sanddollar, *Spisula* (blackened)
	200-220	*Turbo castaneus*, echinoderm plate
4615	20- 40	*Macrocallista maculata*
	40- 60	*Laevicardium* (abundant), *Lithothamnion* (one branch), barnacles, sanddollar, *Turritella*
	60- 80	*Laevicardium*, *Atrina*, echinoderm
	80-100	*Terebra dislocata*, *Chione latilirata*
	120-140	*Discoporella*, *Glycymeris americana*
	140-160	*Lithothamnion* (one, branching) (fragment), *Discoporella*
	160-180	*Chama*, *Turritella*, *Glycymeris*, *Lithothamnion*, *Cardita perplana* (common branching)
	180-200	*Dentalium*, *Olivella*, *Lithothamnion*
	200-220	*Lithothamnion* (balls), *Chama*, *Turritella*, *Ensis*
	220-240	*Lithothamnion*, *Crucibulum*, *Plicatula*
4616	0- 20	*Discoporella*, *Pecten*
	20- 40	barnacle, *Glycymeris americana*, *Vermicularia*, *Turbo castaneus*, *Discoporella*, *Lithothamnion* (balls)
	40- 60	barnacles, branching *Lithothamnion*
	60- 80	*Cardita perplana*, *Glycymeris*
	80-100	*Pecten*, barnacles, *Discoporella*
	100-120	*Turbo castaneus*, *Discoporella*
	120-140	barnacles, *Discoporella*
	140-160	*Vermicularia*, *Nassarius*? sp.
	160-180	*Pecten*, *Chama congregata*, *Chione intapupurea*, *Vermicularia*
	180-200	*Glycymeris pectinata*, *Discoporella*, *Marginella*
	200-220	*Discoporella*, coral (worn branching)
4617	0- 20	*Laevicardium*, *Discoporella*
	20- 40	*Glycymeris*
	40- 60	*Lithothamnion*, *Plicatula*, *Astarte nana*, *Chione intapupurea*, *Atrina*
	60- 80	*Discoporella*, *Lithothamnion*, *Spisula*, *Ensis* *Laevicardium*
	80-100	*Echinochama*, branching bryozoans, *Lithothamnion*, *Pandora*
	100-120	*Lithothamnion*, *Turbo castaneus*
	120-140	*Lithothamnion*, *Turbo castaneus*, *Chama*
	140-160	*Lithothamnion*, *Discoporella*
	160-180	*Lithothamnion*, *Marginella*
	180-200	*Lithothamnion*, *Semele bellastriata*
	200-220	*Lithothamnion*, *Chione intapupurea*, *Plicatula*, barnacle
	220-240	*Glycymeris*, *Marginella*

Table 6-14. Summary of the faunal assemblages in vibracores (continued).

Core No.	Core Interval in Centimeters	Offshore Assemblages (continued)
4618	0- 20	Cardita tridentata, Olivella
	20- 40	Argopecten, Laevicardium
	40- 60	Diplodonta, barnacles
	60- 80	Echinochama, Lithothamnion, Chione intapupurea, Discoporella
	80-100	Semele bellastriata, Discoporella, Crassostrea (worn, black), sanddollar, Lithothamnion

Core No.	Core Interval in Centimeters	Mixed Assemblages (dominantly backbarrier with some shelf species)
4610	140-160	Lithothamnion branches, barnacles, Discoporella
	160-180	Crassostrea? (blackened), Crepidula, Olivella
	180-200	sanddollar, Ostrea? sp., Nassarius obsoletus,
	200-220	Crepidula fornicata, Discoporella
	220-240	Discoporella, Dinocardium? (worn)
	300-320	small phospatic shark tooth
	340	Polinices?, Donax, Glycymeris pectinata
	350	Ervillia
	380	Glycymeris americana, Chione intapupurea
	400	Turbo castaneus, Eucrassatella
	420-440	Astarte nana, sanddollar
	440-460	Nassarius obsoletus, Crepidula fornicata
	460-480	Astarte nana, Spisula, Atrina
4613	98-120	Oliva sayana, Laevicardium, Chama, Glycymeris (worn), Chione latilirata (worn)
	120-140	Macrocallista maculata, Laevicardium, Discoporella, Ensis
	140-160	Ensis (in some clasts), Discoporella (in some clasts)
	160-170	Nassarius obsoletus (fragment), sanddollar
	170-180	coral, Polinices, Spisula, sanddollar, Ensis
4616	260-280	Lithothamnion (fine, common), Nassarium obsoletus, Spisula solidissima, Lithothamnion (worn branches), Discoporella, sanddollars, Chione cancellata, Chama, Turbo castaneus, Caecum, Olivella
	280-300	(less Lithothamnion in fine fraction than above; maybe shallower) Donax, Pteria, sanddollar, Vermicularia, barnacle
4617	240-260	Ensis, Lithothamnion, Spisula
	260-280	Crepidula, Lithothamnion, Donax, oyster (small worn)
4618	100-120	Laevicardium, Crassostrea (blackened), Lithothamnion
	120-140	Neotia (small) linestome? Crassostrea (black)
	140-160	Ilyanassa obsoletus, Crassostrea (black), Lithothamnion
	160-180	Crassostrea (blackened), Lithothamnion

Table 6-14. Summary of the faunal assemblages in vibracores (continued).

Core No.	Core Interval in Centimeters	Waccamaw? Formation
4613	190-210	Break to fragments in a more calcareous-looking matrix. *Anadara* sp.
4614	220-240	*Olivella*, *Glycymeris americana* (blackened), barnacles, *Discoporella*
	240-260	*Glycymeris* (coarse, blackened shell), *Crepidula fornicata*, *Mulinia lateralis*, *Chione latilirata*
	260-280	*Glycymeris pectinata* (in fine sandstone), *Chione latilirata* (in quartz sandstone), *Glycymeris americana*
	280-300	*Astarte nana*, *Glycymeris pectinata*, *Chione latilirata*, *Glycymeris americana*, rare *Lithothamnion* (branches), *Ensis Calliostoma*, *Dentalium*

Core No.	Core Interval in Centimeters	Pre-Pleistocene Sediments
4612	106-120	*Barbatia*, *Marginella*
	140-160	*Discoporella*

NORTHERN LEASE AREA

Core No.	Core Interval in Centimeters	Offshore Assemblages
4605	0- 20	*Pecten*, *Plicatula* (worn, encrusted, blackened), *Crassostrea*, *Ensis*, *Atrina*
	60- 80	*Crassostrea* (blackened, worn)
	80-100	*Laevicardium*, *Discoporella*, *Calyptraea*, *Olivella*
	100-120	sanddollar, *Olivella*, *Discoporella*
	120-140	sanddollar, *Discoporella*, *Olivella*
	140-160	sanddollar, *Cardita perplana*, *Ilyanassa obsoletus*
	160-180	sanddollar, *Pandora*, *Busycon*, *Lithothamnion* branches (blackened), barnacle, *Olivella*, *Cardita tridentata*
	180-200	*Ervillia*
	200-220	sanddollar, *Discoporella*
	220-240	*Olivella*, heart urchin, *Ilyanassa obsoletus*
	240-260	*Olivella*, *Discoporella*
	260-280	*Turritella acropora*, *Lithothamnion*
	280-300	*Crepidula*, *Olivella*
	300-320	*Lithothamnion* (worn), *Ervillia*, *Discoporella*
	320-340	*Argopecten*, *Crassostrea*? sp. (fragment) *Lithothamnion* (worn)
4606	0- 20	*Lithothamnion* (one branch), *Discoporella*, *Laevicardium*
	20- 40	*Olivella*, *Laevicardium*
	40- 60	*Argopecten*, *Olivella*, *Discoporella*
	60- 80	*Lucina blanda*, *Turritella acropora*, *Discoporella*
	80-100	*Argopecten*, *Discoporella*
	100-120	*Turritella acropora*

Table 6-14. Summary of the faunal assemblages in vibracores (continued).

Core No.	Core Interval in Centimeters	Offshore Assemblages (continued)
4606	120-140	barnacles
	140-160	*Discoporella*
	160-180	*Olivella*, *Discoporella*, *Turritella acropora*
	200-220	*Olivella*, *Discoporella*
	220-240	*Discoporella*
	240-260	*Turritella acropora*, *Discoporella*, *Ensis*, *Laevicardium*
	260-280	*Discoporella*
	280-300	*Atrina*, *Pandora*
	300-320	*Discoporella*, *Chione latrilirata*
	320-340	*Chione latilirata*, regular Echinoderm
4607	0- 20	*Discoporella*
	20- 40	*Discoporella*, *Pecten*, sanddollar, *Chama*
	40- 60	*Discoporella*, *Chione intapupurea*
	60- 80	*Olivella*, *Discoporella*, sanddollar
	80-100	*Laevicardium*, branching bryozoans, *Discoporella*
	100-120	*Argopecten*, pteropod, branching bryozoans
	120-140	barnacles, *Discoporella*, Urchin, *Ensis*
	140-160	*Spisula*, *Discoporella*
	160-180	*Macrocallista maculata*, *Discoporella*, branching bryozoans
	180-200	*Macrocallista maculata*, bryozoans (branching), *Turritella*, *Semele nucloides*
	200-220	*Macrocallista maculata*, *Chama*, *Chione intapupurea*
	220-240	*Macrocallista maculata*, *Discoporella*, *Turritella*
4608	0- 20	*Discoporella*, *Semele nucloides*
	20- 40	barnacles, *Discoporella*, *Serpula*
	40- 60	*Laevicardium*, *Discoporella*, *Serpula*, barnacles
	60- 80	*Discoporella*, *Laevicardium*, *Cardita perplana*, *Atrina*, heart urchin, barnacles, bryozoans (branching)
	80-100	*Lithothamnion* branches, barnacles, bryozoans (branching), *Laevicardium*
	100-120	*Laevicardium*, *Discoporella*
	120-140	*Argopecten*, *Varicorbula*, *Laevicardium*
	140-160	*Argopecten*, *Discoporella*
	180-200	*Busycon*? sp., barnacle, *Discoporella*, *Laevicardium*
	200-220	*Glycymeris americana*, *Plicatula*, *Lithothamnion* (branches), *Discoporella*
	220-240	*Laevicardium*, *Lithothamnion* (branch, one)
	240-260	barnacle
	260-280	bryozoans (branching), *Discoporella*, *Laevicardium*, *Argopecten*

Table 6-14. Summary of the faunal assemblages in vibracores (continued).

Core No.	Core Interval in Centimeters	Offshore Assemblages (continued)
4609	0- 20	*Discoporella*, *Chione latilirata*
	20- 40	*Echinochama*, *Argopecten*, *Chione latilirata*, *Glycymeris*, *Discoporella*, barnacles
	40- 60	*Laevicardium*, *Pecten*, *Echinochama*, *Ensis*, *Olivella*, *Chione latilirata*
	60- 80	*Echinochama*, *Chione latilirata*, *Macrocallista maculata*, barnacles, *Discoporella*, *Cardita tridentata*
	80-100	bryozoans (branching), heart urchins
	100-120	barnacles, *Discoporella*, *Chama*, *Plicatula*
	120-140	*Laevicardium*, *Discoporella*, *Glycymeris americana*, *Chama*, bryozoans (branching)
	140-160	*Trachycardium*, *Laevicardium*, *Discoporella*, *Lithothamnion* (rare, branching type)
4620	0- 20	*Discoporella*, *Lithothamnion*
	20- 40	*Atrina*, *Semele bellastriata*, barnacle
	40- 60	*Macrocallista*, *Atrina*
	60- 80	barnacle, *Vericorbula*, *Cardita perplana*, *Chione intapupurea*, *Mulinia*
	80-100	*Discoporella*
	100-120	*Laevicardium*, *Olivella*
	120-140	*Discoporella*
	140-160	*Nassarius trivittatus*
	160-180	sanddollar
	180-200	*Marginella*, *Discoporella*
	200-220	*Tellina agilis*, *Ensis*, *Cardita tridentata*, sanddollar, *Olivella*
	220-240	*Spisula*, *Discoporella*, *Olivella*
	240-260	*Olivella*, coral, sanddollar, *Crepidula*
	260-280	coral, *Chione intapupurea*, *Crepidula*, sanddollar
	280-300	*Ensis*, *Olivella*, *Lucina blanda*
	300-320	*Glycymeris americana*, *Lithothamnion*, *Glycymeris pectinata*
	320-340	*Cardita tridentata*, *Macrocallista*, *Chione intapupurea*
	340-360	*Chione latilirata*, sanddollar
	360-380	sanddollar
4622	0- 20	*Discoporella*, *Atrina*, *Macrocallista maculata*
	20- 40	*Discoporella*, coral, *Phalium*, *Crepidula*
	40- 60	*Mulinia*, *Argopecten*

Table 6-14. Summary of the faunal assemblages in vibracores (continued).

Core No.	Core Interval in Centimeters	Shallow Shelf Assemblages
4600	0- 20	*Discoporella*, *Pecten*?, barnacles
	20- 40	sanddollar, *Olivella*, *Eucrassatella*, *Glycymeris americana*, *Ostrea equestris*, coral, *Crepidula fornicata*
	40- 60	*Mulinia*?
4601	10- 40	*Chama*, *Crassostrea* (worn)
	40- 60	*Laevicardium*, *Lithothamnion*, *Crassostrea*? (worn), *Discoporella*
	60- 80	*Argopecten*
	80-100	*Mulinia* (blackened), *Lithothamnion* (one branch)
	100-120	*Laevicardium*, *Discoporella*
	120-140	*Argopecten*, *Discoporella*
	140-160	*Lithothamnion* (one branch), *Laevicardium*, *Plicatula*, *Ensis*, *Mulinia* (worn)
	160-180	*Discoporella*, *Plicatula*
	180-200	*Glycymeris*, *Lithothamnion* (one, small)
4602	0- 20	*Argopecten*
	20- 40	*Macrocallista maculata*
	40- 60	*Discoporella*, *Glycymeris*
	60- 80	*Discoporella*
	80-100	*Tellina*, *Discoporella*
	120-140	*Discoporella*, *Laevicardium*, sanddollar
	140-160	*Chama*, barnacle, *Spisula*, *Atrina*
	160-180	*Crassostrea* (thick, blackened), *Chama*
	180-200	*Ensis*, *Ervillia*
	200-220	*Nassarium trivittatus*, *Olivella*, *Ensis*, coral
	220-240	*Mulinia*, *Olivella*, *Discoporella*
	240-260	barnacle, *Discoporella*

Core No.	Core Interval in Centimeters	Mixed Assemblages (dominantly backbarrier with some shelf species)
4600	60- 80	*Spisula solidissima*, *Laevicardium*, *Mulinia*, *Olivella*, *Ensis*
	80-100	*Ensis*, barnacle
	100-120	*Mulinia*, *Ensis*
	180-200	*Ensis*, *Plicatula*, *Eupleura*, *Olivella*, *Ensis*
	200-220	*Marginella*, *Spisula*, barnacle, button bryozoans
	220-240	*Ensis*, *Mulinia*, *Discoporella*
	240-250	*Plicatula*, coral, bryozoans (balls)

Table 6-14. Summary of the faunal assemblages in vibracores (continued).

Core No.	Core Interval in Centimeters	Mixed Assemblages (dominantly backbarrier with some shelf species) (cont.)
4602	260-280	*Semele nucloides*, *Discoporella*
	280-300	*Discoporella*
	300-320	*Lucina blanda*, *Discoporella*
	320-340	barnacle, *Atrina*, *Busycon*, *Lithothamnion* (one branch)
	340-360	barnacle, *Chione latilirata*, *Discoporella*
	360-380	sanddollar, *Olivella*
	380-400	Discoporellid-type bryozoan, *Lucina blanda*
	400-420	*Mulinia*, *Spisula*, *Discoporella*
	420-440	*Lithothamnion* (branch, worn), sanddollar, *Ensis*, *Discoporella*
	440-460	*Crepidula*, *Discoporella*, *Ensis*, *Oliva*
	460-480	*Macrocallista maculata*, *Ensis*
4605	340-360	*Olivella*, *Discoporella*
	360-380	*Ervillia*, *Discoporella*
	380-400	*Mulinia*, *Ervillia*, *Discoporella*
	400-420	*Ervillia*, *Argopecten*
4607	240-260	*Discoporella*, barnacles
	260-280	*Chione intapupurea*, *Crassostrea* (blackened), *Ensis*, *Mulinia*
	280	*Anachis avara*
4608	280-300	*Crassostrea*, *Chama*, *Cardita perplana*
	300-320	coral (fresh), *Crassostrea* (worn), bryozoans (branching), *Olivella*, *Crepidula*, barnacle
	320-340	*Nassarius vibex*, *Ilyanassa obsoletus*, *Discoporella*, *Crassostrea* (large, black)
	340-360	*Ilyanassa obsoletus*, *Discoporella*, barnacles
	360-380	roots? organic sediment, tiny *Crepidula*, *Mulinia*
4620	380-400	*Mulinia*, *Ervillia*, *Crassostrea*? (blackened)
	400-420	*Discoporella*
	420-440	*Ilyanassa obsoletus*, *Glycymeris pectinata*
	440-460	*Mulinia*, *Ervillia*, *Chione intapupurea*
	460-480	*Discoporella*, sanddollar
	480-500	*Glycymeris*, *Ervillia*
	540-560	*Ervillia*

Ilyanassa obsoletus (Say, 1822), and Anadara ovalis (Bruguiere, 1789).

The fourth assemblage is a mixed association of backbarrier and shelf species. This assemblage is common within certain portions of the transect where backbarrier deposits have been reworked by erosion on the open shelf. Here is the unusual association of such backbarrier elements as Crassostrea, Ilyanassa, and Mercenaria with open shelf forms such as pteropods, lithothamnion algae, planktic foraminifers, and benthic foraminifers which prefer clear normal oceanic waters. Such a mixed assemblage is found in beds which lie between the backbarrier deposits and the open shelf deposits. It is unusual that shallow shelf beds do not exist adjacent to these beds of mixed assemblage species. The full cycle of deposition is not present in many cores. Thus instead of having a simple progression of backbarrier beds, shallow shelf beds, and open shelf beds, there is a portion of the cycle missing and lagoonal beds have been directly reworked into the open shelf deposits.

Waccamaw Formation

Four of the cores have penetrated into deposits of Waccamaw Formation age (cores 4538, 4543, 4613, and 4614). The bottom of core 4541 may approach the top of this Waccamaw age bed as it has some pebbles of limestone in the base of the core. Also the core 4537 may have struck a high in the top of the Waccamaw surface but the age of the rock fragments (leached calcareous quartz sands) is indeterminent. These Waccamaw age deposits are quite calcareous, with the 4543 core sample containing abundant mollusks including shallow open marine bivalves: Glycymeris americana DeFrance, 1826, Chione intapupurea (Conrad, 1849), Eucrassatella speciosa A. Adams, 1852, Laevicardium sp. frag., Pleuromeris tridentata (Say, 1826), as well as discoporellid bryozoans and coral. Waccamaw Formation age ostracods include the following species identified by J. E. Hazel and R. Forester:

PURIANA CAROLINENSIS Hazel, in press

BENSONOCYTHERE WHITEI (Swain, 1951)

LOXOCONCHA PURISUBRHOMBOIDEA Edwards, 1944

EUCYTHERE DECLIVIS (Norman, 1865)

MALZELLA EVEXA Hazel, in press

BAIRDOPPILLATA aff. B. TRIANGULATA Edwards, 1944

RADIMELLA CONFRAGOSA (Edwards, 1944)

PROTEOCONCHA spp.

PELLUSCISTOMA aff. P. MAGNIVENTRA Edwards, 1944

LOXOCONCHA EDENTONENSIS Swain, 1968

PARADOXOSTOMA spp.

CYTHERURA spp.

MUELLERINA WARDI, Hazel, in press

XESTOLEBERIS sp.

The depositional environment represented by this assemblage is a nearshore, shallow marine low energy environment. Many of these species can tolerate lowered salinities (polyhaline) although no true brackish water species are present, suggesting normal (30 to 38 parts per thousand) salinity. The depth of water herein inferred is based upon the presence of numerous epiphytal species (e.g. PARADOXOSTOMA spp.) that can only live on plants. The current and wave energy level is based upon the large percentage of juveniles present with the adults, which normally does not occur under even moderate energy conditions due to selective sorting of the valves.

STRATIGRAPHY OF THE SHELF SEDIMENT COVER

The surficial sediment of the northern cross-shelf transect (Figure

6-17) exhibits a relatively simple lateral sequence of sediment with an offshore shell assemblage grading into a shallow shelf assemblage on what is presently the shallow shelf. Inlet-backbarrier (lagoon) sequences were penetrated by cores 4525 and 4530. Two radiocarbon dates on core 4525 (22,585 and 25,065 BP) indicate that this lagoonal deposit (with oysters in growth position) was deposited during the last transgression. Underlying pre-Pleistocene rock was penetrated and retrieved in four cores. A well-lithified Paleocene is present at the base of the three shallowest or innermost cores of this transect. Lithified sandstone of unknown age was obtained at the base of core 4530 on the outer shelf. It is highly likely judging from core penetration rates that "hard rock" was penetrated but not retrieved from most of the other cores on this transect.

The southern cross-shelf transect across the wider South Carolina shelf exhibits more complex lateral changes in the unconsolidated sediment cover (Figure 6-17). The uppermost sediment cover, like the northern transect, consists of sediment with an offshore assemblage on the central and outer shelf grading into a shallow shelf assemblage on the inner shelf. As on the northern transect, the offshore assemblage sediment thickens toward the outer shelf. Underlying sediment deposited in the "offshore" environment is sand with an inlet-backbarrier assemblage, the two being separated by a thin band of mixed assemblage sediment (Figure 6-17). Radiocarbon dates point to a Holocene transgression origin of this unit. On the central shelf the inlet-backbarrier and/or mixed assemblage unit is underlain by a shallow shelf assemblage sand. Due to its stratigraphic position this unit must have been deposited as long ago as the Wisconsin sea level regression. On the inner shelf, at a position comparable to the northern transect,

Figure 6-17. Vibracore stratigraphy of the shelf sediment cover. Stratigraphic units plus the depositional environment of the overlying Pleistocene-Holocene unconsolidated sediment cover are shown. Note the extreme vertical exaggeration. Radiocarbon dates shown are mostly for shell material (see Table 6-15).

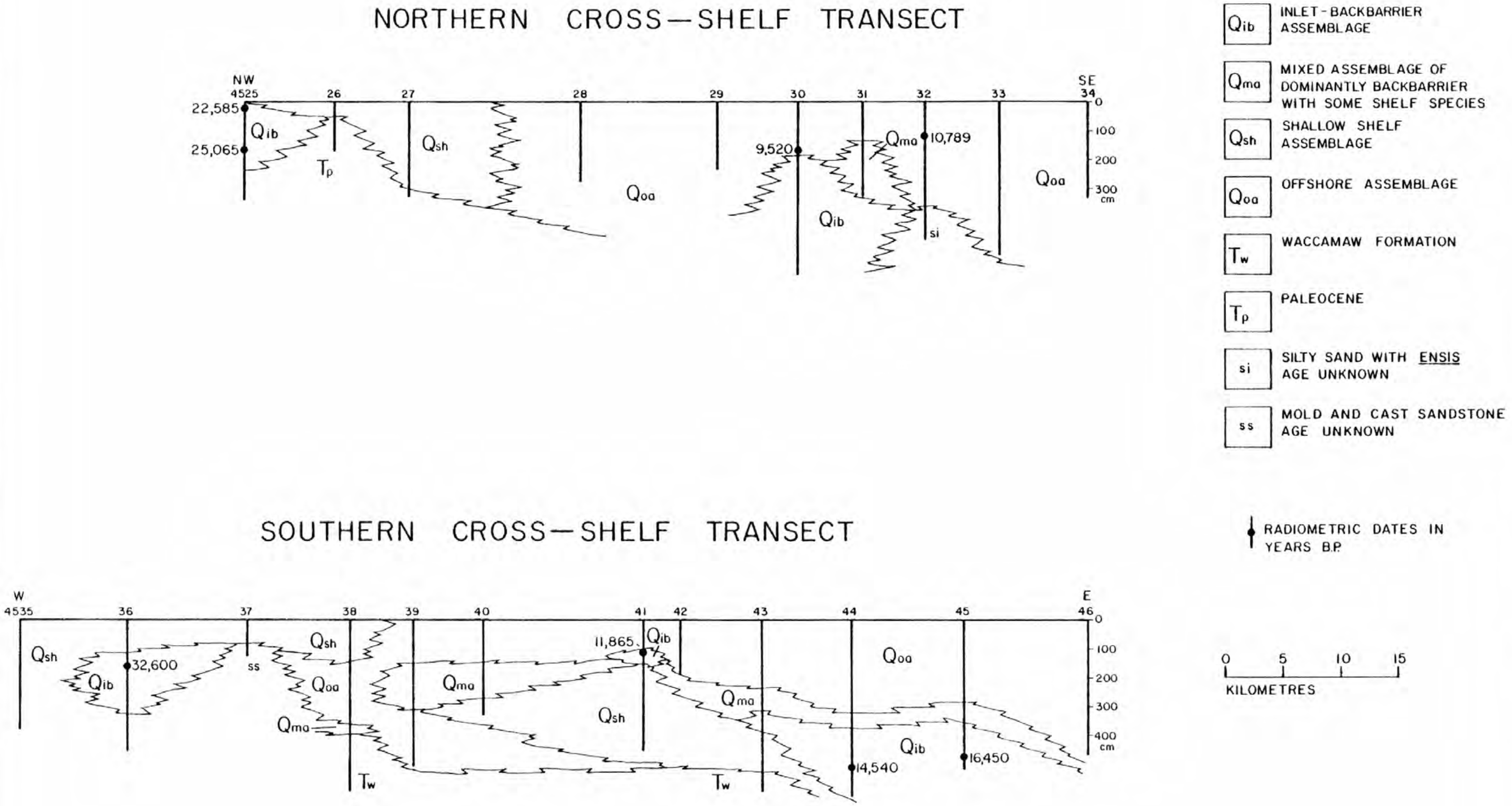
NORTHERN CROSS—SHELF TRANSECT
NW
SE
4525
26
27
28
29
30
31
32
33
34
0
100
200
300
cm
22,585
25,065
9,520
10,789
Qib
Tp
Qsh
Qoa
Qma
si
SOUTHERN CROSS—SHELF TRANSECT
W
E
4535
36
37
38
39
40
41
42
43
44
45
46
0
100
200
300
400
cm
32,600
11,865
14,540
16,450
Qsh
Qib
ss
Qoa
Qma
Tw
Qib
INLET-BACKBARRIER ASSEMBLAGE
Qma
MIXED ASSEMBLAGE OF DOMINANTLY BACKBARRIER WITH SOME SHELF SPECIES
Qsh
SHALLOW SHELF ASSEMBLAGE
Qoa
OFFSHORE ASSEMBLAGE
Tw
WACCAMAW FORMATION
Tp
PALEOCENE
si
SILTY SAND WITH ENSIS AGE UNKNOWN
ss
MOLD AND CAST SANDSTONE AGE UNKNOWN
RADIOMETRIC DATES IN YEARS B.P.
0
5
10
15
KILOMETRES

Figure 6-17

Table 6-15. Age and location of samples (fixed shoreline indicators) used in Figure 6-17.

Number of Plot-Points in Figure 6-20	Latitude/ Longitude	Age in years B.P.	Sample Depth in Meters below MSL	Material Dated	Area	Reference
1	33°55' 74°09'	3,700 36,000 - 2,000	0	salt marsh peat	N.C.	17
2	31°59.66' 80°24.95'	+ 910 32,000 - 1,025	-21.5	*Crassostrea* in lagoonal sediment	Off S.C. coast	This paper core 4536
3	38°40'	28,400 ± 1,800	-14.0	lagoonal silt	Delaware	6
4	33°29.27'	25,065 ± 310	-14.7	lagoonal sediment	Off S.C.	This paper core 4525 20 cm
5	33°29.27' 78°50.27'	22,585 ± 530	-13.2	*Crassostrea* in lagoonal sediment	Off S.C.	This paper core 4525 172 cm
6	30°14' 86°30'	22,042 ±	-28.0	beach coquina	Off N.W. Florida	12
7	31°44.94' 79°53.16'	16,450 ± 155 17,265 ± 235	-58.6	*Crassostrea* (two specimens) in lagoonal sediment	Off S.C.	This paper core 4525 460 cm
8	31°44.94' 79°38.96'	14,540 ± 180	-38/-38.3	salt marsh peat	Off S.C.	This paper core 4544 505-535 cm
9	31°51.30' 79°57.06'	11,865 ± 140	-31	*Crassostrea* in lagoonal sediment	Off S.C.	This paper core 4541 100-110 cm
10	33°03.40' 78°22.99'	10,785 ± 130	-28/-28.5	*Crassostrea* in lagoonal sediment	Off S.C.	This paper core 4532 100-150 cm
11	38°40' 75°04'	10,800 ± 300	-26	peat under lagoon	Delaware	6
12	29°43.70' 84°57.40'	9,950 ± 180	-22	*Rangia cuneata* articulated in growth position in prodeltaic sediments	Off N.W. Florida	19
13	33°08.37' 78°28.66'	9,520 ± 95	-26.8	*Crassostrea* in lagoonal sediment	Off S.C.	This paper core 4530 170-190 cm

the shallow shelf assemblage sand is underlain by lagoonal deposits deposited during the start of the last sea level transgression.

Thus, sediments of the southern cross-shelf transect preserve a slightly more complex series of depositional events than those of the northern transect. It is very important to note the extreme vertical exaggeration of Figure 6-17; i.e., 60-100 km horizontally versus a maximum of 6 m vertically. One overriding characteristic obvious in both the northern and southern transects is the thinness of the unconsolidated sediment cover of Pleistocene-Holocene age. In spite of repeated transgressions and regressions during the Pleistocene, the total amount of sediment contributed to the shelf during this time was very small. If the Swift (1976) model of continental shelf sedimentation is essentially correct, it may be that much of the sand brought down to the shelf during the ice ages is tied up in the present day shoreface wedge or in stranded shoreface wedges on the lower coastal plain.

Perhaps the single most instructive parameter in regard to the stratigraphy of the lease area cores is the set of the megascopic core descriptions. Of the 19 cores that penetrated 50 cm or more of unconsolidated sediment, 11 contain only one recognizable unit; a shelf sand (Figures 6-18 and 6-19). In all cases (cores 4601, 4602, 4605, 4606, 4607, 4609, 4610, 4615, 4616, 4617, and 4620) the unit is believed to represent a layer of sediment mixed under essentially present conditions, that is since the sea level had risen to close to its present location. Evidence that this upper unit is shelf-derived includes the presence of open shelf forms, the high degree of angularity of shell fragments and the presence of delicate fragments such as echinoid plates, razor clams, etc. The abundance of black shells

Figure 6-18. Vibracore stratigraphy of the shelf sediment cover within the boundaries of the proposed northern lease area. Radiometric dates of these cores are shown in Table 6-16.

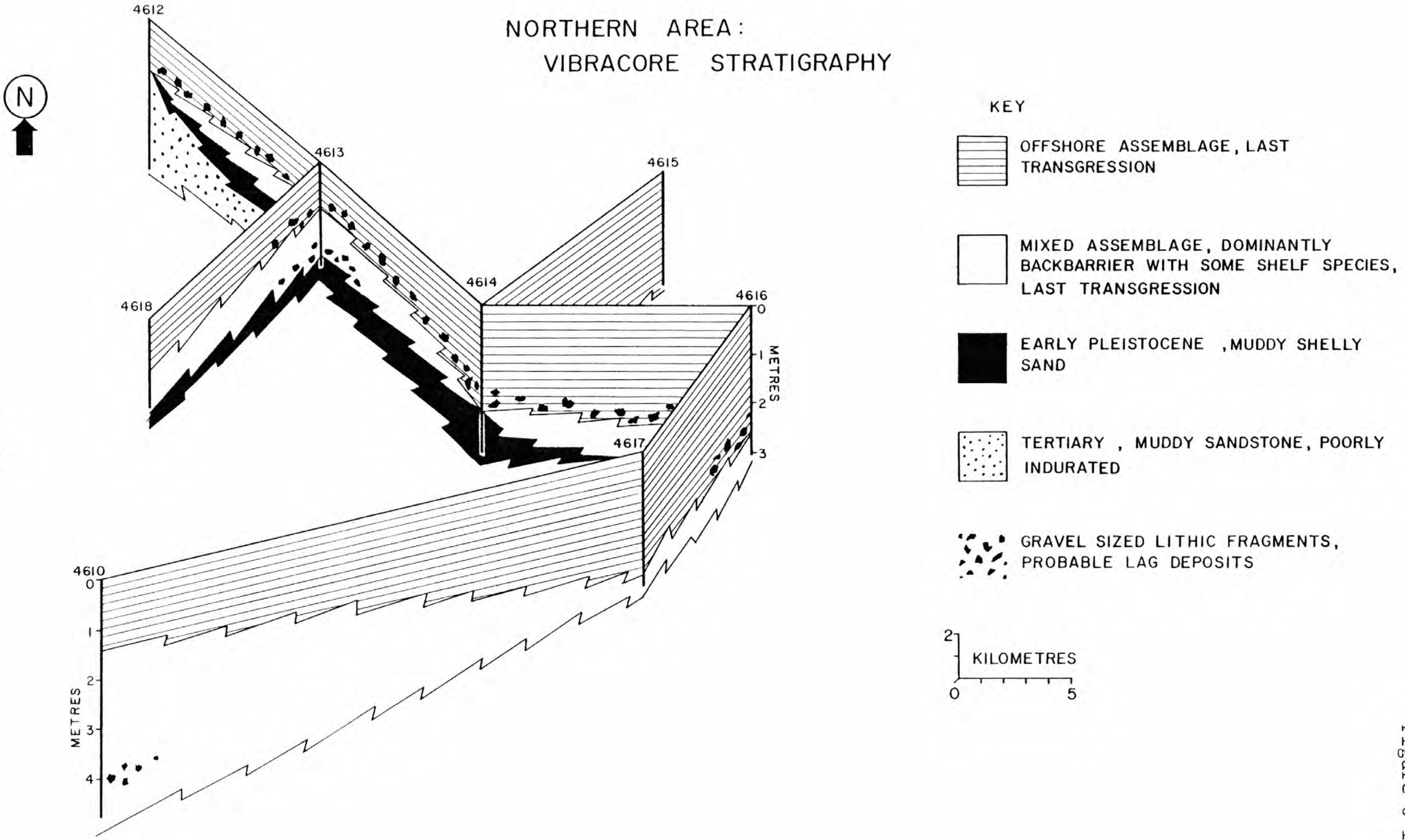

NORTHERN AREA: VIBRACORE STRATIGRAPHY

4612
4613
4615
4614
4618
4616
4617
4610
0
1
2
3
4
METRES
N
KEY
OFFSHORE ASSEMBLAGE, LAST TRANSGRESSION
MIXED ASSEMBLAGE, DOMINANTLY BACKBARRIER WITH SOME SHELF SPECIES, LAST TRANSGRESSION
EARLY PLEISTOCENE, MUDDY SHELLY SAND
TERTIARY, MUDDY SANDSTONE, POORLY INDURATED
GRAVEL SIZED LITHIC FRAGMENTS, PROBABLE LAG DEPOSITS
2
KILOMETRES
0
5

Figure 6-18

Figure 6-19. Vibracore stratigraphy of the shelf sediment cover within the boundaries of the proposed southern lease area. Radiometric dates of these cores are shown in Table 6-16.

SOUTHERN AREA:
VIBRACORE STRATIGRAPHY

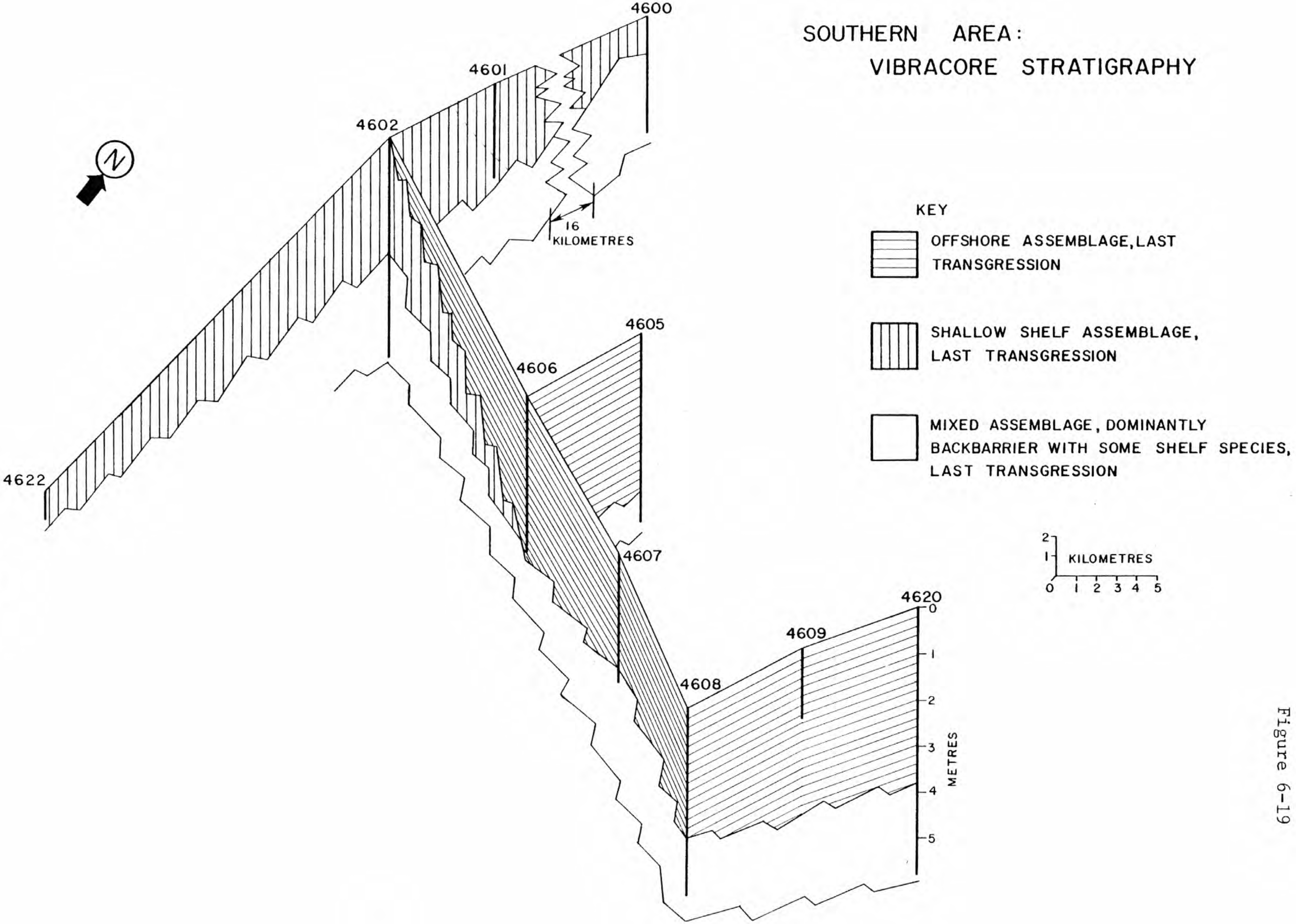
4600
4601
4602
4605
4606
4607
4608
4609
4620
4622
16 KILOMETRES
N
KEY
▤ OFFSHORE ASSEMBLAGE, LAST TRANSGRESSION
▥ SHALLOW SHELF ASSEMBLAGE, LAST TRANSGRESSION
☐ MIXED ASSEMBLAGE, DOMINANTLY BACKBARRIER WITH SOME SHELF SPECIES, LAST TRANSGRESSION
KILOMETRES
0
1
2
3
4
5
METRES

Figure 6-19

Table 6-16. Radiometric (C_{14}) dates from the proposed lease area vibracores.

Core	Core Interval in cm	Apparent Age C_{14} Years B.P.	Material Dated
4613	160-200	$30{,}215 \pm {}^{445}_{475}$	*Spisula*; unabraded
4618	100-160	11,050 ± 140	*Crassostrea*; worn, elongated, black
4618	100-120	4,870 ± 80	*Glycymeris*; unabraded
4620	540-560	$27{,}635 \pm {}^{555}_{595}$	Whole sample oolitic sand
4620	540-560	>44,000	Oolitic sand, inner cores only (treated with 10% HCl until sample was only 18% of original weight)

attests to the fact that some of the shells may have had a lagoonal history but the overall faunal character indicates that mixing and final deposition has occurred in the present environment.

Most cores in the lease areas also bottomed out in well lithified material, judging from penetration rate records. Rocks were obtained in six core bottoms. Certainly, the general statement can be made for this area that the unconsolidated sediment cover is thin, typically less than 6 m and that hard rock frequently underlies it.

Definite shallow water material is present in abundance at the base of two cores, 4608 and 4600. Possible Waccamaw Formation (Lower Pleistocene) may be present in two cores based on macrofauna counts (cores 4614 and 4613, Table 6-14). The oolite and oolitic sediment observed in the base of core 4620 was determined by C_{14} dating to have central portions of the oolites older than 44,000 years with dates of the whole oolites of 27,635 years B.P.

Core 4620 exhibits an interesting sequence which was most likely deposited by a major storm. The core bottoms out in slightly lithified oolite at a depth of about 500 cm. Above this is a 115 cm thick layer of oolitic shelly sand overlain and underlain by non-oolitic sands. Sharp boundaries, lack of mixing and possible grading indicate this is a single event. The presence of the oolites affords a unique opportunity to identify the single event layer. Presumably the oolite source is a surficial outcrop of the same material penetrated at the base of the core. Other storm layers may be present in other cores but would likely be much less "visible" because the material above and below would be the same.

The important observation here is that a single event on the central shelf apparently is capable of locally moving about and depositing more than 1 m of sediment. It would be useful to study this layer with more detailed vibracoring.

SEA LEVEL HISTORY

The establishment of sea level curves based on radiocarbon dates of shoreline indicators is made difficult because of the paucity of datable shoreline indicators as well as the complex interaction of eustatic sea level changes. This has most recently been pointed out in Belknap and Kraft's (1977) study of the Baltimore Canyon trough region.

The Late Pleistocene-Holocene sea level curves most commonly used by geologists, those of Milliman and Emery (1968) and Curray (1965) have been recently brought into question by estimated minimum reconstructed depths for dated in-place shelf edge sandstones of North Carolina (Macintyre _et_ _al_ 1975) and "fixed sample" (including oolites and minimum depth corrected subtidal sandstones) dates from a portion of the shelf off Delaware and Long Island. Macintyre and others (1978) suggested that Curray's sea level curve was closer to reality than Milliman and Emery's on the basis of more than 40 oyster shell dates from the North Carolina shelf. The wide scatter of their data points further suggested that dates on material that can be moved about by the transgressing shoreface are at best only approximate indicators of shoreline position.

Eight datable fixed shoreline indicators obtained from this study (Table 6-15) afford a good opportunity to re-examine the Late Pleistocene-Holocene sea level curves. The dates are from oyster shells in living position, oyster shells associated with a lagoonal faunal assemblage, or in-place salt marsh peat. The new sea level curve (Figure 6-20) closely follows that of Milliman and Emery for the period of time before 22,000 years B.P. (samples 1 through 6, Figure 6-21).

Figure 6-20. Proposed sea level curve for the eastern U. S. Continental Shelf based on C_{14} dates obtained from in-place material.

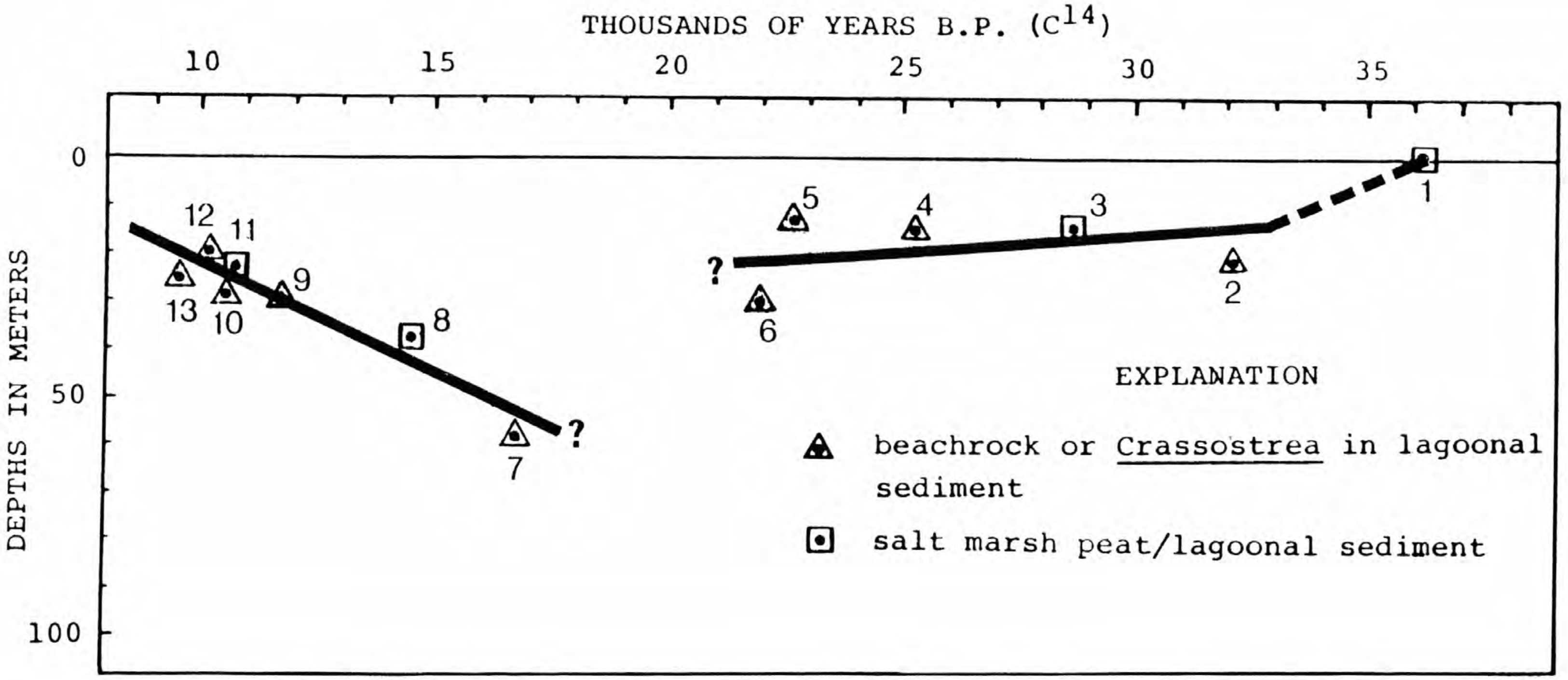
THOUSANDS OF YEARS B.P. (C^{14})
10
15
20
25
30
35
DEPTHS IN METERS
0
50
100
1
2
3
4
5
6
7
8
9
10
11
12
13
?
?
EXPLANATION
beachrock or Crassostrea in lagoonal sediment
salt marsh peat/lagoonal sediment

Figure 6-20

Figure 6-21. Comparison of the sea level curve introduced in this study (Figure 6-20) with those of previous studies.

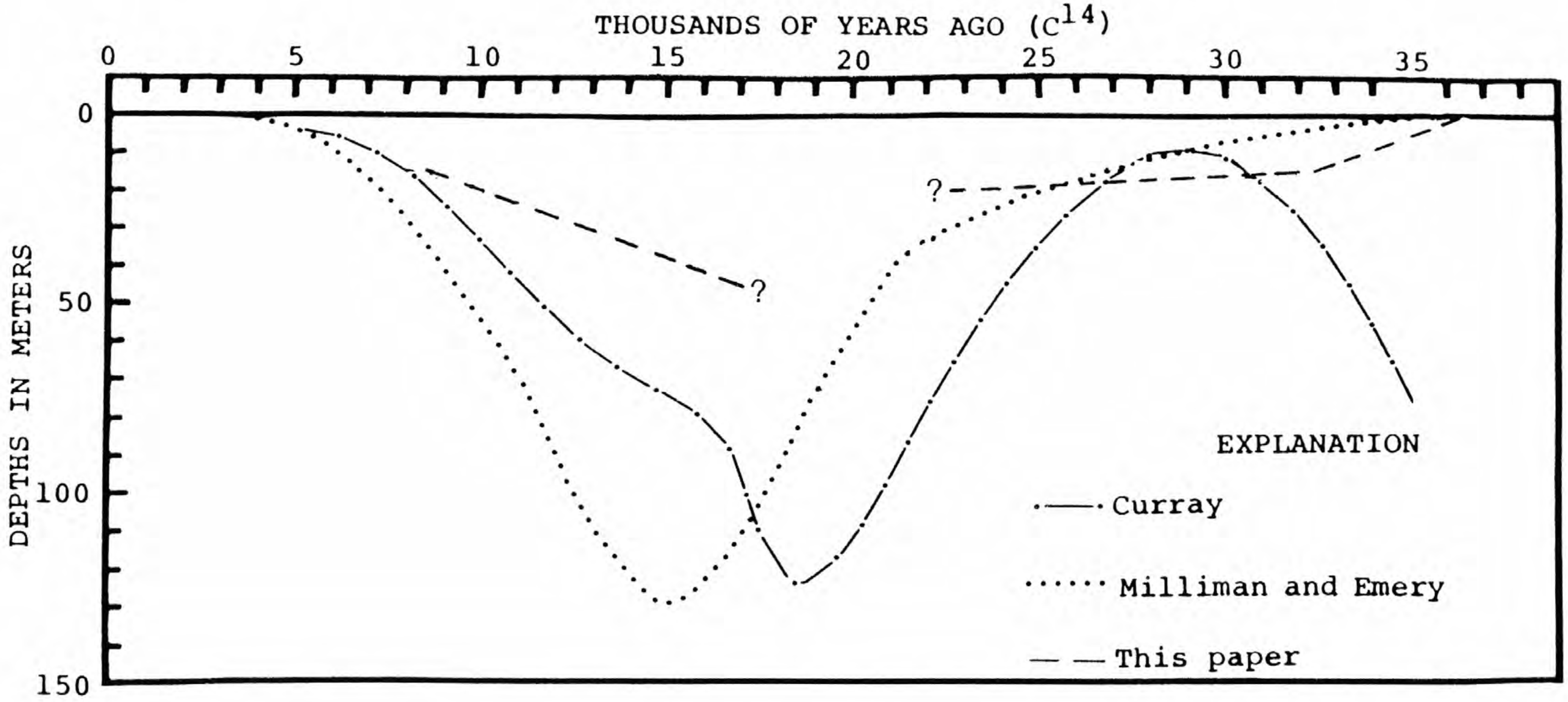
THOUSANDS OF YEARS AGO (C^{14})
0
5
10
15
20
25
30
35
DEPTHS IN METERS
0
50
100
150
?
?
EXPLANATION
Curray
Milliman and Emery
This paper

Figure 6-21

From about 17,000 B.P. to 10,000 B.P. the curve is consistently shallower and more gentle than both of the previously published curves.

DISCUSSION

Implications Regarding Barrier Island Evolution

Most of the original theories of barrier island formation assume that islands were formed near their present position when the Holocene transgression slowed down 5,000 to 7,000 years ago (e.g. Hoyt 1967). Recently Swift (1975) and Field and Duane (1976) have suggested that barrier islands may have formed at the edge of the continental shelf as the sea level first transgressed across it. After initially forming, the barriers are then assumed to have migrated across the shelf at a rate controlled by shelf slope and sea level rise. If this has been the case, backbarrier deposits (which could exist only if a barrier is present) might be expected to be preserved in the outer continental shelf sediment cover.

Sedimentary structure, faunal evidence and radiocarbon dates indicate that lagoon deposits or lagoon derived materials are commonplace in the shelf sediment cover. The clear implication here is that barrier islands must have existed across much of the areal extent of the shelf as the sea level rose during the last transgression. The core evidence, however, does not distinguish between "hopping" barriers or migrating barriers. A number of studies on present-day islands indicates that migration is physically possible and is apparently happening today.

Origin of the Shelf Sediment Cover

The post-Pliocene sediment thickness in the study area probably averages well under 5 m in thickness. The molluscan fauna in this thin veneer of sediment is entirely late Pleistocene or Holocene. Thus, most of the Pleistocene epoch is not represented by fossils in this sediment cover, in spite of the various ice-age transgressions and regressions that must have affected the shelf surface. If the molluscan fauna from each succeeding transgression and regression was preserved, the resulting assemblage would be a confusing mixture of all environments from outer shelf to lagoon.

The lack of early Pleistocene mollusks is probably related to the thinness of the shelf sediment cover. This thin veneer was largely reworked by each transgressing shoreline with incorporation of a new calcareous fraction each time. After sea level regressions, the exposed former shelf surface apparently lost most of its carbonate fraction due to weathering processes just as most material has been removed from Pleistocene shoreface and inner shelf deposits presently on the subaerially exposed lower coastal plain of the southeastern U.S.

The shelf sediment cover is best envisioned as a two component system consisting of carbonate and non-carbonate fractions with greatly different and independent histories. The terms relict or palimpsest conceivably could apply to the non-carbonate component but not to the calcareous material which appears to be largely indigenous. Probably the entire system is best described by Swift's (1976) classification, as autochthonous.

The non-carbonate fraction of the sediment must have been reworked several times during the Pleistocene. Small amounts of material may have been added or subtracted via fluvial processes. Erosion of the underlying pre-Pleistocene materials during each transgression does not appear to be an important source of new sediment since virtually no Tertiary fossils were observed in the Pleistocene-Holocene section of the cores (cf. Pilkey and Luternauer 1967). The lack of such fossils and the general thinness of the sediment cover indicate that shoreface erosion and mixing during a rising sea level affects only the upper few meters of sediment on the shelf.

In both the cross-shelf core profiles of this study the sedimentary structures and the fauna indicate that the upper 1 to 5 m of sediment is "in place." That is, sedimentary structures and fauna indicate deposition generally under present-day conditions. The upper portion of the outer shelf sediment column was deposited on the outer shelf.

Southeastern U.S. shelf sediment has long been considered relict (e.g., Gorsline 1963; Milliman et al 1972). In the sense that the sediment has been cut off from its lines of supply, relict is a suitable descriptive term. However, the thickness of the mixed portion of the sediment cover (Figure 6-22) is such as to indicate a great deal of "in place" movement of sediment on the shelf at the present time.

The "mixing" in the surficial unconsolidated sediment cover must largely have occurred by alternate scouring and filling during storms. The very high percentage of bioturbation argues that sand movement must occur in relatively small surges. Deposition of one meter or more thick sand layers as single events probably is not the usual situation.

Interestingly, the depth below surface of the 15 samples which contained greater than 10% mud (Table 6-11) increases seaward forming a wedge that resembles the lower boundary of the zone of Holocene mixing. It is likely that most of these muddy samples are from undisturbed, low energy depositional units that have not yet been reworked.

After the shoreline has transgressed beyond a given shelf area, subaqueous physical and biological processes continue reworking the sediment now exposed to open shelf conditions. This reworking is both

Figure 6-22. Assumed extent of the Holocene mixing of the shelf sediment cover. Based on the assumption that the presence of even a single outer shelf shell in outer shelf sediment, no matter what the sediment depth, indicates mixing of the sediment when sea level was close to its present position.

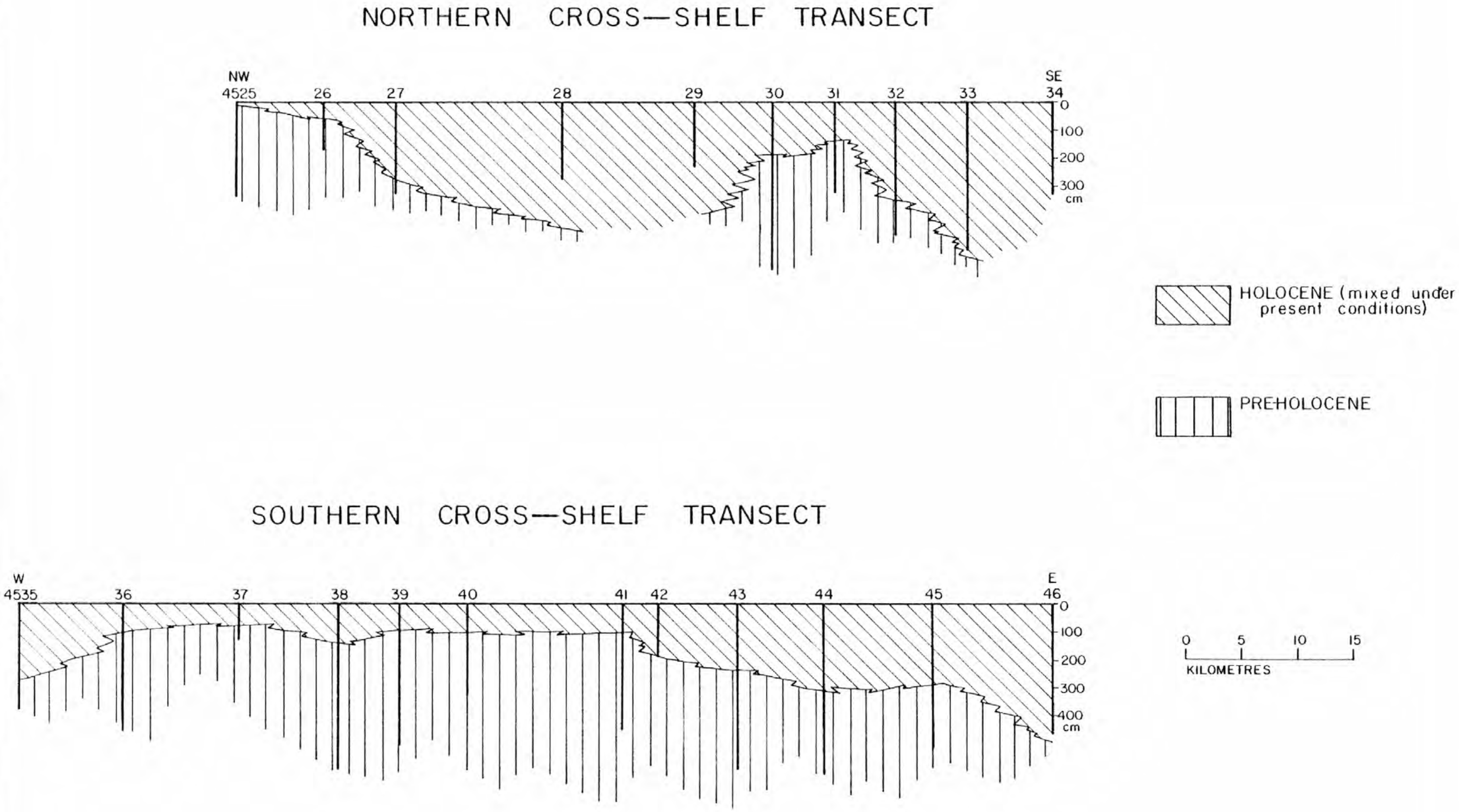
NORTHERN CROSS—SHELF TRANSECT

SOUTHERN CROSS—SHELF TRANSECT

NW
4525
26
27
28
29
30
31
32
33
SE
34
0
100
200
300
cm
HOLOCENE (mixed under present conditions)
PREHOLOCENE
W
4535
36
37
38
39
40
41
42
43
44
45
E
46
0
100
200
300
400
cm
0
5
10
15
KILOMETRES

Figure 6-22

rapid and extensive. An important ramification of this is that the history of most of the Pleistocene is missing in the sedimentary record on the shelf.

Implications Concerning Environmental Impact of Shelf Development

The results of this study indicate that the outer shelf sediment cover has experienced considerable mixing. Because sedimentary structures and faunal components both indicate shelf sediments are in-place, the mixing has likely occurred since the sea level attained close to its present position, i.e. within the last 5,000 to 7,000 years. The time frame and intensity of the mixing and sediment movement processes are important to understand in order to understand potential dispersal of particulate pollutants or contaminants.

Swift (1976) has demonstrated that in the mid-Atlantic shelf region certain sand bodies now on the shelf were probably inherited from a pre-existing shoreface. However, the thickness of the zone of autochthonous sediment in the present study area is sufficiently great to suggest that minor topographic features on the Georgia Embayment shelf surface are likely to reflect present-day processes rather than past nearshore events. That is, the complete mixing of indigenous middle to outer shelf faunas into the shelf sediment cover indicates that significant sand movement has occurred, most likely in response to major storm conditions. On the inner shelf of this study area, however, to water depths of 16 to 20 m, our seismic profiles (Figures 6-4 and 6-5) indicate that some minor topographic features may well be inherited from pre-existing features, e.g. former inlets and tidal deltas. Thus, inner shelf studies may be complicated because of the role of relict topographic features while study of sand bodies on the central and outer shelf may well prove fruitful with regard to understanding shelf dynamics.

LITERATURE CITED

Bailey, E.H. and Stevens, R.E., 1960. Selective staining of K-feldspar and plagioclase on rock slabs and thin sections: Amer. Mineral., vol. 45, p. 1020-1026.

Belknap, D.F., and Kraft, J.C. 1977. Holocene relative sea-level changes and coastal stratigraphic unit on the northwest flank of the Baltimore Canyon trough geosyncline: Jour. of Sed. Pet., vol. 47, pp. 610-629.

Carroll, D., 1970. Clay minerals: A guide to their X-ray identification: Geol. Soc. America Special Paper 126, 80 p.

Cook, D.O., 1969. Calibration of the University of Southern California automatically recording settling tube: Journal of Sedimentary Petrology, vol. 39, pp. 781-786.

Curray, J.R. 1965. Late Quaternary history, continental shelves of the United States in The Quaternary of the United States, Wright and Frey, eds., Princeton University Press, pp. 723-735.

Doyle, L.J., Cleary, W.J., and Pilkey, O.H. 1969. Mica, its use in determining shelf deposition regimes: Marine Geology, vol. 6, pp. 381-389.

Felix, D.W. 1968. An inexpensive recording settling tube for analysis of sands: Jour. of Sed. Pet., vol. 39, pp. 777-780.

Field, M.E., and Duane, D.B. 1976. Geomorphology and sediments of the inner continental shelf, Cape Canaveral, Florida: Coastal Eng. Res. Center, Tech. Mem. No. 42, 83 p.

Folger, D.W. 1972. Texture and organic carbon content of bottom sediments in some estuaries of the United States in Environmental Framework of Coastal Plain Estuaries: Geol. Soc. America Memoir

133, pp. 391-407.

Folk, R.L. 1974. Petrology of sedimentary rocks: Hemphill Publishing Co., Austin, Texas, 182 p.

Gorsline, D.S. 1963. Bottom sediments of the Atlantic shelf and slope off the southern United States: Jour. of Geol., vol. 71, pp. 423-440.

Hoyt, J.H., 1967. Barrier island formation: Geol. Soc. America Bull., vol. 78, pp. 1125-1135.

Kaiser, H. and Specker, H., 1955. Z. Anal. Chem., vol. 149, p. 46.

Macintyre, I.G., Blackwelder, B.W., Land, L.S., and Stuckenrath, R. 1975. North Carolina shelf edge sandstone: Age, environment of origin and relationship to pre-existing sea levels: Geol. Soc. America Bull., vol. 86, pp. 1073-1078.

Macintyre, I.G., Pilkey, O.H., and Stuckenrath, R. 1978. Relict oysters on the United States Atlantic continental shelf: A reconsideration of their usefulness in understanding late Quaternary sea-level history: Geol. Soc. America Bull., vol. 89, pp. 277-282.

Milliman, J.D., and Emery, K.O. 1968. Sea level curves during the past 35,000 years: Science, vol. 162, pp. 1121-1123.

Milliman, J.D., Pilkey, O.H., and Blackwelder, B.W. 1968. Carbonate sedimentation on the continental shelf, Cape Hatteras to Cape Romain: Southeastern Geology, vol. 9, pp. 245-267.

Milliman, J.D., Pilkey, O.H., and Ross, D.A. 1972. Sediments of the continental margin off the eastern United States: Geol. Soc. America Bull., vol. 83, pp. 1315-1334.

Pevear, D. 1968. Clay mineral relationships in recent river, nearshore marine, continental shelf, and slope sediments of the southeastern

United States. Unpublished Ph.D. Dissertations, University of Montana, Missoula, Montana, 163 p.

Pilkey, O.H., and Luternauer, J.L. 1967. A North Carolina shelf phosphate deposit of possible commercial interest: Southeastern Geology, vol. 8, pp. 33-51.

Swift, D.J.P. 1975. Barrier island genesis: Evidence from the Middle Atlantic Shelf of North America: Sediment. Geol., vol. 14, pp. 1-43.

Swift, D.J.P. 1976. Continental shelf sedimentation _in_ Sediment Transport and Environment Management: John Wiley, New York, pp. 311-350.

Uchupi, E., 1965. Maps showing relation of land and submarine topography, Nova Scotia to Florida: U.S. Geol. Survey, Misc. Geol. Inv. Map I-451, scale 1:1,000,000, 3 sheets.

CHAPTER 7

TRACE METAL CONCENTRATIONS IN SEDIMENT CORES FROM THE CONTINENTAL SHELF OFF THE SOUTHEASTERN UNITED STATES

Michael Bothner[1], Phil Aruscavage[2],
Wayne Ferrebee[1], and Joan Lathrop[1]

[1] U. S. Geological Survey, Woods Hole, Massachusetts 02543

[2] U. S. Geological Survey, Reston, Virginia 22092

Chapter 7

Table of Contents

Page

Abstract. 7- 1

Introduction. 7- 1

Methods 7- 2

  Sampling. 7- 2

  Textural Analyses 7- 4

  Trace Metals. 7- 4

Results and Discussion. 7-12

  Texture 7-12

  Trace Metals. 7-17

Conclusions 7-26

Literature Cited. 7-30

USGS LIBRARY - MENLO PARK
3 1820 00087454 9